Poly(lactide-co-glycolide) devices for drug delivery

Campbell, Chris

Award date:
2008

Awarding institution:
University of Bath

Poly(lactide-co-glycolide) Devices for Drug Delivery

Christopher S. J. Campbell

Doctor of Philosophy

University of Bath
Department of Chemical Engineering and
Department of Pharmacy and Pharmacology

September 2008

Abstract

Ovarian cancer is one of the five most common causes of cancer death in women in the USA and UK. It is usually diagnosed when it is well established beyond the ovary in the peritoneum. Intravenous injection of cisplatin is a common palliative therapy for ovarian cancer patients. Intraperitoneal therapy has been shown to improve survival for patients. Poly(lactide-co-glycolide) (PLGA) is a biodegradable polyester which has been proven safe for medical implantation. PLGA microspheres or fibres have been considered in this work as depots for delivering intraperitoneal cisplatin directly to the tumour site. The aims of this work were (1) to develop microsphere depot formulations with improved drug release profiles compared to previous work. (2) Novel cisplatin containing solid and hollow fibres were to be developed and investigated as alternative structures for depot devices. (3) The drug release profiles were to be examined using mathematical models to allow rational comparison of the devices. The suitability of different mathematical models was also considered.

Cisplatin undergoes a ligand exchange in the presence of water, forming a potent electrophile. This charged cisplatin species readily forms DNA-platinum adducts. These adducts are thought to be the major mechanism of toxicity to cancer cells. Charged cisplatin also binds other nucleophiles in cells. Cisplatin binding to other cellular components reduces the amount of cisplatin available for DNA attack. Irreversible protein binding influences cisplatin pharmacokinetics compared to other drugs. Therefore, an additional aim of this project was (4) to investigate irreversible binding of cisplatin to non-DNA targets, such as cisplatin binding to protein.

The surfaces of all implanted medical devices are susceptible to bacterial attachment. Bacteria are able to survive on implants in a hostile environment-resistant slow growth mode. A further aim of this thesis was (5) to investigate attachment of bacteria to PLGA depots.

Cisplatin containing PLGA 50:50 and 65:35 microspheres were prepared using less toxic solvents than those manufactured elsewhere while achieving equivalent release profiles. The particle size distributions of batches of microspheres were measured

using laser scattering. Batches had median diameters of 25-66 μm. Cisplatin containing PLGA 65:35 solid fibres and hollow fibres were fabricated by spinning polymer dissolved in organic solvent into a water bath where solidification (phase inversion) occurred. A novel method was developed for drug delivery applications that included a freeze drying step that maximized encapsulation of the drug. This method may be suitable for improving the drug loading of any fibres used to encapsulate water soluble drugs. The drug loading of solid (15 %) and hollow (27 %) fibres produced by this method was higher than the best drug loading of PLGA microspheres (10 %) produced in this work and elsewhere. Cisplatin release profiles for all three depot structures were determined using atomic absorption spectroscopy (AAS). The devices were also examined using scanning electron microscopy and backscattering electron imaging.

Semi-empirical and mechanistic models derived from Fick's laws of diffusion were successfully used to model the data. The diffusivity of cisplatin in microspheres was lowest in microspheres at 4×10^{-11} cm^2 s^{-1}. The diffusivity of cisplatin in PLGA 65:35 hollow fibres was calculated as 3×10^{-10} cm^2 s^{-1} using a model derived from Fick's second law. Using Higuchi kinetics the diffusivity of cisplatin in PLGA solid fibres was shown to be similar to the diffusivity cisplatin is hollow fibres. The porous structure of solid and hollow fibre matrix produces more rapid diffusion than occurs in the solid matrices of microspheres.

Cisplatin binding to bovine serum albumin (BSA) was determined by combining protein precipitation using cold ethanol with acid digestion and AAS. Cold ethanol precipitation was equivalent to ultrafiltration, the gold standard for removing BSA from solution. Cold ethanol precipitation is here established as a suitable method for *in vitro* investigation of irreversible protein binding phenomena. The rate of irreversible cisplatin binding to protein was found to be $6\pm1\times10^{-5}$ s^{-1} *in vitro*. First order models were successfully used to model *in vitro* data of dynamic cisplatin release and protein binding systems to an acceptable level of accuracy.

Staphylococcus epidermidis is an important pathogen associated with long term implanted polymeric devices such as intravenous catheters. *S. epidermidis* was observed to rapidly bind to PLGA microspheres and fibres *in vitro*. Attached cell

numbers can be reduced by freeze-drying or exposure to 70 % ethanol for 60 seconds. Increasing the amount of depot present increased the number of cells bound. Although bacterial attachment to depot devices does occur, surveillance information of commercial PLGA implants suggests that the infection rates are low (<5 %).

In conclusion, cisplatin containing PLGA 65:35 solid and hollow fibres represent a novel, reproducible formulation for encapsulating higher amounts of cisplatin for an equivalent mass of excipient than other polymer formulations. The fibres developed in this study were able to maintain elevated concentrations of unbound cisplatin in the presence of a biological matrix for approximately 100 hours *in vitro*.

Table of Contents

List of Figures

List of Tables

Acknowledgements

I am very grateful to Semali Perera, Begoña Delgado-Charro, Anthony Smith and Nick Johnson, my large team of supervisors, who have given me encouragement, constructive criticism, and support as necessary during my three years. Semali has always been ready with advice and a smile. Thank you for encouraging me with your unfailingly positive attitude. Begoña has provided an incredible amount of excellent input since I was thrust upon her. Thank you for helping this unexpected student. Anthony has been very kind in offering useful feedback on my work, despite having moved on to greater things. Thanks to Nick for his infectious enthusiasm to start the project rolling.

I would also like to thank the team of technicians for their help. Thanks in particular to John Bishop whose inventions have been extremely useful in the lab and to Richard Bull who has been as helpful as amusing. Thanks to Jo Carter who was invaluable in teaching me the techniques I needed for the bacterial work and found me bench space whenever I needed it. Thanks also to Ursula Potter and Anne O'Reilly in the Centre for Electron Optical Studies for their expertise in electron imaging.

Thanks to Ian Lee for being my lab buddy, Ian Benzeval for being my maths buddy, not to mention the other postgraduates for sharing good times.

I am very grateful to the University of Bath for financial support.

I would also like to thank my parents, not just for financial support, but also as a constant source of love and happiness. Thanks, finally, to Holly for her tireless provision of advice, love, wine, and friendship. Without you I'd probably still be writing up now.

Abbreviations

AAS	Atomic absorption spectroscopy
AIC	Akaike's information criterion
ATP7A	Copper-transporting P-type ATPase 7A
BSA	Bovine serum albumin
CD20	Non-glycosylated phosphoprotein CD20
cfu	Colony forming units
CTR1	Copper-transporting membrane protein 1
DCM	Dichloromethane
DMF	N,N-Dimethyl formamide
ERCC1—XPF	Excision repair cross complementing 1—xeroderma pigmentosum, complementation group F complex
GnRH	Gonadotropin-releasing hormone
IP	Intraperitoneal
IV	Intravenous
LC_{50}	Concentration of a chemical that is lethal to 50 % of a defined group of animals (mg ml^{-1})
LD_{50}	Dose of a chemical that is lethal to 50 % of a defined group of animals (mg)
NER	Nucleotide excision repair
NMP	N-methyl-2-pyrrolidone
PBS	Phosphate buffered saline
PGA	Poly(glycolide)
PLA	Poly(lactide)
PLGA	Poly(lactide-co-glycolide)
PVA	Poly(vinyl alcohol)
rpm	Revolutions per minute
TSA	Tryptone soya agar
TSB	Tryptone soya broth
XPA	Xeroderma pigmentosum, complementation group A

Nomenclature

A	Exposed area of a membrane (cm^2).
A_B	Constant to be determined for solution of Bessel's equation.
A_W	Aggregated constant for pharmacokinetic model.
a	Radius of solid fibre or inner radius of hollow fibre (cm).
α	Positive roots of Bessel function.
α_W	Root of pharmacokinetic polynomial.
B_B	Constant to be determined for solution of Bessel's equation.
B_W	Aggregated constant for pharmacokinetic model.
b	Outer radius of hollow fibre (cm).
β	Random errors.
β_W	Root of pharmacokinetic polynomial.
C	Concentration (mg ml^{-1}).
$C(r, t)$	Concentration in solution at (r) at time = t (mg ml^{-1}).
$C(x, t)$	Concentration in solution at (x) at time = t (mg ml^{-1}).
$C(x, y, z, t)$	Concentration in solution at (x, y, z) at time = t (mg ml^{-1}).
$C(0)$	Starting concentration in solution at time = 0 (mg ml^{-1}).
C_s	Solubility of the drug in the solvent (mg ml^{-1}).
c	Intercept of linear model describing bacterial attachment to microspheres.
c_{12}	Rate constant of transfer from aqueous ($W1$) to peripheral ($W2$) compartment (s^{-1}).
c_{21}	Rate constant of transfer from peripheral ($W2$) to aqueous ($W1$) compartment (s^{-1}).
c_{el}	Rate constant of elimination total cisplatin from central compartment ($W1$) (s^{-1}).
count	Cell count of colony forming units which made weak interactions with microspheres (cfu ml^{-1}).
D	Apparent diffusivity of drug in homogeneous matrix (cm^2 s^{-1}).
D_W	Dose (mg).
d	Coefficient of linear model describing influence of initial culture concentration on bacterial attachment to microspheres.

dd	Coefficient of linear model describing the influence of arbitrary dilution of bacterial culture.
$\Delta C^{\Delta t}$	Change in concentration over small time.
e	Coefficient of linear model describing influence of mass of microspheres present on bacterial attachment to microspheres.
f	Coefficient of linear model describing influence of additional wash step on bacterial attachment to microspheres.
g	Centripetal acceleration of a centrifuge equivalent to the acceleration due to earth's gravity (9.8 m s^{-1})
h	Theoretical distance in Higuchi kinetics describing depth into a slab from which drug has begun eluting.
$init$	Initial concentration of bacteria (cfu ml^{-1}).
$j(r, t)$	Flux of material is the rate of transfer per unit area of section in the direction r (mg cm^{-2}).
$j(x, t)$	Flux of material is the rate of transfer per unit area of section in the direction x (mg cm^{-2}).
j_{12}	Rate constant of transfer of unbound cisplatin from central ($U1$) to peripheral ($U2$) compartment (s^{-1}).
j_{21}	Rate constant of transfer of unbound cisplatin from peripheral ($U2$) to central ($U1$) compartment (s^{-1}).
j_{el}	Rate constant of elimination unbound cisplatin from central compartment ($U1$) (s^{-1}).
k	Release constant using Higuchi kinetics (mg cm^{-2} $s^{-0.5}$).
k_{21}	Rate constant of release from *X2* into *X1* compartment of two compartment model (s^{-1}).
k_{31}	Rate constant of fast release from *X3* into *X1* compartment of three compartment model (s^{-1}).
k_{41}	Rate constant of slow release from *X4* into *X1* compartment of three compartment model (s^{-1}).
k_b	Protein-drug binding constant (s^{-1}).
λ_i	Roots of the denominator polynomial, $Q(s)$, in general partial fraction theorem.
$M(t)$	Amount of drug released at time = t (mg).
$M(\infty)$	Total drug (released after large time) (mg).

$M2(\infty)$	Total drug in depot *X2* compartment of two compartment model (mg).
$M3(\infty)$	Total drug in depot rapidly released from *X3* compartment of three compartment model (mg).
$M4(\infty)$	Total drug in depot slowly released from *X4* compartment of three compartment model (mg).
mass	Mass of microspheres (bacterial attachment studies) (mg).
n	An integer.
P	A point defined using rectangular (x, y, z) or polar (r, θ, z) coordinates.
$P(\cdot)$	Numerator polynomial in general partial fraction theorem.
p	Number of parameters used in a model when calculating AIC.
$Q(\cdot)$	Denominator polynomial in general partial fraction theorem.
R	Microsphere radius (cm).
$R(\cdot)$	A function of radius, r.
r	Radial distance of a point, P from z in polar space (cm).
s	Standard notation used in Laplace operations.
σ^2	Variance.
$T(\cdot)$	A function of time, t.
t	Time (s or h).
θ	Angle from z axis to point, P, in polar space.
$U1$	Concentration of unbound cisplatin in central compartment ($\mu g\ ml^{-1}$).
$U2$	Concentration of unbound cisplatin in peripheral compartment ($\mu g\ ml^{-1}$).
$U3$	Concentration of unbound cisplatin in peritoneal compartment ($\mu g\ ml^{-1}$).
u	An undefined variable.
V	Volume of matrix containing drug (ml).
$W1$	Concentration of total cisplatin in central compartment ($\mu g\ ml^{-1}$).
$W2$	Concentration of total cisplatin in peripheral compartment ($\mu g\ ml^{-1}$).

*W*3	Concentration of total cisplatin in protein bound compartment (μg ml^{-1}).
wash	Number of wash steps (bacterial attachment studies).
X(·)	A function of length, *x*.
X1	Concentration in solution compartment following drug release (mg ml^{-1}).
X2	Concentration in depot compartment for two compartment model (mg ml^{-1}).
X3	Concentration in rapid release compartment of three compartment model (mg ml^{-1}).
X4	Concentration in slow release compartment of three compartment model (mg ml^{-1}).
x	Distance in rectangular space.
y	Distance in rectangular space perpendicular to *x*.
z	Distance in rectangular space perpendicular to *x* and *y* and in polar space.

1 Introduction

1.1 Need for Implantable Drug Release Devices

Modern medicine is able to cure many diseases that were at one time fatal. Some diseases can only be treated toxic drugs which have severe side effects in the patient. To reduce harm to patients such drugs may be administered slowly. This allows the patient to recover from the side effects of the drug at the same time as treating the condition. Drugs can be administered as courses of pills, injections or infusions over hours, days or weeks. This ensures that the effective concentration of the drug in the blood is reached without causing the plasma concentration of the drug to rise to toxic levels.

An estimated 6.7 million people die of cancer every year globally (Parkin et al., 2005). Cancer is difficult to prevent, although risks can be reduced by lifestyle choices, such as not smoking. Cancer is often difficult to diagnose at an early stage as there may be few early symptoms. Cancer drugs are extremely toxic (section 1.3.2) and have limited efficacies for some patients. Cycles of dosing are required for sufficient drug exposure while minimizing the severe side effects. Resident catheters can be used to extend drug delivery duration to several days or weeks. Yet hospitalising patients for extended periods during distressing illness is unpopular with patients and expensive.

Implantable drug release devices can prolong drug exposure at the tumour site and minimise maximum blood plasma concentration of the drug. Depot formulations are currently used for treating some types of tumour (section 1.5.4.4). A depot of chemotherapeutics could improve therapy for other types of cancer. This thesis investigates the possibility of using biodegradable polyesters to act as a depot for platinum drugs, such as cisplatin, for treating ovarian cancer.

1.2 Thesis Outline

This thesis is divided into chapters which outline experimental investigations. Delivery of platinum containing chemotherapeutics to ovarian cancer is considered as a good example of an opportunity for slow release therapy using implantable devices. Section 1 reviews current drug delivery technologies with a focus on platinum therapy for ovarian cancer. Section 2 gives details of the experimental and statistical methods used for this work. Experimental results and discussion are presented in Section 3 with overall conclusions in Section 4.

Section 1 examines the mode of action of platinum therapy for ovarian cancer. It discusses strategies for reducing the toxicities associated with cisplatin therapy. Mathematical analysis of diffusion from drug delivery devices is reviewed. Bacterial contamination of implants is also considered. Section 2 describes the manufacture of microspheres, solid fibres and hollow fibres used in this work. Descriptions of device analysis methods used are included. Methods used for studying attachment of *Staphylococcus epidermidis* to PLGA devices are presented. Section 3 gives details of results of physical analysis of PLGA devices and studies of release kinetics. The binding of cisplatin to biological materials is investigated. The attachment and removal of bacteria from PLGA devices is considered.

1.3 Cancer Treatment

1.3.1 Cancer

Cancer is a major cause of death among populations which have affordable healthcare to control infectious diseases. In the United States an estimated 23 % of deaths were due to cancer in 2004, second only to heart disease as the most likely cause of death (Jemal et al., 2007).

Cancer is the collective term for the 200 or so diseases which occur when healthy body cells are freed from the restrictions of the cell cycle. To grow and maintain a functioning organism, control of cell proliferation must be absolute. Cells which detect that they are damaged commit suicide (apoptosis) and the immune system continuously purges the body of questionable cells. Three types of change occur in cells which become tumours. Cells must be immortalised, growing indefinitely. They

must be transformed meaning they no longer require the normal cell growth factors which would otherwise control them. They must also be able to undergo metastasis whereby cells are able to form colonies in other parts of the body (Lewin, 2000). In addition, tumour cells must not be immunogenic so avoid destruction by the immune system (Shankaran et al., 2001). Once growth is no longer constrained, the cells are able to infiltrate other organs, disrupting them and ultimately resulting in death of the patient.

Cancers develop from the stem cells of the parent tissue. As an organ may consist of many tissues, most organs have several types of cancer associated with them. Cancers are classified by the tissue or organ of origin, morphological appearance of the tumour and spread (progression) of the disease. Although molecular classification of tumours may become possible, for example using genetic microarrays (Golub et al., 1999), these technologies are not yet mature.

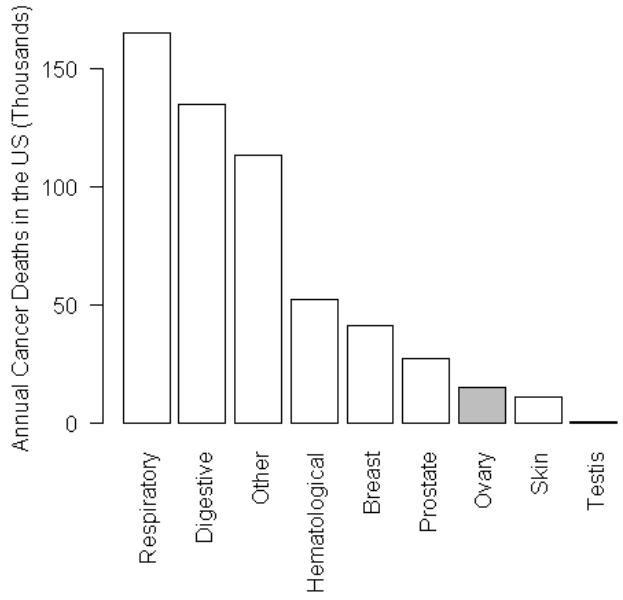

Figure 1: Estimated annual cancer deaths in the US for 2007 by site of cancer.
Ovarian cancer (grey bar) is responsible for 2.7 % of all cancer deaths. Data from Jemal et al., 2007.

Figure 1 shows estimated numbers of cancer deaths for the United States for 2007 for tumours originating at different sites. Cancers of the respiratory and digestive systems account for 35 % of new cases of cancer a year and are responsible for 54 %

of deaths. Non-melanoma skin cancers are not included in the cancer rate estimates as they are rarely fatal and are not reliably reported by some medical practices. The incidence and death rates for individual organs can be quite different. Cancer of the pancreas accounts for 3 % of new cases but 6 % of cancer deaths. Breast cancer accounts for 12 % of new cases but only 7 % deaths. The raised awareness of this disease and the relative ease of screening may be responsible for the relatively high relative survival rate of this disease. Ovarian cancer accounts for 1.6 % of new cases but 2.7 % of deaths (Jemal et al., 2007).

Different types of malignant tumours have characteristic disease progressions whereby if they are not destroyed or removed in the early stages will spread through adjacent tissues and form secondary colonies (metastases) around the body. Metastases are often well dispersed throughout the body, making surgical removal impossible.

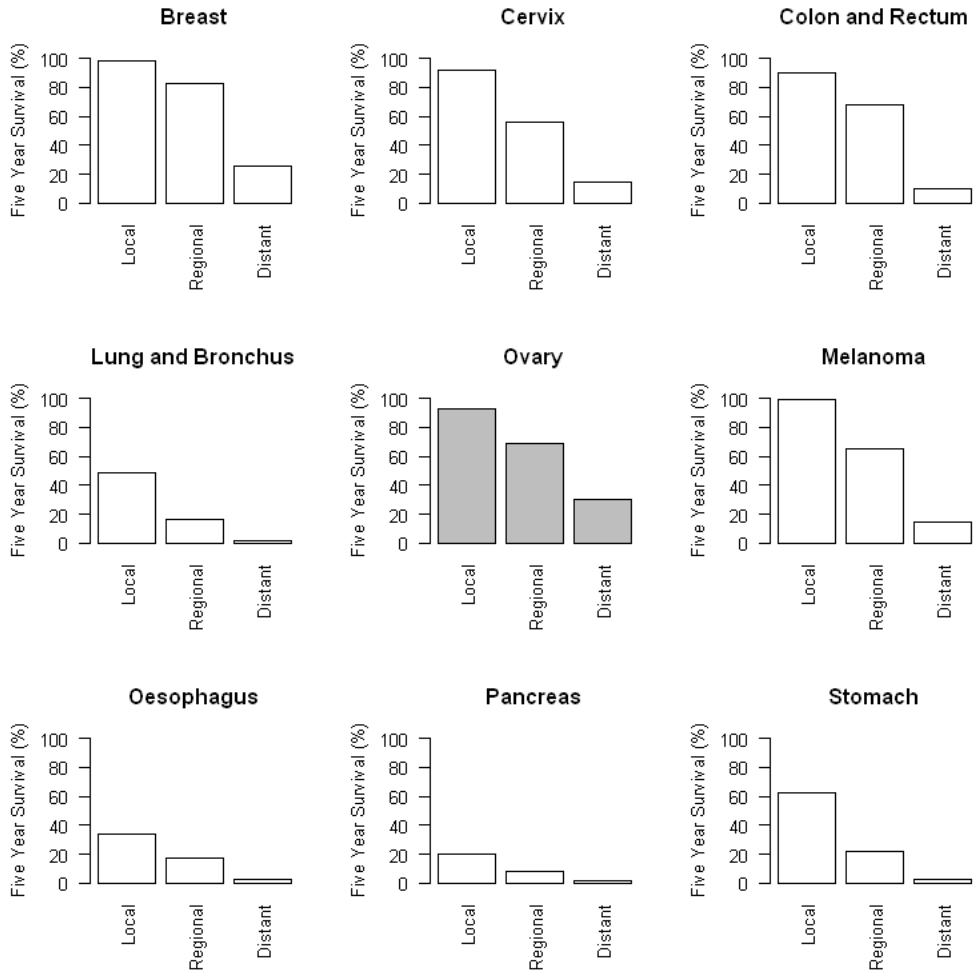

Figure 2: Five year survival of patients with cancers at different sites by progression of disease in the US between 1996 and 2002.

Local disease is constrained within the parent tissue. Survival is higher as affected tissue may be surgically removed. Regional disease has spread beyond originating tissue. Advanced disease is characterised by secondary metastases in distant organs. Data from Jemal, et al., 2007.

Figure 2 compares the five year survival of cancer patients by site and disease progression. Prognosis is better for patients if the disease is recognised during its early stages. Survival from skin cancer is good; 80 % of patients are diagnosed during the early stages, allowing the tumour to be excised. Up to 99 % of patients diagnosed with local melanoma survive for at least five years. Although survival from localised ovarian cancer is good with up to 93 % of patients surviving for at least five years only 19 % of tumours are detected at the early stage. Prognosis is extremely poor for pancreatic cancer. Only 7 % of tumours are detected while the

tumour remains localized and just 20 % of these patients survive for five years following diagnosis. For other patients the survival rate is lower still.

As there are a diverse range of diseases that fall under the umbrella term, cancer, the best approach to treatment varies considerably. Surgery, radiotherapy and chemotherapy are all useful treatment options and may be used alone or in combination. The best treatment for each case depends on the type of cancer, disease progression, and whether the tumour is a solid mass or dispersed through one or more tissues. In addition, more aggressive therapies may not be appropriate for patients who have been weakened by other diseases or old age. In cases where several methods have similar therapeutic value patient may choose treatments based on risks and severity of side effects.

1.3.2 Chemotherapy

Not all tumours can be easily surgically removed or damaged using focussed radiation. Chemotherapy is a successful alternative approach which aims to destroy cancer cells throughout the body. It is particularly useful when the tumour is in close proximity to sensitive vital organs which would be excessively damaged by invasive surgery or high doses of radiation.

Pathogenic microorganisms can be selectively targeted because they are sufficiently different from their host that they have markers and metabolic pathways not shared with humans. Drugs that bind to foreign proteins or block foreign enzymes will not harm the patient. A significant difficulty with extending this approach to cancer is that while invaders such as bacterial pathogens can be targeted using differences from host cells there are few markers for most cancers. Silver bullet approaches aim to solely target cancer cells. Gene therapy may be possible using a cancer cell targeted viral vector which is only able to replicate in telomerase expressing cells (Wirth et al., 2003). Most silver bullet techniques are still many years away from the clinic. Antibody based therapy has been used successfully to deliver radioisotopes to non-Hodgkin's lymphoma which expresses the CD20 antigen (Witzig et al., 2002). Antibody-based approaches are naturally limited to cancers expressing the relevant antigens.

Traditional chemotherapeutics dramatically increase survival rates for some cancers but are highly toxic and are used with the aim of destroying the tumour before the patient. There are three major classes of chemotherapeutic strategies.

- Antimetabolites are small molecules which have a similar structure to normal cell metabolites, most commonly nucleotides. They inhibit cellular machinery when recruited by enzymes, generally inhibiting DNA replication, preventing cell division.
- DNA-affecting compounds cause direct damage to DNA through oxidative damage or chemical modification. Alternatively cell division machinery is attacked through interactions with microtubules or topoisomerases causing entry into apoptosis.
- Cellular protein targeting molecules bind to enzymes or cell surface proteins and reduce the proliferation of cells expressing the target.

Each strategy has associated toxicities. In addition, patients may experience different symptoms determined by properties of the drug, pathways of metabolism, and whether there is an immune response to the treatment. The rate of drug clearance and rate of metabolism will also affect the severity of the side effects. The toxicities of some common chemotherapeutics associated with diseases such as lung, testicular and ovarian cancers are severe.

For adenocarcinoma, the most common lung cancer, surgical removal of early stage disease is the preferred treatment. Unfortunately only a third of patients have disease that can be treated in this way. Surgery for these early stage patients improved chance of surviving five years from 6-22 % with no treatment to 32-63 % in the United States in 1995 (Fry et al., 2000). Prognosis is poor for patients with advanced disease. Patients with distant metastases only survive for an average six months without chemotherapy. Patients with advanced lung cancer treated with cisplatin-docetaxel or gemcitabine-docetaxel chemotherapy survive for a median ten months (Georgoulias et al., 2001). Two thirds of lung cancer patients are given radiotherapy, chemotherapy or a combination. These treatments offer a small but significant survival advantage.

Docetaxel is a DNA-affecting compound which interferes with cell division. Paclitaxel was the first taxane discovered of this class and was initially extracted from the bark of the Pacific yew tree. Docetaxel was developed as a replacement; it is a semi-synthetic taxane which is derived from the more common European yew tree. Taxanes bind to tubulin which stabilises assembled microtubules. This causes an accumulation of microtubules, which initiates apoptosis. Major DNA breaks dues to apoptosis can be observed three days following treatment (Fabbri et al., 2006). As microtubules must be regulated in all dividing cells healthy stem cells are also affected by taxanes.

Gemcitabine is an example of an antimetabolite. It is a pyrimidine nucleoside analogue prodrug which is phosphorylated in the cell and incorporated into DNA during DNA synthesis. Once it has been incorporated DNA polymerase is unable to proceed and the proof-reading enzymes cannot remove it, resulting in apoptosis (Plunkett et al., 1995). As DNA must be replicated by all dividing cells healthy stem cells are also affected by this treatment.

Side effects of both docetaxel and gemcitabine include myelosuppression, nausea and vomiting, muscle and joint pain, constipation or diarrhoea, mild hair loss, peripheral nerve damage, disorders of the skin and nails, fatigue and liver damage.

In the 1970s the best treatment for testicular cancer was bleomycin with vinblastine. This was improved by adding cisplatin (section 1.4) and replacing vinblastine with etoposide. These improvements dramatically improved survival from testicular cancer.

Bleomycin is a DNA-affecting compound which directly damages DNA. It is a glycopeptide antibiotic which is believed to cause DNA cleavage by chelating metal ions to catalyse the production of superoxide and hydroxide free radicals. Oxidative damage affects all body tissues in addition to cancer cells. The lungs suffer extreme damage and severe scarring can impair lung function which is thought to be fatal in up to 3 % of patients (Jones and Vasey, 2003).

Vinblastine is a DNA-affecting alkaloid that binds to tubulin, promoting spiral aggregation of tubulin rather than microtubule formation. Cells become arrested in the M phase of the cell cycle as they cannot form mitotic spindle and the kinetochore and therefore cannot divide.

Etoposide is a non-alkaloid toxin which inhibits topoisomerase II. Like vinblastine and other inhibitors of cell division, etoposide damages stem cells in addition to cancer cells. Side effects include myelosuppression, nausea and vomiting, muscle and joint pain, constipation or diarrhoea, mild hair loss, peripheral nerve damage, disorders of the skin and nails, fatigue and liver damage.

Alkylating agents were the best chemotherapeutics available for treating ovarian cancer in the 1960s. Cisplatin (section 1.4) was introduced in 1973. Carboplatin (section 1.5.1) was introduced in the 1980s. Paclitaxel was first used in the 1990s and replaced cyclophosphamide after survival advantage was shown (McGuire et al., 1996). Doxorubicin has also been used for treating ovarian cancer.

Cyclophosphamide is a nitrogen mustard alkylating agent pro-drug which is oxidised by cytochrome P450s in the liver into its active form (Hengstler et al., 1997). The active metabolite forms DNA cross-links resulting in cell cycle arrest and entry into apoptosis. Aldehyde dehydrogenase converts activated cyclophosphamide into a less toxic form. Cyclophosphamide is therefore most toxic to cells with low concentrations of this enzyme.

Doxorubicin is a DNA-affecting anthracycline antibiotic which intercalates DNA and inhibits DNA, RNA and protein synthesis (Momparler et al., 1976). Cardiotoxicity is the dose limiting toxicity. Other toxicities include nausea and vomiting, myelosuppression and hair loss.

Development of novel classes of chemotherapeutics is one approach to cancer treatment. However, the pipeline of bringing new drugs to market is agonizingly slow. Drugs typically take ten years after identification of a suitable lead to approval. The drug must be economically viable, safe and effective. Even successful drugs may not be widely available to patients if they are too expensive.

An alternative approach is to reduce the toxicity of existing compounds and optimize the path of delivery of the drug or drugs. Since each type of cancer poses unique challenges, the best method of drug delivery should be considered for each type of disease.

1.3.3 Ovarian Cancer

Ovarian cancer is the fourth most common cause of cancer death in women in the United Kingdom with around 6000 new cases diagnosed each year. In the United States it is the fifth most common cause of cancer death with 22,400 new cases diagnosed each year (Jemal et al., 2007). The majority of cases are malignancies of the ovarian epithelium in post-menopausal women. In younger patients malignancies are frequently germ-cell tumours. Around 5-10 % cases are hereditary; these are generally due to inherited mutations in tumour suppressor genes. Such cases occur around 10 years earlier (Holschneider and Berek, 2000).

Ovarian cancers are derived from three different types of parent tissue. The most common are surface epithelial-stromal tumours are from ovarian surface lining cells. Sex cord-stromal tumours are derived from hormone producing cells and may continue to express oestrogen and inhibin (La Marca and Volpe, 2007). Germ cell tumours are the most common type of tumours in young women or girls. As there are a range of cancer types it is likely that no single marker will be discovered; early diagnosis is difficult.

Stage	Summary	Five Year Survival (%)
I	Cancer confined to one or both ovaries.	82-93
II	Includes pelvic extensions.	51-70
III	Includes peritoneal metastases.	17-37
IV	Distant metastases.	12-25

Table 1: Staging of ovarian cancer and five year survival rates by stage from Holschneider et al, 2000.

Ovarian cancer is usually asymptomatic in the early stages of the disease. If it is diagnosed at stage I while restricted to the ovaries (Table 1) prognosis is very good with five-year survival rates of 82-93 % (Holschneider and Berek, 2000). At stage II the cancer has begun to spread into the pelvis but is still difficult to detect. Three quarters of cases are diagnosed with advanced disease. Normally ovarian cancer is diagnosed at stage III when cells have proliferated into the peritoneum. The tumour cells form a plaque across the diaphragm and omentum which blocks lymph drainage of the peritoneum. Without drainage the abdomen swells as the volume of tumour cell containing fluid (ascites) increases. By the time symptoms have appeared it is impossible to remove all of the tumour cells by surgery. Five-year survival is much lower at 17-37 %. If disease is not diagnosed before stage IV, where metastases have spread to peripheral sites around the body, survival falls to 12-25 % (Holschneider and Berek, 2000).

Most patients require a combination of surgery and chemotherapy. An initial surgical operation to investigate the stage of the disease is common to allow accurate staging of the disease. Surgery is carried out to remove the ovaries and visible tumour mass in the peritoneum is also often removed (cytoreduction or debulking). Work by Eisenkop et al. revealed a 62 month median survival of 139 patients with advanced ovarian cancer following removal of all visible tumour (Eisenkop et al., 1997).

The prognosis of disease is worse once cancer cells have escaped from the ovary, are present in both ovaries, are well differentiated or have unusual numbers of chromosomes (aneuploidy) (Trope et al., 2000). The disease is also likely to relapse in older patients or if malignant cells are present in the ascites.

Radiotherapy is not suitable as a first line therapy as the tumour cells are well dispersed around the abdomen by the time of diagnosis. Evidence that radiotherapy is useful for consolidating treatment following chemotherapy (Petit et al., 2006, Sorbe, 2003) or for salvage therapy following chemotherapy (Morton and Thomas, 1996) is not conclusive.

Intravenous cisplatin or carboplatin is a popular choice for treating ovarian cancer, often with paclitaxel (section 1.4.4).

1.4 Cisplatin

1.4.1 Properties of Cisplatin

The cell growth inhibiting effects of platinum complexes were discovered by Rosenberg et al. in 1964. Active platinum salts were accidentally created in a cell culture experiment by electrolysis of a platinum electrode (Rosenberg et al., 1965). The most active compound, *cis*-dichlorodiammine platinum (II) which came to be known as cisplatin, was shown to reduce animal tumour mass. Cisplatin is a deep yellow powder when solid. It is slightly soluble in water with a limit of solubility in the range 1.0-2.4 mg ml^{-1} depending on temperature (de Kroon et al., 2005, Burger et al., 2002). The diffusivity of cisplatin in water has been estimated as 6×10^{-6} cm^2 s^{-1} (Saltzman and Radomsky, 1991). Cisplatin is poorly lipophilic; its lipophilicity parameter, $\log P_{oct}$, is -2.3±0.05 (Hall et al., 2004). After development and trials Food and Drug Administration approval was granted in 1978 under the name Platinol.

1.4.2 Pharmacokinetics of Cisplatin

Cisplatin is usually administered by intravenous infusion (section 1.4.4). For determining cisplatin pharmacokinetics, acid digestion of samples is used to break down biological molecules present. The platinum concentration is then determined without interference from the sample matrix. This technique has good sensitivity for determining low platinum concentrations. In this way the pharmacokinetics of cisplatin can be calculated from the total cisplatin concentration.

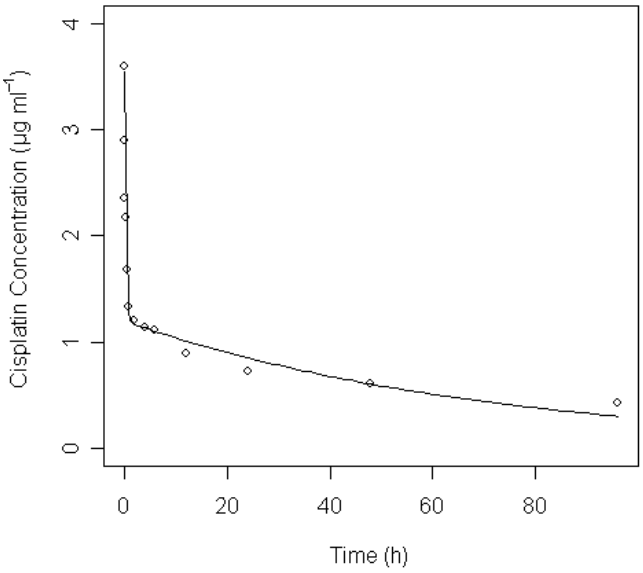

Figure 3: Mean plasma cisplatin concentration following cisplatin infusion.
Infusion duration 15 min. Data from Erlichman et al., 1987.

Figure 3 shows typical cisplatin pharmacokinetics following a single bolus infusion of cisplatin over 15 min (Erlichman et al., 1987). Following cisplatin administration the drug becomes dispersed in the blood and quickly reaches equilibrium with well perfused tissues such as the lungs and liver. The drug is then distributed through the rest of the body (except the brain which is kept separate by the blood-brain barrier). This is modelled as transfer of drug into the peripheral compartment. The peripheral compartment represents fatty tissues and other tissues which have a poor blood supply. The distribution into these tissues takes longer to reach equilibrium. Drug molecules enter the peripheral compartment at a concentration determined by the partition coefficient of the drug in that tissue when the concentration of drug is high in the blood. Drug in the peripheral compartment will slowly diffuse back into the blood as the drug is eliminated from the central compartment. This causes the blood plasma concentration of total cisplatin falls in a biphasic manner.

Two (Korst et al., 1998) and three compartment (Erlichman et al., 1987) models have been used for describing cisplatin pharmacokinetics. The two compartment model is an adequate model for the behaviour of total plasma cisplatin. This model requires two assumptions; firstly, that the body can be treated as the two separate

well perfused and poorly perfused compartments. Secondly, that drug is only transported between the compartments and eliminated as a diffusion-limited first order process with no active transport. These assumptions are acceptable as long as the model produces useful, predictive results.

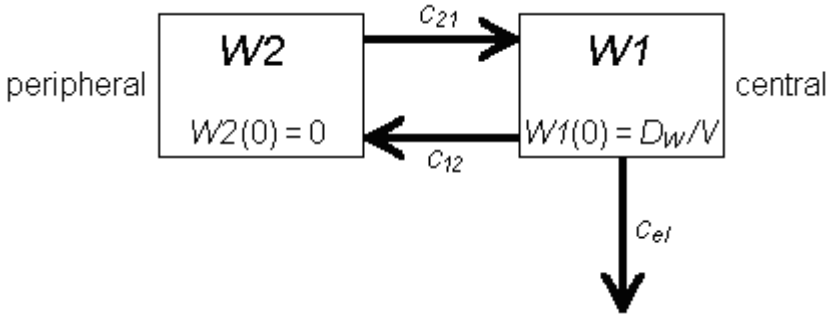

Figure 4: Pharmacokinetic model of total cisplatin in the body following intravenous injection.

A bolus of cisplatin, D_W is injected into the central compartment with volume V. The concentration in the central compartment, $W1$, is determined by the rates of transport of cisplatin, c_{12}, c_{21} and c_{el}, into and out of that compartment.

Figure 4 shows a two compartment pharmacokinetic model where an initial dose, D_W, is injected into the blood of a patient, becoming rapidly mixed throughout the whole volume, V, of the central compartment. The concentration of cisplatin in the central compartment, $W1$, is determined by the rate of transfer into, c_{12}, and out of, c_{21}, the peripheral compartment, the concentration of cisplatin in the peripheral compartment, $W2$, and the rate constant for elimination, c_{el}. The elimination rate constant comprises of drug elimination by the kidneys and removal of the drug from the circulation by reactions with drug targets or other metabolism.

$$\frac{dW1}{dt} = c_{21}W2 - c_{12}W1 - c_{el}W1 \quad \textbf{(1)}$$

$$\frac{dW2}{dt} = c_{12}W1 - c_{21}W2 \quad \textbf{(2)}$$

Rate equations (equations 1 and 2) can be determined for this two compartment model (Figure 4). From the rate equations the predicted concentration of cisplatin in

the central compartment (which includes the blood), equation 3, can be derived (Appendix B).

$$W1 = A_W \exp(-\alpha_W \cdot t) + B_W \exp(-\beta_W \cdot t) \quad \textbf{(3)}$$

The concentration of drug in the blood can be predicted from equation 3 if the empirical constants A_W, B_W, α_W, and β_W are known. Assuming the two compartment model shown in Figure 4, the transport constants, c_{12}, c_{21} and c_{el}, can be linked to A_W and B_W.

For many drugs the two compartment model is a good tool for predicting drug exposure. Such drugs reversibly bind to plasma proteins and are released from binding, maintaining a constant unbound:bound ratio as unbound drug is cleared. Cisplatin binding to proteins is effectively irreversible. Although the amount of cisplatin present in the blood decreases relatively slowly with a half-life of 58-96 h (Sweetman, 2004) this does not represent the total amount of cisplatin available for cancer cell killing. The total cisplatin plasma concentration includes unbound and protein-bound cisplatin.

Cisplatin in aqueous solution undergoes a reversible ligand exchange of a chloride ion for water. The forward reaction is described as aquation. A potent charged electrophile is formed. The aquated cisplatin species readily form DNA-platinum adducts. These adducts are thought to be the major mechanism of toxicity to cancer cells (section 1.4.3). However, aquated cisplatin species will also form adducts with other nucleophiles in the blood and in cells. When the chloride concentration is high (>50 mM), the equilibrium is towards uncharged cisplatin (Cheung et al., 1987, Wenclawiak and Wollmann, 1996). As the concentration of chlorine is 84-122 mM in blood, the concentration of aquated cisplatin is low. However, the equilibrium is displaced towards aquation by the removal of aquated cisplatin. Aquated cisplatin binds to plasma nucleophiles, shifting the equilibrium. There is no significant dissociation following binding (Sullivan and Krieger, 1992).

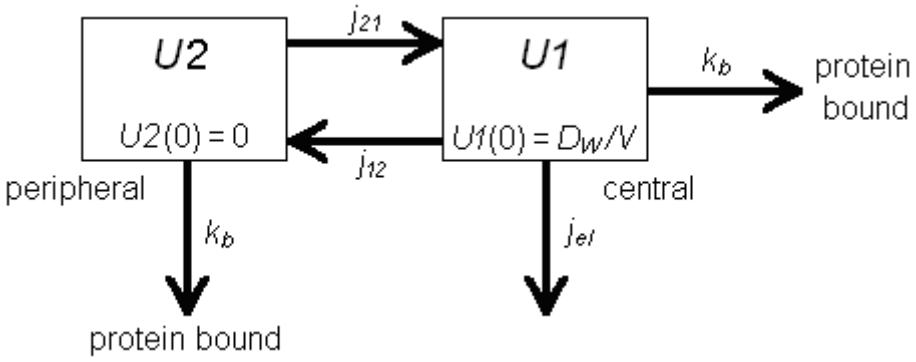

Figure 5: Pharmacokinetic model of unbound cisplatin in the body following intravenous injection incorporating protein binding.

A bolus of cisplatin, D_W is injected into the aqueous compartment with volume V. The concentration of unbound cisplatin in the central compartment, $U1(t)$, is determined by the rates of transport of cisplatin, j_{12}, j_{21} and j_{el}, and k_b into and out of that compartment. In addition, clearance of unbound cisplatin occurs in the peripheral compartment, $U2$.

Figure 5 shows a two compartment model treating protein binding as an additional source of elimination. In this model the concentration of unbound cisplatin in the plasma, $U1(t)$, is determined by k_b and j_{el}. In addition, cisplatin is also cleared by protein binding from the peripheral compartment. Ovarian cancer occurs in the ovaries and peritoneum which is well perfused with blood and can be modelled as part of the central compartment. Alternatively, the peritoneum can be modelled as a separate compartment (section 1.6.3).

The model for $U1$ has the same form as equation 3 but the parameters incorporate the protein binding constant, k_b. The disadvantage of this model is that because $\alpha_W \beta_W$ depends on four constants, the values of the parameters cannot easily be determined. In addition, this model does not take into account protein binding of cisplatin in the peripheral compartment. Increasing the number of compartments may improve the physiological description of the model but may not improve the usefulness of the model. It is important to consider that the amount of toxicity to the tumour may not correspond to the exposure to total cisplatin, but instead, the exposure to unbound cisplatin (section 1.4.3). Unbound cisplatin has a half-life of 1.3 h (Urien and Lokiec, 2004).

1.4.3 Intracellular Action of Cisplatin

Cisplatin is thought to enter cells by a combination of passive diffusion and facilitated diffusion (Kartalou and Essigmann, 2001). Passive diffusion of cisplatin across the cell membrane is likely to be slower than for other small molecules due to the slightly polar nature of the molecule (Kelland, 2007). The polarity is caused by the small positive charge on the ammonia the small negative charge on the chlorine group. In addition, the hydrogen bonds between the ligands and the water molecules of the hydration shell will also reduce the rate of diffusion across the cell membrane. Dissolved cisplatin undergoes a ligand exchange reaction, called aquation, where a chloride ion is replaced with a water molecule (Figure 6). This exchange creates a positively charged ion called aquated cisplatin. Aquated cisplatin is unable to cross cell membranes since lipid membranes are a good barrier to ions. CTR1 (copper-transporting membrane protein 1) is the main protein responsible for delivering copper into cells (Lee et al., 2001). Mounting evidence suggests that copper transporters, such as CTR1 and chaperones mediate cisplatin uptake (Ishida et al., 2002). High intracellular concentrations of copper cause ATP7A (copper-transporting P-type ATPase 7A) to be delivered to the surface membrane, causing copper efflux (La Fontaine and Mercer, 2007). It has been shown that increased expression of ATP7A corresponds with tumour resistance (Samimi et al., 2003). This evidence suggests that cisplatin is transported into and out of the cell via the copper homeostasis machinery.

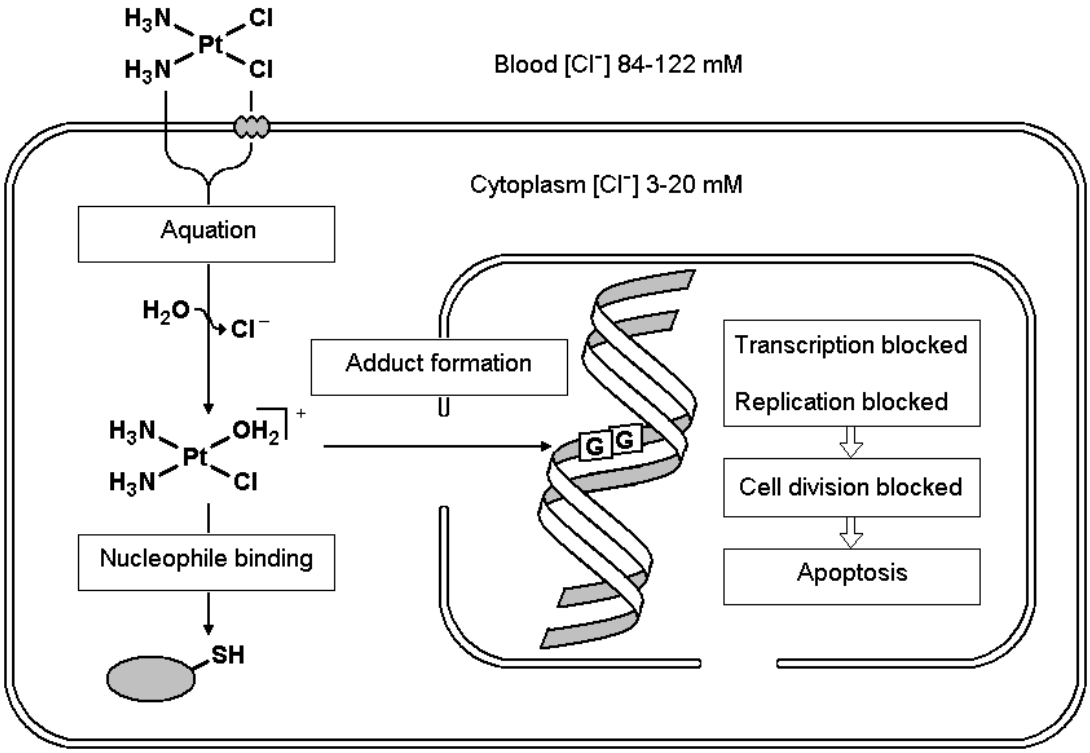

Figure 6: Mechanism of cisplatin tumour toxicity.

Cisplatin enters the cell by facilitated and passive diffusion where it is rapidly hydrolysed (aquation) to form a strongly electrophilic charged species. If aquated cisplatin is not removed by binding to proteins it selectively binds guanine residues in the DNA. Blockade of DNA and RNA polymerase causes the cell to enter programmed cell death (Kartalou and Essigmann, 2001, Kelland, 2007).

The physiological chloride concentration in blood plasma is ~100 mM. The presence of nucleophiles in blood will increase the rate of aquation by removing the charged species from solution. Nonetheless, cisplatin remains relatively stable in extracellular matrices due to the excess chloride ions present (Sweetman, 2004). Once cisplatin has entered the cell the lower chloride level (~4 mM) means that the equilibrium is shifted towards aquation (Figure 6). Cisplatin hydrolysis therefore occurs at a faster rate inside cells (Reedijk, 2003). A potent electrophile is formed in the cell at 8×10^{-5} s^{-1} (Knox et al., 1986, Wenclawiak and Wollmann, 1996). Aquation of the platinum group creates the highly reactive electrophile that will attack surrounding nucleophiles such as sulphydryl groups in proteins or nitrogen donor atoms on nucleic acids, especially guanine.

Cisplatin is able to form two covalent cross-links in the DNA strands. *In vitro* studies show that 90 % of DNA-cisplatin adducts are between adjacent guanine residues or between guanine-adenine (Eastman, 1986). It is likely that the mono-aquated platinum binds the DNA and the cross-link occurs subsequently (Eastman, 1986). Intra-strand cross-links are thought to be major disrupting lesions. Guanine-guanine cross-links have been shown to cause kinks in a DNA strand (Takahara et al., 1996). Morphological changes to DNA will disrupt interactions between DNA and the nuclear machinery. High levels of DNA damage cause replicating cells to enter the apoptosis pathway rather than division (Kartalou and Essigmann, 2001). It is thought that DNA-cisplatin adducts cause cell division to become blocked in G2 before the start of mitosis (Sorenson, 1990). Cells which do not enter mitosis within a few days enter apoptosis and die.

This gross DNA damage can be very effective at cell killing and can completely kill tumours. Cisplatin/etoposide/bleomycin combination therapy for testicular cancer achieves cure rates of between 80 % (Einhorn, 2002) and 95 % (Kartalou and Essigmann, 2001). This cure rate is so high because testicular cancer is hypersensitive to cisplatin. Testicular tumour cells exhibit low XPA (xeroderma pigmentosum, complementation group A) protein concentration. This causes low ERCC1—XPF (excision repair cross complementing 1—xeroderma pigmentosum, complementation group F complex) levels (Kelland, 2007) which means that nucleotide excision repair (NER) is defective and the adducts cannot be removed. The accumulation of damage triggers apoptosis. For other tumours, such as ovarian cancer, which are not repair-defective the cure rate is much lower.

Severe dose-limiting toxicities include hearing loss (ototoxicity), damage to the kidneys (nephrotoxicity) and epithelium of the gastrointestinal tract (mucositis), and immunosuppression. In addition nausea and vomiting can be so bad in the first month of therapy that patients sometimes consider withdrawing from treatment. The cost of anti-emetics alone can be more than the chemotherapeutics. Patients may also experience hair loss.

Cisplatin is thought to kill cells by trapping cells in G2 of cell division. This is achieved through the formation of DNA-cisplatin adducts. This would suggest that

cisplatin toxicity should be restricted to dividing cells. However, there is evidence that systemic toxicity is not solely due to DNA-cisplatin adducts. Additional mechanisms of toxicity in non-dividing cells have been proposed.

When aquated cisplatin reacts with glutathione, the conjugate can be metabolised to toxic thiols. Investigations into nephrotoxicity in kidney samples suggest that the production of thiols is involved in cisplatin-induced kidney damage. Townsend et al., 2003 inhibited the enzymes which metabolise cisplatin-glutathione adducts to unstable reactive thiols in kidney proximal tubule cells. This halved toxicity to the cells (Townsend et al., 2003). This suggests that the metabolites may be more toxic than cisplatin to systemic, non-dividing cells and be the primary cause of nephrotoxicity. Patients' are protected from severe nephrotoxicity during intravenous cisplatin therapy by being kept well hydrated before and during treatment (Hayes et al., 1977).

It has also been proposed that the platinum group directly catalyses the production of free radicals. Cisplatin induced ototoxicity (hearing loss) may be caused by production of reactive oxygen species. Electron paramagnetic resonance detects the spins on free radicals. This technique has been used to show direct evidence of free radical formation by cisplatin in the presence of cochlear material (Clerici et al., 1996).

The main mechanism of cisplatin toxicity is cisplatin-DNA adduct formation. Mitosis is prevented in dividing cells which triggers apoptosis. Alternative pathways may be a significant source of toxicity, causing cell death in healthy non-dividing cells.

1.4.4 Cancer Treatment with Cisplatin

Cisplatin is a successful therapeutic that has improved survival for many patients with lung, neck, head, testicular and ovarian cancers. Cisplatin chemotherapy improved the complete cure rate for testicular cancer from 5-10 % with original therapy to at least 80 % today (Einhorn, 2002).

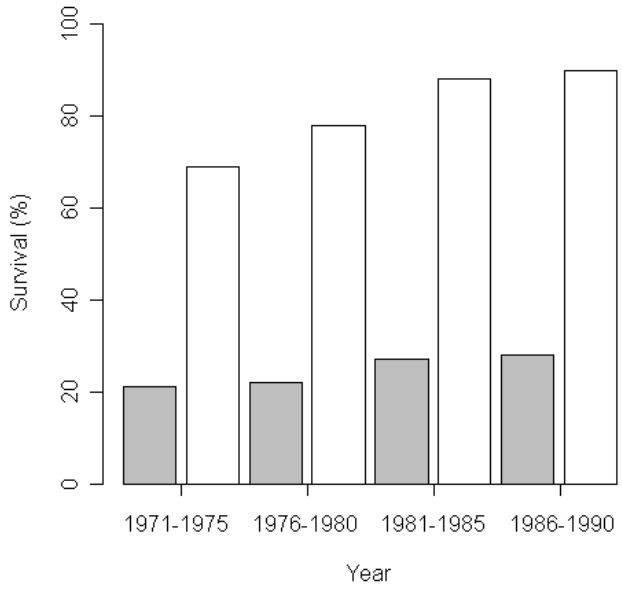

Figure 7: Five year survival for ovarian and testicular cancer patients since 1971. Percentage of patients with ovarian (grey bars) and testicular cancer (white bars) in the UK who survived for five years following diagnosis during the 1970s and 1980s (Office for National Statistics, 1995).

Cisplatin is also used to treat ovarian cancer with significant but less impressive results than for testicular cancer (Figure 7). The addition of cisplatin to cyclophosphamide-doxorubicin therapy increased the proportion of patients that showed a partial or complete response to therapy from 48 % to 76 % (Omura et al., 1986).

A typical course of cisplatin consists of at least six cycles of cisplatin solution, a dose of 75 mg m^{-2} which is typically ~120 mg per patient. This is administered intravenously at 1.0 mg ml^{-1} in saline solution with hydration before and after delivery. This saline solution has a high chloride concentration to keep the cisplatin in the inactive form for as long as possible during delivery. Dose is reduced in patients with low kidney function (a glomerular filtration rate of less than 55 ml min^{-1}). This dose is administered every 21 days as long as the tumour shows response (Graham and Falk, 2005). Hydration with up to two litres of fluid before treatment and infusion with excess fluid containing an osmotic diuretic such as mannitol diminishes the extent of the kidney damage (Sweetman, 2004).

1.4.5 Failure of Cisplatin Treatment

Relapses following treatment are due to tumour resistance to cisplatin. If the tumour is not completely destroyed by the first treatment then mutations may appear which confer resistance against cisplatin toxicity making further treatment ineffective. Further cisplatin treatment has reduced effectiveness. There is no standard treatment and prognosis is poor. Some resistant cell lines have been shown to be able to tolerate fifty times more platinum-DNA adducts. Failure of therapy can occur by a number of mechanisms before and after toxic platinum-DNA adducts have been formed.

Before binding has occurred cisplatin availability can be modulated by the tumour. Cisplatin is a polar molecule which enters cells slowly. Uptake is influenced by sodium and potassium ion concentrations, pH, presence of reducing agents and transporters.

The amount of cisplatin entering and leaving the cell are strongly influenced by the copper homeostasis machinery (section 1.4.1). Loss of the copper transporter, CTR1 by tumour cells increases resistance to cisplatin. CTR1 negative cells have low accumulation of cisplatin. Tumour cell populations treated with cisplatin undergo a reduction in CTR1 levels (Kelland, 2007). In addition, an increase of the copper efflux transporter ATP7A increases resistance of tumour cells to cisplatin.

Some resistant cell lines remove platinum-DNA adducts four times faster than sensitive cells (Eastman and Schulte, 1988). In addition, treated populations show increased glutathione which sequesters cisplatin before it can bind to the DNA. This conjugate can be transported out of the cell by the ATP-dependent glutathione S-conjugate export pump (Kartalou and Essigmann, 2001).

Following binding, the efficacy of the adducts in causing cell death can be reduced by a number of pathways. DNA repair and removal of adducts or tolerance to adducts increases tumour resistance. Nucleotide excision repair (NER) removes incorrect or damaged nucleotides. Evidence for this mechanism can be seen in cell lines where increased NER coincides with increased cisplatin resistance (Kelland,

2007). ERCC1-XPF is the protein complex that makes the incision for this pathway. Small inhibiting RNA for ERCC1 increases sensitivity of tumour cells to cisplatin (Kelland, 2007).

1.5 Reducing Cisplatin Toxicity

1.5.1 Cisplatin Analogues

The rate of release of reactive platinum can be changed by changing the ligand to reduce the rate of aquation to form the active species. The analogues carboplatin and oxaliplatin are successful chemical alternatives to cisplatin that have higher lethal concentrations for 50 % of patients (LC_{50}s), but which require higher concentrations to reach an equivalent effective dose.

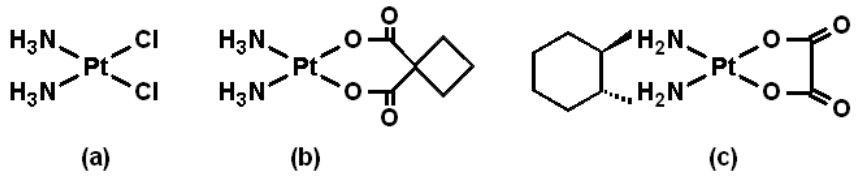

Figure 8: (a) Cisplatin and its analogues, (b) Carboplatin and (c) Oxaliplatin.

The dose limiting toxicity for carboplatin is immune suppression. For oxaliplatin it is damage to the peripheral nerves which connect the central nervous system with the rest of the body (peripheral neuropathy), possibly due to blockade of sodium channels in sensory neurons (Wilson et al., 2002).

Cisplatin rapidly becomes aquated by a substitution of a chloride ion for water with a rate constant of 8×10^{-4} s^{-1} at 37°C (Wenclawiak and Wollmann, 1996). Carboplatin aquation has a rate constant of the order of 10^{-6} s^{-1} (Knox et al., 1986). The differences in rate of DNA adduct formation of cisplatin and carboplatin are similar orders of magnitude to the differences in aquation rates, suggesting that aquation is rate limiting. The bidentate cyclobutanedicarboxylato group of carboplatin hydrolyses at a rate of 10^{-5} s^{-1} after adduct formation. This is faster than before DNA binding and correlates with the rate of interstrand adduct formation of DNA bound carboplatin. The slower rate of aquation of carboplatin means that there is less irreversible binding of carboplatin to plasma components.

Although carboplatin may exhibit less severe toxicities, prolonged exposure may lead to allergy-like reactions. In a study by Markman et al., 1999, episodes of hypersensitivity to carboplatin were found to be rare in patients who have received fewer than six courses of carboplatin with no episodes occurring among 205 patients at risk. Hypersensitivity was more frequent in patients who had more than six courses with 22 episodes among 83 patients at risk (Markman et al., 1999). This increase in risk of hypersensitivity with repeated exposure suggests that carboplatin may not be suitable for sustained release for extended periods. Cisplatin hypersensitivity reactions are believed to occur but at a rate of 1-5 % patients when administered alone (Von Hoff et al., 1979, Zweizig et al., 1994).

In a study of 417 patients given cisplatin or carboplatin alongside cyclophosphamide (section 1.3.2) no significant differences in response (57 % and 59 %) and median survival (100 weeks and 110 weeks) were found (Swenerton et al., 1992). The main finding from such trials are that carboplatin exhibits more acceptable toxicities than cisplatin (Alberts et al., 1992) rather than significant improvement of response for either drug.

Oxaliplatin, *trans*-cyclohexane-1,3-diamineoxalato platinum (II), is a tetravalent platinum compound. Oxaliplatin also hydrolyses slower than cisplatin with a rate constant of the order of 10^{-6} s^{-1} at 25°C (Gao et al., 2003). Some experimental tumours which are resistant to the divalent cisplatin and carboplatin are not resistant to oxaliplatin. This may be due to the bulky diaminocyclohexane ring remaining following adduct formation. Resistance to platinum adducts can be due to repair of the DNA strand or bypass of the damaged site by the replication machinery. The incorporation of the larger blockade may reduce access of repair and replication proteins by steric hindrance. As nephrotoxicity is low, hydration is not required with oxaliplatin treatment. Around 15-18 % of patients show allergic reactions to oxaliplatin; allergies can develop from first exposure but symptoms tend to be mild (Fu et al., 2006).

The development of cisplatin analogues continues with many promising candidates entering late phase trials. Satraplatin may shortly be approved for treatment of

hormone-refractory prostate cancer. Picoplatin is a promising candidate for treating small-cell lung cancer.

1.5.2 Regional Delivery

Chemotherapy drugs are extremely toxic (section 1.3.2) and typically have narrow therapeutic windows. Intravenous injection is systemic, exposing the whole body to the chemotherapeutic agent during treatment. Regional drug delivery aims to create high drug concentrations at the tumour site and lower concentrations throughout the rest of the body than by intravenous injection. Drugs with high ratios of toxicity to efficacy are described as having high therapeutic indices. Regional delivery increases the therapeutic index of a drug by increasing the dose that can be safely delivered while reducing the toxicity to the rest of the body. A high therapeutic index is important because there is variability in the reaction of each patient to a certain dose of drug. A safe dose for one patient could be fatal for another. Patients are less likely to suffer extreme side effects if there is a wide margin of safety.

Ovarian cancer is difficult to diagnose in the early stages and is normally diagnosed by the symptoms of stage III of the disease, especially ascites. By this stage a tumour plaque has formed a coating on the surface of the diaphragm and omentum and is effectively impossible to remove by surgery. Soluble anti-tumour drugs have a low residence time in the peritoneum. Much work has been focussed on attempting to increase the retention of chemotherapeutics in the peritoneum, potentially increasing efficacy and reducing side-effects. Intraperitoneal (IP) therapy is an attractive method for treating ovarian cancer. A catheter is passed directly into the peritoneal cavity and aqueous cisplatin delivered in a large volume (generally two litres) of saline.

Injecting cisplatin into the peritoneal cavity of rats produced IP cisplatin concentrations ten to twenty times higher than serum levels. However, cisplatin only penetrated 1-2 mm into tumour nodules despite the improved exposure (Los et al., 1990). This suggests that IP delivery is only suitable for patients who have had debulking surgery to remove the majority of the tumour nodules. Prolonging exposure of drug to the peritoneum may allow progressive penetration into tumour nodules as the tumour progressively dies back.

Ovarian cancer spreads through the lymphatic and venous systems in addition to the peritoneum (Burghardt et al., 1991). Chemotherapy targeting solely the peritoneum may be insufficient for treating the disease.

There have been eight clinical trials investigating the effect of IP cisplatin as a first line therapy. Clinical trials accept patients with diseases at a range of stages of progression and treat them with differing treatments. Even if the selection criteria for the study are very strict, there is still great variability in survival times of patients following diagnosis. These factors mean that detecting a real change in overall survival using an alternative treatment requires a large number of patients to reliably determine the distributions of survival of the two groups. Many trials do not have enough patients do detect differences in survival that could not be attributed to chance. These trials do not have sufficient statistical power to make rigorous assessments of the treatment of interest. The most statistically sound way to determine the affect of a treatment is perform a meta-analysis on the aggregated the results of every relevant randomised trial. By examining the survival of a very large number of patients from many studies significant differences can be identified, if present. There have been eight studies including intraperitoneal platinum agents as a first line therapy:

- Alberts et al., 1996 found that intravenous (IV) cyclophosphamide or with IV or IP cisplatin chemotherapy showed prolonged median survival. Abdominal pain was worse for IP patients but other side effects such as low white blood cell count and tinnitus were reduced under IP therapy (Alberts et al., 1996).
- Armstrong et al., 2006 compared IV paclitaxel and IV cisplatin with IV paclitaxel followed by IP cisplatin and IP paclitaxel. IP therapy improved survival although the dosing schedules and toxicities were higher (Armstrong et al., 2006).
- Gadducci et al., 2000 compared epidoxorubicin and cyclophosphamide with IV or IP cisplatin. IP therapy showed a slight but not significant improvement in survival (Gadducci et al., 2000).

- Kirmani et al., 1995 compared both cisplatin and cyclophosphamide delivered by IV or IP infusion. No significant differences were found between the groups (Kirmani et al., 1995).
- Markman et al., 2001 compared IV cisplatin and paclitaxel with IV carboplatin, IP cisplatin and paclitaxel. IP cisplatin improved progression free survival but bone marrow suppression was more severe (Markman et al., 2001).
- Polyzos et al., 1999 compared IV cyclophosphamide combined with either IV or IP carboplatin. Differences in survival between the groups were not significant (Polyzos et al., 1999).
- Yen et al., 2001 compared IV cyclophosphamide plus adriamycin or epirubicin with or without an additional dose of IP cisplatin. Differences in survival between the groups were not significant (Yen et al., 2001).
- Zylberberg et al., 1986 compared a multidrug cocktail of adriamycin, fluorouracil, bleomycin, vincaleublastin, ifosfamide and cisplatin delivered either entirely IV or in part IP. Results were not significant due to low patient numbers (Zylberberg et al., 1986).

A meta-analysis of the eight studies investigating intraperitoneal cisplatin or carboplatin as an addition to standard treatment following surgery has shown an improvement in survival (Jaaback and Johnson, 2006). Hazard ratio is a metric for comparing two treatments. To identify if a new regime of chemotherapy increases the survival for one group of patients compared to another, the median survival of the standard treatment group is divided by the median survival of the trial group. A ratio of significantly less than one suggests an improvement in treatment. If the ratio is one then there is no improvement using the trial regime. If the ratio is greater than one then the trial regime is more toxic than any improvement due to treatment effects.

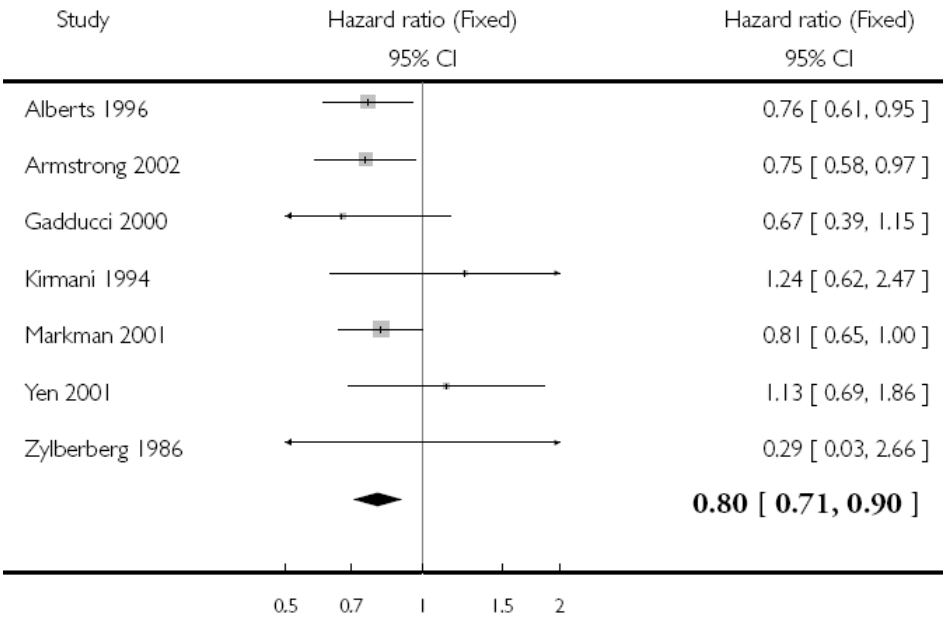

Figure 9: Meta-analysis of the effect of intraperitoneal (IP) cisplatin on time to death of ovarian cancer patients.

Hazard ratio of chemotherapy with and without IP cisplatin is 0.8, favouring IP delivery. Grey boxes show relative weights of trials. From Jaaback and Johnson, 2006.

Figure 9 shows the hazard ratios of chemotherapy with or without IP platinum therapy. The combined hazard ratio is 0.8 (95 % confidence intervals 0.7-0.9) in favour of IP cisplatin. This means that including IP cisplatin in chemotherapy for ovarian cancer prolongs survival for some patients.

A theoretical advantage of cisplatin for IP therapy over analogues such as carboplatin is its low molecular mass. During IP therapy transfer of cisplatin into the tumour is diffusion limited. This is because the drug is delivered directly to the site of action so does not need to be transported to the site of action. The tumour nodules are bathed with chemotherapeutic rather than being delivered through the bloodstream. The inverse relationship between diffusion and solute mass has been confirmed using rat models in which ten-fold concentrations of carboplatin were required to reach an equivalent penetration to cisplatin (Los et al., 1991). In addition, the increased stability of carboplatin may allow sufficient time for the peritoneal and serum concentrations to reach equilibrium before any advantage of peritoneal administration is able to occur.

1.5.3 Prolonged Delivery

Prolonged drug delivery over hours, days or weeks may offer improvement in efficacy of disease treatment with a reduction of side effects. Prolonged delivery of doxorubicin, for example, has been shown to cause less heart failure at high cumulative doses (450 mg m^{-2}) compared to bolus delivery for breast carcinoma patients (Hortobagyi et al., 1988).

There are several strategies for prolonged delivery of drugs. The most widely used is intravenous (IV) catheter. A catheter feeds to a major blood vessel and drugs are passed into the bloodstream by injection into an external port such as a Hickman line or a subcutaneous port such as BardPort®. The main reason for failure of treatment by this route is either infection of the implant (section 1.7.1) or blockage of the catheter line. Prolonged delivery may be achieved using daily low doses or continuous infusion. Daily doses offer less fluctuation in patient drug plasma concentration than less frequent bolus injections but there will still be variability. Continuous infusion can be used to achieve stable drug plasma concentrations but requires connection to an external pump. This requires hospitalisation for the duration of delivery which carries associated costs and may be distressing for the patient.

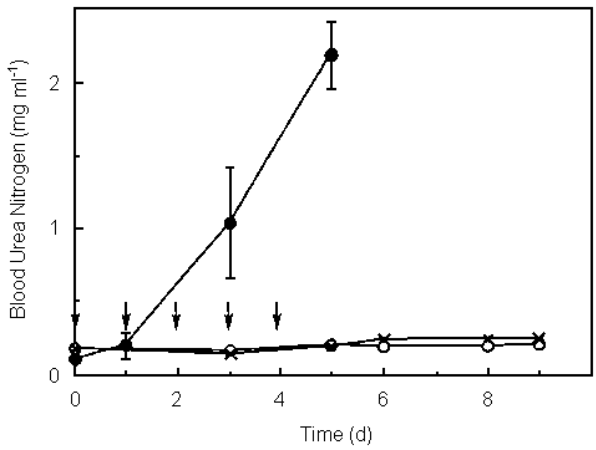

Figure 10: The effect of cisplatin on blood urea nitrogen.

Blood urea nitrogen is an indicator of renal impairment. Dose administered by single (●) or intermittent (at arrows) bolus (o) injection. Control was intermittent bolus of 0.9 % saline solution (x). Adapted from Nagai and Ogata, 1997.

Tests of dosing schedules in a rat model showed a negation of severe nephrotoxicity using doses administered over four days rather than a single bolus injection (Figure 10). This was achieved despite having an equivalent exposure to the drug by comparison of areas under the concentration against time curves (Nagai and Ogata, 1997).

Tumour response to drugs may be cell cycle dependent. The major mechanism of cisplatin toxicity depends on blockading cells in the G2 phase of the cell cycle (section 1.4.3). By maintaining high concentrations of cisplatin for prolonged periods of time, a larger proportion of the population of tumour cells will be exposed at the relevant part of the cells cycle. Cisplatin which has not become protein bound is the critical concentration to be maintained (section 1.4.2). Since protein binding is effectively not in equilibrium for cisplatin, unlike for other drugs, it is important that prolonged delivery is able to maintain therapeutic unbound cisplatin levels.

In a pilot clinical study Chen et al., 1990 administered cisplatin at 10 mg m^{-2} day^{-1} over 14 days with anthracycline antibiotic, aclarubicin. Diuretics were not used. The mean plasma level of unbound cisplatin was $0.4\text{-}1.3\times10^{-6}$ mg ml^{-1} during infusion compared to a total platinum concentration of 0.2-1.2 mg ml^{-1} (Chen et al., 1990). Following the end of infusion the level of unbound platinum dropped significantly over the following 12 hours while the total platinum did not decrease appreciably. This study suggests that unbound cisplatin concentrations can be maintained during prolonged drug delivery.

These studies suggest that prolonged delivery of cisplatin may offer reduced toxicity compared to IV delivery of a single bolus. Prolonged release can also be achieved by sustained release from a drug depot (section 1.5.4). Sustained release of cisplatin from implantable microspheres or fibres offers the reduced toxicity of prolonged delivery. In addition, the risks associated with resident catheters and costs of extended hospitalization are avoided.

1.5.4 Depot Formulation

1.5.4.1 Polymers for Drug Delivery

Both continuous infusion and regional delivery of cisplatin can be shown to be advantageous; these advantages can be exploited by formulating the drug with a polymer excipient for slow release therapy. A solid depot system can be injected directly to the site of action, the peritoneum, to which the drug will be released over the course of several weeks. As there will be no resident catheter the risk of infection is far lower than by intravenous infusion. The depot contains the entire dose for the treatment cycle minimising the number of health personnel interventions required for treatment.

Choice of polymer is important in depot design. Besides having very low toxicity, interactions of the drug with the polymer matrix must also be understood. The properties of both polymer and drug determine whether it will remain active upon formulation and at what rate it will be released under physiological conditions. The profile of release should match the required regime of the treatment. An ideal candidate for drug delivery would have low toxicity during its entire life cycle in the patient. Real world considerations mean that the entire process of manufacture must be affordable to patients and provide a good rate of return to investors.

Drug release from the depot will occur by diffusion from the matrix. The matrix must become wetted to allow the drug to become solubilised. Wetting will occur as water penetrates the depot. Differences in dynamics of the hydration front influences drug release (Jamzad et al., 2005). Matrix degradation may also be required to increase the permeability of the matrix. Pores in the polymer will further complicate rates of drug release.

As the diffusivity of the drug in the polymer affects the rate of diffusion controlled release, the choice of polymer will determine release kinetics. To the author's knowledge, diffusivity of cisplatin has not been reported for any polymer matrices. Polymer selection has been based on empirical observations of release. The diffusivity will also change with time as the polymer degrades. Diffusion of small molecules occurs at a higher rate in lower molecular mass polymer matrices

(Braunecker et al., 2004). This is because glass transition temperature of a polymer is usually higher when the molecular mass is higher. The closer the environmental temperature is to the glass transition temperature, the higher the long-range mobility of the polymer chains. Lower molecular mass polymer chains will be more mobile than higher molecular mass polymer chains at a fixed temperature. More mobile polymer chains will allow faster diffusion of small molecules in that matrix. Other factors such as the size and shape of the polymer device, the rate of polymer hydrolysis, and the physiological conditions to which the device is exposed will have an effect on the rate of release.

Concerted efforts have been made to exploit biodegradable polymers as slow release delivery devices for a range of proteins, peptides and other pharmaceuticals. These systems have advantages and disadvantages; a delivery system which is excellent for one pharmaceutical may be of no value for another. Polymers of interest are generally preferred to already be commonly used for some medical purpose. Dextrin is used clinically in dialysis solutions. A dextrin-doxorubicin conjugate with a drug loading of 8-12 % by weight degraded by enzymes in the plasma over seven days releasing oligosaccharide conjugated doxorubicin species (Hreczuk-Hirst et al., 2001). The breakdown products of this polymer are non-toxic and non-enzymatic degradation is very low so the formulation is stable. Conjugating sugars to cisplatin however is likely to be difficult, expensive and reduce drug efficacy.

Cisplatin has been encapsulated in liposomes with the aim of either triggering drug release at the tumour site, or anticipating direct fusion of the liposomes with tumour cells. Iga et al., 1991 fabricated cisplatin liposomes with a drug loading of 13 %. Using an implanted heater to disrupt the liposomes, they demonstrated targeted release in a mouse model (Iga et al., 1991). Elevated internal temperatures are painful for patients and the technique was not developed further. An improved method of liposome fabrication yielded nanocapsules with a drug loading as high as 49 % by weight (Burger et al., 2002). At 37°C drug was released more rapidly than from typical polyester microsphere formulations. The first order release constant (section 1.6.2) of these liposomes has been calculated here to be approximately 3×10^{-5} s^{-1}, higher than the release constant of four published microsphere formulations (section 1.5.4.5) analysed in section 3.4.1. These capsules were more

toxic to cancer cells *in vitro* than drug in solution, possibly due to direct delivery of cisplatin into the cells by liposome-cell fusion. A possible drawback of liposome formulation could be preferential uptake of these submicron particles by phagocytic immune cells, potentially leading to higher immunosuppression than standard cisplatin chemotherapy.

Responsive drug release systems have been investigated, in which the drug is released in the presence of a stimulus such as pH, temperature change, or electric field strength. Unfortunately these polymers are frequently toxic and do not degrade in the patient so must be left in place or surgically removed (Jeong et al., 1997). Responsive polymers are not especially advantageous for treating ovarian cancer where a constant release of cisplatin is required rather than release at a rate relating to an additional parameter.

Some attempts have been made to prolong the time that the drug depot remains in circulation in the blood. Colloidal poly(ethylene glycol)-poly(aspartic acid) copolymer micelles containing 39 % by weight cisplatin showed prolonged blood residence. These submicron particles (28 nm) did not appear to be preferentially taken up by the spleen but accumulated in liver tissue at three times the concentration of the tumour (Nishiyama et al., 2003). Pegylation has also been used to reduce detection of liposomes by the immune system (Newman et al., 1999) but suffered from leaching of polyethylene glycol before complete release.

Lactic acid and glycolic acid polymers and copolymers have a number of characteristics making them suitable for depot delivery (section 1.5.4.2) and have investigated as a promising excipient for cisplatin (section 1.5.4.5). Rational improvements to drug release profiles from polymer depots can be made using mathematical models (section 1.6).

1.5.4.2 Poly(lactide-co-glycolide)

Poly(lactide-co-glycolide) (PLGA) is an aliphatic, biocompatible polyester. It hydrolyses in water to produce lactic acid and glycolic acid which may be metabolised by the body or excreted. Lactic acid has a chiral centre which has some influence on the physical properties of its polymers (and the chemical properties of

its degradation properties). When the polymer is manufactured from at or close to 100 % glycolic acid or enantiomerically pure lactic acid, the polymer may demonstrate semi-crystalline character. For other lactide:glycolide ratios the random sequence of backbone prevents regular, crystalline structures from forming. Similarly, a racemic mixture of D- and L-lactic acid will introduce sufficient disorder into the polymer chain that semi-crystalline behaviour will not be observed. PLGA is generally manufactured from the racemic mixture of D- and L-lactic acid. PLGA is therefore usually an amorphous solid at room and physiological temperatures. By using PLGA with intermediate lactide:glycolide ratios there is a reduction in the risk of crystalline regions forming during the processing or degradation of the devices, thus reducing the risk of device fracture.

There are a number of routes for PLGA polymerisation. The most common method of manufacture is under high pressure using stannous octoate as a catalyst. Glycolic acid is very reactive and so may form side products during PLGA synthesis. The molecular mass and composition of the chains determine the physical properties of the polymer. Lactic and glycolic acid polymers can also be blended to increase the range of properties available.

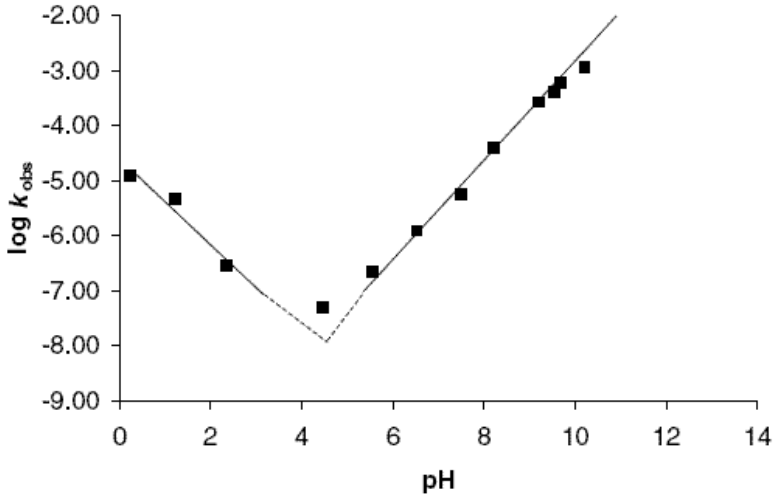

Figure 11: Log observed degradation rate against pH of lactic acid oligomers (de Jong et al., 2001).

Experiments with immobilised PLA oligomers showed acid catalysed ester hydrolysis below pH 4 and base catalysed hydrolysis above pH 4 (de Jong et al., 2001). This is suggested by the change of end terminal hydrolysis with pH shown in

Figure 11 with a typical observed rate of hydrolysis of 10^{-7}-10^{-6} s^{-1}. This range of degradation rate is in accord with observations that microspheres made from PLGA 50:50 with molecular mass 21 kDa degrade at a rate of 5×10^{-7} s^{-1} (Tracy et al., 1999).

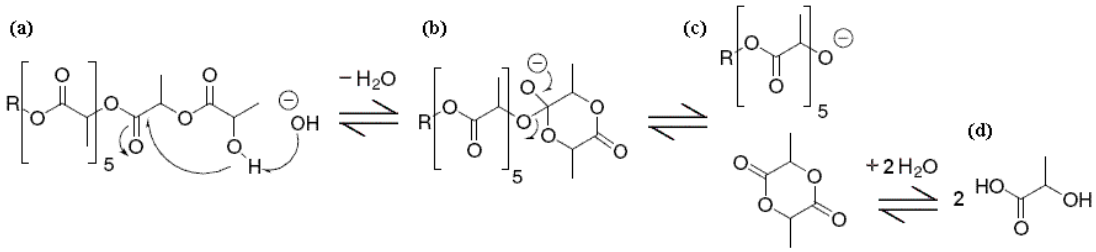

Figure 12: Proposed mechanism of base catalysed ester hydrolysis (de Jong et al., 2001).

The proposed mechanism for base catalysed ester hydrolysis is shown in Figure 12. The nucleophilic hydroxyl end group attacks the second carbonyl leading to the formation of a six-membered ring as an intermediate (b). A base interacting with the hydroxyl end group increases the nucleophilicity of the oxygen atom, catalysing the reaction (de Jong et al., 2001). Lactide rapidly hydrolyses to lactic acid in water. This model may be relevant at physiological pH as the number of end groups increases. It should be noted that glycolide does not have the steric hindrance of the additional methyl group and so PLGA chains may also undergo standard ester hydrolysis at these residues.

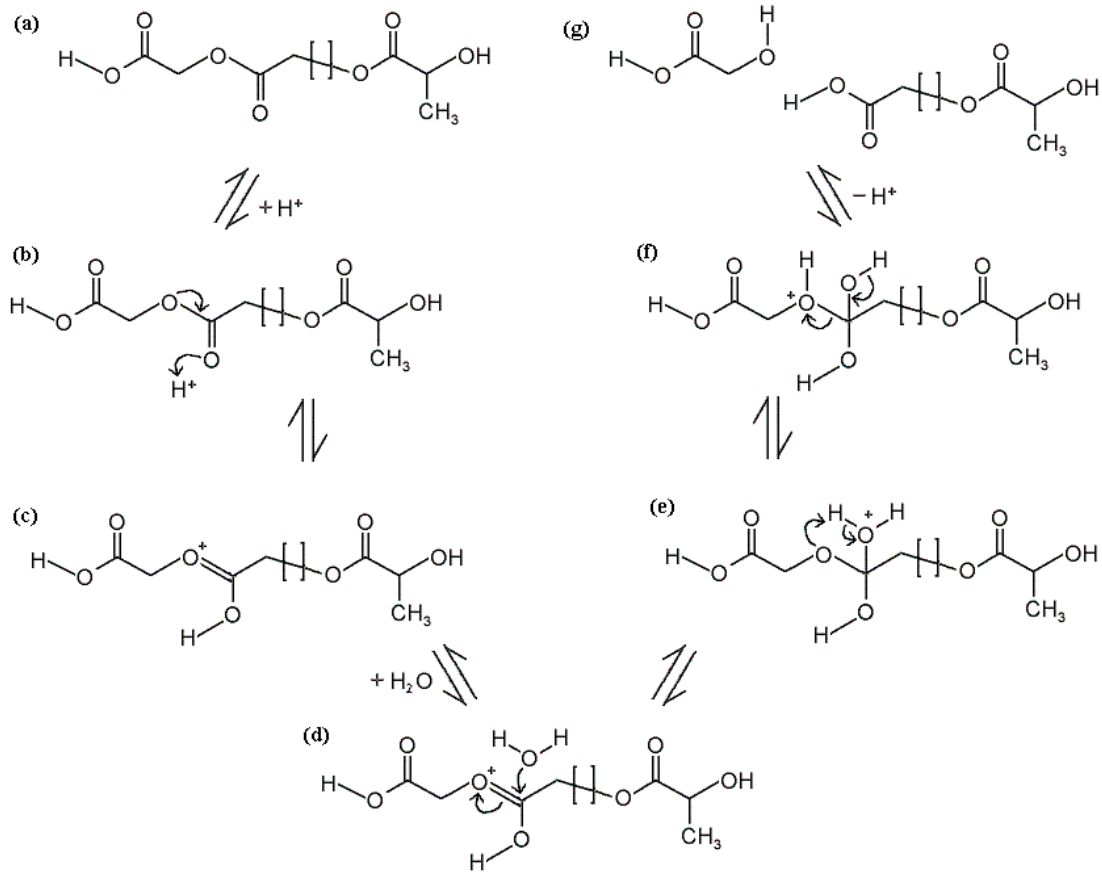

Figure 13: Reaction scheme showing acid catalysed hydrolysis of PLGA.
Brackets represent continuation of polymer chain.

Figure 13 shows acid catalysed hydrolysis of an ester bond of a PLGA chain (a) based on the text-book model of ester hydrolysis. Hydrolysis is initiated by protonation of the carbonyl; this increases its electrophilicity (c). This facilitates nucleophilic attack by water (d). A proton is transferred to generate a good leaving group (e). The equilibrium is driven towards ester hydrolysis when water is in excess. Ester hydrolysis can occur at any point along the polymer chain resulting in PLGA chains and oligomers of varying length.

Hydrolysis will continue, releasing lactic and glycolic acid monomers for metabolism. D-lactic acid is the biologically preferred isomer and is rapidly metabolised (at a rate of 950 mg kg^{-1} h^{-1} in rats without increasing blood lactate) and although L-lactate is poorly metabolised it is rapidly excreted (Cori and Cori, 1929). As the structures degrade fragments of the microspheres may be cleared by phagocytes.

Lactide and glycolide polymers have been in use in medicine since the 1960s as biodegradable sutures (Cutright et al., 1971). They have also been used for orthopaedic applications. Bone fracture fixing pins hold damaged bone in place and allow the bone to bear increasing load as it is repaired and the pin subsequently dissolves (Muggli et al., 1999). Interference screws are used during reconstructive anterior cruciate ligament surgery to secure the graft in the femur and tibia. PLA interference screws have allowed successful repair without need for second surgery (Bach et al., 2002). Suture anchors are used to fix sutures firmly in place during reattachment of soft tissue to bone. Biodegradable sutures have similar strength to metal anchors but do not need to be removed (Warme et al., 1999). An additional advantage of polymer orthopaedic implants over metal implants is that they do not prevent magnetic resonance imaging of the repair site. PGA and PLGA have also been used as tissue scaffolds for smooth muscle cells (Kim et al., 1999) and bone marrow stromal cells (Kim et al., 2005). Biodegradable polyesters have also been used extensively for drug delivery systems (section 1.5.4.4) which have also been shown to be biocompatible (Anderson and Shive, 1997).

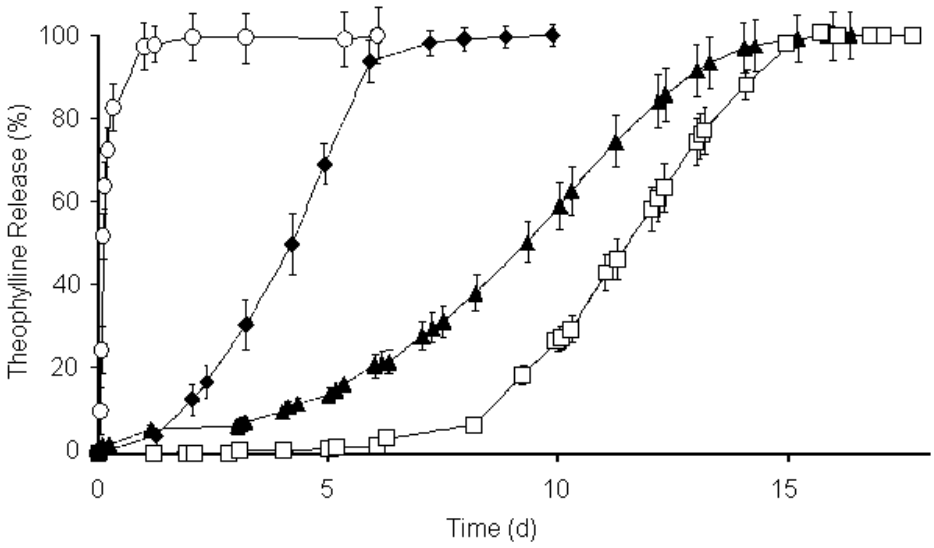

Figure 14: Drug release profiles of theophylline from PGA.
PGA had molecular weights of 6 kDa (o), 13 kDa (●), 24 kDa (▲) and 36 kDa (□). Adapted from Braunecker et al. 2004.

Figure 14 shows release of theophylline from PGA pellets with a range of molecular weights. Drug release was faster from PGA pellets with lower molecular weight (Braunecker et al., 2004). For systems in which the scale of drug release corresponds

to the scale of polymer degradation the release profile may be adjusted by rational selection of polymer excipient with an appropriate molecular weight. By controlling how the polyester is deposited, well defined structures can be formed (such as microspheres or hollow fibres) which release drugs at a predictable rate.

Properties of Ideal Polymer for Drug Delivery	Properties of PLGA for delivering cisplatin
Non-Toxic	✓ Non-toxic
Not antigenic or inflammatory	✓ Negligible
Readily excreted, non-toxic metabolites	✓ Metabolised or excreted
High drug loading to minimise excipient	✓ Moderate (10 %)
Formulation simple	✓ Optimisation ongoing
Financial viability	✓ Excipient currently on market

Table 2: Table comparing the ideal properties of polymers for drug delivery and the properties of PLGA for delivering cisplatin.

Table 2 summarises the suitability of PLGA as a slow release excipient for cisplatin. As well as being a safe polymer it is also possible to develop the system by controlling the lactide:glycolide ratio, molecular mass and device structure, allowing a tailored delivery profile.

1.5.4.3 PLGA Microspheres

PLGA microspheres have been fabricated by a range of routes (Watts et al., 1990), commonly by dissolving the polymer in an organic solvent, creating an oil phase. Oil and water mixtures will disperse spontaneously, forming an emulsion of droplets less than one micrometre in diameter if the interfacial tension is reduced to zero by an emulsifying agent. Most PLGA microspheres have been manufactured by agitation of an oil in water suspension where the interfacial tension is greater than zero. PLGA microsphere formation occurs in two stages. The first is the suspension step. Initially a dope of polymer dissolved in an organic solvent is dispersed in an aqueous medium (or continuous phase) using a mechanical homogeniser (Niwa et al., 1993, Araki et al., 1999, Tamura et al., 2002, Huo et al., 2005, Matsumoto et al., 2005) or ultrasonication (Ishihara et al., 2005). A suspending agent, such as poly(vinyl

alcohol) (PVA), is used to lower the interfacial tension between the oil and water. The dope is immiscible with the aqueous medium so an oil in water suspension is formed. Mixing must be continuous to maintain the suspension. The suspension step can also be carried out using an immiscible oil instead of water as the continuous phase (Ike et al., 1992, Fujiyama et al., 2003). A potential hazard of oil in oil suspension is that more toxic contaminants are present in place of water. This additional oil must be carefully removed from the final formulation. Water-soluble molecules have been incorporated in microspheres by a double emulsion step of water in oil followed by oil in water (Okada, 1997).

The second step is extraction of the polymer solvent leaving spherical droplets of polymer. A high concentration of solvent plasticizes the polymer, decreasing the glass transition temperature of the polymer. The lower the glass transition temperature of the polymer, the more the polymer chains move at the temperature of manufacture. Initially, the solvent is able to rapidly diffuse out of the oil phase into the aqueous phase. As more solvent is extracted, the oil phase becomes a progressively poorer solvent the polymer chain becomes less extended in solution (Artursson et al., 1990), interacting more with other PLGA chains and the glass transition temperature increases. As the glass transition temperature increases, the polymer chains move less, reducing the diffusivity of the solvent in the oil phase. This decreases the rate at which the solvent is extracted. The outer layer of the droplet solidifies first, leaving a molten centre. Depending on how long the droplet is exposed to water the droplets of polymer may completely harden as the remaining solvent dissolves away or retain a viscous liquid centre. Evaporation of the solvent from the reaction vessel allows additional hardening of the microspheres (although this will be reduced for solvents with higher boiling points). This reverse-phase (or oil in water) technique gives a normal distribution of micrometre-scale spheres (microspheres) rather than haphazard structures formed by uncontrolled precipitation.

All factors which effect the destabilization processes of the solvent/polymer suspension and interactions between the oil and aqueous phases will influence particle formation. Creaming or sedimentation are destabilization effects which are determined by the difference between the density of the solvent and the continuous

phase, the radius of the droplets, and the viscosity of the mixture. Particles may aggregate, increasing the destabilization of the suspended droplets, even if they do not coalesce due to their hard surfaces. The solubility of the solvent in the continuous phase and the volatility of the solvent will determine the rate of diffusion of the solvent into the continuous phase by altering the concentration gradient microsphere formation and so the size and porosity of the particles. The choice of continuous phase, solvent, polymer, suspending agent, drugs and any other additives will alter the electrical charge on the surface of the suspended droplets (or Zeta potential) which will alter the behaviour of the suspension. In addition, factors such as method and degree of agitation of the emulsion, , ratio of polymer to solvent, ratio of solvent to external phase, temperature of all phases, humidity, dimensions of the mixing vessel and so on will have some effect on the nature of the microspheres formed.

Water (with suspending agent such as polyvinyl alcohol) is preferred as a suitable continuous phase due to its low cost and lack of toxicity.

Dichloromethane (DCM) is a solvent of PLGA commonly used for microsphere manufacture. It has a low boiling point of 40°C (Appendix A) which means that most of the solvent will be removed during the solvent evaporation step in microsphere production. DCM is a class 2 solvent according to the International Conference on Harmonisation which means that the concentration should be limited to 600 ppm (ICH Q3C (R3), 2005).

Replacing DCM in microspheres should lead to less chance of toxicity due to accidental high levels resulting from a fault during manufacture. PLGA nanospheres have been made using a mixture of acetone and methanol as the PLGA solvent (Kawashima et al., 1998).

Ethyl acetate is a suitable replacement solvent for microsphere production. The solubility of ethyl acetate in water is 8.4 g in 100 g water at 20°C(Altshuller and Everson, 1953). Destabilization process that increase the tendency of a suspension to separate. Differences in density can cause creaming or sedimentation of the oil phase. For example, DCM has a density of 1.3 g cm^{-3} (Appendix A), suggesting that

sedimentation effects may be partially responsible for destabilizing the suspension of DCM in water. The density of ethyl acetate is close to that of water, reducing the destabilizing effect on the suspension. The most appealing attribute of ethyl acetate is low toxicity. Ethyl acetate is a class 3 solvent as it is less toxic with an LD_{50} three times higher than that of DCM (Appendix A). Ethyl acetate concentration should be minimised by good manufacturing practice but is less hazardous for medical applications than DCM. This improved safety rating makes it better to take to the clinic and so is preferred for manufacture of microspheres.

1.5.4.4 Market Approved PLGA Microspheres

A number of PLGA implantable microsphere formulations are currently in clinical use. Decapeptyl SR® (licensed as Trelstar Depot® in the US) is a PLGA microsphere formulation licensed by the British regulatory body (the Medicines and Healthcare products Regulatory Agency) in January 2002. PLGA technology was developed by Debio R.P., Switzerland and is manufactured by a solvent-free method. The active ingredient is triptorelin acetate, a gonadotropin-releasing hormone (GnRH) analogue at 2 % drug loading. Lupron Depot® is an equivalent PLA matrix, administered as a subcutaneous or intramuscular injection, which releases leuprolide, another GnRH analogue at 10 % drug loading for treating prostate cancer (Okada, 1997, TAP Pharmaceutical Products Inc., 2003).

The mechanism of action is the same for both products. At higher than normal concentrations these GnRH agonists suppress rather than stimulate sex hormone (such as testosterone and oestrogen) production by desensitising the pituitary gland. The resulting reduction of testosterone reduces stimulation of prostate cancer tumour cells. Similarly, inhibiting oestrogen release ends stimulation of endometriosis or painful fibroids in the uterus. Decapeptyl SR® may also be administered to delay early onset (precocious) puberty. Both Decapeptyl SR® and Lupron Depot® are available in formulations that release for one or three months.

Leuprolide is a relatively large molecule (molecular mass 1209.4 g mol^{-1}). The molecular mass of the PLA used for Lupron Depot® is low (15 kDa) but the hydrophobicity of PLA acts to control the drug release. These two factors allow sustained release of the drug for up to three months. Polyesters are especially well

suited to hormone delivery as the agents are active at low concentrations and the mechanism of action is required over prolonged periods.

Risperdal Consta® is a PLGA microsphere formulation of risperidone for intramuscular injection. Risperidone is a common antipsychotic for treating schizophrenia. It is a receptor antagonist with an inhibitory constant in the nanomolar range for four key neurotransmitter receptors, although the precise mechanism of action is uncertain. This formulation consists of PLGA 75:25 and has 38 % drug loading (Janssen Pharmaceutical Products Inc., 2006). Risperidone is released following initial polymer degradation between weeks three and eight following injection. Risperdal Consta® is useful clinically as it increases patient compliance while providing a useful dosing schedule and can extend the period over which treatment is effective.

Although risperidone is a relatively small molecule (molecular mass 410.5 g mol^{-1}) the release is controlled by the high lactide:glycolide ratio and high molecular mass (90 kDa) of the PLGA used in the formulation.

The success of these formulations suggests that there would be acceptance of a similar formulation of cisplatin microspheres by physicians and patients. It also suggests that microspheres are financially viable provided that they offer advantages over alternative therapies.

1.5.4.5 Cisplatin Microspheres

Injecting cisplatin microspheres directly into the peritoneum has advantages over IV delivery of particles. IP microspheres would have lower exposure to phagocytic cells in the liver and spleen. Formulation of cisplatin into microspheres also changes the rate of platinum delivery. Rather than IV infusion over a few hours, cisplatin can be released over days. A depot of drug in microspheres can produce high drug exposure at the treatment site. In addition, the maximum plasma concentration of drug is reduced. No external access is required once the microspheres have been injected.

Ike et al., 1992 made PLA microspheres with 4 % cisplatin loading. This formulation released 85 % of the cisplatin after one day. They also found that larger beads (2 mm

diameter) released cisplatin more slowly and this rate was dependent on the polydispersity of the molecular mass of the PLA (Ike et al., 1992).

Araki et al., 1999 produced PLA-albumin cisplatin microcapsules with a cisplatin loading of 8.5 %. The formulations produced were less toxic and less effective than an equivalent dose of cisplatin as a solution (Araki et al., 1999). This observation could be explained by assuming that a proportion of the cisplatin dose became inactivated by binding to albumin in the formulation. Reduced toxicity of the albumin and cisplatin containing formulation supports the hypothesis that unbound cisplatin is the active species for tumour cell killing (section 1.4.3).

Hagiwara et al., 1993 prepared cisplatin loaded PLA microspheres by an oil in oil emulsion method with a loading of 9 %. Release profile of the formulation was 40-50 % burst release followed by 20-30 % slow release of cisplatin over the following three weeks (release profiles not shown). These microspheres had an LD_{50} almost twice as high as cisplatin solution in mice. The microspheres were used to treat a mouse model of ovarian cancer which had a mean survival time of 21±5 days if left untreated. Comparing cisplatin solution at 2.5 mg kg^{-1} to cisplatin microspheres at 5 mg kg^{-1} survival was increased from 28±7 to 35±10 days (Hagiwara et al., 1993a). These doses correspond to 19 % and 21 % of the LD_{50} respectively.

These microspheres were then used in a pilot study of 13 patients with malignant ascites resulting from gastric, colon or pancreatic cancer. Cancer cells were cleared or reduced in 12 of the patients but there was negligible improvement in survival time due to a lack of treatment for other tumours distributed around the body (Hagiwara et al., 1993b). These results suggest that this approach is not suitable as a sole method of treatment for gastric, colon or pancreatic cancer. For these diseases the tumour cells are not entirely contained within the peritoneal cavity. For ovarian cancer however, many patients will only have small tumour nodules (<0.5 mm diameter) which will largely be confined to the peritoneal cavity. Subsequent preparations by the same group were reported as cisplatin PLGA 75:25 microspheres by oil in oil emulsion with a drug loading of 3 %. There was a 21 % burst release and 95 % release over two weeks (Fujiyama et al., 2003).

Kumagai et al., 1996 prepared cisplatin PLGA microspheres with a drug loading of 5 % (release profiles not shown). When implanted into rats the microspheres had an LD_{50} which was four times higher than cisplatin solution. The microspheres were used to treat a rat model of ovarian cancer; untreated rats had a mean survival time of 9±3 days. The LD_{50} of cisplatin solution for the rats was 14 mg kg^{-1} and 53 mg kg^{-1} for cisplatin microspheres. Comparing cisplatin solution at 2.4 mg kg^{-1} (the equivalent of a clinical dose) with a dose of 9.6 mg kg^{-1} cisplatin in microspheres survival of rats was increased from 48±23 to 74±18 days. This is a valid comparison as these doses correspond to 17 % and 18 % of the LD_{50} of solution and microsphere formulation respectively (Kumagai et al., 1996).

Tamura et al., 2002 compared cisplatin distribution following injection with IP cisplatin solution and IP or subcutaneous PLA microspheres containing 5 % cisplatin. As expected the peak concentration of cisplatin was much higher following cisplatin treatment than microsphere treatment (Tamura et al., 2002).

Huo, et al., 2005 made PLGA 75:25 microspheres of 5-30 μm by solvent evaporation of DCM in PVA solution. These were injected into healthy rabbits. These microspheres were found to accumulate in the lung (Huo et al., 2005). By comparison with other cisplatin microsphere formulations it is likely that the claimed drug loading of 17 % is an overestimate. As only 70 % of the claimed total loading was released after 28 days with a negligible rate of release it is likely that the true drug loading was closer to 12 %.

Matsumoto, et al. 2005 made PLA and PLGA 50:50 microspheres by homogenisation of the polymer with DCM and cisplatin in PVA solution and solvent evaporation (Matsumoto et al., 2005).

Author	Polyester	Molecular Weight (kDa)	Dope Solvent	Continuous Phase
Ike, 1992	PLA	12	DMF	Castor Oil
Araki, 1999	PLA	20	DCM	PVA
Fujiyama, 2002	PLGA 75:25	17	DMF	Paraffin
Tamura, 2002	PLA	9 + 22	DCM	PVA
Huo, 2005	PLGA 75:25	20	"	"
Matsumoto, 2005	PLA/PLGA 50:50	20 + 20	"	"

Table 3: Polyester and solvents used for manufacture published cisplatin microspheres.

Table 3 summarises the polymer, dope solvent and continuous phase of published cisplatin microspheres. Cisplatin microspheres have been examined as a formulation for chemotherapy. Little effort has been made to rigorously characterize the release kinetics of such sustained release formulations. A brief analysis of these formulations may allow meaningful comparisons to be made. Other hurdles still to be overcome are the reproducibility of cisplatin release and scale-up of production and a demonstration that the formulation can provide a significant improvement in treatment over current standard therapy.

1.5.4.6 Microsphere Phagocytosis

Foreign bodies are detected by the immune system even if they do not elicit an immune response. Small particles such as polymer microspheres are well known to be cleared by phagocytes (Tabata and Ikada, 1988). Nanocapsules have been used to deliver drugs to treat pathogens which are resident within phagocytic cells and so hard to treat by conventional means. For example PLGA microspheres of 4 μm diameter have even been used to deliver drugs to phagocytic cells (Prior et al., 2002). PLGA microspheres as large as 10 μm have even been used as a medium for an experimental vaccine for cattle and was shown to be well phagocytosed by antigen presenting cells (O'Brien and Guidry, 1996). This means that PLGA microspheres below 10 μm could accentuate damage to the immune system compared to venous

administration. A PLGA delivery system should have released most of its drug load before becoming small enough to be phagocytosed.

Avgoustakis *et al.* introduced cisplatin PLGA-mPEG nanospheres (0.1-0.2 μm) into the bloodstream of model animals and demonstrated that a proportion of the particles appeared to be evading the immune system. These particles were designed to accumulate in solid tumours. Unfortunately, the drug loading was very low at just 0.1 % by weight. In addition the mPEG was shed faster than the PLGA particles degraded which may expose phagocytic cells to high doses of cisplatin (Avgoustakis et al., 2002).

1.5.4.7 Disadvantages of Depot Formulation

An important disadvantage of depot formulations is the difficulty of recovering the large quantity of drug implanted. Even if the general risk of poor response to a treatment is low the consequences of unexpected toxicity can be severe. Cisplatin causes major dose related toxicity including cumulative nephrotoxicity, immunosuppression, ototoxicity, nausea and vomiting. Under current dosing the kidney is protected by pre-treatment hydration and diuresis. Nephrotoxicity may be less severe under the lower peak cisplatin concentrations associated with slow release. Immunosuppression and ototoxicity increase with extended dosing schedules. In addition anaphylactic-like reactions have been reported (Brunton et al., 2005).

When the patient undergoes sudden side effects it may be clinically necessary to withdraw treatment. If a month's dose of drug has been administered then this may not be feasible. With microsphere formulations, it may be good practice to administer a standard IV solution dose of drug before committing to the treatment with a depot system. Alternatively implanted fibres have similar release profiles but can be more easily removed in case of adverse reactions to the therapy.

Another potential drawback that needs to be investigated is the effective bioavailability of drugs which are released slowly. Many drugs exhibit reversible binding to plasma proteins. Cisplatin is continually removed from solution by irreversible binding to nucleophiles in cells and in the plasma During slow release

concentrations will remain low and with a large portion of the active drug being sequestered by peritoneal fluid nucleophiles, the effective concentration may be further lowered.

1.5.4.8 PLGA Fibres

Rather than dispersing polymer in an organic solvent in an aqueous medium to create droplets, a stream of polymer can be extruded into the aqueous medium to create a continuous fibre of polymer. A dope of PLGA dissolved in NMP with powdered drug as a suspension can be extruded from a needle or spinneret (Perera and Tai, 2006) into a water bath. The NMP is extracted into the water leaving a coagulated PLGA fibre containing encapsulated drug.

For manufacturing fibres the solvent must be very soluble to allow a skin to rapidly form, creating the fibre structure. The most suitable solvent for manufacturing fibres is n-Methyl-2-Pyrrolidone (NMP) (Appendix A). This is a class 2 solvent meaning that the concentration should be controlled. Residual NMP should be maintained below 4840 ppm when used to manufacture polymer excipients (ICH Q3C (R3), 2005).

A spinneret is a spinning orifice with two concentric needles. Polymer dope is extruded through the outer orifice and water through the inner orifice. The polymer then enters the water bath as a continuous stream with solvent diffusing out of the nascent fibre into the water bath and the fibre bore.

Polyethersulphone (Wang et al., 1996, Qin and Chung, 1999) and polyimide (Wallace et al., 2006) hollow fibres have been used for gas or liquid separation. PLGA hollow fibres have been used for bone tissue engineering (Ellis and Chaudhuri, 2006) and as nerve tract guidance channels (Wen and Tresco, 2006). PLGA fibres have also been used as coronary stents (Tamai et al., 2000).

Solid or hollow polymer fibres may also be of interest for drug delivery. Depot morphology influences release behaviour. Fibres may exhibit improved drug release characteristics. A potential disadvantage of fibres is that they may cause pain to patients if implanted due to their larger size and are more difficult to administer since

they cannot be injected. An advantage of fibres over microspheres is that fibres can more easily be recovered from the patient in the event of severe adverse reactions to the drugs. Another advantage of fibres is that fibre extrusion may readily be adapted into a continuous process allowing scale-up, whereas microspheres must be made by a batch process.

1.6 Modelling Drug Release

1.6.1 Mathematical Models

Slow release drug delivery devices release their payload at a rate that is determined by the physical characteristics of the drug, matrix and solvent. Although many groups have shown interest in developing sustained release formulations for cisplatin release (full review in section 1.5.4.5), few have reported meaningful results of analysis of release kinetics. To allow comparisons between formulations, mathematical models can be fitted to drug release data. These fits are sometimes based on theory that allows general predictions to be made about the behaviour of the devices.

Mathematical models can increase understanding of physical systems. Empirical models make fewer assumptions but do not make predictions about the underlying process. Simple empirical models such as averages or straight lines are useful for generalising trends in a system. More complex empirical models may reduce the residual error (the total difference between the values predicted by the model and the data) but do not allow extrapolation of the data or improve understanding of the system.

A semi-mechanistic empirical model is an empirical model that can be usefully interpreted by relating the parameters to physical events. A rate constant only gives predictions under the experimental conditions in which it was deduced but does allow comparisons between formulations under the same conditions. If the experimental conditions are close to the conditions of interest (physiological conditions in the case of drug delivery) then useful predictions can be made.

Mechanistic models attempt to interpret data with physical significance. Calculating a diffusion coefficient can allow predictions of release profiles under conditions other than experimental conditions in which it was deduced. It should be noted that a mechanistic model is still a model. It may allow improved predictions to be made but it is not reality. A mechanistic model is only an interpretation of the system so predictions may differ from observations.

1.6.2 Semi-Empirical Models

First order models are used extensively for pharmacokinetic analysis. They are used for compartmental and non-compartmental analysis of patients during analysis of drug distribution, although the individual rates are usually treated as aggregated parameters (section 1.4.2). First order models are also appropriate for use as semi-empirical models for studying drug release from depots. When a solid matrix containing a water soluble drug is introduced into an aqueous environment the drug will leach into the aqueous phase. The more that drug leaves the matrix means that the amount remaining to subsequently be released is reduced. Diffusion of a concentrated analyte can be assumed to dissipate away from the concentrated region assuming a favourable or irreversible equilibrium. It can be assumed that the driving force for mass transfer is proportional to the difference between the outer surface concentration and the concentration of analyte in an analyte-rich region (Glueckauf and Coates, 1947). For drug release from a depot under sink conditions the rate of drug release will be determined by the concentration of drug in the depot and the constant representing the rate of release.

Rate equations are derived from simplified schematics of material transfer. The concentrations in each compartment, here depot and solution, can be derived by integrating the rate equations.

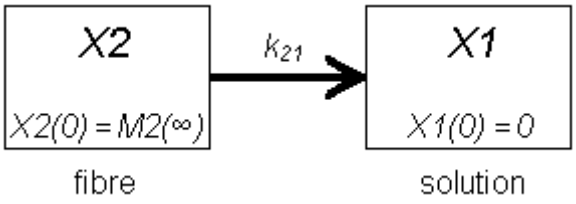

Figure 15: Two compartment drug release model.

X2 is the amount of drug remaining in the depot. This is released at a concentration dependent rate k_{21}. *X1* is the amount of drug which has been released from the depot into the surrounding solution.

Figure 15 shows the scheme of cisplatin release from a fibre (or microsphere), where *X1* is the amount released, $M2(\infty)$ is amount of cisplatin in the depot which will be released after a long time and k_{21} is the rate of the release process. Initially (at time = 0) all of the cisplatin, $M2(\infty)$, is in the fibre and none has been released into solution.

$$\frac{dX1}{dt} = k_{21} \cdot X2 \qquad \textbf{(4)}$$

After the fibre is implanted it releases drug at a rate determined by the release constant and the concentration of drug remaining in the fibre (equation 4). Integrating the equations for the two compartments (described in Appendix C) produces the first order equation that describes the amount of drug present in the volume of each compartment.

$$X1 = M2(\infty) \cdot \left(1 - e^{-k_{21}t}\right) \qquad \textbf{(5)}$$

$$X2 = M2(\infty) \cdot e^{-k_{21}t} \qquad \textbf{(6)}$$

This release scheme is described by equation 5 and the remaining drug in the depot is described by equation 6. A single exponential, also known as the linear driving force (LDF) model (Sircar and Hufton, 2000), is simple to implement and so is widely used (Messaritakia et al., 2005, Machida et al., 2000). First order kinetics can be used to model drug release from solid matrices. An exponential release curve should give parameters which are true for each formulation under the corresponding

experimental conditions. The release constant represents the fraction of drug remaining in the depot released after a unit of time. Rate of release is proportional to the release constant (equation 4). The release constant, k_{21}, can be used to compare how quickly drug is released from different formulations under the same conditions.

For some depot formulations the initial burst of drug release can occur to a greater extent than predicted by a single exponential. As the apparent rate of release changes the previous model is no longer appropriate. Such an effect could be caused by a skewed distribution of drug crystals towards the surface of the depot such that drug is released faster than would be expected for homogenous distribution of drug in the matrix. A second exponential term can be added to represent the readily released drug. Adding parameters should always reduce the residual error of the model; a more complex model cannot be justified unless the improvement in predicting power justifies the reduction in degrees of freedom.

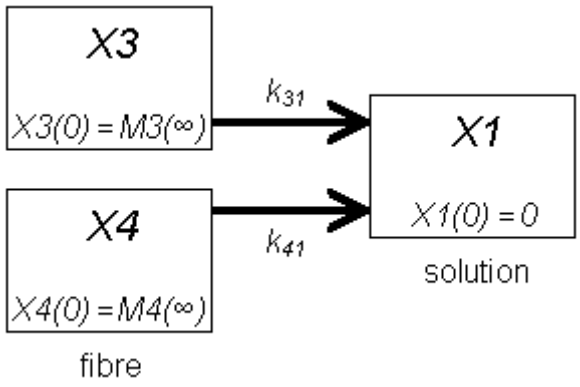

Figure 16: Three compartment model showing release of two pools of drug in the fibre into solution.

X3 and *X4* are the amounts of cisplatin remaining in the fast and slow compartments of the device respectively. This is released at concentration dependent rates k_{31} and k_{41}. *X1* is the amount of cisplatin which has been released from the depot into the surrounding solution.

Figure 16 shows the release scheme which in physical terms these represent a surface pool, $M3(\infty)$, of readily released cisplatin at rate k_{31} and a well dispersed pool, $M4(\infty)$, of slowly released cisplatin at a rate, k_{41}. The sum of drug in both pools $M3(\infty)$ and $M4(\infty)$ is the total drug loading.

$$X1 = \{M3(\infty) + M4(\infty)\} - M3(\infty) \cdot e^{-k_{31} \cdot t} - M4(\infty) \cdot e^{-k_{41} \cdot t} \quad \textbf{(7)}$$

The amount of drug released can be derived from the rate equations (Appendix C) to give the model shown in equation 7.

Empirical models are useful for describing release profiles. They are simple to implement and are robust to fit computationally. Their scope is limited to a quantitative understanding of the system. To attempt to examine the underlying physics of the systems mechanistic models are required. These are derived from Fick's laws of diffusion and are described in sections 1.6.4 and 1.6.5.

1.6.3 Cisplatin Release and Protein Binding

Many drugs exhibit reversible binding to plasma proteins. This is not a mechanism of drug clearance because as drug in the plasma is eliminated, the equilibrium of bound to unbound drug is displaced towards unbound. Most drugs are effectively entirely cleared from the central compartment. This is a good approximation of total drug fate as drugs are usually eliminated by renal filtration or liver metabolism. The kidneys and liver are active in the central compartment. Since the entire absorbed dose is eventually eliminated from the central compartment the area under the concentration-time curve is independent of the rate of drug release (section 1.4.2).

The peritoneum is usually considered as part of the central compartment. There is some evidence that concentrations of unbound cisplatin are higher in the peritoneum compared to the blood plasma during IP cisplatin release (Kumagai, et al., 1996).

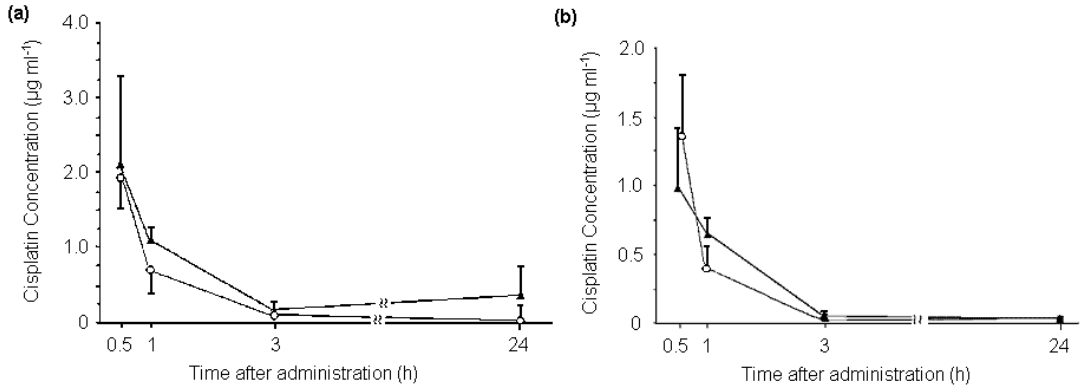

Figure 17: Concentration of unbound cisplatin in (a) peritoneum and (b) plasma.
Concentration of cisplatin measured following administration of cisplatin microspheres (▲) or cisplatin solution (o) (Kumagai et al., 1996).

Figure 17 shows the concentration of cisplatin in the peritoneal fluid and the blood plasma that had not become protein bound. Cisplatin was measured following release from 9.6 mg kg^{-1} IP microspheres or 2.4 mg kg^{-1} IP cisplatin solution. Concentration of unbound cisplatin was higher in (a) the peritoneum than (b) the plasma at equivalent times. At 24 h the concentration of cisplatin was higher in the peritoneum of rats treated with microspheres than in those treated with cisplatin solution. The concentration of cisplatin is higher in the peritoneum than in the plasma which may justify the use of an additional compartment to describe the pharmacokinetics of sustained, regional delivery of cisplatin to pharmacokinetic models such as Figure 5.

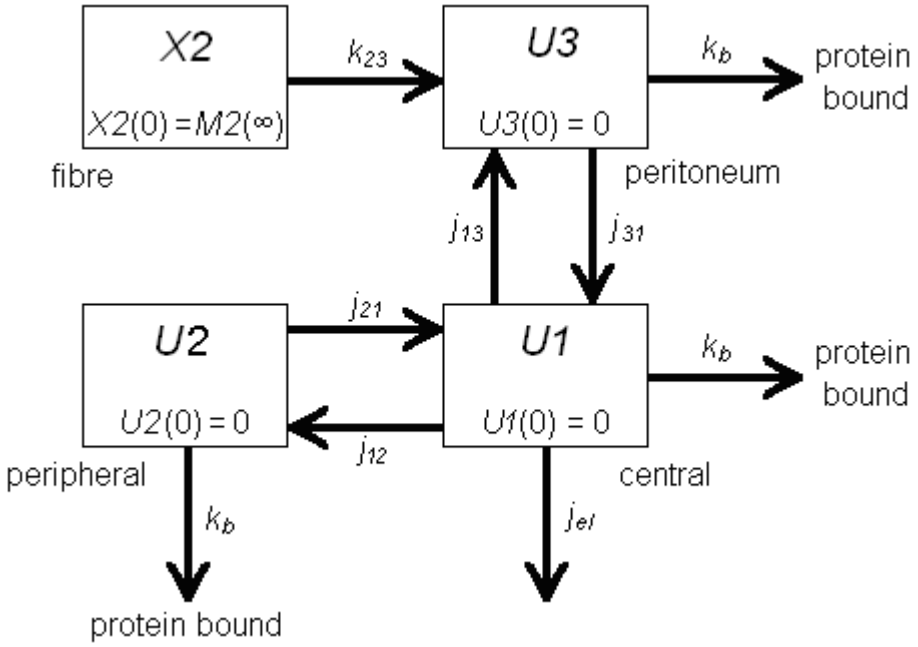

Figure 18: Four compartment model for release of cisplatin from a fibre.

A dose of cisplatin, *M2*(∞), is released from a fibre, *X2*, with a rate constant k_{23} into the peritoneum of a patient, *U3*. Cisplatin rapidly exchanges with the central compartment, *U1*, with rate constants j_{13} and j_{31} and becomes protein bound from central, peripheral and peritoneal compartments with rate constant k_b. There is distribution with the peripheral compartment, *U2* from the central compartment with rate constants j_{12} and j_{21}.

Figure 18 is an extension of Figure 5 incorporating a compartment for regional drug release (section 1.6.2) into the peritoneum and a compartment for sustained release (Figure 15) from an dose of drug, *M2*(∞), implanted microsphere or fibre depot. For this model, the rate of elimination of unbound cisplatin depends on the concentration of drug in the peripheral, peritoneal and central compartments, the protein binding constant, k_b, and the elimination constant of unbound cisplatin, j_{el}. The elimination constant j_{el} includes renal filtration and binding of cellular or other non-plasma components.

Regional delivery is able to increase the area under the concentration-time curve of that compartment to the drug relative to the central compartment, even if the overall residence time of the drug in the body is unchanged (Benet, 1985). Cisplatin becomes protein bound in the peritoneum as well as in the central and peripheral compartments. Unbound cisplatin concentration in the peritoneum can be measured experimentally if a patient has a catheter for ascites drainage. This may allow

correlations between plasma and peritoneal unbound cisplatin concentrations to be assessed. Therefore, the peritoneum is a valid compartment to incorporate into the pharmacokinetic model. The peritoneum has been treated as a separate compartment for carboplatin pharmacokinetics (Miyagi et al., 2005).

Since the cisplatin-protein binding constant, k_b, cannot be calculated from pharmacokinetic data (Appendix B), complex pharmacokinetic models such as Figure 18 could be solved by supplying fixed values for the model. For example, the determination of free cisplatin concentrations released from a fibre in the presence of protein would be useful for assessing the impact of protein binding in the performance of an IP cisplatin depot.

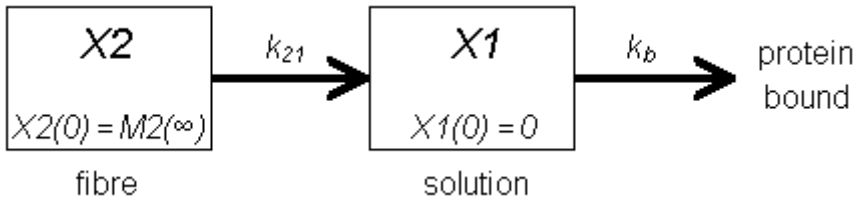

Figure 19: Two compartment model for cisplatin release and protein binding.
M2(∞) is the amount of cisplatin remaining in the fibre, *X2*, which is released at a concentration dependent rate with a rate constant k_{21}. *X1*(*t*) is the amount of cisplatin which has been released from the fibre but which is subsequently removed by binding to BSA with rate constant k_b. The unbound cisplatin in *X1* corresponds to unbound cisplatin to which the patient is exposed.

Rate equations for drug release from a depot such as a microsphere or fibre and protein binding following release can be derived from a two compartment model (Figure 19). The amount of drug remaining in the fibre decreases at a rate defined as k_{21}. The rate of drug removed from the system is defined by k_b. The predicted concentration in solution (equation 8) can be derived from these rate equations (Appendix D).

$$X1 = \frac{k_{21} M2(\infty)}{(k_b - k_{21})} \cdot \left(e^{-k_{21}t} - e^{-k_b t}\right) \qquad \textbf{(8)}$$

Initially the amount of cisplatin in the fibre, $X2$, is the drug loading, $M2(\infty)$, and there is no cisplatin in solution, $X1$. The concentration of cisplatin solution will initially increase as it is released from the depot. As the concentration of cisplatin increases, protein binding will occur faster. The concentration peaks when the amount of cisplatin being released equals the amount becoming bound. As the rate of drug release falls the concentration of cisplatin in solution will fall.

Equation 8 will be appropriate for determining the concentration of drug in solution if a two compartment model was sufficient for analysing drug release in water. If the release profile is more complicated and required three compartment model treatment then an equivalent three compartment profile may be more appropriate.

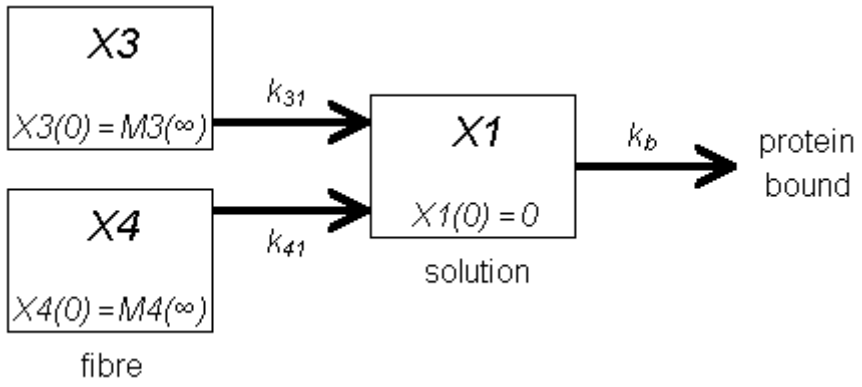

Figure 20: Three compartment model showing release of two pools of cisplatin from the fibre into solution and removal of cisplatin from solution by protein binding.
$M3(\infty)+M4(\infty)$ is the amount of cisplatin remaining in the fibre, $X3+X4$, which is released at a concentration dependent rate with a rate constants k_{31} and k_{41}. $X1(t)$ is the amount of cisplatin which has been released from the fibre but which is subsequently removed by binding to BSA with rate constant k_b. The unbound cisplatin in $X1$ corresponds to unbound cisplatin to which the patient is exposed.

From the rate equations of the three compartment model (Figure 20) the amount of cisplatin in solution in the presence of protein (equation 9) can also be derived (Appendix D).

$$X1 = \begin{pmatrix} \dfrac{k_{31} \cdot M3(\infty)(-k_b + k_{41}) + k_{41} \cdot M4(\infty)(-k_b + k_{31})}{(-k_b + k_{31})(-k_b + k_{41})} \cdot e^{-k_b t} \\ + \dfrac{k_{31} \cdot M3(\infty)}{(-k_{31} + k_b)} \cdot e^{-k_{31} t} \\ + \dfrac{k_{41} \cdot M4(\infty)}{(-k_{41} + k_b)} \cdot e^{-k_{41} t} \end{pmatrix} \quad \textbf{(9)}$$

This model may give better predictions if the release profile of the device deviates from single exponential release. As there are five parameters, this model will have fewer degrees of freedom than the two compartment model. Unless the additional parameters significantly improve the fit to the data the two compartment model will generally be preferred.

1.6.4 Fick's First Law Mechanistic Model

Rather than analysing diffusion data, empirically mathematical modelling can incorporate characteristics of the physical process. This means that the diffusivity, a general parameter that describes the movement of a molecule through a defined matrix can be directly calculated. The movement of small molecules in a medium is governed by Fick's laws of diffusion. Fick's first law for diffusion in one dimension can be written as a rate equation where $j(x, t)$ is the flux of material in the direction x, D is the diffusion coefficient, $C(x, t)$ is the concentration and x is distance in one direction (equation 10).

$$j(x,t) = -D\frac{\partial C(x,t)}{\partial x} \quad \textbf{(10)}$$

The flux, $j(x, t)$, is the rate of transfer per unit area of section of the matrix. The diffusion coefficient incorporates Brownian diffusion as well as mechanical restrictions to mobility such as tortuosity of the path of the small molecule out of the matrix. Because the model is derived assuming that the matrix is perfectly homogenous when it is actually heterogeneous, matrices made from the same material but with different structures may demonstrate different apparent diffusivities. This model also requires that the solute is homogenously dissolved in the matrix and elutes from the inert support. If instead the drug is encapsulated as

large aggregates with no direct contact between water and the drug, the drug will dissolve into the matrix as it is removed, maintaining the drug concentration at the maximum solubility of the drug in the matrix. In this case, the drug concentration is buffered by the crystals and the release profile may be expected to behave more like a mass transfer system (section 1.6.2).

Kinetics based on Fick's first law predicts that initial drug release is dependent on the square root of time. This model assumes that the homogeneous matrix contains a higher concentration of drug than the solubility of the drug in the bathing fluid and that the rate of dissolution of drug into the polymer is faster than the rate of diffusion of the drug in the matrix. The most common implementation in the field of drug delivery is Higuchi kinetics (Higuchi, 1961). Higuchi proposed that an infinitely thick flat membrane under perfect sink conditions can be used to represent initial release of drug from a polymer depot (Appendix E). The model assumes that the drug loading of the matrix is much higher than the solubility of the drug in the release medium.

$$\frac{M(t)}{A} = \sqrt{DC_s\left(2M(\infty)/V - C_s\right)\cdot t} \qquad \textbf{(11)}$$

Equation 11 is the Higuchi model where $M(t)$ is the amount of drug released across the exposed area, A, after time t, D is the diffusivity of the drug in the matrix medium, $M(\infty)/V$ is the total amount of drug initially present in the matrix per unit volume and C_s is the solubility of the drug in the solvent.

$$M(t) = k\sqrt{t} \qquad \textbf{(12)}$$

The constants in the Higuchi model can be aggregated to give equation 12 which can be determined by fitting the model to drug release data where k is a constant relating to diffusion controlled release (equation 13). The Higuchi model makes a number of assumptions but effectively only has one parameter, k for a single sample under fixed conditions. It should be noted that k is not a rate constant and has the dimensions mg $s^{-0.5}$.

$$D = \frac{(k/A)^2}{C_s(2M(\infty)/V - C_s)} \quad \textbf{(13)}$$

From *k*, the Higuchi model can be used to estimate the diffusivity. The advantage of the Higuchi model is that it is defined by a single parameter, *k*, and may be fitted as a linear model as a function of the square root of time. The most significant flaw of this model is that it is only true for part of the release profile as the depot is not actually an infinite slab. It has been estimated that this transport equation is applicable to the first 60 % of drug release (Ritger and Peppas, 1987). In addition, the Higuchi model is only defined for one dimension and does not take device morphology into account.

1.6.5 Fick's Second Law Mechanistic Models

To overcome the limitations of models derived from Fick's first law, release models can instead be derived from Fick's second law. Fick's second law for diffusion states that the rate of change of concentration in a matrix is proportional to the rate of change of concentration gradient at that point. Drug delivery devices are three dimensional objects so Fick's second law requires a solution in three dimensions.

$$\frac{\partial C(x,y,z,t)}{\partial t} = D\left(\frac{\partial^2 C(x,y,z,t)}{\partial x^2} + \frac{\partial^2 C(x,y,z,t)}{\partial y^2} + \frac{\partial^2 C(x,y,z,t)}{\partial z^2}\right) \quad \textbf{(14)}$$

Fick's second law in three dimensions can be written in the form of equation 14 where *D* is the diffusion coefficient, *C*(*x, y, z, t*) is the concentration and *x, y,* and *z* are locations in rectangular coordinates. It is assumed that the diffusivity is the same in every direction; such media are described as isotropic. Depending on the boundary conditions which define the morphology of the depot the diffusion model can be derived. From this the diffusivity can more accurately be estimated for spheres (section 1.6.5.1), solid cylinders (section 1.6.5.2), and hollow cylinders (section 1.6.5.3).

1.6.5.1 Spherical Model

The diffusivity and release profile of microspheres can be calculated by using the spherical Fickian model and assuming that the microspheres are perfect spheres with diameter equal to the median diameter of the sample. It is also assumed that as drug reaches the surface of the fibre it is instantly removed. Spherical matrices such as microspheres are symmetrical in three dimensions so treating x, y, and z as equal, Fick's first law (equation 10) can be expressed in terms of r (equation 15) where $C(r, t)$ is the concentration, D is the diffusivity and r is the radius.

$$j(r,t) = -D\frac{\partial C(r,t)}{\partial r} \tag{15}$$

This can be used to derive Fick's second law (equation 14) in terms of r using finite element analysis (Appendix F). This technique considers the amount of material being released from the microsphere through a very thin spherical shell, which has an internal surface area of $4\pi r^2$ and external surface area $4\pi(r+\Delta r)^2$. Since the amount passing through the shell equals the change in concentration across the shell multiplied by the volume of the shell, the change in concentration with respect to radius and time can be determined in terms of the flux across the shell (equation 16).

$$\frac{\partial C(r,t)}{\partial t} = -\frac{\partial j(r,t)}{\partial r} - \frac{2}{r}j(r,t) \tag{16}$$

Substituting for Fick's law (equation 15) produces the result of Fick's second law for cylindrical coordinates (equation 17).

$$\frac{\partial C(r,t)}{\partial t} = D\left(\frac{\partial^2 C(r,t)}{\partial r^2} + \frac{2}{r}\frac{\partial C(r,t)}{\partial r}\right) \tag{17}$$

Substituting $u = C(r, t)r$, where u is the substituted variable, into equation 17 produces equation 18, the equation for linear flow in one dimension (Crank, 1975).

$$\frac{\partial u}{\partial t} = D\frac{\partial^2 u}{\partial r^2} \quad \textbf{(18)}$$

There are four boundary conditions for this equation. Firstly, because u is the concentration multiplied by the radius, $u = 0$ when $r = 0$ at $t > 0$. Secondly, the microsphere is under sink conditions during release so $u = 0$ when $r = a$ at $t > 0$ where a is the radius of the microsphere. Thirdly, $u = rC_0$ at $t = 0$ at $0 < r < a$, where C_0 is the constant surface concentration of drug. Finally, the sphere is initially at uniform concentration, C_1.

For a sphere the solution of Fick's second law for drug release can be expressed as a Taylor series of exponentials (equation 19) as described by Crank, 1975, p91.

$$M(t) = M(\infty)\cdot\left(1 - \frac{6}{\pi^2}\sum_{n=1}^{\infty}\frac{1}{n^2}\exp\left(-n^2\pi^2\frac{D}{R^2}t\right)\right) \quad \textbf{(19)}$$

$M(\infty)$ is the total drug in the device which is completely released after infinite time. As sphere radius (R) is effectively a bulk parameter that will depend on the size distribution of the particles it should be combined with diffusivity (D) for parameter estimation. As n increases the output converges with the solution; the solution can be approximated using a high value for n. This mechanistic model can give information about the underlying process of the drug release from a spherical device. Unlike a Fick's first law model it describes the profile even at long values of time (weeks).

1.6.5.2 Solid Cylinder Model

The diffusivity and release profile of solid fibres can be calculated by using the cylindrical Fickian model and assuming that the fibres are infinitely long, perfect cylinders with radius, a, equal to the mean radius of the fibre. It is also assumed that as drug reaches the surface of the fibre it is instantly removed. A long, cylindrical device such as a fibre can be analysed in polar coordinates by substituting $x = r\cos\theta$ and $y = r\sin\theta$ into equation 14 as shown by Figure 21. To describe point, P, at (x, y, z) the substitution defines P at (r, θ, z).

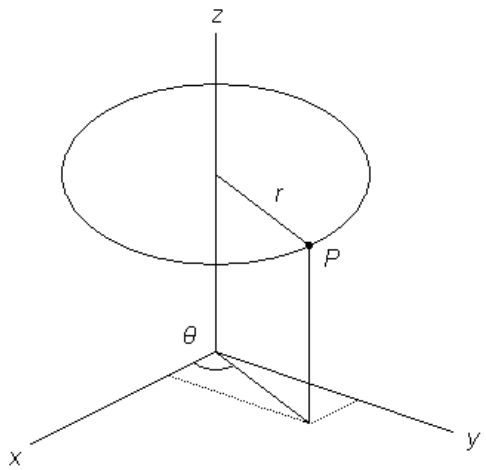

Figure 21: Polar coordinates.
A point, *P*, in three dimensional coordinates (*x, y, z*) can also be described in polar coordinates by (*r, θ, z*), where $x = r\cos\theta$ and $y = r\sin\theta$ (Sten-Knudsen, 2002).

The fibre is assumed to be radially homogenous for all angles of θ and along its length for all values of z. Therefore, concentration is treated as not being a function of z or θ so the terms in equation 20 can be excluded from the concentration profile.

$$\frac{\partial C(r,\theta,z)}{\partial z} = \frac{\partial C(r,\theta,z)}{\partial \theta} = 0 \qquad \textbf{(20)}$$

As the only independent variable is the radius of the cylindrical surface, concentration is only a function of radius and time. Flux, from Fick's first law (equation 15), is the same at every point on the cylindrical surface and is always perpendicular to the cylinder axis. As for spherical systems (section 1.6.5.1) Fick's second law can be derived for cylindrical systems using finite element analysis (full derivation in Appendix G). An amount of material passes through a cylindrical ring with internal surface area $2\pi r\Delta z$ and external surface area $2\pi(r+\Delta r)\Delta z$. As above (section 1.6.5.1), this amount equals the change in concentration multiplied by the volume thereby allowing the change in concentration to be determined with respect to the flux.

$$\frac{\partial C(r,t)}{\partial t} = -\frac{\partial j(r,t)}{\partial r} - \frac{1}{r} j(r,t) \qquad \textbf{(21)}$$

Substituting for Fick's law (equation 15) produces the result of Fick's second law for cylindrical coordinates (equation 22) (Sten-Knudsen, 2002).

$$\frac{\partial C(r,t)}{\partial t} = \frac{1}{r}\frac{\partial}{\partial r}\left(rD\frac{\partial C(r,t)}{\partial r}\right) \quad \textbf{(22)}$$

The method of separation of variables (as described by Crank, 1975, p17) can be used to solve this expression where time and space variables are convoluted. It is assumed that the time and space dimensions of $C(r, t)$ has a solution that can be treated as two independent functions, $R(r)$ and $T(t)$, which can be multiplied together (equation 23).

$$C(r,t) = R(r)T(t) \quad \textbf{(23)}$$

These functions can be substituted into equation 22 to give equation 24.

$$\frac{\partial R(r)T(t)}{\partial t} = \frac{1}{r}\frac{\partial}{\partial r}\left(rD\frac{\partial R(r)T(t)}{\partial r}\right) \quad \textbf{(24)}$$

Since $R(r)$ is not a function of time and $T(t)$ is not a function of radius, equation 25 can be expressed as two separate ordinary differential equations.

$$\frac{1}{T(t)}\frac{dT(t)}{dt} = \frac{D}{R(r)}\left(\frac{d^2R(r)}{dr^2} + \frac{1}{r}\frac{dR(r)}{dr}\right) \quad \textbf{(25)}$$

As both sides are equal they can be treated as separate differential equations for time and space and solved by setting both sides equal to $-\alpha^2 D$. Treating the time function of equation 25 as an ordinary differential equation allows the function $T(t)$ to be defined (equation 26).

$$\frac{1}{T(t)}\frac{dT(t)}{dt} = -\alpha^2 D$$

$$\frac{1}{T(t)}dT(t) = -\alpha^2 D dt$$

$$\ln(T(t)) = -\alpha^2 Dt$$

$$T(t) = \exp(-\alpha^2 Dt) \quad \textbf{(26)}$$

To solve the space function, $R(r)$, for fibres to be determined $-\alpha^2 D$ is substituted into the other side of equation 26.

$$\frac{1}{R(r)}\left(\frac{d^2R(r)}{dr^2} + \frac{1}{r}\frac{dR(r)}{dr}\right) = -\alpha^2$$

$$\frac{d^2R(r)}{dr^2} + \frac{1}{r}\frac{dR(r)}{dr} + \alpha^2 R(r) = 0 \quad \textbf{(27)}$$

Equation 27 is in the form of a Bessel equation (Crank, 1975).

$$R(r) = A_B \cdot J_0(r) + B_B \cdot Y_0(r) \quad \textbf{(28)}$$

A Bessel equation has the solution given in equation 28 where A_B and B_B are constants, $J_0(r)$ is a Bessel function of the first kind of order zero, and $Y_0(r)$ is a Bessel function of the second kind of order zero. These functions are damped but infinitely oscillating.

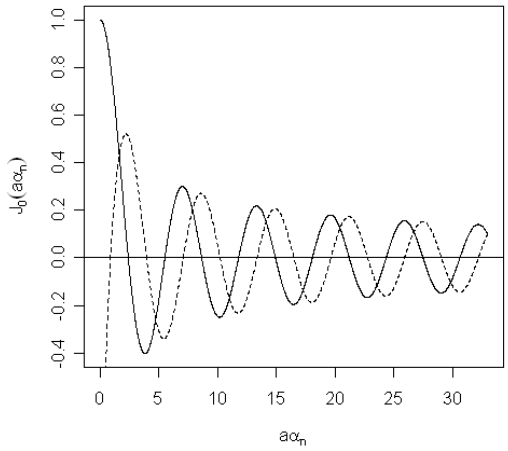

Figure 22: Bessel functions.

Bessel function of the first kind of zero order, $J_0(a\alpha_n)$, (solid line) and of the second kind of zero order, $Y_0(a\alpha_n)$, (dashed line) calculated using R. The first ten in the infinite series of positive roots of $J_0(a\alpha_n)$ are shown in Table G1.

Bessel functions of the first, J_0, and second, Y_0, kind of zero order have the form shown in Figure 22. A Bessel function of the first kind of order zero, $J_0(r)$, has a defined value at $r = 0$. A Bessel function of the second kind of zero order, $Y_0(r)$, diverges at the origin which means that B_B can be set to zero for physical models of solid fibres so that the result has physical meaning.

$$R(r) = A_B \cdot J_0(r) \tag{29}$$

By combining the definitions of the time function (equation 26) and the space function (equation 29) gives the explicit solution, equation 30, which is defined when the boundary conditions are satisfied. The concentration, $C(r, t) = C_0$ when $r = a$, for all time, $t \geq 0$, and $C(r, t) = C_0$ at $0 < r < a$, when $t = 0$.

$$C(t,r) = \sum_{n=1}^{\infty} A_{Bn} J_0(\alpha_n r) \exp\left(-D\alpha_n^2 t\right) \tag{30}$$

The boundary condition is satisfied by equation 30 as long as α_n is the series of positive roots of the Bessel function of the first kind of zero order (equation 31) divided by a.

$$J_0(a\alpha_n) = 0 \quad \textbf{(31)}$$

For a long fibre where diffusion from the end of the fibre is negligible the solution of Fick's second law for drug release can be expressed as a Taylor series of exponentials (equation 32) as described by Crank, 1975 p73.

$$M(t) = M(\infty) \cdot \left(1 - \sum_{n=1}^{\infty} \frac{4}{(a\alpha_n)^2} \exp(-D\alpha_n^2 t) \right) \quad \textbf{(32)}$$

The amount of drug released depends on fibre radius (a), diffusivity (D), total drug ($M(\infty)$) and α_n which is the series of roots of Bessel's equation of the first kind of order zero. The true value can be approximated using an arbitrarily large number of roots.

The cylindrical model has been successfully used to determine the diffusivity of hydrocortisone in polycaprolactone (1.6×10^{-10} cm^2 s^{-1}), ethylene-vinyl acetate (1.2×10^{-11} cm^2 s^{-1}) and PVA terpolymer (4.3×10^{-12} cm^2 s^{-1}) (Fu et al., 1976). This model should also be able to describe the release of cisplatin from PLGA fibres.

1.6.5.3 Hollow Fibre Model

The diffusivity and release profile of hollow fibres can be calculated by using the cylindrical Fickian model determined as for a solid fibre in section 1.6.5.2 using equation 22. For a hollow fibre there are different boundary conditions that must be considered. It is assumed that the fibres are infinitely long, perfect hollow cylinders with inner radius, a, and outer radius, b. Continuing to assume sink conditions $C(r, t) = 0$ at $t > 0$ and $r = a$, or $r = b$. Fick's second law (equation 22) is true between the outer and inner radius of the cylinder, $a < r < b$. Release of drug from a hollow cylindrical device such as a hollow fibre is described by equation 33 from Crank, 1975, p83 (Appendix H).

$$M(t) = M(\infty) \cdot \left(1 - \frac{4}{(b^2 - a^2)} \sum_{n=1}^{\infty} \frac{J_0(a\alpha_n) - J_0(b\alpha_n)}{\alpha_n^2 \{J_0(a\alpha_n) + J_0(b\alpha_n)\}} \exp\left(-D\alpha_n^2 t\right) \right) \quad \textbf{(33)}$$

Equation 33 predicts drug release from a hollow fibre with inner radius a and outer radius b where a_n is a positive root of equation 34.

$$J_0(a\alpha_n) Y_0(b\alpha_n) - J_0(b\alpha_n) Y_0(a\alpha_n) = 0 \quad \textbf{(34)}$$

The Fickian model for the hollow fibre is useful for estimating the diffusivity of cisplatin in the fibre. The diffusivity should be more comparable between formulations than rate constants or other empirical measures. Quantitative predictions cannot be made in the same way from the empirical models.

1.6.6 Model Comparison

Statistical computing packages are able to greatly extend analysis of scientific data. Models can be fitted to the data and then compared to allow the most likely mechanism to be determined. Alternatively, different models can offer equally valid interpretations of the same dataset. Statistical testing provides objective measures for decisions to be made as to how well different models fit a dataset.

$$y_i = f(\beta, x_i) + \varepsilon_i \quad \textbf{(35)}$$

A model (equation 35) representing data, y_i can be described as being a function of its independent variable, x_i, with model parameters, β, and also independent, randomly distributed errors, $\boldsymbol{\varepsilon_i}$. A useful method of fitting non-linear models to data is by minimizing the sum of the squared residuals.

$$S(\beta) = \sum_{i=1}^{n} [y_i - f(\beta, x_i)]^2 \quad \textbf{(36)}$$

The differences between the data, y_i, and the predicted values of the independent variable, $f(\beta, x_i)$ at each data point, from $i = 1, \ldots, n$ are the residuals. The minimum value of the sum of the squared residuals, $S(\beta)$, is calculated by finding the points of

inflection where the gradient of equation 36 is zero. These equations must be solved numerically and in R this is achieved using a convergence criterion that minimizes the distance between the data point and the predicted value (Bates and Watts, 1981).

Analysis of variance is an extended form of Student's t-test. To determine whether a set of values are different from the whole population the ratio of between-group and within-group variance, the F statistic, is examined. When F is large the probability that the groups belong to the same population is low. If we are comparing models then a saturated linear model can be fitted and parameters removed until removing a parameter introduces a significant change. This approach can be used to compare models as better models will produce less variance in the residuals. The method is modified for categorical data and the technique is called analysis of covariance.

Models can be selected by comparing how well the data is explained by the model with how many parameters are used in the model. Akaike's Information Criterion (AIC) (Akaike, 1974) allows comparison of mathematical models of data by trading off the number of parameters used against the residual error.

$$AIC = 2p - 2\ln(L) \tag{37}$$

AIC is calculated from statistical fitting parameters using equation 37; p is the number of parameters including the sum of squares, L is the likelihood function and 2 is the numeric penalty for each parameter. AIC values can only be used to compare different models of a dataset, not between datasets. The model with the lowest AIC is preferred by this method. AIC can be used in conjunction with hypothesis testing methods such as analysis of variance/covariance during model comparison. The advantage of AIC is that unlike hypothesis testing there is no concern that the sequence of analysis will affect the results.

$$L(\beta,\sigma^2) = \frac{1}{(2\pi\sigma^2)^{n/2}} \exp\left\{ -\frac{\sum_{i=1}^{n}[y_i - f(\beta, x_i)]^2}{2\sigma^2} \right\} \tag{38}$$

The likelihood of a model with parameters, β, with random errors distributed with variance σ^2 is calculated using equation 38. Comparison with equation 36 shows that minimizing the sum squared of the residuals maximises the likelihood of the model.

1.7 Infection of Implants

1.7.1 Infection

Bacteria which manage to penetrate one of the physical barriers to entering the body are destroyed by the immune system. This effective system is generally only overcome when it is in a weakened state or by organisms which have specifically evolved to subvert its defences in some way. Even normal body cells are vigilant and send distress signals to the immune system or commit suicide if they detect that they are under attack.

Any surface is susceptible to suffer bacteria attachment (Smith, 2005). Even if a surface is chemically resistant to bacterial attachment, small organic molecules will rapidly foul the surface in normal conditions. Microorganisms have a wide array of surface properties with differing surface charges and different degrees of hydrophobicity or hydrophilicity. A surface which has tailored physicochemical properties to be resistant to bacterial attachment cannot be resistant to every infectious organism. Even within a single species, mutants can show a range of affinities for a surface. Some *Staphylococcus aureus* mutants have been shown to attach to polystyrene surfaces although the wild type does not (Gross et al., 2001). Once a surface has become fouled with small molecules or other microorganisms, further surface infection can occur. Following initial attachment, the microorganisms secrete a matrix of biological polymers (such as polysaccharides and proteins) which is able to develop into a highly structured community including other species. Such a closely packed and firmly attached bacterial mass, or biofilm, matures into complex structure that protects the cells from the immune system and the effects of anti-microbial agents.

The problem of surface fouling is magnified in clinical situations. Implanted objects are frequently used for a variety of medical purposes such as mechanical repair,

introduction of medicines or drainage of fluids. Inert surfaces rapidly become covered with a conditioning film of biological material such as small molecules and host matrix proteins (Heilmann, 2003). The physicochemical characteristics of the surface as well as the environmental conditions will determine how quickly bacteria to which the surface is exposed may become attached. Bacteria can contaminate the implant during manufacture, handling, implantation or even from the bloodstream. The skin of healthcare workers and patients is a common source of bacteria.

Environmental stresses trigger global gene regulators; these cascade to regulate bacterial virulence and so adopt a range of stress response phenotypes (Foley et al., 1999). This means that stresses in the host bloodstream such as low iron availability and immune system attack trigger entry of bacteria into the slow-growth or dormant state preparing bacterial cells for hostile environments (Warner and Mizrahi, 2003). One stress response is an increase in production of polysaccharide intercellular adhesin which is involved in cell-cell binding, biofilm formation and attachment to biomaterials (Cramton et al., 2001). Stressed cells also demonstrate other characteristics such as low metabolic activity and can be said to enter a persister state (Brown and Smith, 2003) in which antibiotic resistance is many orders of magnitude higher than during growth stages (Keren et al., 2004).

After initial reversible contact there is a phase of protein mediated strong binding. The cells produce a defensive matrix of extracellular polysaccharides to develop a biofilm. Rate of biofilm growth will depend on environmental conditions. In ideal conditions for bacterial growth severe encrustation can occur within 24 hours (Donlan, 2001).

Bacteria encrusting surfaces and encased in biofilm have excellent resistance to the immune system, stressful conditions and antimicrobial treatments. Biofilms are medically important as the colony matures it sheds cells which may cause bacteremia. To avoid this risk catheters which become colonised by biofilm are generally removed (von Eiff et al., 2005). This would interrupt or end a catheter based IV slow release regime.

Coagulase-negative *Staphylococci* are gram-positive, human skin commensals. While normally harmless, they represent the most frequent causative agents of catheter and foreign body related infections. The majority (87 %) of bloodstream infections in intensive care units were caused by catheterisation and 39 % of these infections were coagulase-negative *Staphylococci* (compared to 12 % *S. aureus*) (Richards et al., 2000). *S. epidermidis* is the most successful of these species and is found in nearly 80 % of biomaterial related infections. *S. epidermidis* is able to colonise a medical implant prior to insertion, via a direct pathway between the skin to the implant (in the case of catheters) or from the blood following a subsequent wound. Cells in the biofilm mode of growth are difficult to control with antibiotics. Strains of *S. epidermidis* which do not form biofilm are not normally associated with disease.

1.7.2 Bacterial Attachment to Implants

Any form of implant for medical treatment may potentially suffer from colonisation by microorganisms. Before implementing a new method of treatment it is important to attempt to quantify the risks involved. Even objects prepared under perfectly aseptic conditions and a contamination free implantation can become subsequently infected by bacteria which have entered the body by another route, for example dental surgery. Normally these bacteria are rapidly destroyed by the immune system. If they are able to form a protective biofilm colony on an implant there is a danger of creating a centre for repeated infection. Clinically, polymer implants are known to occasionally become infected. Abscess formation following injection of Lupron Depot® suggests that the site of microsphere injection site becomes infected in up to 5 % of cases (TAP Pharmaceutical Products Inc., 2003). Risperdal Consta® follow up data suggest that this figure may be lower at 0.1-1.0 % of doses (Janssen Pharmaceutical Products Inc., 2006).

S. epidermidis is a good choice of experimental organism as it is easier to work with than the more pathogenic *S. aureus* while being medically relevant as a very common coloniser of implants. It is important to remember that no one set of physicochemical conditions will be repellent to all bacteria. In addition, the properties of the surface will never prove impregnable to colonisation because no surface is truly unadulterated. Organic material will coat any surface (Heilmann,

2003), especially *in vivo* where there are large quantities of protein and other organic molecules.

Ideally all biopolymer devices would be manufactured under sterile conditions. If this is not possible then the PLGA device must be sterilized. Unfortunately the properties which make the polymer suitable for implantation become a hindrance to effective sterilization. Extreme conditions such as autoclaving will destroy the polymer. Gamma irradiation (Gilding and Reed, 1979), ethylene oxide and radio frequency glow discharge plasma (Holy et al., 2001) reduces the molecular mass of the polymer, potentially altering the release properties. Antibiotic cocktails can destroy certain classes of microbes but do not guarantee sterilization and may create further problems for patients with allergies.

Ethanol solution, typically at 70 % is frequently used as an effective, broad-spectrum antiseptic. Ethanol has the advantage of having a relatively low toxicity and low cost although it is capable of causing tissue damage at high concentrations. Even 70 % ethanol treatment causes some damage to PLGA structures (Shearer et al., 2006) and cannot guarantee sterilization as it will not destroy some viruses and bacterial spores. In addition, bacteria living in the hostile (dry, nutrient-depleted) environment of microspheres are likely to be in a stress-resistant vegetative state even if they are not spore forming.

Aseptic production and administration remains the best approach to disease prevention. Devices for sterile injection of microsphere are already used to prevent infection before implantation. If ethanol treatment can be shown to display reproducible effects on a device then it may be a suitable treatment method after production as a risk reducing measure to prevent inadvertent injection of infected implants.

1.8 Aims and Objectives

This review of the current state of ovarian cancer treatment shows that paclitaxel in combination with platinum drugs is the best treatment currently available. Second generation platinum agents have reduced side effects but have not yet been shown to improve survival. Intraperitoneal delivery has been shown to offer improved therapy

to ovarian cancer patients. Depot delivery of cisplatin to the peritoneum may offer further improvements in efficacy with reduced toxicity to patients with this disease. Findings from this thesis will also offer a review of mathematical tools available to rational investigation of diffusion controlled drug releasing depots.

The aims of this research are to:

1. Fabricate microspheres with improved release profiles compared to previous formulations.
2. Manufacture novel fibres and assess as potential drug delivery devices. Solid and hollow fibres have not been widely studied as drug delivery devices.
3. Apply mathematical models to the drug release profiles to allow rigorous comparison of formulations. Real datasets will also allow critical evaluation of the usefulness of empirical and mechanistic mathematical models.
4. Investigate irreversible protein binding of cisplatin to proteins. As unbound cisplatin is thought to form the cytotoxic species, quantifying the amount of unbound cisplatin in solution is an important goal.
5. Quantify bacterial attachment to drug depots using *Staphylococcus epidermidis*, a common implant pathogen. All surfaces are liable to bacterial attachment. Cisplatin is a toxic molecule which limits bacterial growth. Once the cisplatin payload has been released from a depot, the surface will serve as a potential focus for infection until the polymer has fully degraded. A method for comparing attachment of bacteria to different depots would be a useful tool for development of biomedical applications.

2 Experimental Methods

2.1 Drug Release from Delivery Devices

2.1.1 Materials

Cisplatin powder was obtained from Lianyungang Unionrun Foreign Trade Co., Jiangsu, China. Poly(vinyl alcohol) (PVA) was purchased from Sigma-Aldrich (UK).

Poly(lactide-co-glycolide) (PLGA) was obtained from Alkermes (Birmingham, Ohio, USA). Three different lactide:glycolide polymers were selected to allow comparisons of release rates from depots made from each. PLGA 50:50 (lot LP-178) had a molecular weight of 51-72 kDa. PLGA 65:35 (lot LX4-72) had a molecular weight of 90-140 kDa. PLGA 75:25 (LX4-74) had a molecular weight of 290 kDa.

Analytical grade ethyl acetate, N-methyl-2-pyrrolidone (NMP), dichloromethane (DCM) and cyclohexane were from Fisher Scientific (UK).

2.1.2 Manufacture of Microspheres

Microspheres were fabricated by oil in water suspension precipitation (section 1.5.4.3). A dope solution consisting of polymer dissolved in an organic solvent is homogenised with an aqueous phase to create a suspension. The solvent dissolves in the aqueous phase leaving a precipitate of polymer droplets of the order of 10 to 100 μm in diameter. Ethyl acetate was used rather than dichloromethane (DCM) due to its lower toxicity (MSDS data in Appendix A). The solubility of ethyl acetate is 8.4 g in 100 g water at 20°C(Altshuller and Everson, 1953). The amount of ethyl acetate in the dope added to the aqueous phase was below this solubility threshold. This means that the solvent has the opportunity to dissolve extensively into the aqueous phase. PLGA was added to ethyl acetate at 10% by weight. This was mixed on a rolling bed until it had completely dissolved forming a viscous polymer solution, or dope, for device manufacture. For batches to which drugs were added, 40 % weight of polymer was mixed with the dope at this stage.

Batch	PLGA	Polymer in dope (%)	Cisplatin in dope (%)
M1, M3, M4, M7	50:50	9.5-9.7	3.2-4.9
M8, M14, M17, M20, M21, M25, M26, M27	65:35	9.6-9.7	3.2-3.9
M18	65:35	13.3	4.7
M19	65:35	16.9	5.9
M16, M22	65:35	9.6-9.7	-

Table 4: Batches of PLGA microspheres manufactured and ranges of polymer and cisplatin concentrations in the dope.

Polymer and cisplatin in dope calculated as percentage of total mass including polymer, solvent and drug.

Table 4 summarizes the conditions of manufacture of PLGA 65:35 and 50:50 microspheres. The recipe used was derived from methods reported elsewhere(Watts et al., 1990). Additional batch details are noted in Appendix K.

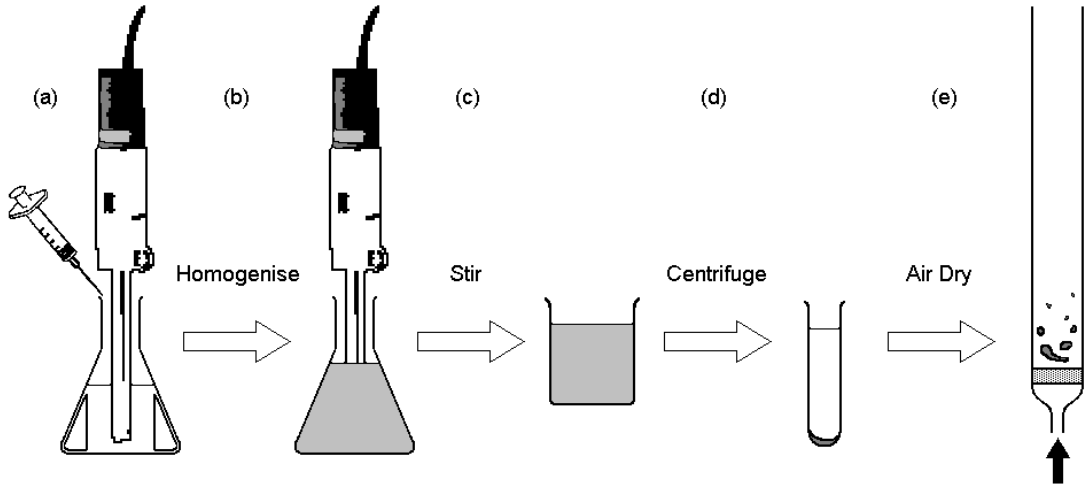

Figure 23: Manufacture of PLGA microspheres.

(a) Dope added to PVA solution. (b) Mixture homogenised for 13 minutes at 9500 rpm. (c) Suspension stirred for 4 hours at 500 rpm. (d) Suspension centrifuged at 500 *g* for 3 minutes, the supernatant decanted and the pellet of microspheres resuspended in distilled water. (e) Suspension filtered and the cake air dried for 12 hours.

Figure 23 summarises the method used to manufacture PLGA microspheres. An aliquot of dope (6 g) was taken from the stock using a syringe and added to 150 ml of 0.2 % poly(vinyl alcohol) (PVA) aqueous solution at 5°C. To create the emulsion the mixture was mechanically homogenised at 9500 rpm for 13 min in a baffled conical flask. Flasks with baffles were used to improve mixing throughout the volume. The suspension was poured into a beaker to be stirred with a magnetic bead at 500 rpm for 3-5 h to allow for solvent evaporation and microsphere hardening. The suspension was centrifuged at 500 *g* for 3 min and the supernatant discarded. This process was repeated four times until the dope had been used up and combined into a single batch for processing.

To remove surfactant, residual solvent and undersized microspheres the microspheres were washed with distilled water. For this, the suspension was centrifuged at 150 *g* for three minutes and the supernatant discarded. The microspheres were then resuspended in distilled water. This was repeated twice. The pellet was resuspended and filtered using Whatman M100 glass filter paper (pore size 1.47 μm). The filter cake was air dried overnight in a stream of air. Due to the low toxicity of ethyl acetate (Appendix A) it was not quantitatively confirmed that the solvent was completely removed by this washing protocol. The solidification of the microspheres as the solvent is removed increases the glass transition temperature of the polymer (section 1.5.4.3), thereby increasing the diffusivity of the solvent in the polymer at the temperature of manufacture. Therefore, the more the solvent is extracted, the lower the rate of further extraction. Varying amounts of residual solvent in different batches may result in a source of between batch variation both in the amount of drug initially present in the microspheres and in the diffusivity of the drug being released by the formulation. Due to the high boiling point of ethyl acetate (77°C) air drying may not completely remove the solvent. Freeze-drying samples with residual solvent in the centre may produce large voids on complete drying (section 3.3.1).

The dry microspheres were separated by physical sieving in a stack of sieves with mesh sizes 106, 90, 53 and 38 μm. Particles above 90 μm were discarded. Particles below 90 μm were either recombined or maintained as two fractions of particles

below 38 μm and particles between 38 and 90 μm. Microspheres were stored in a refrigerator at 5°C.

2.1.3 Manufacture of Solid Fibres

Preliminary studies found that PLGA 75:25 microspheres appeared to encapsulate less cisplatin than PLGA 50:50 with PLGA 65:35 encapsulating the most by the microsphere method described above. Therefore, most fibres were manufactured using PLGA 65:35. PLGA 65:35 was dissolved in N-methyl-2-pyrrolidone (NMP) (18 % by weight). Cisplatin (50 % by weight of PLGA) was added immediately (F2, F4) or after the PLGA had completely dissolved (F3).

Batch	PLGA	Polymer in dope (%)	Cisplatin in dope (%)
F1	75:25	16.4	1.8
F2-F4, F7	65:35	16.2-16.4	8.1-8.4
F6	65:35	16.0	9.8◊
F5	65:35	16.3	-

Table 5: Batches of PLGA fibres manufactured and polymer and cisplatin concentrations in the dope.

Polymer and cisplatin in dope calculated as percentage of total mass including polymer, solvent and drug. ◊ Carboplatin was used instead of cisplatin for F6 fibres.

Table 5 shows the concentrations of the polymer dope used for manufacturing solid fibres.

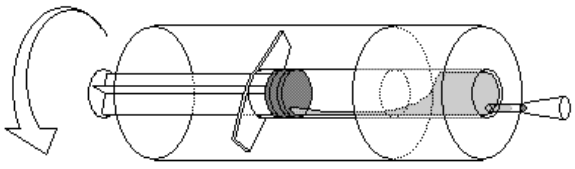

Figure 24: Polymer dissolved in syringe for spinning.

This method reduced waste as it could be spun directly without an additional transfer step. A cardboard support allowed the dope to be mixed using a rolling bed.

To reduce waste during transfer of polymer dope the PLGA was dissolved in NMP in a sealed syringe and mixed on a rolling bed. The syringe was rolled in a support as

shown in Figure 24 so that no modification of the syringe was necessary. Immediately before spinning the fused plastic cap can be removed with a scalpel, the air expelled and the syringe connected to the spinneret with tubing.

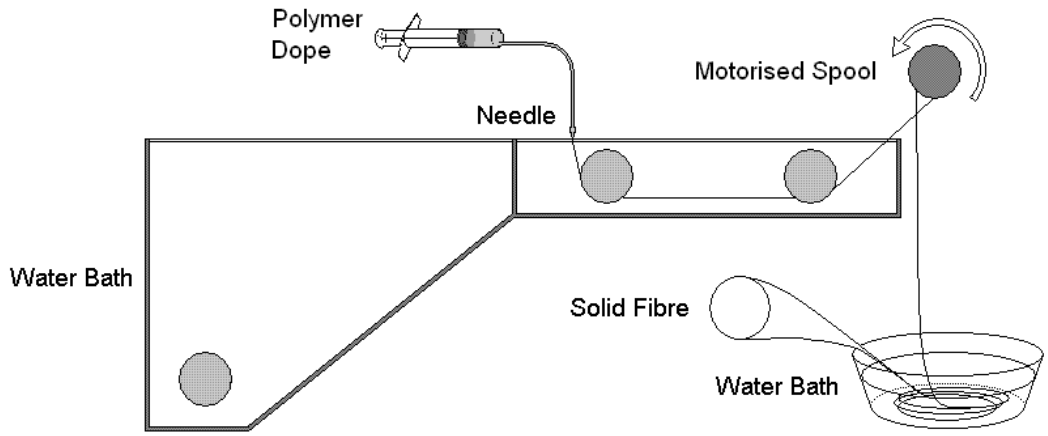

Figure 25: Schematic of solid fibre spinning process.
Dope is extruded through a needle at 60 ml h^{-1} into a water bath before being collected by a motorised spool into a second hardening bath.

Figure 25 shows the manufacture of PLGA solid fibres. The dope was driven from the syringe at 60 ml h^{-1} using a syringe pump and extruded through a needle into a water bath. Rollers ensure that the fibre does not float during the phase inversion process. The fibres were collected at 14 rpm into a second water bath. Fibres are soaked in the water bath to allow the NMP to completely dissolve into the water, ensuring that there is no solvent remaining in the finished fibre. This could otherwise be toxic or cause degradation of the fibre. Fibres were then dried. The concentration of residual NMP was not quantitatively determined following this washing protocol. The solidification of the fibres as the solvent is removed increases the glass transition temperature of the polymer, thereby increasing the diffusivity of the solvent in the polymer at the temperature of manufacture. Therefore, as more solvent is extracted, the rate of further extraction decreases. Varying amounts of residual solvent in different batches may result in a source of between batch variation both in the amount of drug initially present in the fibres and in the diffusivity of the drug being released by the formulation. Freeze-drying samples with residual solvent in the centre caused large voids to form on complete drying (section 3.3.2).

Cisplatin is water soluble (section 1.4.1). Since excessive soaking would completely remove the drug, during the manufacture of F1 fibres different drying methods were trialled. A third of the fibre (F1-F) was soaked for one hour and then freeze-dried using a Heto PowerDry LL3000. A third of the fibre (F1-A) was soaked for one hour and then air dried at 30°C. The remaining fibre was soaked overnight (F1) and then freeze dried.

The fibres were wrapped around cardboard supports to increase the rate of solvent removal and to prevent the fibre becoming fused together during drying. Determining the drug loading showed that the majority of cisplatin had been lost from F1 fibres while cisplatin remained in F1-F and F1-A fibres. Subsequent fibres were soaked for one hour and then freeze dried overnight to retain cisplatin while removing solvent. Detailed batch notes are given in Appendix K.

2.1.4 Manufacture of Hollow Fibres

Hollow fibres were manufactured as for solid fibres except that the dope was extruded through a spinneret (Perera and Tai, 2006) at 200 ml min^{-1} with distilled water flow through a central bore cavity.

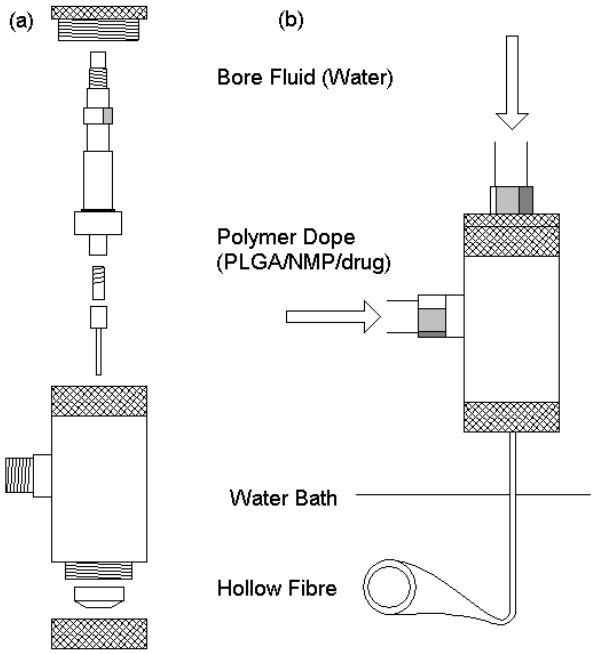

Figure 26: Hollow fibre spinneret.

(a) Exploded schematic of the spinneret (Perera and Tai, 2006). (b) Fibre is directly extruded into water with water pumped through the central needle to create the hollow core.

Sample F8 was a blank containing only made solely from PLGA and n-methyl-2-pyrrolidone (NMP). Figure 26 shows the spinneret used for manufacturing hollow fibres. Polymer is extruded from the spinneret with distilled water flowing through the central bore. The central bore creates support for the nascent fibre allowing an air gap to be incorporated between the spinneret and the bath. This reduces the chance of blockage during spinning.

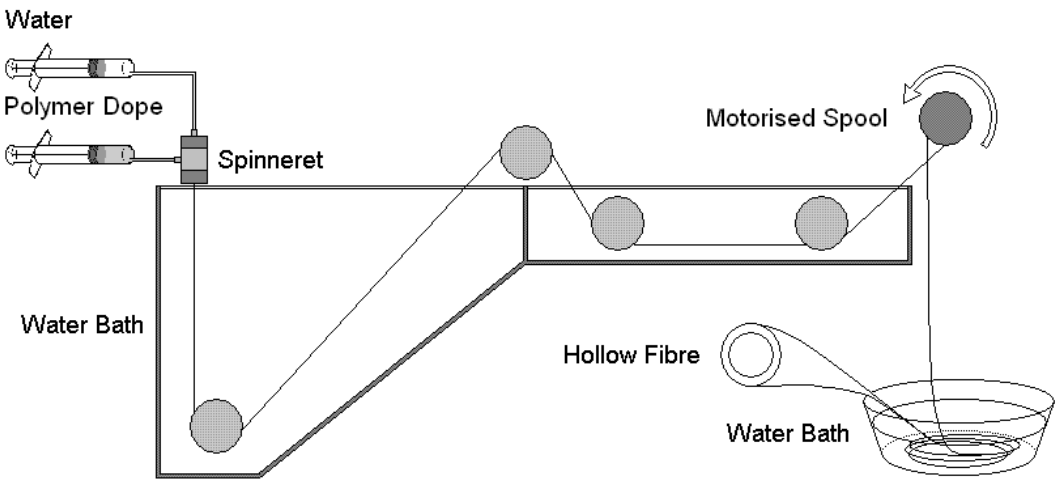

Figure 27: Schematic of hollow fibre spinning process.

Dope is extruded through the spinneret at 200 ml h^{-1} with water pumped into the fibre bore at 180 ml h^{-1} into a water bath before being collected by a motorised spool into a second hardening bath.

Due to their larger size and more fragile structure the hollow fibres were spun into a deep water bath to give them enough time to begin to harden before the fibres are passed through the spools (Figure 27) and then collected via a second bath into a final water bath for soaking. Due to their larger surface area to volume ratio compared to solid fibres, hollow fibres were able to be handled sooner after collection into the hardening bath. This allowed fibres with higher drug loadings to be produced. Although the residual NMP in the fibres was not quantified, the less porous structure of the matrix following freeze-drying (section 3.3.3) suggests that the fibre contained less solvent than solid fibres. This is because molten polymer inside a solid polymer shell occupies a smaller volume, meaning that voids will form when the solvent is completely removed.

Batch	PLGA	Polymer in dope (%)	Cisplatin in dope (%)
F9, F10	65:35	16.3	8.2
F8	65:35	16.3	-

Table 6: Batches of PLGA hollow fibres manufactured polymer and cisplatin concentrations in the dope.

Table 6 shows the concentrations of the polymer dope used for manufacturing hollow fibres. Batch measurements are noted in Appendix K.

2.2 Device Analysis Methods

2.2.1 Laser Scattering Analysis of Microspheres

Microsphere particle size distributions were measured using a Malvern Mastersizer with a 100 mm lens (for particles of 0.5-180 μm). Particle size was calculated using the Mie scattering model. The microspheres were dispersed in cyclohexane with 1 mg ml^{-1} lecithin as a stabiliser. Distribution was scanned at least four times for each sample.

2.2.2 Physical Characterisation of Fibres

Diameter of fibres was measured fibres using a digital micrometer (n = 16). Approximately 50 cm of each fibre was weighed and the volume determined by displacement of water in a measuring cylinder.

2.2.3 Scanning Electron Microscopy

A sample of microspheres (M4) were sieved (between sieves with mesh size 90 and 38 μm) and separated into large (38 to 90 μm) and small (<38 μm) fractions. Microspheres were freeze dried and mounted on specimen plates with carbon tabs. Samples were sputter coated with gold. Imaging was carried out on a JEOL JSM 6310 electron microscope at 5 keV accelerating voltage.

A sample of microspheres was sieved (between pans with mesh size 90 and 53 μm) to isolate a fraction of large (53 to 90 μm) particles. The microspheres were mixed with a suspension of *Staphylococcus epidermidis* (~1×10^4 cfu ml^{-1}) and incubated at room temperature for five minutes. The sample was then centrifuged at 100 *g* for 1 min to sediment the microspheres only. The supernatant was aspirated and discarded. The microspheres from the pellet were fixed with 2 % glutaraldehyde in 0.1 M sodium cacodylate buffer followed by 1 % osmium tetroxide. The sample was then freeze dried using a tissue drier, mounted on specimen plates with carbon tabs, and sputter coated with gold. Imaging was carried out on a JEOL JSM 6310 electron microscope at 10 keV accelerating voltage.

Samples of fibres (F3, F4, F10) were oven dried overnight at 30°C and cut into small sections, then pressed onto carbon tabs on specimen plates. Samples were carbon coated prior to imaging. SEM and backscattering images of fibres were taken using a JEOL 6480LV scanning electron microscope. Backscattering maps were performed on a JEOL JSM 6310 electron microscope at 15 or 20 keV accelerating voltage. Areas of high electron reflectivity by backscattering imaging were validated as cisplatin by spot X-ray analysis. No additional preparation was required for X-ray analysis as X-rays emitted by the excited samples were directly captured *in situ* using the JEOL JXA8600 Superprobe electron probe microanalyser attachment of the electron microscope.

2.2.4 Digital Image Analysis

Photographs of hollow fibres were taken using a digital camera. Hollow fibre wall thicknesses were estimated by taking measurements at twelve positions around the circumference using ImageJ (Abramoff et al., 2004). Fibres were cut with a scalpel using a gentle sawing motion to minimise disruption to the profile of the cross-section.

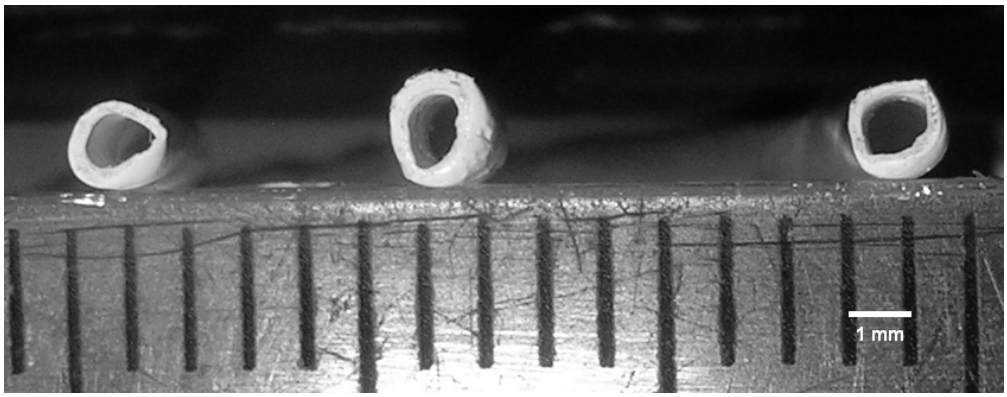

Figure 28: Photograph of hollow fibres.
Digital photograph scale was calibrated using ImageJ and twelve measurements of wall thickness were taken for each fibre at ten cross-sections. Diameter of each fibre was measured at six points at each of ten cross-sections. Bar is 1 mm.

The images where calibrated using a ruler (Figure 28). Although this method may have limited precision it is sufficient for comparisons between fibres and gives a good estimation of the variability of the thickness of the fibres.

Release of cisplatin from fibres was examined by digital image analysis of SEM and backscattered images. Samples of F3, F4 and F10 fibres were soaked in distilled water at 30°C for 1, 5 or 21 hours and oven dried at 30°C overnight. Unsoaked fibre samples were also placed in the oven to control for the effect of temperature. SEM and backscattered images were taken of cross-sections of fibre samples (n = 4). Images were analysed using ImageJ.

Images were calibrated using the embedded scale bar. Area of fibre cross-section was measured by manually selecting the outline of the fibre in the scanning electron micrograph.

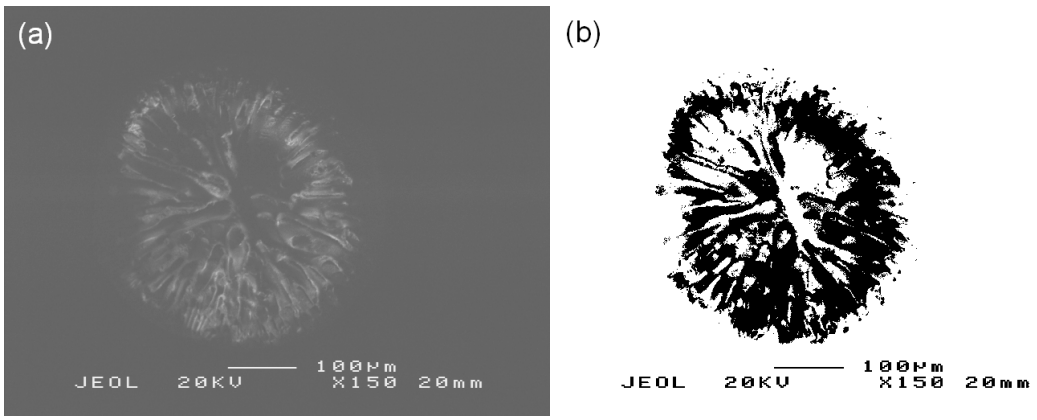

Figure 29: Estimate of cisplatin area from backscattered electron image.
(a) Backscattered electron image of F3 fibre. (b) Threshold mask. Bar is 100µm.

The area of cisplatin was estimated by setting the threshold of the backscattered image to just before random speckles appeared in the threshold mask (Figure 29b). As setting the threshold is subjective quantitative data must be treated with caution. The area of the mask is related to the amount of drug present in the fibre. The measured area cannot be directly compared to quantity of drug remaining in the fibre. This area may be used to observe the qualitative pattern of cisplatin dissolution from the fibre by comparing fibres soaked for different lengths of time.

2.3 Atomic Absorption Spectroscopy

2.3.1 Materials

Platinum standard for concentration calibration and bovine serum albumin fraction V (BSA) for the protein binding studies were purchased from Sigma-Aldrich (UK). Analytical grade ethanol, 37 % hydrochloric acid (HCl) and 70 % nitric acid (HNO_3) and Amicon Bioseparations Cetrifree micropartition ultrafiltration filters (Fisher Scientific, UK) were from Fisher Scientific (UK). Acetylene was from BOC (UK).

2.3.2 Calibration

Cisplatin release from delivery devices was quantified using a Perkin Elmer Model 3110 for atomic absorption spectroscopy (AAS) at 265.9 nm.

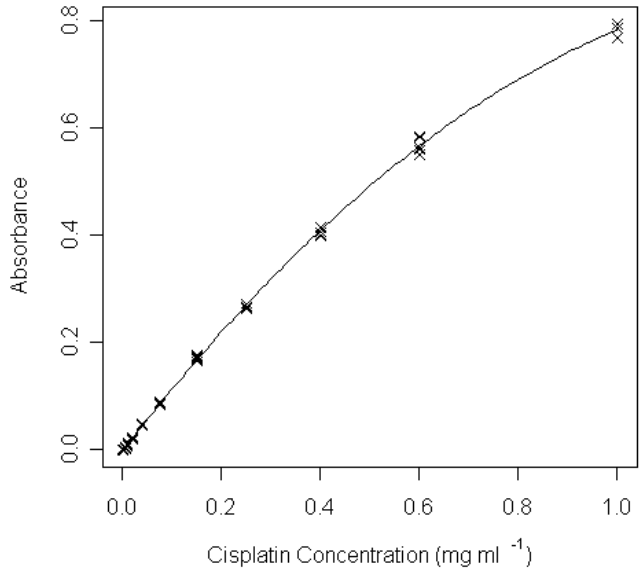

Figure 30: Typical calibration curve for analysis of cisplatin from PLGA devices. Equation of the quadratic fit is $y = -0.41x^2 + 1.19x - 0.00$.

To compensate for fluctuations in the fuel and oxidant pressure the instrument was manually calibrated using a working curve. The dilution series consisted of twelve platinum standards in HCl 2.0 M from 1.000 mg ml^{-1} to 0.001 mg ml^{-1}. The method was validated by dissolving powdered cisplatin in water for comparison with the standard.

Where sample concentrations were low enough that the Beer-Lambert law was obeyed a linear fit was used for the calibration. At higher concentrations a quadratic equation was needed (Figure 30). The third parameter was excluded when not significant. Standards were run throughout data collection to confirm that there was no change in response of the instrument. In cases where a significant change in response was noted a new calibration curve was generated for subsequent samples. Absorbance was measured using a 2.0 s integration time and an aspiration rate of 3.0 ml min^{-1}.

To compensate for the density dependent differences in 2.0 M HCl and water matrices the appropriate diluent was use depending on the matrix of the samples being analysed.

$$\frac{M_r(Pt) \cdot \text{Concentration (Pt)}}{M_r(PtCl_2(NH_3)_2)} = \text{Concentration } (PtCl_2(NH_3)_2) \quad \textbf{(39)}$$

The amount of cisplatin present was calculated from the mass ratio of the molecular mass (M_r) of platinum in cisplatin (Equation 39). For example, an aliquot of 0.50 mg ml^{-1} platinum standard solution should have the same absorbance as 0.75 mg ml^{-1} cisplatin solution.

To confirm that cisplatin detection was not affected by the presence of a PLGA digest matrix cisplatin was added to samples of PLGA 75:25 F1 fibre and then digested using *aqua regia*. Nominal cisplatin concentration was plotted against the concentration determined by AAS.

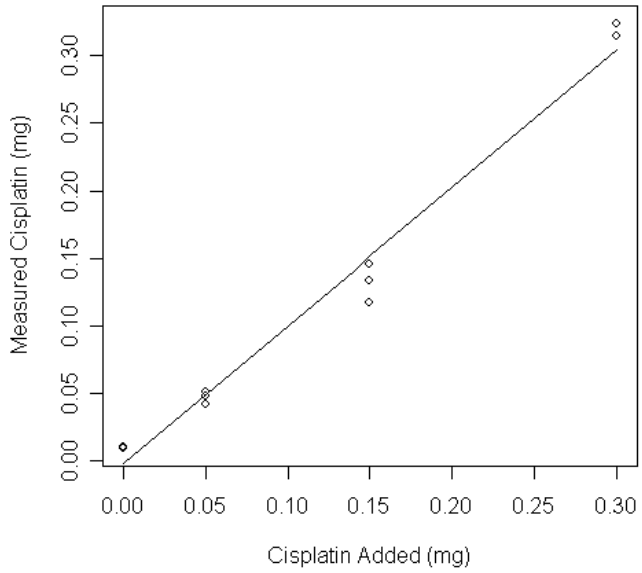

Figure 31: Validation of acid digestion for cisplatin quantification using AAS.
Correlation between amount of cisplatin added to PLGA 72:25 F1 fibres as a series of spikes and the amount of cisplatin calculated from atomic absorption spectroscopy measurements (n = 3). Equation of linear fit is $y = 1.02\ x - 0.00$.

Figure 31 shows the comparison of the amount of cisplatin added to samples of F1 PLGA 75:25 fibres to the amount of cisplatin measured. There is a close correlation ($r^2 = 0.98$) of these values with a relationship of 1.0 ($p = 4.4 \times 10^{-9}$) which validates this method for cisplatin analysis.

2.3.3 Cisplatin Loading

Drug loading was calculated by digesting 21.6±0.7 mg F2 and F3 fibre pieces at 105°C with 1.0 ml aqua regia (three parts concentrated HCl to one part HNO_3) until near dryness twice. Once dry the samples were redissolved in 1.0 ml HCl 2 M. Samples with the blank were spiked with cisplatin before digestion to check for loss of platinum. Material appeared to be retained in the crucibles so the digestion was repeated and a second set of samples was collected in 1.0 ml HCl 2M.

2.3.4 Release of Cisplatin from Microspheres

Cisplatin release profiles were determined for microspheres in distilled water (Table 7) at 37°C. At each sampling time point the microspheres were sedimented by centrifugation, the release medium was decanted and the microspheres were

resuspended in fresh water. This strategy maintained the release environment at close to sink conditions. The concentration in each sample was measured using atomic absorption spectroscopy (AAS). Plotting the amount released into each sample gave a cumulative release profile of the formulation.

#	Sample	Mass (mg)	Volume (ml)
2	M3	200	20
3	M3, M4	100	15
4	M7, M8	150	15
5	M14, M16	100	20
6	M7, M13, M17	100	15
7	M17, M18, M19, M20, M21, M22	100	10

Table 7: Nominal mass of microspheres and volume of water used as release medium.

The samples were stored at room temperature for analysis by atomic absorption spectroscopy (AAS). Absorbance values for platinum were converted into cisplatin release profiles as described above. Amount of cisplatin released by each sample was normalised to facilitate comparisons. Two and three compartment empirical, Higuchi and spherical Fickian models were fitted to cumulative release curves by non-linear least squares regression using the statistics package R (R Development Core Team, 2007).

2.3.5 Release of Cisplatin from Solid Fibres

Cisplatin release profiles were determined for 5 mg portions of solid fibre in 1 ml distilled water at 37°C. At each time point the release medium was collected and replaced with fresh water. Absorbance values for platinum were converted into release profiles as described above. Two and three compartment empirical, Higuchi and cylindrical Fickian models were fitted to cumulative release curves by non-linear least squares regression using the statistics package R.

2.3.6 Release of Cisplatin from Hollow Fibres

Cisplatin release profiles were determined as above for 5 mg portions of hollow fibre in 1 ml distilled water at 37°C. At each time point the release medium was collected and replaced with fresh water. Absorbance values for platinum were converted into release profiles as described above. Two and three compartment empirical, Higuchi and hollow cylinder Fickian models were fitted to cumulative release curves by non-linear least squares regression using the statistics package R.

2.3.7 Cisplatin Binding to Albumin

Cisplatin becomes inactivated *in vivo* by binding of aquated cisplatin to nucleophiles such as glutathione, DNA and proteins. Albumin is a well characterised model protein that can be used as a representative cisplatin binding target. Albumin can be removed from solution by ultrafiltration or cold ethanol precipitation allowing the concentration of unbound cisplatin to be determined. Characterising the profile of concurrent cisplatin release from a polymer depot and binding to protein will improve understanding of the pharmacokinetics of drug release and test the usefulness of the mathematical models described above (section 1.6.3).

Typically serum albumin concentration is approximately 44 mg ml^{-1} and a therapeutic dose of cisplatin needs to attain a serum concentration of the order of 10 μg ml^{-1}. To validate that cisplatin could be accurately detected under these conditions known amounts of cisplatin were incubated with bovine serum albumin (BSA) solution, digested and measured using AAS.

For cisplatin standards cisplatin powder was dissolved in distilled water. Each sample was heated to 105°C on a hot plate in a crucible to concentrate the sample. To destroy the protein the sample was then further heated with 1.0 ml *aqua regia* (0.25 ml 70 % HNO_3 and 0.75 ml 37 % HCl) until most liquid had evaporated. This was repeated and the almost dry crucible was allowed to cool before the addition of 2.0 ml 2.0 M HCl for AAS.

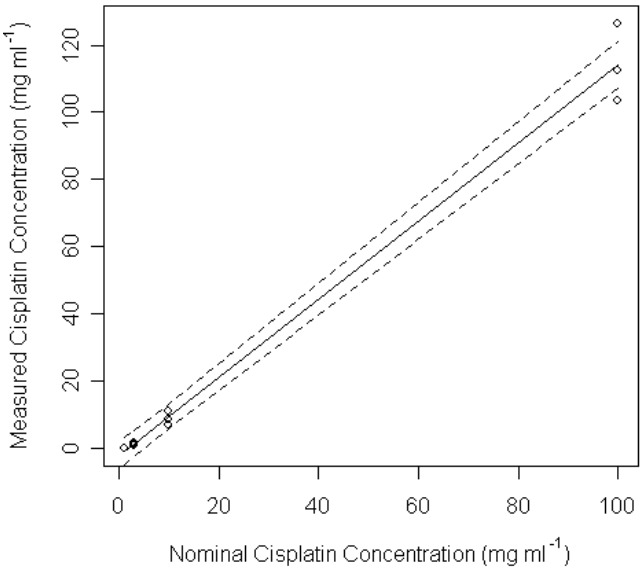

Figure 32: Cisplatin concentration measured by AAS after digestion of protein against concentration of cisplatin in samples.

Nominal concentration calculated from mass of cisplatin added (n = 3). Solid line shows linear model of these data and dashed lines show the 95 % confidence interval.

Figure 32 shows that the concentration of cisplatin measured by chemical digestion of protein and analysis by AAS are close to the expected values based on the amount of cisplatin powder added to the samples. Although the value of the intercept was not significant the gradient, 1.2±0.04, was significant ($p = 3\times10^{-11}$) by linear regression. This suggests that there is a small positive systematic error in this experiment. This analysis does not incorporate errors in weighing the cisplatin powder. These could be high (~20 %) due to static charging which can occur when weighing small quantities of powders. During manufacture of drug depots amounts weighed were large enough that static would not be significant. Acid digestion enabled the determination of total cisplatin concentration in the presence of biological molecules. Although it is useful to be able to determine total cisplatin concentration, only unbound cisplatin is able to cause tumour killing. It is necessary to develop a method to determine the concentration of the unbound fraction.

Therefore a protocol was developed to determine protein binding kinetic parameters for cisplatin solution. The principle is to use cold ethanol precipitation (Ma et al.,

1996) to remove the protein bound fraction from solution. This involves mixing a sample of the release medium with two volumes of cold ethanol, incubating at -20°C and then centrifuging. The supernatant was acid digested to remove residual protein that would interfere with the AAS analysis. Once the cisplatin solution was mixed with the BSA solution aliquots were removed at sequential time points and the protein removed by ethanol precipitation. The concentration of unbound cisplatin was determined with time. A preliminary experiment with 0.02 and 0.04 mg ml^{-1} cisplatin demonstrated the proof of this concept.

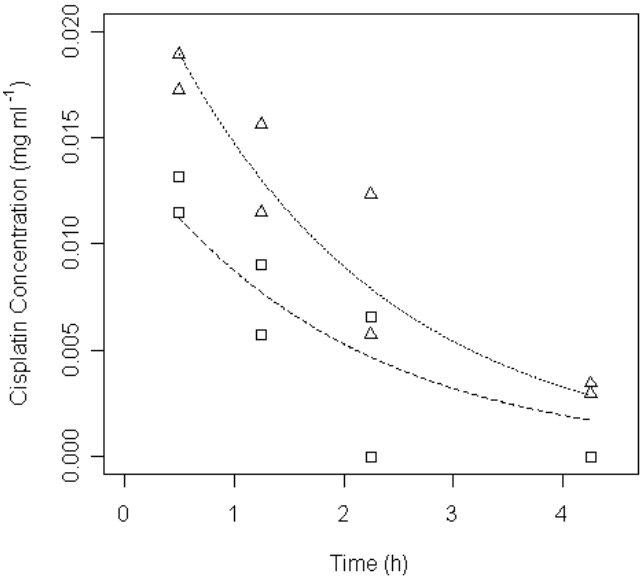

Figure 33: Unbound cisplatin concentration measured by AAS against time.
Solutions of 0.02 mg ml^{-1} (□) or 0.04 mg ml^{-1} (Δ) (n=2) added to BSA solution. Lines shown are fitted to the data assuming a single binding constant for both series.

Figure 33 shows the decrease of unbound cisplatin concentration caused by binding to BSA. The absorbance values measured were low meaning that the experiment was at the limit of detection and therefore numerical values must be treated with caution. There was a clear reduction in cisplatin concentration over four hours. Assuming that the binding constant was the same for both datasets the binding constant, k_b, was of the order of 1×10^{-4} s^{-1} calculated using the Solver function of Excel. Following this

preliminary experiment a complete experiment was carried out validating the use of ethanol precipitation as an alternative to ultrafiltration.

To compare whether protein precipitation is equivalent to ultrafiltration the two methods were directly compared. Samples (8 ml) were prepared containing 0.10 mg ml^{-1} cisplatin with and without 0.44 mg ml^{-1} BSA. At each of five time points an aliquot was withdrawn and the unbound cisplatin was collected using either ultrafiltration or ethanol precipitation (n = 4) to remove the protein. For ultrafiltration, 0.70 ml of sample were withdrawn, placed in Amicon Bioseparations Cetrifree micropartition ultrafiltration filters and centrifuged at 4000 *g* for 10 min and stored at -20°C until analysis. For ethanol precipitation, 0.67 ml of sample were pipetted into 1.33 ml cold ethanol, mixed and stored for 2 h at -20°C before centrifugation at 20 000 *g* for 30 min. The methods of protein extraction were found to be equivalent (section 3.5.1).

2.3.8 Binding of Cisplatin Released from PLGA Depots to Albumin

2.3.8.1 Release from Microspheres

Samples of microspheres (M21, M25, M26, and M27) were suspended in distilled water (118 mg in 8 ml). Samples were well mixed and 0.56 ml of each was quickly added to six of twenty-four Eppendorf tubes. Distilled water or 100 mg ml^{-1} BSA (0.44 ml) was added to each sample and incubated at room temperature. At each time point the tubes were spun at 500 *g* for 3 min to pellet the microspheres and then 0.67ml of release medium was withdrawn and added to 1.33 ml cold (-20°C) ethanol. The remaining release medium was aspirated and discarded. Fresh release medium (1.0 ml water or 0.44 mg ml^{-1} BSA) was added to the microsphere samples. The samples for each time point were spun at 20 000 *g* for 10 min and stored at -20°C for analysis. These samples were subsequently evaporated in ceramic crucibles (discarding the protein pellet) and digested with aqua regia at 105°C until near dryness twice. Once dry the samples were dissolved in 1.0 ml HCl, 2 M.

2.3.8.2 Release from Solid Fibres

Fibres (F1, F2, and F3) were cut into 5.0±0.17 mg pieces. Release medium (1 ml distilled water or 0.44 mg ml^{-1} BSA at 37°C) was added to each sample (n = 6) and incubated at 37°C. At each of ten time points 0.67 ml of release medium was

withdrawn and added to 1.33 ml cold (-20°C) ethanol. The remaining release medium was aspirated and discarded. Fresh release medium (1 ml) was added to the fibre samples. The samples for each time point were spun at 20 000 *g* for 10 min and stored at -20°C for analysis. These samples were subsequently evaporated in ceramic crucibles (discarding the protein pellet) and digested with aqua regia at 105°C until near dryness twice. Once dry the samples were redissolved in 1.0 ml 2.0 M HCl.

2.3.8.3 Release from Hollow Fibres

Fibres (F10) were cut into pieces weighing 5.6±1.0 mg. Release medium (1 ml distilled water or 0.44 mg ml^{-1} BSA at 37°C) was added to each sample (n = 8) and incubated at 37°C. At each of eight time points 0.67 ml of release medium was withdrawn and added to 1.33 ml cold (-20°C) ethanol. The remaining release medium was aspirated and discarded. Fresh release medium (1 ml) was added to the fibre samples. The samples for each time point were spun at 20 000 *g* for 10 min and stored at -20°C for analysis. These samples were subsequently evaporated in ceramic crucibles (discarding the protein pellet) and digested with aqua regia at 105°C until near dryness twice. Once dry the samples were redissolved in 1.0 ml 2.0 M HCl.

2.4 Determination of Peritoneal pH

Samples of ascites were obtained with informed consent from a stage IIIc ovarian cancer patient. Peritoneal fluid was taken from the abdominal drain catheter and pH was measured immediately using a pH meter. The pH meter was calibrated using standards.

2.5 Bacterial Attachment to Drug Delivery Devices

2.5.1 Materials

Staphylococcus epidermidis strain ATCC35984 was purchased from LGC Promochem (Teddington, UK), revived and then stored under liquid nitrogen for later use. Solid potassium phosphate (KH_2PO_3 and K_2HPO_3) was obtained from Fisher Scientific, UK and dissolved in distilled water to 1.0 M. Phosphate buffered saline (PBS) 0.1 M, pH 7.4 was made from 5 ml 1.0 M KH_2PO_3, 20 ml 1.0 M K_2HPO_3 and 225 ml distilled water and sterilized in a Rodwell Scientific Instruments Series 56 autoclave at 121°C (2.1 bar), for 15 minutes. Peptone, Tryptone soya broth

(TSB) and tryptone soya agar (TSA) were obtained from Sigma Aldrich, UK and were also sterilised in an autoclave.

2.5.2 Bacterial Attachment to Microspheres

As bacterial attachment to implanted devices is a fact, the degree of attraction between PLGA 50:50 microspheres and *S. epidermidis* was investigated. *S. epidermidis* ATCC 35984 was grown overnight in tryptone soya broth (TSB) at 37°C without agitation to approximately 10^7 cfu ml^{-1}. The culture was centrifuged at 1000 *g* for 10 min, the nutrient media removed and the pellet of cells resuspended in the same volume of PBS. The culture was diluted 1:10 four times. To determine the concentration of the culture for each repetition of the experiment, test plates were made, plating 100 µl of 10^{-4} and 10^{-5} dilutions.

A 1 ml aliquot was added to each container with or without microspheres. The samples were incubated for one hour at room temperature with a density of bacteria of 10^3 cfu ml^{-1}. The microspheres were separated from the culture by centrifuging the mixture at 100 *g*; this sedimented the microspheres but not the free bacteria. The supernatant was aspirated and discarded. To reduce numbers of cells remaining in the liquid surrounding the microspheres but not attached, 1 ml PBS was added, mixed, centrifuged at 100 *g* and aspirated. To determine the number of cells loosely associated with the microspheres, samples were incubated with sterile PBS for one minute. Tubes were centrifuged at 100 *g* and 100 µl was spread plated onto TSA. This experiment was carried out four times.

2.5.3 Freeze Drying to Kill Bacteria Attached to Microspheres

Blank and cisplatin-containing microspheres (M22 and M20, 1.3 g) were freeze dried in Sterilin containers by pouring liquid nitrogen onto the samples and freeze-dryed with a Heto PowerDry LL3000. The microspheres were then suspended in sterile distilled water (13 ml).

S. epidermidis ATCC 35984 was grown overnight in tryptone soya broth (TSB) at 37°C and agitated at 60 rpm to approximately 10^8 cfu ml^{-1}. The culture was centrifuged at 1000 *g* for 10 min, the nutrient media removed and the pellet of cells resuspended in the same volume of peptone. This culture was diluted 1:10 three

times. A 1 ml aliquot of dilute culture was added to each container of microspheres. The samples were incubated overnight at room temperature with a density of bacteria of 2×10^4 cfu ml^{-1}.

Samples were spun at 1000 *g* for 10 minutes and the supernatant discarded. Half of the pellets were freeze dried at -59°C, half stored at room temperature. Pellets were resuspended in peptone and plated on tryptone soya agar (TSA).

2.5.4 Bacterial Attachment to Fibres

Samples of fibre (F5, 50 cm and 100 cm) were added to Sterilin containers and sanitised by shaking with 5 ml ethanol (70 %) for one minute and then rinsed with 5 ml PBS for one minute. In addition containers without fibre were treated in the same way as a negative control to quantify the amount of bacteria transferred by the container alone. PBS (9 ml) was added to each of these containers.

S. epidermidis ATCC 35984 was grown to approximately 10^8 cfu ml^{-1} in tryptone soya broth (TSB) as above. The culture was centrifuged at 1000 *g* for 10 min, the nutrient media removed and the pellet of cells resuspended in the same volume of PBS pH 7.4. This culture was diluted 1:10 three times. A 1 ml aliquot was added to each container. The samples were incubated at room temperature for 15 minutes with a density of bacteria of 3.4×10^3 cfu ml^{-1}.

For each sample two independent series of six two-fold dilutions were made in a 96-well plate. From each dilution series 10 µl was spotted onto a TSA plate and incubated overnight and the colonies counted and the data were analysed using R.

The experiment was repeated with F1 fibres. Samples of F1 fibre (50 cm, 100 cm, 150 cm) were added to Sterilin containers and sanitised by shaking with 5 ml ethanol (70 %) for one minute and then rinsed with 5 ml PBS for one minute. In addition containers without fibre were treated in the same way as a negative control to quantify the amount of bacteria transferred by the container alone. Sterile PBS (9 ml) was added to each of these containers.

S. epidermidis ATCC 35984 was grown to approximately 10^7 cfu ml^{-1} in tryptone soya broth (TSB) as above. The culture was centrifuged at 1000 *g* for 10 minutes, the nutrient media removed and the pellet of cells resuspended in the same volume of PBS pH 7.4. This culture was diluted 1:10 three times. A 1 ml aliquot was added to each container. The samples were incubated at room temperature for 45-105 minutes with a density of bacteria of 1.5×10^3 cfu ml^{-1}, plated and analysed as above.

2.5.5 Ethanol to Kill Bacteria Attached to Fibres

Samples of fibre (F5, 50 cm) were added to Sterilin containers and sanitised by shaking with 5 ml 70 % ethanol (Fisher Scientific, UK) for one minute, then rinsed with 5 ml PBS for one minute. PBS (9 ml) was added to each of these containers.

S. epidermidis ATCC 35984 was grown overnight in tryptone soya broth (TSB) at 37°C and agitated at 60 rpm to approximately 10^8 cfu ml^{-1}. The culture was centrifuged at 1000 *g* for 10 minutes, the nutrient media removed and the pellet of cells resuspended in the same volume of PBS. This culture was diluted 1:10 three times. A 1 ml aliquot was added to each container. The samples were incubated at room temperature for 15 minutes with a density of bacteria of 1.2×10^4 cfu ml^{-1}. The diluted culture was decanted and 5 ml 70 % ethanol was added to the samples for 30 or 60 seconds or not at all. The ethanol was decanted and sterile 5 ml PBS was added to each container for 5 minutes.

For each sample two independent series of six two-fold dilutions were made in a 96-well plate. Spread plating is resource and labour intensive. To increase the number of measurements for each sample, serial dilutions were made in 96-well plates and spot plated. From each dilution series 10 µl was spotted onto a TSA plate and incubated overnight and the colonies counted.

3 Results and Discussion

3.1 Laser Scattering Analysis of Microspheres

PLGA 50:50 and 65:35 microspheres were manufactured by oil in water emulsion. This process produces microspheres with a wide particle size distribution. In addition the non-spherical particles are produced at the interfaces between the bulk solution and with the foam at the surface of the fluid and between the bulk solution and the walls of the vessel. The oversized particles are not desirable in the formulation as their haphazard structures may result in unpredictable release characteristics. In addition, non-spherical particles may skew the particle size distribution during laser scattering analysis due to their variable profile in the path of the laser beam. Therefore, all microspheres were sieved to below 90 μm using a mesh sieve prior to analysis.

Samples were dispersed in cyclohexane and kept in suspension in the analysis cell using a magnetic flea. Static and surface charging effects can cause microspheres to aggregate. Aggregates would be measured as larger particles, skewing the measured size distributions. To reduce aggregation the particles were ultrasonicated immediately prior to analysis. In addition, 1 % lecithin was added to the cyclohexane. This surfactant is intended to reduce between-particle interactions.

Label	Lactide:glycolide	10th Percentile (μm)	Median Diameter (μm)	90th Percentile (μm)
M1	50:50	13	53	127
M7	50:50	6	32	72
M8	65:35	7	35	75
M17	65:35	6	29	74
M18	65:35	10	39	75
M19	65:35	17	66	118
M20	65:35	10	42	98
M21	65:35	5	59	73
M22	65:35	4	25	54

Table 8: Tenth, fiftieth and ninetieth percentiles of microsphere particle diameter as determined by laser scattering analysis.

The median diameter of cisplatin microspheres made by homogenisation of PLGA/ethyl acetate in PVA solution was 25-66 μm (Table 8). By laser scattering particle size analysis the logarithm of the volume distribution plotted against the particle diameter showed different particle size distributions even between microspheres made under the same conditions (M17, M20, M21).

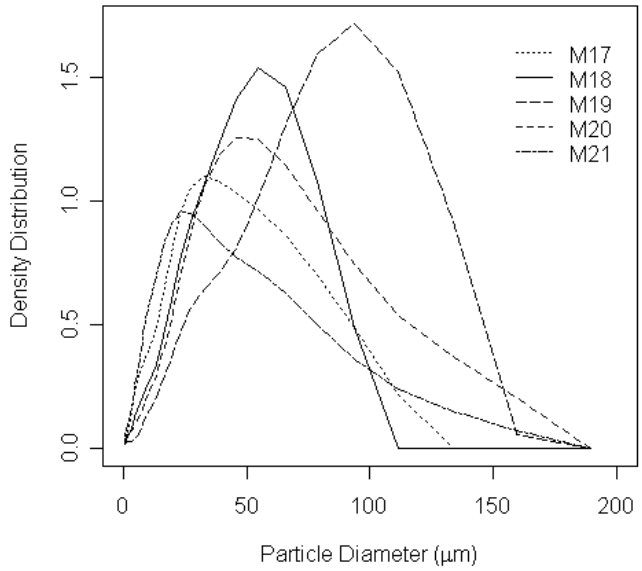

Figure 34: Particle size distribution of PLGA 65:35 cisplatin microspheres (M17-M21) determined by laser scattering.

Density distribution, Q3×log(2×*R*), against particle diameter, 2×*R*, shows that for these samples, most particles are 20-100 µm in diameter.

Figure 34 shows the particle size distribution of cisplatin microspheres. The differences in particle size distributions could be due to the profile of the oil in water emulsion during manufacture. Alternatively, similar starting particle size distribution formulations could be filtered to different extents due to differences in the sieving end point. Extent of static charging could alter the behaviour of the microspheres during sieving. Surface charging could also affect aggregation in cyclohexane suspension, despite the precautions taken. As expected sieving does not provide a clear particle size cut off. Whether this is a challenge for formulation depends on to what extent particle size effects drug release profiles (sections 3.4.2 and 3.4.3).

3.2 Physical Characterisation of Fibres

The diameter of sixteen pieces of each fibre was measured using a digital micrometer. Approximately 50 cm of each fibre was weighed and the volume determined by displacement of water in a measuring cylinder.

Sample	Diameter (mm)	Density (mg cm^{-3})
F1	0.44±0.06	210
F2	0.48±0.03	290
F3	0.48±0.05	270
F4	0.52±0.11	290
F5	0.59±0.02	240
F6	0.97±0.16	270
F7	0.65±0.05	220
F8	1.10±0.38	510
F9	1.27±0.08	280
F10	1.49±0.15	360

Table 9: Diameter and estimated density of PLGA fibres.
Diameters given as mean ± standard deviation.

Table 9 show the diameters and densities (sample calculations in Appendix J) of fibres. The lower density of the solid fibres (F1-F7) may be due to the larger pores (Figure 37) than present in the hollow fibres (F8-F10) (Figure 44). The differences in morphology could be caused by a higher concentration of residual NMP in solid fibres following soaking due to the lower surface area to volume ratio compared to hollow fibres (section 3.3). The carboplatin containing fibre, F6, was extruded through a larger orifice than other fibres due to the higher dope viscosity. The hollow fibres, F8 to F10, were extruded through a spinneret. The outer diameter of F9 fibres was calculated as 0.144±0.017 cm and of F10 fibres as 0.154±0.032 cm by image analysis of digital photographs. Analysis of covariance determined that the micrometer values were 0.012±0.005 cm lower than the image analysis values for these fibres (p = 0.03). This difference could be due to a slight crushing of the fibre during measurement.

3.3 Electron Microscopy Imaging

3.3.1 Microspheres

Microspheres were filtered using a stack of mesh filters of mesh sizes 106, 90, 58, and 38 μm. Particles greater than 90 μm were discarded. Particles less than and greater than 38 μm were imaged separately. Scanning electron microscopy images were taken of microspheres stuck to carbon tags.

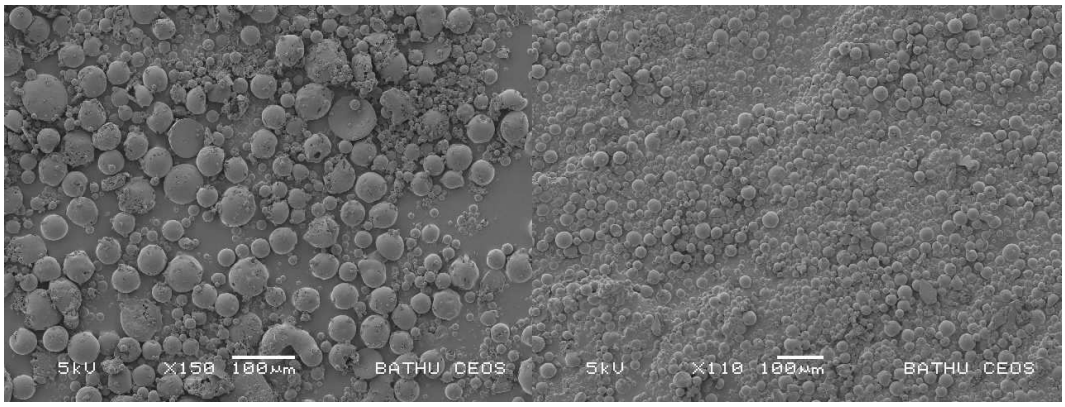

Figure 35: SEM image showing PLGA 65:35 microspheres.
Microspheres (M4) filtered to 38-90 μm and <38 μm. Bar is 100 μm.

The 38-90 μm fraction contained particles smaller than 38 μm. These particles are retained in the upper filters by electrostatic interactions with each other or larger particles. It was observed that larger fractions of microspheres tended to be less spherical. Non-spherical particles can be seen in Figure 35. Particle size distributions could not reliably be calculated from images because overlapping particles are not readily detected by imaging software. Small microspheres appeared to be more spherical and less misshapen than large microspheres. Some large microspheres had fractured to reveal their internal structure.

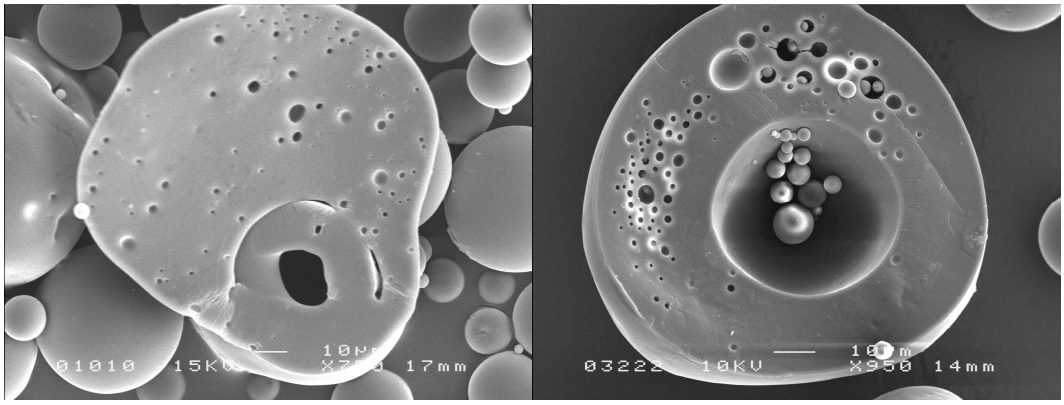

Figure 36: SEM image showing fractured PLGA 75:25 and 65:35 microspheres.
Microspheres which had fractured during freeze drying were observed in some images. Bar is 10 µm.

Figure 36 shows microspheres which had fractured, revealing their internal structure. This may have been caused by freeze drying, although it is also possible that shear forces during sieving were responsible. Fractured microspheres were composed of solid matrices with small internal pores. Although some pores were connected the majority were discrete. Some microspheres appeared to have engulfed other microspheres with shell-like pores surrounding some regions of a microsphere. This type of structure reflects the properties of the suspension from which the microspheres were formed. These cavities may have been formed during freeze-drying of microspheres with molten centres produced by the reduction in the rate of diffusion of the solvent following outer skin formation. The low porosity of these microspheres suggests that diffusion of drug will be slow as there are few aqueous channels to allow faster movement.

3.3.2 Fibres

Scanning electron microscopy and back scattering electron microscopy was performed on solid fibres. While SEM detects secondary electrons which are emitted from the carbon coating of the sample, back scattering detects electrons which are reflected directly back from the electron beam by the sample if it meets an electron opaque material such as platinum atoms.

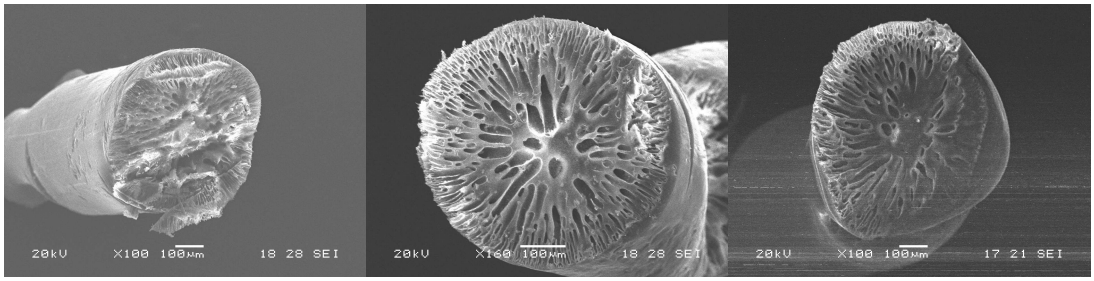

Figure 37: SEM images showing PLGA 65:35 solid fibres (F2, F3 and F5).
Bar is 100 µm.

Figure 37 shows a cross-section of F2, F3 and F5 fibres. The fibre had a smooth solid surface and a porous internal structure.

The increased porosity may caused by the higher concentration of residual NMP in the solid fibre during freeze-drying. The higher solvent concentration is caused by the longer diffusion path for solvent molecules between the centre of the fibre and the aqueous phase in solid fibres compared to hollow fibres. The excess solvent means that the polymer in the centre of the fibre has a lower glass transition temperature and is fluid. When the solvent it removed by freeze-drying the volume of the polymer is reduced, and as it aggregates voids are formed. An alternative theory is that the high porosity of the fibres is caused by the rapid entry of water into the stream of polymer dope during spinning. As the NMP dissolves into the water the polymer aggregates into a solid matrix leaving channels in the fibre. However, the water may not be able to freely enter into these small (~10 µm) channels given the relative hydrophobicity of high molecular mass PLGA. The low density of solid fibres (Table 9) compared to solid fibres could possibly be due to the larger pores present (Figure 37) compared to hollow fibres (Figure 44).

Once these channels become water filled they may be expected to increase the overall rate of diffusion of drug from the fibres since small molecules diffuse faster in water than in glassy matrices. However, the rate at which these pores become water-filled may be relatively slow due to the high contact angle of water with PLGA.

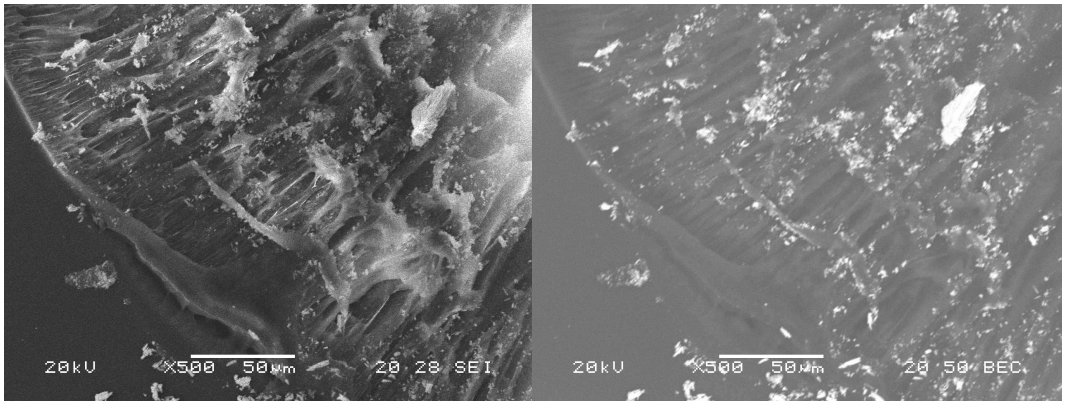

Figure 38: SEM and electron back scattering images of the same region of PLGA 65:35 cisplatin solid fibre (F2).
Images of fibre show co-localisation of crystalline structures and electron dense regions corresponding to cisplatin crystals. Bar is 50 µm.

Figure 38 shows SEM and back scattered images of the same region of F2 fibre. Structures which are electron opaque show as white on the back scattered image while electron transparent material is grey. As the small atoms (hydrogen, carbon) which comprise PLGA are known to be poorly electron reflective and the only expected large atoms are platinum and chlorine it is likely that white regions correspond to cisplatin crystals.

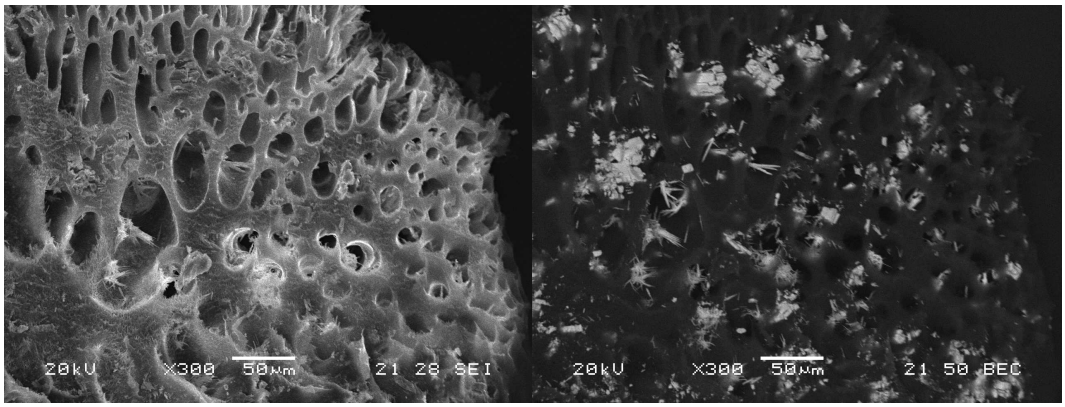

Figure 39: SEM and electron back scattering images of the same region of PLGA 65:35 cisplatin solid fibre (F3).
Images of fibre show co-localisation of crystalline structures and electron dense regions corresponding to cisplatin crystals. Bar is 50 µm.

Figure 39 shows needle shaped crystal structures in the pores of the F3 matrix which are revealed to be cisplatin crystals by back scattering imaging. Image analysis suggests that mean and median particles are around an order of magnitude larger in F3 fibres.

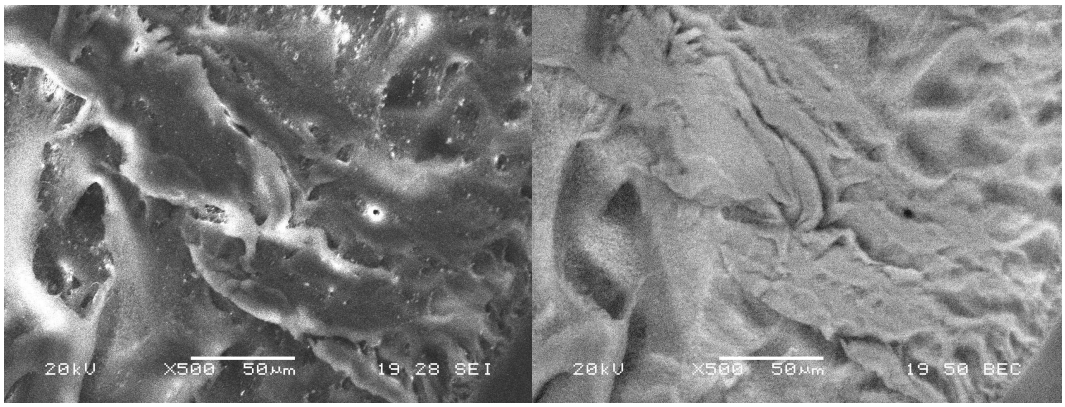

Figure 40: SEM and electron back scattering images of the same region of blank PLGA 65:35 solid fibre (F5).
Images of fibre show no crystal structures and no electron dense regions. Bar is 50 µm.

Figure 40 shows the SEM and back scattering image of F5 fibres. The absence of notable bright regions in the back scattering image is expected as F5 are blank.

Regions of F2, F3 and F5 fibres which appeared brightest under backscattering were analysed by X-ray microanalysis. The electron beam was focussed on the fibre and the X-rays generated by atoms which had been excited by the electrons were collected. The wavelength of the X-rays generated will be determined by electron transition energies in the excited atoms. As these transitions are distinctive, atoms can be identified based on their fingerprint on the X-ray spectrum.

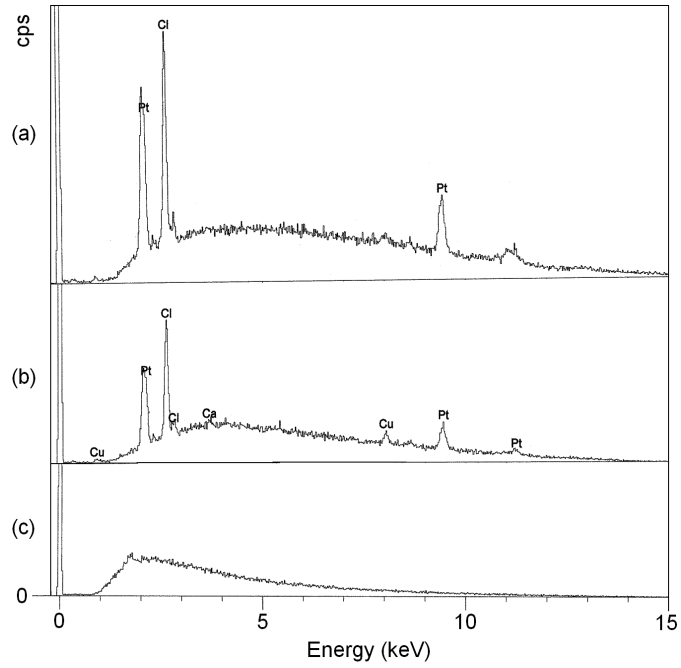

Figure 41: X-ray microanalysis of PLGA 65:35 solid fibres.

Two batches of fibres, (a) F3 and (b) F2, contained cisplatin. Peaks correspond to platinum and chlorine. One batch was a drug-free control, (c) F5, and shows no major peaks indicating that sample contains no elements heavier than sodium.

Figure 41 shows X-ray microanalysis plots for F2, F3 and F5 fibres. The hump of background radiation is braking-radiation (or Bremsstrahlung) emitted as the electrons slow down as they interact with the sample. The peak at the origin is caused by the beryllium window. The window screens low energy X-rays from low atomic weight atoms lower than sodium (Gedcke, 1972). Peaks from the polymer, such as carbon signals, are not detected. The detector units, counts per second, is not an absolute value as it depends on many factors and in addition is not consistent across the energy axis.

These plots show peaks corresponding to the strongest wavelengths of platinum (Mα/Mβ at 2.1 keV and Lα at 9.4 keV) and chlorine (Kα at 2.6 keV) in F2 and F3 fibres but not F5 fibres. This makes it very likely that a platinum salt is present. Small peaks which could correspond to trace amounts of copper and calcium were detected for F2 fibres. This contamination could have occurred at any of several stages during manufacture or analysis. They are not a significant contaminant of the polymer as they are not present in F5 fibres.

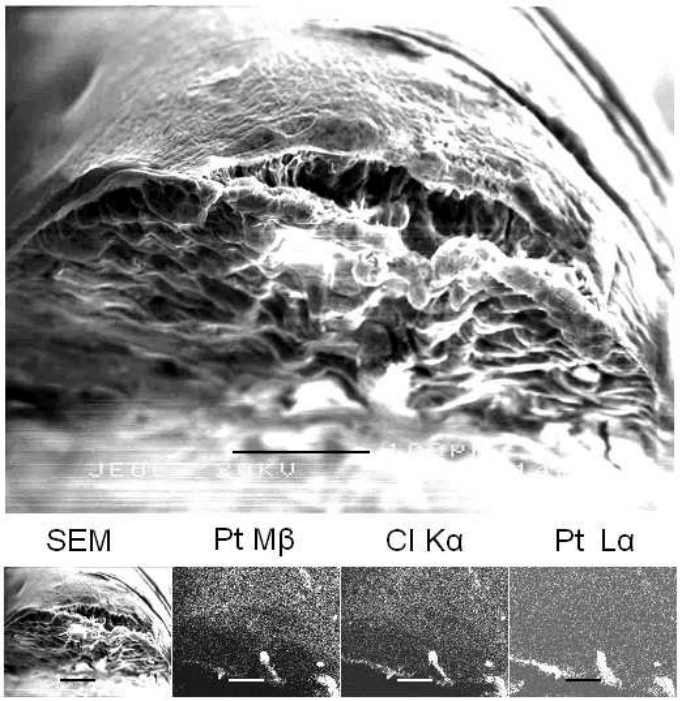

Figure 42: SEM image of PLGA 65:35 cisplatin solid fibre (F2) and associated X-ray maps.

X-ray maps recorded at wavelengths corresponding to platinum Mβ and Lα bands and chlorine Kα band. Bar is 100 μm.

To confirm that the platinum and chlorine were co-localised in the fibre X-ray maps were collected for F2 and F3 fibres. Figure 42 shows an SEM of F2 PLGA 65:35 cisplatin fibre and associated X-ray microanalysis maps. From the co-localisation of peaks at wavelengths corresponding to platinum Mβ and Lα bands and chlorine Kα bands it can be inferred that cisplatin is the major electron reflecting species in the fibre. These images show a single large cisplatin crystal with smaller particles dispersed throughout the fibre.

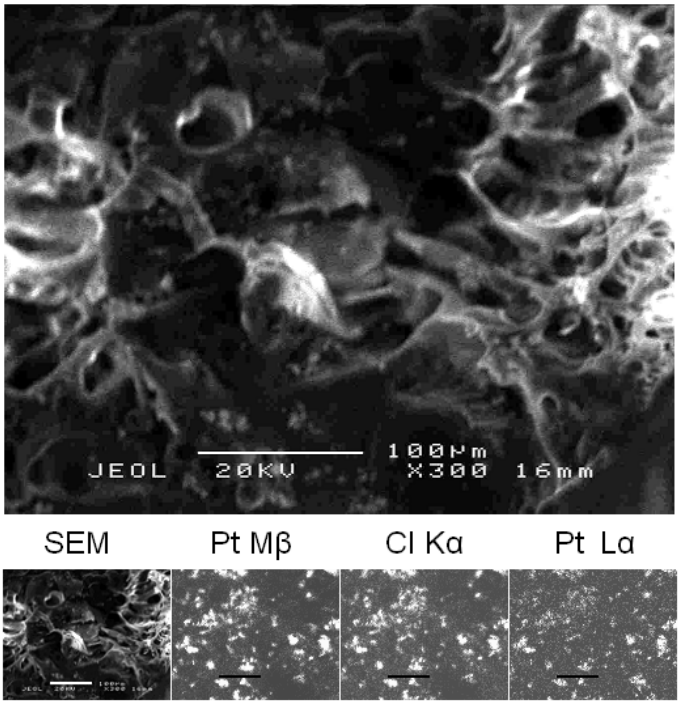

Figure 43: SEM image of PLGA 65:35 cisplatin solid fibre (F3) and associated X-ray maps.

X-ray maps recorded at wavelengths corresponding to platinum Mβ and Lα bands and chlorine Kα band. Bar is 100 µm.

Figure 43 shows an SEM of F3 PLGA 65:35 cisplatin fibre and associated X-ray microanalysis maps. As for F2 fibres the platinum and chlorine bands overlap but appear as a number of large crystals rather than smaller finely dispersed crystals.

Cisplatin particles appear in fibres as crystals, generally associated with pores rather than finely dispersed in the polymer matrix. Cisplatin was added to the dope early for F2 fibres and late for F3 fibres. Cisplatin in F2 fibres is more finely dispersed than for F3 fibres where individual crystals can be seen. It is possible that crystals of cisplatin had time to disaggregate in the F2 dope and become well dispersed during the extended mixing period.

Large crystalline aggregates of cisplatin dispersed in the matrix with direct contact between water and the drug avoided suggests that the system may act like a reservoir device. This is not satisfactorily modelled using the Higuchi equation (section 1.6.4), since the drug will dissolve into the matrix as it is removed, maintaining the drug

concentration at the maximum solubility of the drug in the matrix. Very finely dispersed crystals where the cisplatin is dissolved in the matrix will behave as described by Higuchi kinetics, eluting from an inert support. Differences between the release profiles of F2 and F3 fibres could be predicted from these X-ray maps.

SEM was also used to examine cisplatin containing PLGA 65:35 hollow fibres (F10).

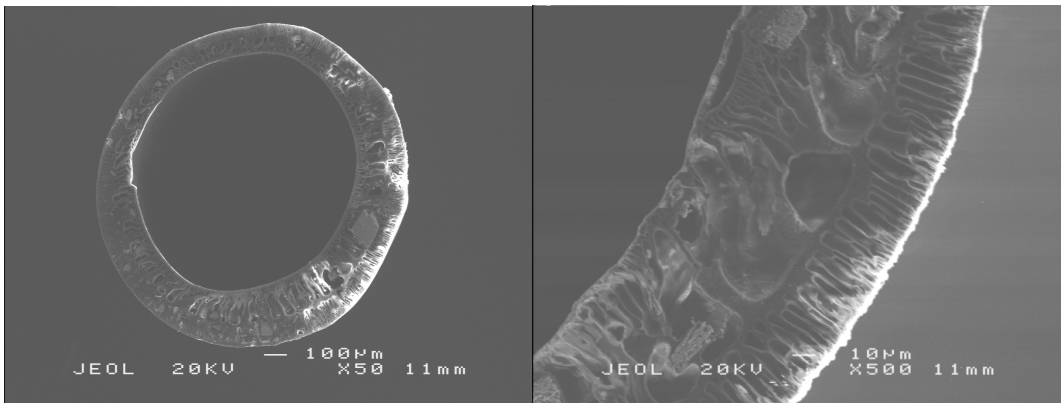

Figure 44: SEM images of PLGA 65:35 fibre (F10) and close up of section of wall. Bar is 100 µm and 10 µm.

Figure 44 shows a cross-section through the wall of a PLGA 65:35 hollow fibre. The matrix structure is similar to that observed for solid fibres (Figure 37) but different from microspheres (Figure 36). This suggests that there may be differences during matrix solidification during suspension solidification and phase inversion processes. Due to the short diffusion path length between the centre of microspheres and the aqueous phase, the matrix is not excessively porous. Conversely, water soluble organic solvents such as NMP rapidly partition out of the stream of dope. As the polymer loses its solvent and water begins to enter the fibre, voids are left in the structure, creating finger-like pores. These pores will create a faster alternative pathway for cisplatin release compared to the more dense structure of microspheres. This may be an advantage for fibres since their larger physical size may otherwise hinder drug release too much.

The effect of soaking F3, F4 and F10 fibres was studied following 1, 5 and 21 hours in distilled water. The aim was to determine whether drug dissolved throughout the

fibre matrix or from the edge in as assumed using the Higuchi model. The presence of finger-like pores suggests that drug will not be released from the outside in as water is able to more rapidly penetrate deep into the fibre.

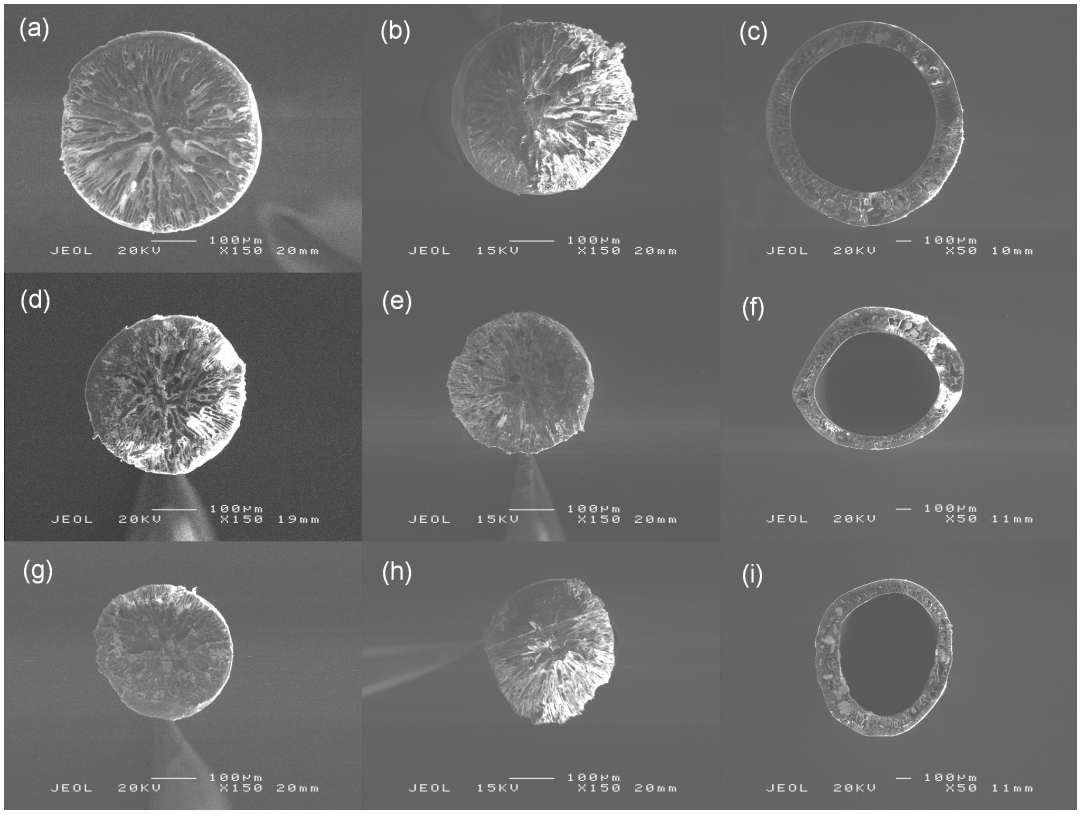

Figure 45: SEM images of PLGA 65:35 fibres after soaking in distilled water.
SEM images of F3 (a, d, g), F4 (b, e, h) and F10 (c, f, i) fibres before soaking (a, b, c), and after soaking for 5 h (d, e, f) and 21 h (g, h, i). Bar is 100 µm.

SEM images showed that fibres decreased in size after only a few hours in an aqueous environment (Figure 45). In addition the fibres appeared to become less symmetric. The backscattered images showed a trend of decreasing cisplatin. There was no clear pattern of cisplatin being removed from the edge of the fibre first with the advance of the solvent front predicted by the Higuchi model (section 1.6.4). This is due to the porous nature of the fibres.

For each data series, the area of the fibre and area of cisplatin were plotted against time. A linear model was fitted to these data. Plotting the area of the fibre against time showed that after soaking for 21 hours the fibres had shrunk. Solid F3 fibres

had decreased in area by a third and hollow F10 fibres were half the area. The gradient for F4 fibres cannot be interpreted individually as it was not strongly significant ($p = 0.099$). The area of cross-section and the area of drug both decreased so there was no significant change in the ratio of cisplatin area to fibre area.

To determine whether the decrease in fibre size and decrease in cisplatin area was significant for these structures the data were normalised and combined. Each data point was divided by the intercept (the mean initial area) of its linear model to give relative area. The mean initial area from the model was used rather than the mean at before soaking because each sample is an independent sample, not the same sample measured repeatedly.

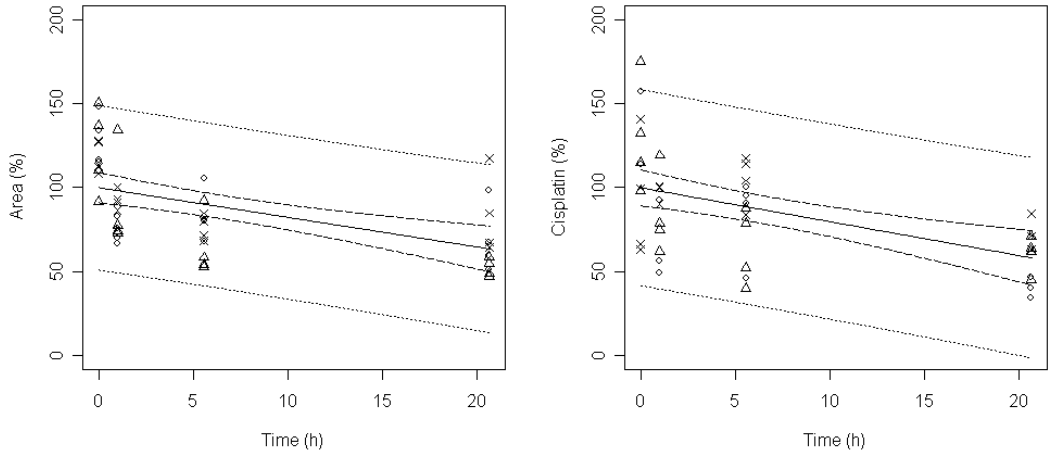

Figure 46: Decrease of normalised area of cross-section and area of cisplatin of PLGA 65:35 fibres.

Batches of PLGA 65:35 fibres, F3 (o), F4 (×) and F10 (Δ), were soaked for up to 21 hours, dried and imaged by SEM and backscattered electron imaging. Area of fibre and cisplatin for each sample was measured using R. Mean area used to normalise data was intercept of individual batch plots. Solid line is least squares best fit of combined data, dashed line is 95 % confidence interval of the model and dotted line is 95 % prediction interval.

Figure 46 shows the change in relative fibre and cisplatin area with time. There appears to be a large variability in the relative area of the fibres. This is because cross-sectional area varies with the radius squared. Analysing the aggregated data for all fibres predicted a decrease in cross-section area of -1.8±0.4 % h^{-1} ($p = 1\times10^{-4}$). This suggests that there would be changes in device morphology within a few hours of implantation. Assuming that the PLGA in the fibres degrades at a rate of

approximately 5×10^{-7} s^{-1} (see section 1.5.4.2) after 21 h, 4 % of the ester bonds will have hydrolysed. This is insufficient to explain the decrease of fibre cross-section of 37 %.

Analysing the combined cisplatin area data gave an estimated release gradient of -2.0±0.5 % h^{-1} ($p = 2\times10^{-4}$). Assuming that this linear gradient is an initial rate estimate of the exponential release model (equation 6) the rate constant can be calculated.

$$\frac{dX2}{dt} = -k_{21}M2(\infty)\cdot e^{-k_{21}t} \quad \textbf{(40)}$$

Equation 40, the differential of the two compartment model, can be solved for the boundary condition $t = 0$ and $dX2/dt$ = -2.0±0.5 % h^{-1}. This is the equivalent of a release constant of 6×10^{-6} s^{-1}. This calculation suggests that 34 % of the cisplatin has been released after 21 h. The estimate is approximately half the rate calculated from release curves (see section 3.4.4). It is possible that this discrepancy could be removed by analysing image intensity. Areas of dispersed drug in the matrix included in the image mask could not be distinguished from an equivalent area of solid crystal. Difficulties and expense involved with calibrating image intensity against drug loading do not make this a practical alternative to directly measuring drug release.

The average ratio of area of cisplatin to area of cross-section estimated as the intercept of the linear models is 29 %. This is close to the drug loading estimated for fibres. If the area of drug released corresponds to a decrease in the area of cross-section of the fibre then 17 % of the decrease is accounted for by the loss of cisplatin. This is insufficient to completely explain the 37 % decrease of area. A possible explanation for the larger than expected decrease in fibre area is that as the cisplatin is released the fibre contracts as the cisplatin crystals no longer support the structure. The reduction in the area of cross section of the fibres may be explained by the fibre becoming more hydrophilic as it begins to degrade. This may allow water to enter the finger-like pores and then crush some of them due to the attractive surface tension force between water on the pore walls.

These data show that the process of cisplatin release from a PLGA matrix does not occur by diffusion from a static matrix but rather a continual evolution in the size and porosity of the matrix with time.

3.4 Drug Release from Delivery Devices

3.4.1 Analysis of Published data of Release of Cisplatin from PLGA Microspheres

Although many formulations of cisplatin microspheres have been produced (section 1.5.4.5) very little kinetic analysis has been performed on the release profiles by the authors themselves. The release profiles of cisplatin microspheres produced by other authors were estimated from graphs in their papers. Due to the limited amount of data available only the two compartment model (equation 5) was fitted to the data (apart from Huo, 2005).

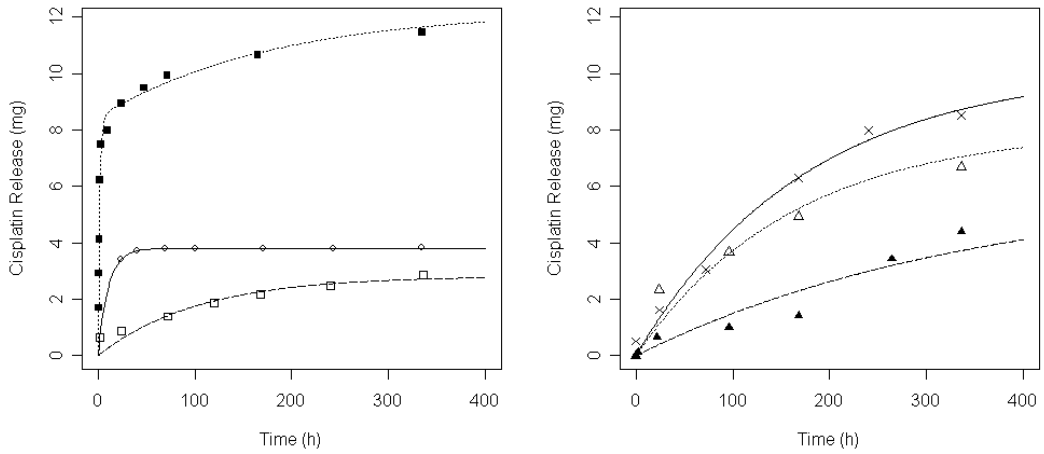

Figure 47: Published release profiles of cisplatin microspheres.
Data transformed to show release from 100 mg microspheres. Data from Ike, 1992 (o), Fujiyama, 2002 (□), Huo, 2005 (■), Araki, 1999 (×), Tamura, 2002 (▲) and Matsumoto, 2005 (∆). Lines show two compartment model, apart from Huo, 2005 which is three compartment model.

Figure 47 shows the release profiles of six formulations of cisplatin microspheres from the literature. Data were extracted from digital images in published papers using ImageJ (Abramoff et al., 2004). The two compartment model was fitted to these data using R. Data were published as percentage of total release. To allow

comparison between formulations the data were multiplied by the nominal drug loading claimed by the respective authors.

Author	Release constant (s^{-1})	Estimated release (%)	Nominal microsphere drug loading (%)
Ike, 1992	2.6E-05	95	4
Araki, 1999	1.6E-06	120	9
Fujiyama, 2002	2.7E-06	94	3
Tamura, 2002	7.9E-07	121	5
Huo, 2005	1.1E-04†	60	17
Matsumoto, 2005	1.7E-06	80	10

Table 10: Estimated percentage of cisplatin released and first order rate constant for six published polyester microsphere formulations calculated using a two compartment model†.

Data were extracted from digital images using ImageJ. Two compartment model was fitted to data using R. † Huo, 2005 data was a better fit to a three compartment model.

Table 10 shows the estimated first order rate of drug release for six published PLGA microsphere formulations (section 1.5.4.5). Data from Huo, et al., 2005 fit a three compartment model better than a two compartment model when the models were compared using ANOVA ($p = 7\times10^{-4}$) and AIC. Based on the three compartment model 72 % of the nominal cisplatin loading was released with a burst release constant of 1.5×10^{-4} s^{-1} and slow release constant of 1.5×10^{-6} s^{-1}. The claimed drug loading of microspheres by Huo, et al., 2005 was 17 %. However, based on the release profile reported, less than 72 % was released over the reported timescale. This suggests that the effective drug loading was 12 %. The difference could be due to an overestimation of the drug loading during sample analysis or due to inactivation of cisplatin by binding to the matrix (see effect of microsphere aging in section 3.4.3). The release profile of cisplatin from microspheres by Huo, et al., 2005 is not appropriate for sustained release as the majority of the drug in the depot is released within a few hours. Cisplatin microspheres in the literature have a drug loading of 3-12 %.

The groups who have previously reported the characteristics of cisplatin microspheres have used low molecular mass polyester (Table 3) of ~20 kDa. For this work high molecular mass PLGA (~100 kDa) was used (section 2.1.1). This was to attempt to reduce the rate of cisplatin release (section 1.5.4.2). In addition, spinning fibres requires a viscous dope. Higher molecular mass polymer has a higher viscosity. To ensure suitable spinning characteristics high molecular mass PLGA was used for spinning fibres. To allow comparisons to be made between formulations, microspheres were also manufactured using high molecular mass PLGA.

The release of cisplatin from the BSA containing microspheres of Araki, et al., 1999 was measured as total platinum. Since protein bound and unbound cisplatin was not determined separately, the amount of unbound drug is not recorded. The slower release is likely due to the release of BSA-cisplatin adduct which was able to form during formulation manufacture. Diffusivity of a species through a matrix is determined partly by its size. The large size of BSA (66 kDa) is responsible for the apparent slow release of BSA-cisplatin compared to unbound cisplatin. The tumour killing of these BSA containing microspheres was lower than cisplatin solution, suggesting that the hypothesis that unbound cisplatin is the major agent of tumour killing (section 1.4.3) is correct. Therefore, although the microspheres of Araki, et al., 1999 appear to have the most favourable release profile, the efficacy of the formulation as a successful chemotherapeutic is questionable.

The microspheres with the most favourable characteristics reported for continuous release of cisplatin to date are those of Tamura, et al., 2002 and Matsumoto, et al., 2005 with drug loadings of 6-8 % and release constants of $0.8\text{-}2\times10^{-6}$ s^{-1}.

3.4.2 Cisplatin Release from PLGA 50:50 Microspheres

PLGA 50:50 microspheres were manufactured by oil in water emulsion (section 2.1.2). PLGA 50:50 was dissolved in ethyl acetate and dispersed in dilute PVA solution using a mechanical homogeniser. The microspheres were allowed to harden for four hours. The mixture was centrifuged and waste continuous phase-solvent solution was decanted and discarded. The microspheres were washed by resuspension in distilled water followed by centrifugation and removal of the

supernatant. This was repeated three times. The particles were then filtered and dried in a stream of air. The microspheres were then filtered using a sieve with a 90 µm mesh and the oversized portion discarded. The drug release profile of independent batches of PLGA 50:50 (M3 and M7) was determined in two experiments for known masses of microspheres in distilled water by AAS (sections 2.3.4). Rate of diffusion is proportional to the concentration gradient (section 1.6.5). Therefore, the rate constant will decrease if cisplatin accumulates in solution. The release medium was kept at sink conditions by completely refreshing the release medium at each time point. Sink conditions ensured that the release rate was not affected by an increase in drug concentration in the release medium.

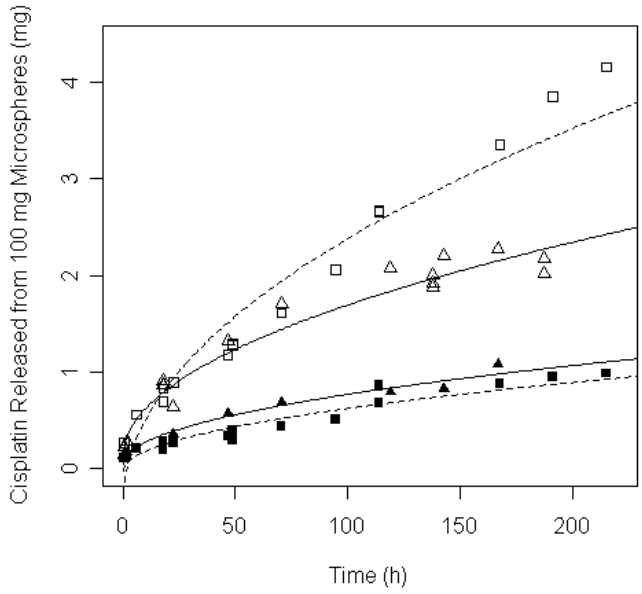

Figure 48: Cisplatin release from PLGA 50:50 microspheres.
Cumulative release from equivalent of 100 mg large (38-90 µm) (■, ▲) and small (0-38 µm) (□, ∆) PLGA 50:50 M3 (■, □, dashed lines) and M7 (▲, ∆, solid lines) microspheres into distilled water over nine days (n = 3). Lines show Higuchi model.

Figure 48 shows release of cisplatin from two batches of PLGA 50:50 microspheres which had been separated by mesh sieves to below 38 µm and between 38 and 90 µm. Twice as much cisplatin was released from small M7 microspheres than from the large fraction. Four times more cisplatin was released from small M3 microspheres after sixteen days than large microspheres. A mixture of large and small M3 microspheres had an intermediate profile (not shown).

The two batches of PLGA 50:50 microspheres showed similar release characteristics with the major difference being in the drug loading of the small microspheres. The lower drug loading of M7 microspheres is probably due to additional leaching of cisplatin from the microspheres during washing. The washing step is likely to be the major source of between-batch variation and should be carefully controlled.

The two compartment and Higuchi models could be fitted to each of the release profiles for large and small microspheres (Appendix L). There were insufficient data to fit three compartment and Fickian models.

Akaike's Information Criterion (AIC) (Akaike, 1974) allows comparison of mathematical models of data by comparing residual error with the number of parameters used (section 1.6.6). The AIC of both two compartment and Higuchi models were similar for these data which suggests that neither is better at explaining the data. The models can be used for different purposes. The two compartment model provides a release constant that can be used to compare release kinetics over long time scales. The Higuchi model can be used to estimate the diffusivity from equation 13, which may offer greater mechanistic insight.

The Higuchi constant, k, was $1.1 \pm 0.04 \times 10^{-3}$ mg $s^{-0.5}$ for large microspheres. The surface area of the sample can be estimated as 130 cm^2 (Appendix I) based on an approximate mean radius of 30 μm and a density of 780 mg cm^{-3}. Diffusivity of cisplatin from the microspheres can be estimated from the experimental values using equation 13. The solubility of cisplatin, C_s, is 2 mg cm^{-3} (section 1.4.1). The concentration of cisplatin in the sample ($M(\infty)/V$) was 1.2 % of the 100 mg sample or 0.012 mg mg^{-1}. This calculation predicts a diffusivity of 1×10^{-12} cm^2 s^{-1} which is within the range expected for a small molecule diffusing in a glassy matrix.

For small microspheres the Higuchi constant was $3.4 \pm 0.13 \times 10^{-3}$ mg $s^{-0.5}$. Using 10 μm as the approximate mean radius of the microspheres, the surface area of the sample was estimated as 380 cm^2. The concentration of cisplatin in the sample was 4.9 % of the 100 mg sample or 0.049 mg mg^{-1}. This calculation predicts a diffusivity of 5×10^{-13} cm^2 s^{-1}. Given the uncertainty present in the estimate reliable

determination of differences between these fractions cannot be rigorously claimed. Additional uncertainty was generated by using a rough approximation of the surface area. A more precise calculation could have been performed based on a particle size distribution. However, dynamic light scattering measurements were not performed for these samples due to the limited amount of sample available.

The two compartment model release rate constant, k_{21}, for large particles was $2.5\pm0.44\times10^{-6}$ s^{-1} and for small microspheres was $1.4\pm0.43\times10^{-6}$ s^{-1}. The difference in release constants corresponds to the difference seen in the diffusivities of cisplatin in large and small microspheres. Cisplatin loading was four times higher in small particles suggesting that loading is strongly dependent on particle size. This is an unfavourable characteristic of the method of oil in water microsphere production as larger (38-90 μm) microspheres would be preferred in a therapeutic formulation (section 1.5.4.6). In addition, variability in the particle size distribution has been shown for these formulations (section 3.1).

The rate of release of the PLGA 50:50 microspheres reported here was slower than release from the PLA microspheres of Ike, et al., 1992. The release profiles of PLGA 50:50 microspheres were similar to those achieved by the PLGA 75:35 microspheres of Fujiyama, et al., 2002 and the PLA microspheres of Tamura, et al., 2005 (section 3.4.1). The current recipe is an improvement over those reported formulations as the release profile is equivalent but the microspheres were manufactured using ethyl acetate rather than DMF or DCM, which are more toxic solvents (Appendix A).

3.4.3 Cisplatin Release from PLGA 65:35 Microspheres

PLGA 65:35 microspheres were manufactured by oil in water emulsion (section 2.1.2). PLGA 65:35 was dissolved in ethyl acetate and dispersed in dilute PVA solution using a mechanical homogeniser. The microspheres were allowed to harden for four hours. The mixture was centrifuged and waste continuous phase-solvent solution was decanted and discarded. The microspheres were washed by resuspending them in distilled water followed by centrifugation and removal of the supernatant. This was repeated three times. The particles were then filtered and dried in a stream of air. The microspheres were then filtered using a sieve with a 90 μm mesh and the oversized portion discarded. The drug release profile was determined

in four experiments for known masses of microspheres in distilled water by AAS (sections 2.3.4 and 2.3.8.1).

The level of batch variation in the production of PLGA 65:35 microspheres was determined by nonlinear mixed effects modelling. Four batches (M14, M17, M20, M21) were made under the same conditions from polymer dope made with 10 % PLGA to ethyl acetate. Two batches were made with 14 % (M18) and 18 % (M19) PLGA to ethyl acetate instead. The integrity of the baseline was confirmed for each experiment with blank (M13, M16) or phenolphthalein (M22) microspheres.

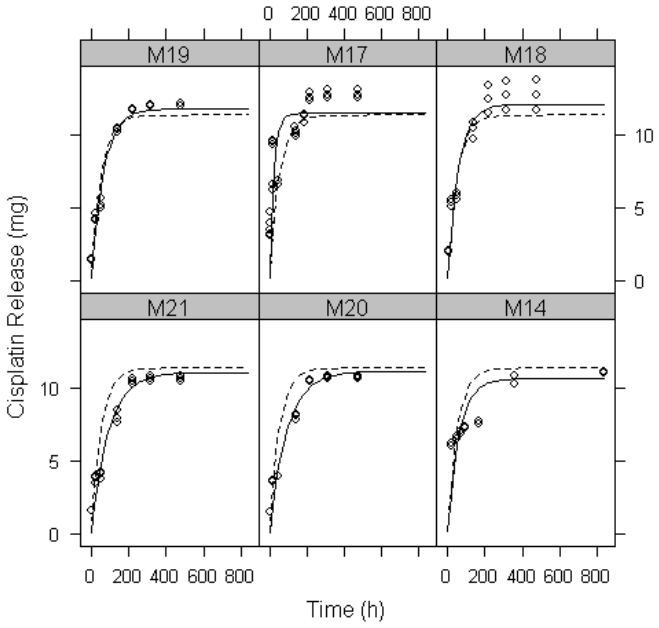

Figure 49: Cisplatin release from PLGA 65:35 microspheres.
Cumulative cisplatin release from 100 mg of six batches of PLGA 65:35 microspheres into distilled water over twenty days. Batches made with 14 % (M18) and 18 % (M19) polymer did not appear to have different release profiles from those made with 10 % (M17, M20, M21) polymer (n = 3). Data for M14 (n = 2) and M17 (n=3) were included. Dashed line shows two compartment model average for all batches. Solid line shows two compartment model for each batch (parameters in Table 11).

Figure 49 shows release of cisplatin from six independently manufactured batches of microspheres. The release profiles of all batches were similar. The two compartment model was fitted to the grouped data.

Batch	Release constant k_{21} (s^{-1})	Drug loading $M2(\infty)$ (mg)
M19	4.0E-06	12.1
M17	1.6E-05	11.2
M18	4.3E-06	12.6
M21	3.2E-06	10.8
M20	3.0E-06	10.9
M14	6.5E-06	9.5

Table 11: Parameters for cisplatin release for six batches of PLGA 65:35 microspheres calculated using a two compartment model.

Two compartment model was fitted to combined microsphere data (Figure 49) using R.

Table 11 shows the parameters for the two compartment model for each batch of PLGA 65:35 microspheres. There is some between batch variation of the release constant for PLGA 65:35 microspheres but the drug loading was reproducible. There appeared to be no correlation between the median particle size (Table 8) and the release rate constant (Table 11) for these batches. Non-linear mixed effects modelling of the two compartment model calculated that $M2(\infty) = 11.3 \pm 0.63$ mg and $k_{21} = 5.27 \pm 3.23 \times 10^{-6}$ s^{-1} (mean ± standard deviation) for the combined data.

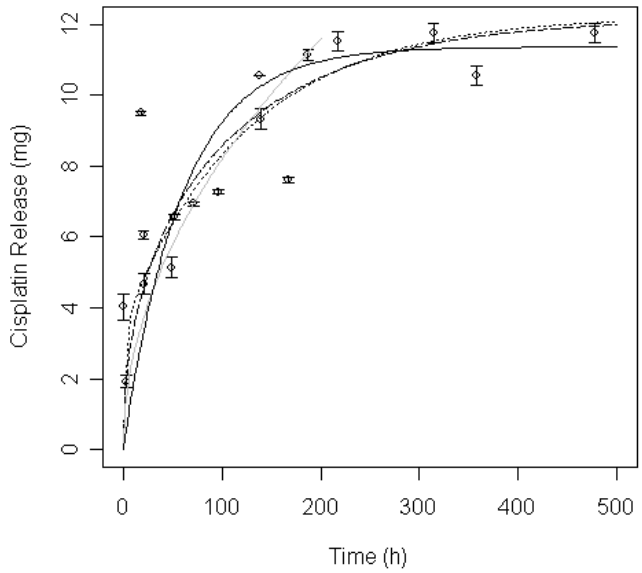

Figure 50: Four mathematical models were fitted to microsphere release data.
Two compartment (solid line), three compartment (dotted line), spherical Fickian (dashed line) and Higuchi (grey line) models were fitted to release data for PLGA 65:35 microspheres. Higuchi model was fitted only to data of the first 200 h of release. Data points of combined data with standard errors shown.

Figure 50 shows the four mathematical models (section 1.6) to which the data for the release of cisplatin from PLGA 65:35 microspheres were fitted. The spherical Fickian and three compartment models were found to have more explaining power as determined using Akaike's Information Criterion (AIC) compared to the two compartment model (Appendix L). The Fickian and three compartment models predicted similarly shaped release profiles. Although the two compartment model offers an acceptable description of the data it underestimates the amount of drug initially released (<48 h). As a large proportion of the drug (~50 %) is released during the first 48 h the suitability of using the two compartment to describe drug release from microspheres is called into question. The systematic error is of a similar order to the magnitude to the variance of the release profiles. This means that the systematic error may be small enough to ignore for some applications where only an approximation is needed, given the robustness of a single exponential.

It is not appropriate to use the Higuchi model with the complete dataset as this model assumes that the depot is infinitely deep (section 1.6.4). The data corresponding to only the first 200 h of release were fitted to the Higuchi model. The AIC cannot be used to compare the Higuchi model with the other models since the AIC assumes that the models have the same error structure (section 1.6.6). Although the comparison cannot be statistically rigorous, comparing the diffusivity as calculated by the Higuchi model with the spherical Fickian model is still of interest.

The Higuchi constant, k, was $1.34 \pm 0.00 \times 10^{-2}$ mg $s^{-0.5}$. The surface area of the sample can be estimated as 130 cm^2 (Appendix I) based on an approximate mean radius of 20 μm and a density of 780 mg cm^{-3}. Diffusivity of cisplatin in the microspheres can be estimated from the fitted value of k using equation 13. The solubility of cisplatin in water, C_s, is 2 mg cm^{-3}. The concentration of cisplatin in the sample is 11.3 % of the 100 mg sample or 0.113 mg mg^{-1} (Appendix I). This calculation estimates that the diffusivity of cisplatin in the microspheres is 1.3×10^{-10} cm^2 s^{-1} which is within the range expected for a small molecule diffusing in a glassy matrix.

The rate of cisplatin release is determined by the effective diffusivity of cisplatin in the formulation, D, and the particle radius, R according to the solution of Fick's second law for spheres (section 1.6.5.1). The Fickian model has been extended as the sum of the release profile as a function of the experimentally determined particle size distribution (Ritger and Peppas, 1987). However, this would require the calculation of the drug loading for each fraction of the particle size distribution as well as an accurate assessment of the distribution itself. More complicated interpretations of this model are computationally more demanding without offering major improvements in the accuracy of the estimate. To maintain the robustness of the calculation, R can also be more simply interpreted as the median particle size. By non-linear least squares regression for the first 120 terms in the Taylor series D/R^2 was calculated to be $1.02 \pm 0.13 \times 10^{-5}$ s^{-1}. The median radius of the six microsphere batches used in these experiments was estimated to be 20 μm. Using this approximation, the diffusivity was calculated as 4.1×10^{-11} cm^2 s^{-1}. This value is an order of magnitude lower than that predicted by Higuchi kinetics. This value may be a more accurate prediction as it takes the morphology of the microspheres and the finite nature of the drug depot into account.

The rate of drug release from the microsphere samples was estimated from the release data by dividing the amount of drug released since the previous sampling by the time elapsed since the previous sampling. The rate equation for the two compartment model was plotted by combing rate equation 4 with concentration equation 6. This can be used to define the rate in terms of the starting amount of drug, $M2(\infty)$, the release constant, k_{21}, and the amount of time elapsed since implantation, t (equation 41).

$$\frac{dX1}{dt} = k_{21} M2(\infty) \exp(-k_{21} t) \quad \textbf{(41)}$$

The rate equation for the three compartment model was plotted by combing rate equation 67 with the appropriate analogues to concentration equation 6, giving equation 42.

$$\frac{dX1}{dt} = k_{31} M3(\infty) \exp(-k_{31} t) + k_{41} M4(\infty) \exp(-k_{41} t) \quad \textbf{(42)}$$

These two and three compartment rate models were used to analyse the rate data. Analysing the rate data rather than the release profiles has the advantage that the large changes in rate during the early release will have proportionally less error than the smaller changes later towards the end of release. Since the fit will be dominated by the higher concentration, more accurate data, rate estimates should be improved.

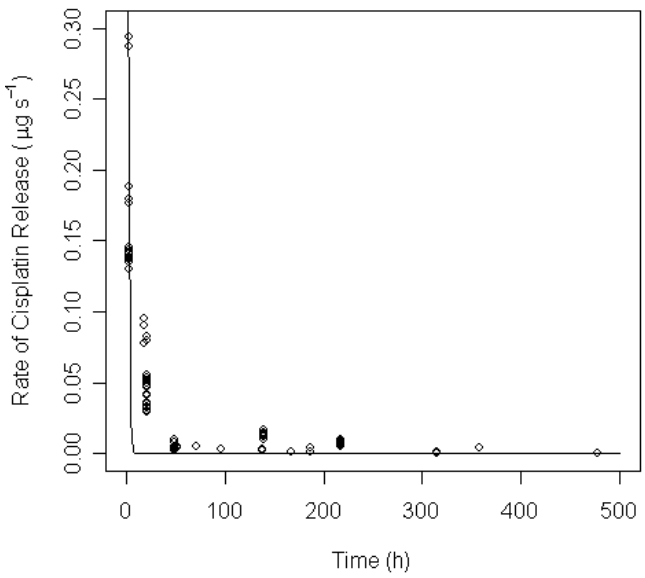

Figure 51: Rate of release of cisplatin from PLGA 65:35 microspheres.
Release rates were calculated by dividing the amount of cisplatin released from 100 mg microspheres since the previous sampling by the time elapsed since the previous sampling. Solid line shows two compartment model rate equation.

Figure 51 shows the cisplatin release rate against time for PLGA 65:35 microspheres. The release rate is initially high but quickly drops to close to zero during the first two days of release. The two compartment model estimated total cisplatin released as $M2(\infty) = 12.0 \pm 0.2$ mg (parameter ± standard error). The model was skewed by the very high initial release rate with $k_{21} = 2.7 \pm 0.08 \times 10^{-4}$ s^{-1} which is two orders of magnitude faster than when calculated using the release profile. The two compartment model describes the initial rate of release well but does not include the additional information about the slower release component. This supports the earlier observation that the three compartment model was a better fit than the two compartment model in that it distinguished between early and late release rates. The three compartment model did not converge on a solution. A larger dataset may be required to achieve convergence for this more complicated model. The sensitivity of the three compartment model suggests that it is not robust enough to be routinely used for analysing release profiles.

The release characteristics of additional samples of microspheres were determined both in water and in albumin solution (section 2.3.8.1). One batch of microspheres had been stored for five months at 5°C (<90 µm, M21). Three batches were freshly manufactured and sieved to between 38 and90 µm (M25, M26, and M27). The cisplatin concentration resulting from release from these four samples in the presence of protein was determined and the results are reported in section 3.6.2.

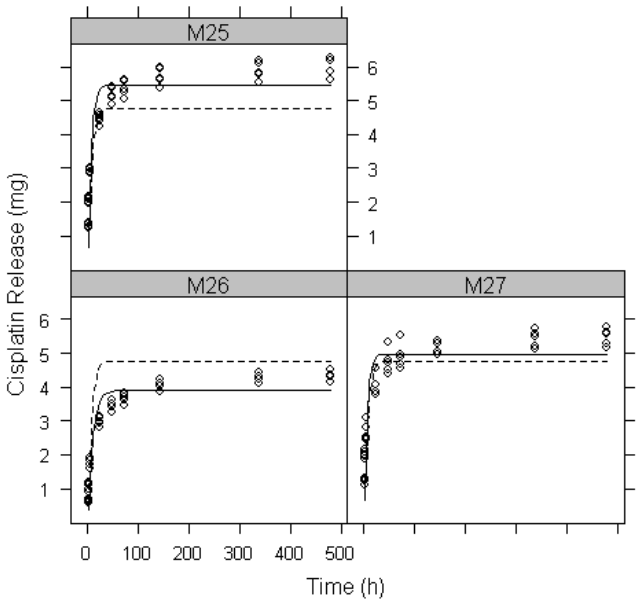

Figure 52: Release of cisplatin from large (38-90 µm) PLGA 65:35 microspheres.
Cumulative release of cisplatin from 100 mg of three independent batches of PLGA 65:35 microspheres (M25, M26 and M27) (n = 6). Microspheres had been sieved to between 38 and 90 µm. Dashed line shows two compartment model average for three batches. Solid line shows two compartment model for each batch (parameters in Table 12).

Figure 52 shows release of cisplatin from three independently manufactured batches of large microspheres. Although the drug loadings were lower than for samples which included smaller microspheres, the release profiles were of a similar form with negligible cisplatin being released after 200 h. Sample M26 released less cisplatin than the other two samples. This could be due to an inadvertently prolonged wash step or a different ambient temperature on the day of manufacture, causing decreased drug retention. An alternative source of error for these samples is the proportion of fine particles below 38 µm retained in the larger fraction during filtering.

Batch	Release constant k_{21} (s^{-1})	Drug loading $M2(\infty)$ (mg)
M25	4.6E-05	5.5
M26	2.6E-05	3.9
M27	4.8E-05	5.0

Table 12: Parameters for cisplatin release for three batches of PLGA 65:35 microspheres calculated using a two compartment model.

Two compartment model was fitted to combined 100 mg of large microsphere (M25, M26 and M27) data (Figure 52) using R.

Table 12 shows the parameters of the two compartment model for PLGA 65:35 microspheres M25-M27 which had been filtered to between 38 and 90 μm. Using non-linear mixed effects modelling to fit the data to the two compartment model it was calculated that the drug loading, $M2(\infty) = 4.78 \pm 0.65$ mg and the first order release constant, $k_{21} = 4.04 \pm 0.87 \times 10^{-5}$ s^{-1} (mean ± standard deviation) for the combined data. This is less than half the drug loading of the equivalent mass of microspheres taken from a sample comprised of particles of the complete particle size distribution (<90 μm) (Table 11). This supports the observation in section 3.4.2 that large microspheres (39-90 μm) have a higher drug loading than small (<38 μm) microspheres.

The data were also fitted to the spherical Fickian and three compartment models. The Fick's second law model was calculated using the first 120 terms of the Taylor series (parameters of the Fickian, two and three compartment models are shown in Appendix L). The Higuchi model was not applicable since the data was collected until complete release. As was observed for the samples M14-M21, the three compartment model described the data better than the two compartment model (the AIC was lower). The spherical Fickian model described a similar profile. The Fickian model was used to calculate the diffusivity assuming a mean particle radius of 30 μm. Diffusivity was 1.3×10^{-11} cm^2 s^{-1} for M25 and M27 and 7.1×10^{-11} cm^2 s^{-1} for M26 microspheres. The diffusivity of cisplatin in these large microspheres (38-90 μm) is within an order of magnitude of the diffusivity of cisplatin calculated from the combined microsphere data with the complete particle size distribution (<90 μm). Given the approximations used for calculating the radius of the particles differences

between these samples can not be conclusively determined. Although the rate constants are different between large and small microspheres, for both types of sample the Fickian and three compartment models were a better fit. This suggests that although the two compartment model may give a useful approximation of the release profile, it does not give an accurate mechanistic description. The assumption that cisplatin is released from microspheres at a constant rate with only the amount of remaining drug in the depot determining how much drug is released is not accurate.

The release profiles of cisplatin from a batch of microspheres when freshly made (section 2.3.4) and after five months cold storage (section 2.3.8.1) were compared.

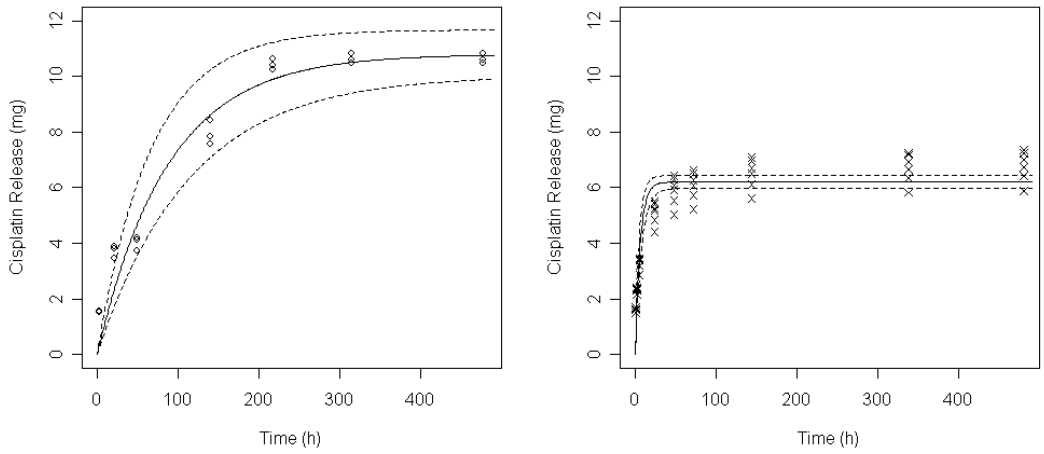

Figure 53: Effect of ageing on microspheres.

Release was determined for M21 microspheres when they were freshly made (o) and after five months (x). Less cisplatin was released after ageing and release was quicker.

Figure 53 shows the effect of storing PLGA 65:35 microspheres at 5°C for five months. Approximately 10 mg cisplatin was released from 100 mg fresh microspheres over 200 h. Five months later, the same batch only released 6 mg from 100 mg microspheres over 50 h. The loss of cisplatin is probably due to reaction of cisplatin with the PLGA matrix. This is a disadvantage of slow release cisplatin formulations as it suggests that the shelf-life of the formulation is only a few months. Strategies to increase the length of time for which cisplatin slow release devices can be stored could include freeze-drying and storage at -20°C. Alternatively, a desiccant

could be used to keep the formulation dry to slow the rate of polymer hydrolysis and cisplatin decomposition and binding.

PLGA 65:35 cisplatin microspheres formulations show similar release characteristics to the best microspheres manufactured elsewhere (section 3.4.1). The drug loading is high at 11 %, similar to Huo, et al., 2005 but the release constant is two and a half orders of magnitude lower. The release constant of these formulations is around 5×10^{-6} s^{-1} which represents a similar control of release to formulations reported by Tamura, et al., 2002 and Matsumoto, et al., 2005 but with superior drug loading.

3.4.4 Cisplatin Release from Solid Fibres

Solid fibres were spun from a dope solution of PLGA 65:35 dissolved in NMP and were formed by phase inversion of the dissolved polymer into a solid fibre (section 2.1.3). The fibre must harden in water as the residual solvent must be allowed to fully diffuse out of the fibre and dissolve in the water bath. PLGA fibres are traditionally hardened overnight for solvent removal from the fibre (Ellis and Chaudhuri, 2006). As cisplatin also dissolves in water a prolonged hardening step will lower the drug concentration. For microsphere manufacture the drug loading is limited by cisplatin dissolving into the continuous phase during emulsion, hardening and washing. The fibre can be handled from approximately 30 minutes following spinning. This observation has been exploited in this work to allow the drug loading to be increased. To prevent excess cisplatin being lost from the fibres, once the fibres were strong enough to be handled they were wrapped around cardboard supports. These coils of fibre were then freeze dried to remove water and remaining solvent. This method produced solid fibres with drug loadings higher than those previously seen for microspheres.

Solid fibres are larger structures that are easier to handle than microspheres. Their higher weight reduces handling difficulties which can be experienced due to static charging. Experimentally, fibres have the advantage that no depot material is lost as may occur when decanting release medium containing microspheres. In the event of a patient suffering an allergic reaction or other serious toxicity to the drug, a fibre can more easily be completely removed than microspheres. In addition, the mechanical properties of fibres could be used to provide physical support as a woven

patch or coiled stent. Fibres can also be more readily manufactured by a continuous process. Solid fibre manufacture could be a continuous method for manufacturing implantable pellets.

Label	Drug Loading (%)	Diameter (mm)
F1	0	0.44±0.06
F2	11	0.48±0.03
F3	24	0.48±0.05
F4	15	0.52±0.11
F5	0	0.59±0.02

Table 13: Drug loading estimated from release profile and diameter measured using a digital micrometer of cisplatin PLGA 65:35 fibres.
Diameter given as mean ± standard deviation (n = 12).

Table 13 shows the drug loading and diameter of PLGA 65:35 solid fibres. The drug loading is estimated from the cylindrical Fickian model. The drug loading of F2 and F3 fibres was measured as 10 % and 9 % by acid digestion of the fibre (section 2.3.3). The fibres were digested using *aqua regia* and the cisplatin was dissolved in HCl for analysis. The discrepancy for F3 fibres was probably caused by incomplete dissolution of the cisplatin in HCl. This is because 21 mg F3 fibre contained 5 mg cisplatin. As the loading was not expected to be so high, 1 ml HCl was used to dissolve this sample. As the solubility of cisplatin in water is 2 mg ml^{-1} the drug loading was underestimated more than two-fold. The cylindrical Fickian model appears to produce good estimates of the drug loading.

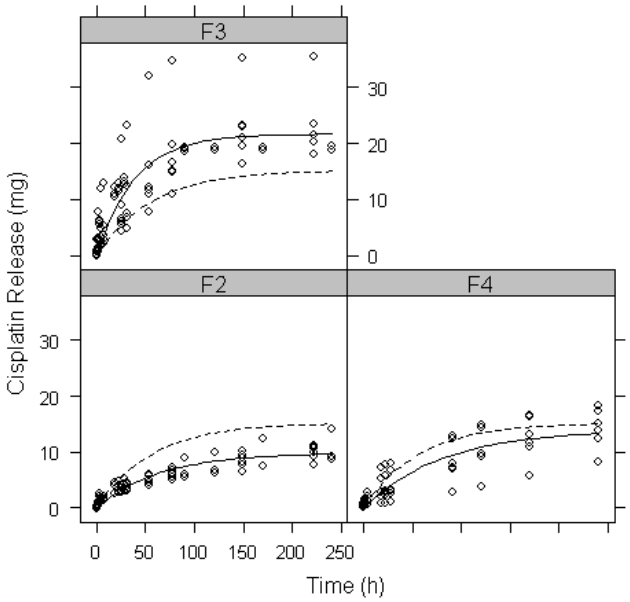

Figure 54: Release of cisplatin from PLGA 65:35 solid fibres.

Cumulative release of cisplatin from equivalent of 100 mg of three independent batches of PLGA 65:35 solid fibres (F2, F3, and F4). Dashed line shows two compartment model average for three batches. Solid line shows two compartment model for each batch (parameters in Table 14).

Figure 55 shows release of cisplatin from three independently manufactured batches of solid fibres. The two compartment model was fitted to the grouped data. The release profiles of all batches were quite different. One batch of fibres (F3) had a higher drug loading than the other batches but more variation in the release profile. Images of the cross-section of F3 fibres show heterogeneous distribution of large cisplatin crystals in the matrix (Figure 39). The variation observed in the release profile is probably caused by this poor dispersion of drug. This batch was manufactured from a dope to which cisplatin was added after the polymer had dissolved. For the other batches (F2, F4) the cisplatin was added at the same time as the polymer meaning that the drug had more time to become well dispersed.

Batch	Release constant k_{21} (s^{-1})	Drug loading $M2(\infty)$ (mg)
F3	7.4E-06	21
F2	4.2E-06	9.9
F4	3.0E-06	15

Table 14: Parameters for cisplatin release for three batches of PLGA 65:35 solid fibres calculated using a two compartment model.

Two compartment model was fitted to combined fibre data (Figure 54) using R.

Table 14 shows the parameters for the two compartment model for each batch of PLGA 65:35 solid fibres. There is significant batch variation of the release profiles. Non-linear mixed effects modelling of the two compartment model calculated that $M2(\infty) = 15 \pm 5$ mg and $k_{21} = 5 \pm 0.2 \times 10^{-6}$ s^{-1} (mean ± standard deviation) for the combined data. One batch (F3) had a higher drug loading and a rate constant that was twice as high as for the other batches. As each batch has different release characteristics they should be analysed separately (parameters in Appendix M).

F2 fibre was cut into 5 mg fragments and release into 1 ml distilled water was determined using AAS (section 2.3.5). To maintain sink conditions the release medium was decanted for analysis and 1 ml fresh water was added.

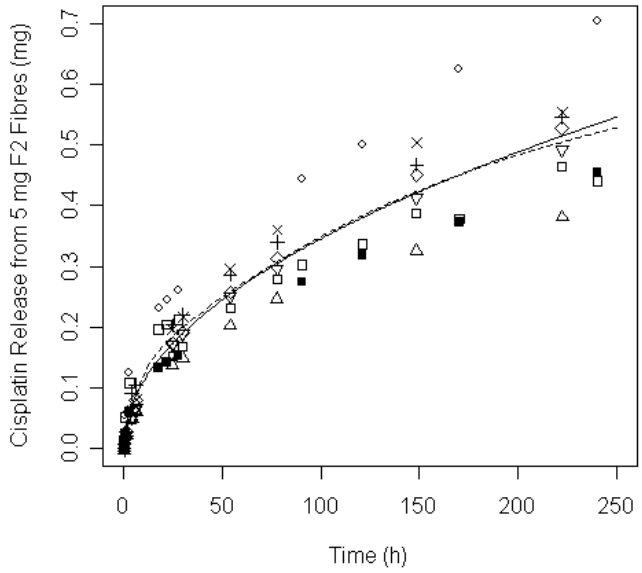

Figure 55: Release of cisplatin from PLGA 65:35 (F2) solid fibres.

Cumulative cisplatin release from 5 mg of PLGA 65:35 F2 fibres into distilled water over ten days (n = 9). Solid line shows Higuchi model. Dashed line shows three compartment model.

Figure 55 shows release of cisplatin from F2 fibres over ten days. Data from two independent experiments was combined to increase the analysis reliability. As the release profile has not levelled off during the experiment, the spherical Fickian model did not converge towards significant parameters. The Higuchi model produced the significant parameter, k, as $5.8 \pm 0.1 \times 10^{-4}$ mg $s^{-0.5}$ ($p < 2 \times 10^{-16}$). The diffusivity can be estimated using equation 13 assuming that each sample of fibre has a surface area of approximately 1.4 cm^2 (Appendix J). Based on a drug loading of 9.9 % and a density of 290 mg cm^{-3} the diffusivity, D, is estimated as 1.5×10^{-9} cm^2 s^{-1} which is within the range expected for a small molecule diffusing in a glassy matrix. This value is two orders of magnitude higher than the diffusivity calculated using Higuchi kinetics for microspheres. This difference could be caused by open pores in the fibre allowing faster diffusion than would be possible in a solid membrane. The drug loading is higher than for microspheres produced in this work and elsewhere. Parameters calculated are given in Appendix M.

The release profile of F3 fibres was determined in the same way. The only difference in manufacture between F2 and F3 fibres was that cisplatin was added to the dope after the polymer had fully dissolved rather than concurrently with the polymer.

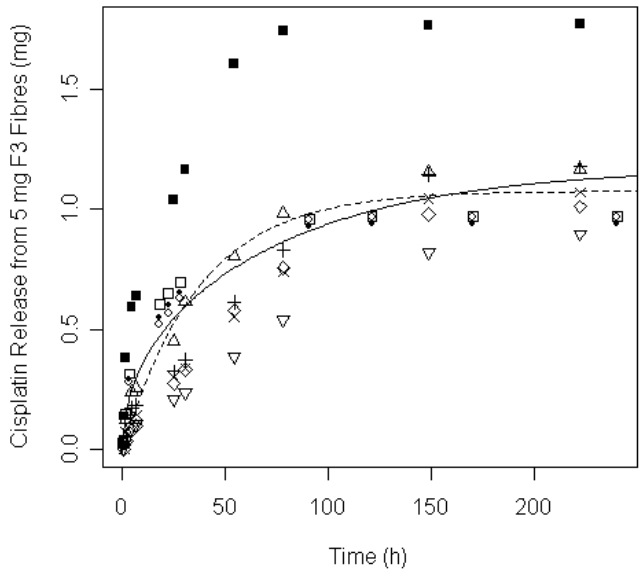

Figure 56: Release of cisplatin from PLGA 65:35 (F3) solid fibres.
Cumulative cisplatin release from 5 mg of PLGA 65:35 F3 fibres into distilled water over ten days (n = 9). Solid line shows cylindrical Fickian model. Dashed line shows two compartment model.

Figure 56 shows the release profile of F3 fibres. The fibres appear to contain more cisplatin than F2 fibres. One sample showed much greater release than others. This may have been due to a single large crystal being entrapped within the fibre and in addition to smaller, well dispersed crystals. The single replicate with the widely different profile may influence the analysis. However, with only nine replicates, it is not rigorous to exclude the series as an outlier as it may reflect the true properties of the fibre. The non-homogeneity in this sample suggests that adding cisplatin to the spinning dope after the polymer has dissolved produces poor fibres. If a drug depot contains an uncertain amount of cisplatin then the dose of drug cannot be controlled. A high dose could be extremely toxic for a patient. A low dose could be ineffective at controlling the disease. Since the therapeutic margin is small for cisplatin a depot which cannot be rigorously controlled is not appropriate for clinical use.

The parameters of the analysis using the four models are given in Appendix M. The two compartment empirical model calculated the drug loading to be 22 %. Not all of the parameters of the three compartment model were significant. The Higuchi model was a worse fit than the two compartment empirical model. The Higuchi model calculates the diffusivity to be 4×10^{-9} cm^2 s^{-1} using equation 13 from $k = 1.5\times10^{-3}$ mg $s^{-0.5}$, surface area of 1.5 cm^2, drug loading of 22 % and density of 270 mg cm^{-3}. This suggests that cisplatin travels almost four times faster in F2 fibres than F3 fibres. This difference may be an artefact of the pattern of the data influencing the model. Alternatively, it may be due to differences in the matrix structure. Release appears complete by around 100 h for F3 fibres. The qualitative observation that release is still occurring from F2 fibres after 200 h suggests that the Higuchi model has correctly identified real differences between these fibres. Not only are F3 fibres highly variable, they also have faster drug release, which is undesirable for continuous delivery devices.

The cylindrical Fickian model had the lowest AIC for this sample. By non-linear least squares regression for the first 120 terms in the Taylor series of the cylindrical model, D was calculated to be $3.4\pm1.0\times10^{-10}$ cm^2 s^{-1} assuming that the fibre had a constant diameter of 0.024 cm. This is an order of magnitude slower than the value calculated using the Higuchi model. The Fickian model is derived from a more complete physical model. Since the Fickian model is valid for the entire release profile it is likely that the estimate of diffusivity derived in this way is closer to the true value.

The release profile of F4 fibres was determined in the same way. F4 fibres were manufactured in the same way as F2 fibres with the cisplatin and polymer dispersed in NMP at the same time.

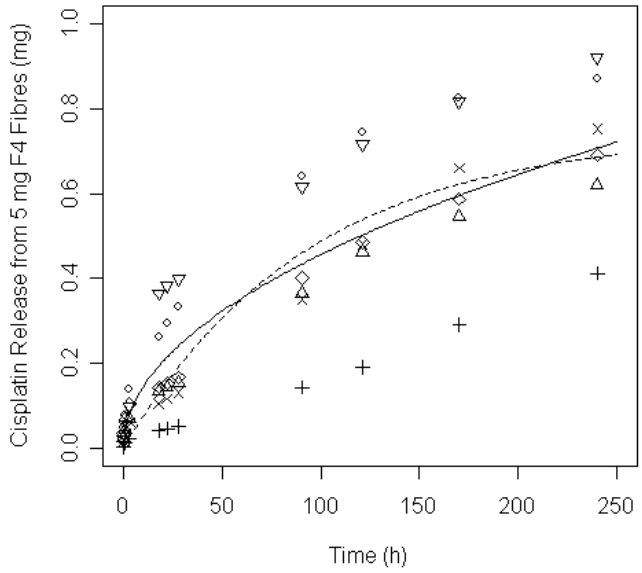

Figure 57: Release of cisplatin from PLGA 65:35 (F4) solid fibres.
Cumulative cisplatin release from 5 mg of PLGA 65:35 F4 fibres into distilled water over ten days (n = 6). Solid line shows Higuchi model. Dashed line shows two compartment model.

Figure 57 shows the release profile of F4 fibres. The fibres appear to have similar cisplatin loadings to F2 fibres. One replicate had a lower release rate, possibly with lower drug content. Although low drug content is safer than high content, this is still not a desirable property of the solid fibre. Variability in the drug loading could be caused by settling of suspended cisplatin during spinning.

The more linear profile of one replicate and the lack of a clear plateau meant that the empirical models were not good fits to the data. The Higuchi model was a better fit to the data than the empirical models. The two compartment empirical model predicted a drug loading of 15 %. By the Higuchi model (equation 13) the diffusivity is predicted to be 2×10^{-9} cm^2 s^{-1} using $k = 7.6\times10^{-4}$ mg s$^{-0.5}$, surface area of 1.4 cm^2, drug loading of 15 % and density of 290 mg cm^{-3}. The cylindrical Fickian model did not converge for this dataset so no significant parameters were generated.

Batch	Diffusivity (Higuchi) (cm^2 s^{-1})	Diffusivity (Fickian) (cm^2 s^{-1})
F2	2×10^{-9} ***	9×10^{-9}
F3	4×10^{-9} ***	3×10^{-10} ***
F4	2×10^{-9} ***	1×10^{-12}

Table 15: Diffusivity of cisplatin in PLGA 65:35 solid fibres calculated by Higuchi and Fickian models.

Model parameters, where significant at $p < 0.001$, are marked ***.

Table 15 shows the diffusivity of cisplatin as calculated by the Higuchi and cylindrical Fickian models. There is considerable variability in the diffusivity calculated by both models, with almost three orders of magnitude difference in the values calculated for F4 fibres. For this batch the Fickian model was a poor fit for the data and the parameters were not significant. This suggests that the non-significant parameters can be ignored. There was an order of magnitude difference between the significant parameters for release from F3 fibres. These fibres had the greatest within batch variation in the release profile. Therefore the diffusivity probably lies in the range indicated by these values.

This analysis suggests that for release profiles the simpler and more robust Higuchi model is more likely to achieve a likely estimate for the diffusivity. The diffusivity of cisplatin in PLGA 65:35 should be constant as long as the matrix is homogenous and has the same microscopic structure. However, images of the cross-section of these fibres (Figure 37) show that the microscopic structure of solid fibres is heterogeneous and may vary between (and within) batches. To be considered as a successful drug delivery formulation, the variability between and within batches must be reduced.

These results show that spinning solid fibres is a promising method for producing PLGA matrices with higher cisplatin loading than microspheres. A drug loading of up to 15 % for F4 fibres is an improvement over polyester microspheres produced here and elsewhere. The advantage of a high drug loading is that less excipient is implanted in the patient. Cisplatin should be added to the dope at the same time as

the PLGA rather than subsequently. Cisplatin is released from fibres manufactured in this way in a diffusion controlled manner for a period of ten days.

3.4.5 Cisplatin Release from Hollow Fibres

Hollow fibres were manufactured using a spinneret to create fibres with a hollow central bore. Fibres were spun from a dope solution of PLGA 65:35 dissolved in NMP and were formed by phase inversion of the dissolved polymer into a solid fibre (section 2.1.4). The fibre must harden in water as the residual solvent must be allowed to fully diffuse out of the fibre and dissolve in the water bath. PLGA fibres are traditionally hardened overnight for solvent removal from the fibre (Ellis and Chaudhuri, 2006). As cisplatin also dissolves in water a prolonged hardening step will reduce the drug loading. The fibre can be handled from approximately 30 minutes following spinning. This observation has been exploited in this work to allow the cisplatin loading of hollow fibres to be increased above that previously observed for polyester microspheres. To prevent excess cisplatin being lost, once the fibres were strong enough to be handled, they were wrapped around cardboard supports. These coils of fibre were then freeze dried to remove water and remaining solvent. This method produced solid fibres with drug loadings higher than those previously seen for microspheres.

Batch	Drug Loading (%)	Outer Diameter (mm)	Wall Thickness (mm)
F9	21-22	1.44±0.17	0.32±0.09
F10	27-28	1.54±0.32	0.30±0.12

Table 16: Drug loading and size of PLGA 65:35 hollow fibres.
Outer diameter (n = 60) and wall thickness (n = 120) of hollow fibres (mean ± standard deviation) calculated from photographs of cross-sections using ImageJ.

Table 16 summarizes the properties of F9 and F10 fibres. The fibre dimensions were determined from images of cross sections (see section 2.2.4). The release profile of F9 and F10 fibres was determined as for solid fibres.

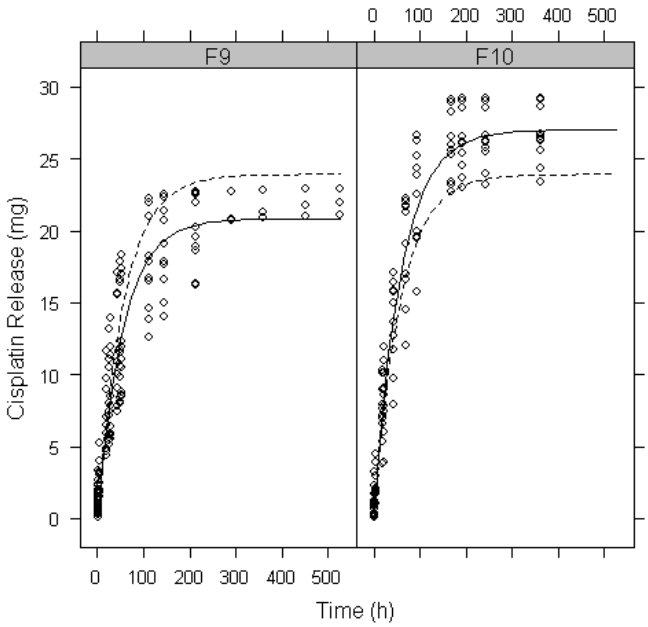

Figure 58: Release of cisplatin from PLGA 65:35 hollow fibres.

Cumulative release of cisplatin from equivalent of 100 mg of two independent batches of PLGA 65:35 hollow fibres (F9 and F10). Dashed line shows two compartment model average for two batches. Solid line shows two compartment model for each batch (parameters in Table 17).

Figure 58 shows release of cisplatin from two independently manufactured batches of hollow fibres. The release profiles of both batches were similar with high drug loading of over 20 % with significant drug release over 200 h. F10 fibres had a higher drug loading than F9 fibres. The two compartment model was fitted to the grouped data.

Batch	Release constant k_{21} (s^{-1})	Drug loading $M2(\infty)$ (mg)
F9	5.0E-06	21
F10	4.8E-06	27

Table 17: Parameters for cisplatin release for both batches of PLGA 65:35 hollow fibres calculated using a two compartment model.

Two compartment model was fitted to combined fibre data (Figure 58) using R.

Table 17 shows the parameters for the two compartment model for each batch of PLGA 65:35 hollow fibres. There is significant batch variation of the release

profiles. Non-linear mixed effects modelling of the two compartment model calculated that $M2(\infty) = 23.9 \pm 3.1$ mg and $k_{21} = 4.9 \pm 0.12 \times 10^{-6}$ s^{-1} (mean ± standard deviation) for the combined data. The batches were also analysed separately (Appendix N).

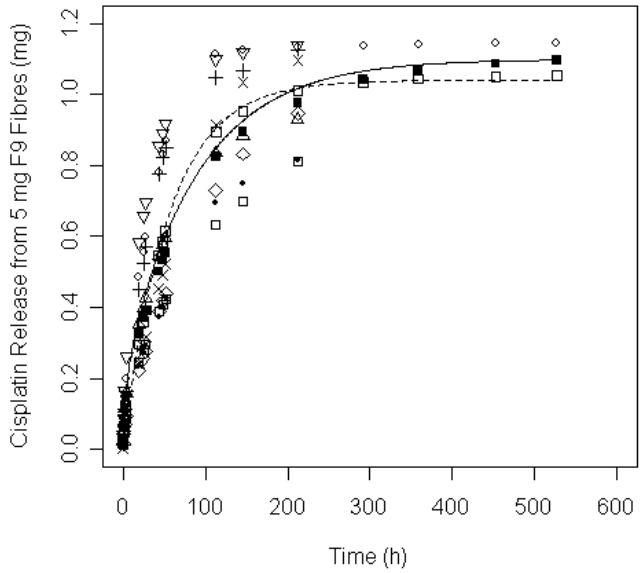

Figure 59: Release of cisplatin from PLGA 65:35 (F9) hollow fibres

Cumulative cisplatin release from 5 mg of PLGA 65:35 F9 fibres into distilled water over nine days (n = 7) and 24 days (n=3). Solid line shows hollow cylindrical Fickian model. Dashed line shows two compartment model.

Figure 59 shows the release profile of F9 fibres. The two compartment empirical model calculated the drug loading as 21 %. One of the parameters of the three compartment model was not significant. The Higuchi model was a less good fit to the data than the two compartment model. The diffusivity was 5×10^{-9} cm^2 s^{-1} for F9 fibres. This was calculated from the Higuchi model using equation 13, where $k = 1.7 \times 10^{-3}$ mg s$^{-0.5}$, surface area was 1.4 cm^2, drug loading was 21 % and density was approximately 270 mg cm^{-3}.

The hollow cylinder Fickian model was the best fit to the F9 data out of the four models. By non-linear least squares regression for the first 120 terms in the Taylor series of the cylindrical model, D was calculated as $3.3 \pm 0.3 \times 10^{-10}$ cm^2 s^{-1}.

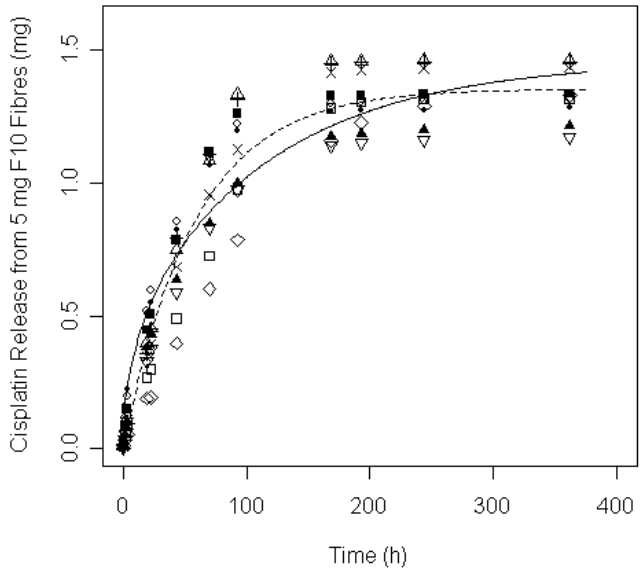

Figure 60: Release of cisplatin from PLGA 65:35 (F10) solid fibres

Cumulative cisplatin release from 5 mg of PLGA 65:35 F10 fibres into distilled water over sixteen days (n=10). Solid line shows hollow cylindrical Fickian model. Dashed line shows two compartment model.

Figure 60 shows the release profile of F10 fibres. The two compartment empirical model predicted a drug loading of 27 %. Two of the parameters of the three compartment model were not significant because the initial release was not a major proportion of the release profile. The Higuchi model was a poor fit to this complete dataset. By the Higuchi model the diffusivity is predicted to be 4×10^{-9} cm^2 s^{-1} by equation 13 using $k = 1.5\times10^{-3}$ mg $s^{-0.5}$, an estimated surface area of 1.4 cm^2, drug loading of 27 % and an estimated density of 270 mg cm^{-3}.

The cylindrical Fickian model had a similar AIC to the two compartment model. This suggests that both models have a similar explanatory power for the data. By non-linear least squares regression for the first 120 terms in the Taylor series of the cylindrical model D was calculated to be $2.3\pm0.3\times10^{-10}$ cm^2 s^{-1} assuming that the fibre had a constant diameter of 0.024 cm.

Batch	Diffusivity (Higuchi) (cm^2 s^{-1})	Diffusivity (Fickian) (cm^2 s^{-1})
F9	5×10^{-9} ***	3×10^{-10} ***
F10	4×10^{-9} ***	3×10^{-10} ***

Table 18: Diffusivity of cisplatin in PLGA 65:35 hollow fibres calculated by Higuchi and Fickian models.

Model parameters were significant at $p < 0.001$ where marked ***.

Table 18 shows the diffusivity of cisplatin as calculated by the Higuchi and cylindrical Fickian models. Since the Fickian model has significantly improved explaining power over the Higuchi model for both batches it seems probable that the Fickian model offers a better description of this system. Therefore the diffusivity of cisplatin in PLGA 65:35 hollow fibres is 3×10^{-10} cm^2 s^{-1}. The release profiles of both batches appear to be reliable given the high drug loading achieved.

The diffusivity of cisplatin in PLGA hollow fibres calculated using the Higuchi model (4×10^{-9} cm^2 s^{-1}) is similar to the diffusivity of cisplatin in PLGA solid fibres (2×10^{-9} cm^2 s^{-1}). This difference is similar to the difference in the rate constant for first order drug release. This suggests that properties of the matrix structure dominate the release rate rather than overall morphology of the depot.

The diffusivity of cisplatin in PLGA microspheres is much lower (1×10^{-10} cm^2 s^{-1}) than for fibres. This suggests that the matrix structure is similar between solid and hollow fibres. This outcome is expected as both formulations are manufactured by phase inversion of a stream of polymer dope into water. The matrices of solid (Figure 37) and hollow (Figure 44) fibres appeared similar under SEM (section 3.3.2) with finger-like pores orthogonal to the central axis of the fibre. Microspheres had a denser matrix that contained fewer, spherical pores (Figure 36).

Two different independent batches of hollow fibres were manufactured. These batches had very similar properties and low within batch variation. The mean drug loading for these batches was 24 % which is substantially higher than for microspheres and solid fibres. Drug was released over five days. Hollow fibres

represent a great improvement in formulation over microspheres for sustained cisplatin delivery with a 42 % reduction in the amount of PLGA needed to be implanted for an equivalent dose.

3.4.6 Effect of Ethanol Treatment on Cisplatin Release from Solid Fibres

Ethanol can be used to reduce the microbiological burden of surfaces in clinical applications. Treating microspheres and fibres was found to reduce the density of *S. epidermidis* (section 3.7.4). Because of that, this study has addressed the effect of this treatment on PLGA fibres. Solid fibres (F9 and F10) were treated with 70 % ethanol for one minute and then the release profile was determined.

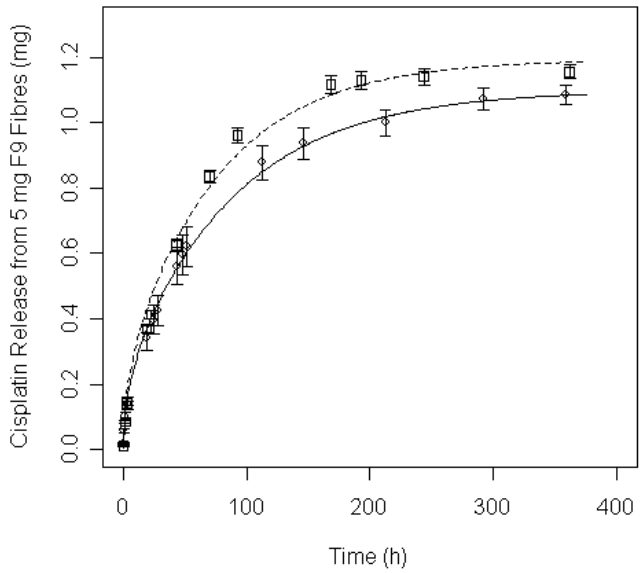

Figure 61: Effect of ethanol treatment on cisplatin release from PLGA 65:35 hollow fibres (F9).

Mean and standard error of cumulative cisplatin release from 5 mg of PLGA 65:35 F9 fibres into distilled water over sixteen days with (□) and without (○) ethanol treatment (n=10). Solid line shows cylindrical Fickian model for untreated fibre. Dashed line shows cylindrical Fickian model for ethanol treated fibre.

Figure 61 shows the effect of treatment with 70 % ethanol for one minute on F9 PLGA 65:35 hollow fibres. The diffusivity of cisplatin in F9 fibres is calculated by the cylindrical Fickian model to be $2.2\pm0.3\times10^{-10}$ cm^2 s^{-1} (95 % CI 1.7-

2.8×10^{-10} cm^2 s^{-1}) before ethanol treatment and increased to $2.7\pm0.3\times10^{-10}$ cm^2 s^{-1} (95 % CI $2.1\text{-}3.2\times10^{-10}$ cm^2 s^{-1}) after treatment (Appendix N).

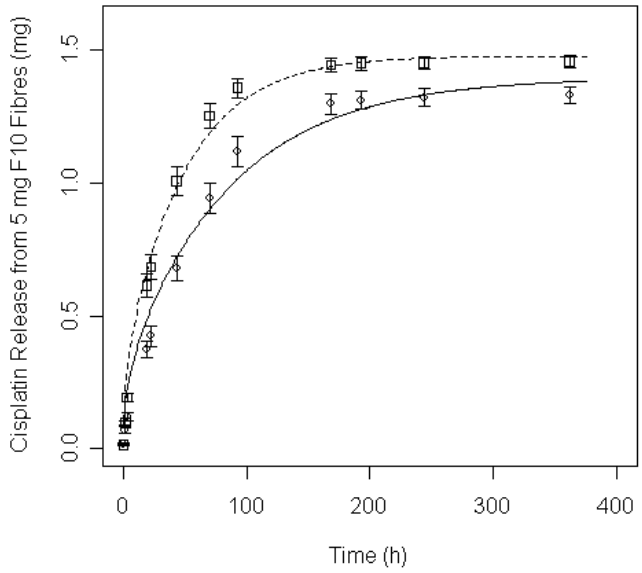

Figure 62: Effect of ethanol treatment on cisplatin release from PLGA 65:35 hollow fibres (F10).

Mean and standard error of cumulative cisplatin release from 5 mg of PLGA 65:35 F10 fibres into distilled water over sixteen days with (□) and without (○) ethanol treatment (n=10). Solid line shows cylindrical Fickian model for untreated fibre. Dashed line shows cylindrical Fickian model for ethanol treated fibre.

Figure 62 shows the effect of treatment with 70 % ethanol for one minute on F10 PLGA 65:35 fibres. The diffusivity of cisplatin in F10 fibres is calculated by the cylindrical Fickian model to be $2.3\pm0.3\times10^{-10}$ cm^2 s^{-1} (95 % CI $1.7\text{-}2.9\times10^{-10}$ cm^2 s^{-1}) before ethanol treatment and doubled to $4.4\pm0.3\times10^{-10}$ cm^2 s^{-1} (95 % CI $3.8\text{-}5.1\times10^{-10}$ cm^2 s^{-1}) after treatment.

For both F9 and F10 fibres the diffusivity of the fibres increased. Damage of PLGA structures by ethanol has been reported elsewhere (Shearer et al., 2006). The effect of treatment is likely to be real as it could be expected that ethanol causes disruption of the structure of the fibre and increased wetting of the polymer surface.

3.4.7 Carboplatin Release from Solid Fibres

Carboplatin is a cisplatin analogue with reduced toxicity, reduced efficacy at equivalent doses and negligible irreversible protein binding in the plasma (section 1.5.1). Carboplatin is more soluble in water than cisplatin and so harder to encapsulate in polyesters at high doses than cisplatin. To compare the formulation properties of carboplatin with cisplatin, PLGA 65:35 solid fibres were manufactured by phase inversion spinning (section 2.1.3). So that an equivalent amount of platinum was present in cisplatin and carboplatin containing fibres, the mass of carboplatin added to the polymer dope was higher than the equivalent mass of cisplatin. Carboplatin containing dope was too viscous to spin through the spinning needle. Carboplatin containing solid fibre (F6) was made by extrusion through a 5 ml pipette tip instead. Therefore, no morphological analysis was performed on carboplatin containing fibres. The major differences in manufacture suggested that SEM observation would not be useful for comparisons with cisplatin containing fibres. Fibres were observed to have a rough surface, possibly caused by the presence of large crystals incorporated in the matrix. This suggests an irregularity of the drug distribution that may make this formulation unsuitable for drug delivery applications.

Batch	Drug Loading (%)	Outer Diameter (mm)
F6	3-5	0.97±0.16

Table 19: Drug loading and diameter of carboplatin PLGA 65:35 solid fibre (F6). Diameter given as mean ± standard deviation (n = 12).

The wider diameter of the fibre (Table 19) than other solid fibres (Table 13) means that the cylindrical Fickian model is less applicable as the surface area of the ends of 5 mg fibres is a larger proportion of the total surface area.

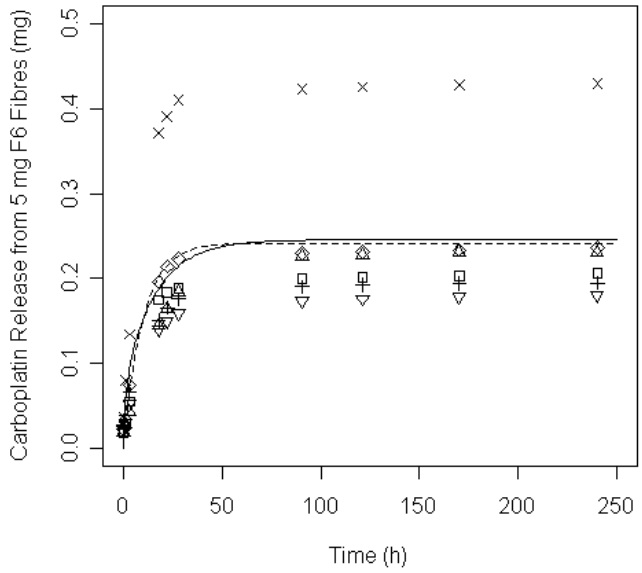

Figure 63: Carboplatin release from PLGA 65:35 (F6) solid fibres.
Cumulative carboplatin release from 5 mg of PLGA 65:35 F6 fibres into distilled water over ten days (n = 6). Solid line shows cylindrical Fickian model. Dashed line shows two compartment model.

Carboplatin was completely released from F6 fibres within 48 hours, around four times faster than for cisplatin. This faster rate of release would be expected as carboplatin is around seven times more soluble than cisplatin. The rate of diffusion of carboplatin is not even higher due to its higher molecular mass compared to cisplatin. The diffusivity of carboplatin in PLGA 65:35 solid fibres was $7.0 \pm 2.3 \times 10^{-9}$ cm^2 s^{-1} from fibre with a mean radius of 0.49 mm using non-linear least squares fitting to the cylindrical Fickian model (Appendix O).

One replicate released twice as much drug as the others. This is likely due to the incorporation of a large carboplatin crystal in that part of the fibre. This is an undesirable property for a drug delivery device which must give a reproducible release profile to be safely used. Micronisation of the carboplatin before it is added to the spinning dope may improve homogeneity of drug dispersal.

3.4.8 Summary of Release Studies

Ovarian cancer is one of the five most common causes of cancer death in women in the USA and UK. The tumour is generally well established in the peritoneum when diagnosed. Intraperitoneal therapy has been shown to improve survival for patients. Poly(lactide-co-glycolide) (PLGA) is a biodegradable polyester which has been proven safe for medical implantation. PLGA microspheres or fibres have been considered in this work as depots for delivering intraperitoneal cisplatin directly to the tumour site. PLGA 65:35 microspheres have been manufactured using the ethyl acetate that is a safer than solvents used for previously published formulations, such as DCM (Table 3). The microspheres produced by this improved method have higher cisplatin loadings than previously reported. Formulations with higher drug loading require less excipient.

PLGA 65:35 solid fibres have been manufactured with a typical drug loading of 15 % and an equivalent release constant to microspheres. PLGA 65:35 hollow fibres have been manufactured with a typical drug loading of 21 % and an equivalent release constant to microspheres. In addition, between batch and within batch variation of hollow fibres was relatively low compared to microspheres and solid fibres. Manufacturing fibres can be readily adapted to act as a continuous process, making scale up easier to achieve than for microspheres. Fibres could be sliced into pellets for intraperitoneal delivery of cisplatin. Carboplatin solid fibres were manufactured for comparison with cisplatin formulations. The longer residence time of carboplatin in an active form in blood plasma may reduce the advantage of regional delivery. The drug loading was lower for carboplatin (5 %) than for cisplatin solid fibres (15 %). Carboplatin was almost completely released within 24 h.

First order models such as the two compartment model are robust model and allow rapid comparison between formulations. The rate constants of the three formulations are similar ($3\text{-}5\times10^{-6}$ s^{-1}). Due to differences in the PLGA matrix the diffusivity of cisplatin in microspheres is an order of magnitude slower than in solid or hollow fibres. An additional exponential (three compartment model) improved the description of the data for microsphere formulations but was not necessarily an

improvement for fibres. The Higuchi model is only appropriate to describe early release from drug depots but is robust and can converge on a solution even for poor datasets. The Fickian models offer a good mechanistic description of drug release and can generate a physical parameter, the diffusion coefficient, directly. The disadvantage of this model is that is may not achieve convergence for poor or incomplete datasets. The diffusivity was determined for fast releasing F3 fibres but did not have sufficient information to resolve clear parameters for the more slowly releasing F2 and F4 solid fibres.

The Higuchi model systematically overestimated the diffusivity compared to the Fickian models. This is expected since increasing the range to which the model is fitted decreases the gradient of the model. This increases the value of k in equation 12. Since the Higuchi constant, k, is proportional to $\sqrt{D}$ fitting the Higuchi model to more than the initial release will increase the calculated diffusivity.

All models are approximations to reality, so considering several is the best way to inform interpretation of diffusion data.

3.5 Peritoneal pH

Release of cisplatin from PLGA depot devices was determined in water. This ensured that the release conditions or cisplatin detection were not disrupted by complex background matrices. Although PLGA degradation is pH sensitive (section 1.5.4.2) the change of pH of water was not detectable during release experiments. In addition, cisplatin was released from PLGA depots before major changes in the molecular mass could have occurred. For treating cancer patients, the PLGA devices would be implanted in the peritoneum. Significant physiological changes can occur at tumour sites. If the pH of the peritoneum is greatly altered during ovarian cancer the rate of drug release could be affected, reducing the efficacy or increasing the toxicity of the treatment. To determine whether the peritoneum deviates from physiological pH during ovarian cancer, the pH of samples of peritoneal fluid was determined for a stage III patient.

Peritoneal fluid was taken from the abdominal drain catheter and pH was measured immediately using a pH meter. The pH of the fluid was measured five times over five days. The pH was 7.4±0.1 (mean ± standard deviation). This is in agreement with the normal range of 7.4-8.1 for peritoneal pH (Noh, 2003). This suggests that rate of PLGA hydrolysis should not vary due to pH dependent effects. Therefore the rate of drug release should not be altered in the peritoneum by pH effects as it should remain close to neutral. Peritoneal fluid is a complex mixture of cells, small molecules, proteins and salts in solution. To determine the effect of the presence of nucleophilic groups, drug release was determined in the presence of a model protein solution (section 3.6).

3.6 Protein Binding of Cisplatin

3.6.1 Removal of Cisplatin from Solution by Albumin

Cisplatin exerts its therapeutic action by covalent attack of DNA (section 1.4.3). If cisplatin is sequestered by binding to nucleophiles in the serum or cell it is no longer available to cause tumour killing. Cisplatin binds to biological molecules with very high affinity. Unlike most drugs, unbound and protein bound cisplatin are not in equilibrium. Cisplatin becomes permanently bound nucleophiles. A well studied model protein is albumin. Albumin is present at ~40 mg ml^{-1} in serum. It is unlikely that albumin bound cisplatin retains therapeutic efficacy. Albumin contains a nucleophilic cysteine residue which is attacked by cisplatin (Espósito and Najjar, 2002). Cisplatin that is released from a biodegradable depot and passes into a cell will be sequestered by nucleophiles such as glutathione. As removal of cisplatin by pathways other than renal clearance is significant, the effect of permanent binding is important for fully understanding cisplatin therapy. Albumin was used as a model to demonstrate the effect of concurrent drug release and removal from solution. To detect the concentration of cisplatin remaining in solution at each time point the albumin was removed by cold ethanol precipitation of the protein (section 2.3.7).

A potential pitfall of this approach is that co-precipitation is indistinguishable from irreversible binding using this method. Adding ethanol to water reduces the solubility of cisplatin in the water. The solubility of cisplatin in 20 % ethanol in water solution is 1 mg ml^{-1}(Peleg-Shulman et al., 2001). However, for these experiments, 1 mg cisplatin is being released into 1 ml over several days with the release medium being repeatedly refreshed. The cisplatin concentration should be sufficiently low that free cisplatin is not precipitated during addition of the sample to ethanol. To confirm that cisplatin was not precipitating due to the change in solubility caused by the ethanol, the release profiles of F2 and F3 solid fibres were determined by release of cisplatin into water (section 2.3.5) and into water followed by ethanol precipitation, evaporation, chemical digestion and resuspended in 2 M HCl (section 2.3.8.2). The release profiles of the fibres (Figure 55 and Figure 56) show the combined datasets from two experiments where different sampling time

points were used. Despite the differences in experimental methods, both sets of data follow the same release pattern. This implies that no cisplatin had been removed by precipitation at the ethanol precipitation step when no BSA is present. To verify covalent cisplatin-protein binding, second method may be used. Appropriate techniques would be electrophoresis of the protein before and after binding, analysis of free thiols in the protein sample, or UV analysis to detect changes in the UV spectrum due to cisplatin binding.

Preliminary experiments showed that detection of low concentrations of cisplatin was possible in the presence of protein. The binding of cisplatin in solution to protein was compared by ultrafiltration and ethanol precipitation. Due to the heteroscedasticity of the dataset linear regression was performed using quasi-Poisson family linear model simplification. By linear regression from the saturated model (filtration method, time and the interaction) filtration method was found not to be a significant parameter ($p = 0.45$) using the F test.

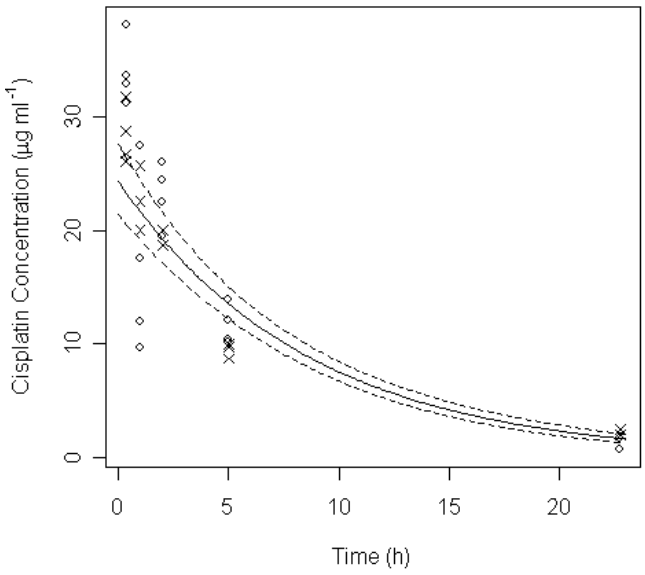

Figure 64: The concentration of unbound cisplatin in solution in the presence of BSA.

Protein removed by ultrafiltration (o) or protein precipitation (x) (n = 4). Solid line shows exponential of linear model of logarithm of data and dashed lines are 95 % confidence intervals.

The removal of unbound cisplatin from solution can be modelled as an exponential decay of the form;

$$C(t) = C(0) \cdot \exp(-k_b t) \quad \textbf{(43)}$$

where $C(t)$ is the concentration at time t, where $C(0)$ is the starting concentration and k_b is the binding constant.

The binding constant for the combined dataset is $6.1 \pm 0.92 \times 10^{-5}$ s^{-1}. This rate may be slightly underestimated if the concentration of binding sites on the BSA has fallen significantly during the course of the experiment. The rate of aquation determined elsewhere is 8×10^{-5} s^{-1} (Knox et al., 1986, Wenclawiak and Wollmann, 1996). The rate of aquation determines the maximum rate of observed protein binding so these values do not contradict each other.

3.6.2 Cisplatin Release from Microspheres and Binding to Albumin

In solution cisplatin binds to BSA. This reaction is effectively irreversible at biologically relevant concentrations. The concentration of unbound cisplatin in solution is predicted to be described by a two or three compartment model of protein binding (section 1.6.3). The rate of drug release will initially be high causing the concentration of drug in solution to rise. As the concentration of unbound cisplatin increases, the rate of protein binding will increase. The concentration of unbound cisplatin then decreases as both rates fall.

The concentration of unbound cisplatin was determined as above in the presence of a depot suspension of PLGA 65:35 microspheres (section 2.3.8.1). Drug concentration was measured by complete replacement of the release medium. The difference caused by the removal of cisplatin in the release medium should not affect measured results. The system is dynamic. Cisplatin is initially released at a faster rate than protein binding. This means that the concentration of unbound cisplatin will return to almost the same concentration as if the solution had not been removed. Therefore, instantaneous samplings should be equivalent whether or not the solution is replaced at each time point. In addition, this method avoids the possibility that the rate of

cisplatin-protein binding decreases as the number of nucleophilic sites on the BSA molecules falls.

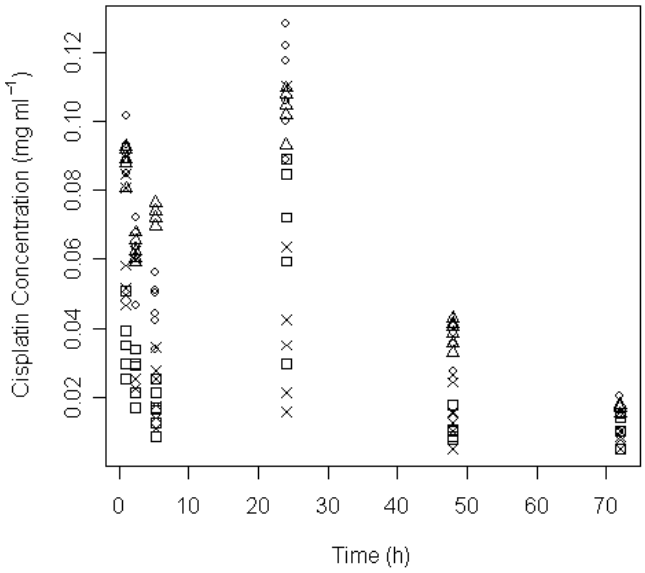

Figure 65: Unbound cisplatin concentration in BSA solution during cisplatin release from PLGA 65:35 microspheres.

Cisplatin concentration resulting from release from 8.3 mg PLGA 65:35 microspheres M21 (o), M25 (x), M26 (□) and M27 (Δ) and removal from solution by binding to BSA and cold ethanol precipitation (n=6).

Figure 65 shows the concentration of cisplatin in 1 ml BSA solution in the presence of 8.3 mg PLGA 65:35 microspheres. The concentration initially appears to fall but is higher than expected after 24 hours than would be predicted by a protein binding constant of 6×10^{-5} s^{-1} (section 3.6.1). Attempting to fit the two compartment protein binding model produced large errors for the final three time points (line of fit not shown).

The unexpectedly high values at 24 hours could be due to an unconsidered experimental variable such as transfer of microspheres into the digested portion of the sample. This is possible because the microspheres had to be removed from suspension by centrifugation which does not pellet all microspheres. Alternatively the longer sampling time between the third and fourth sample could mean that the rate of protein binding changed as the number of unoccupied binding sites reduced. This unusual profile makes definitive predictions for microspheres difficult.

Nevertheless, it is possible to see that the presence of BSA decreased the concentration of unbound cisplatin.

Subsequent experiments were carried out with fibres rather than microspheres that cannot be accidentally transferred into the sample for analysis. In addition, samples were taken at intermediate time points to provide more time points for the profile.

3.6.3 Cisplatin Release from Solid Fibres and Binding to Albumin

The irreversible binding of cisplatin to BSA during drug release from solid fibres was determined as above (section 2.3.8.2). The concentration of unbound cisplatin in solution is predicted to be described by a two or three compartment model of protein binding (section 1.6.3).

The release profile of PLGA 65:35 F2 (Figure 55) and F3 (Figure 56) solid fibres was determined in water (section 3.4.4). Concurrently the concentration of unbound cisplatin as it was released from fibres and bound to BSA was determined in BSA solution. Bound cisplatin was removed by cold ethanol precipitation of protein as for microspheres. The concentration of unbound cisplatin was determined as above in the presence of a depot suspension of PLGA 65:35 microspheres. Drug concentration was measured by completely replacing the release medium. Drug is initially released at a faster rate than protein binding. This means that the concentration of unbound cisplatin will return to almost the same concentration as if the solution had not been removed. Therefore, instantaneous samplings should be equivalent whether or not the solution is replaced at each time point. In addition, this method avoids the possibility that the rate of cisplatin-protein binding decreases as the number of nucleophilic sites on the BSA molecules falls.

Assuming that the three compartment model (section 1.6.3) is appropriate for describing the release and binding profiles, the amount of protein bound can be calculated using equation 44.

$$X_{bound} = M3(\infty) + M4(\infty) - \frac{k_b M3(\infty)}{(k_b - k_{31})} e^{-k_{31}t} - \frac{k_b M4(\infty)}{(k_b - k_{41})} e^{-k_{41}t} - \frac{k_{31}(k_{41} - k_b)M3(\infty) + k_{41}(k_{31} - k_b)M4(\infty)}{(k_{31} - k_b)(k_{41} - k_b)} e^{-k_b t} \quad \textbf{(44)}$$

The variance associated with the release profile was larger than the values for the cisplatin concentration due to the large difference in scale between the measurements. To demonstrate the difference between the proportion of drug released and the proportion of drug which had become bound, the three compartment model was applied to the normalized data to produce a mean profile of proportional cisplatin release in the presence of water only. The concentration profile in the presence of albumin was then normalized by dividing by the mean maximum cisplatin release from the paired experimental samples in water. The data were then subtracted from the mean proportional release profile and fitted to the three compartment model, using the values for $M3(\infty)$, $M4(\infty)$, k_{31}, and k_{41} from the mean proportional release profile (Figure 66). Using this model, k_b was calculated as 2×10^{-4} s^{-1}. The errors associated with this estimate cannot be calculated since the release profile has been coerced to fit by using the model as the background. However, individual datasets cannot any more rigorously be used since a different sample from the same batch was necessarily used for each repeat in the experiment.

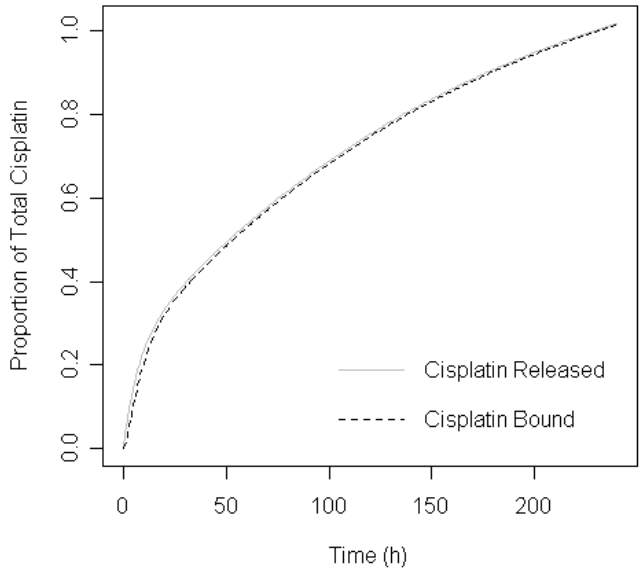

Figure 66: Proportion of cisplatin released from F2 fibres and proportion that has become protein bound.

Mean proportional cisplatin release was calculated by normalizing the release data and applying the three compartment model. The proportion of bound cisplatin was calculated by subtracting the normalized cisplatin concentration in the presence of cisplatin from the mean proportional release. The release constant, k_b was calculated as 2×10^{-4} s^{-1} using the three compartment model (equation 44). Data points have been omitted for clarity.

Since analysis of the relative amount of bound cisplatin was statistically unsound due to the high degree of processing needed for the data, the two (equation 8) and three (equation 9) compartment models were used directly for component of drug in solution. Although both the two and three compartment models were significant for F2 fibres, the three compartment model incorporating protein clearance did not converge to significant parameters for F3 fibres. However, the two compartment model was significant (Table 20 and Table 21).

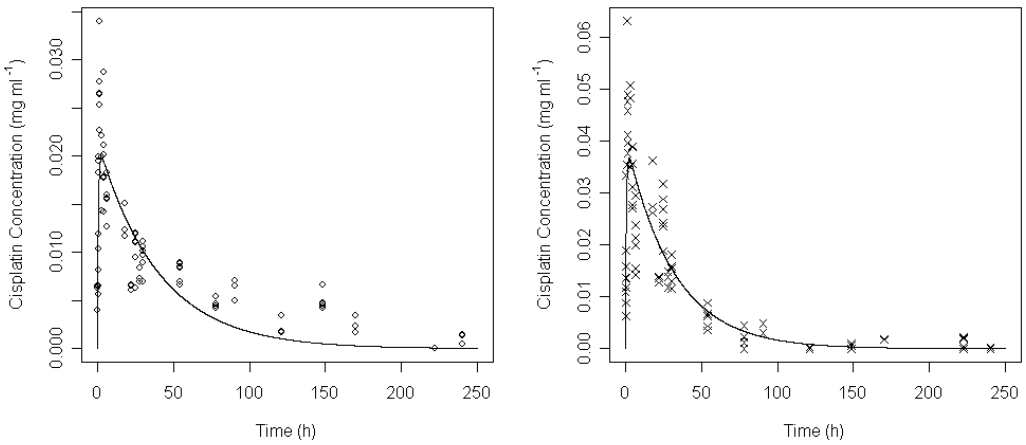

Figure 67: Unbound cisplatin concentration in BSA solution during cisplatin release from PLGA 65:35 solid fibres.

Cisplatin concentration resulting from release from 5 mg Fibres F2 (o), F3 (x), and removal from solution by binding to BSA (n=9). Solid line is predicted value using two compartment model with parameters shown in Table 20 and Table 21.

Figure 67 shows the concentration of cisplatin as it is released from F2 and F3 fibres (compared to Figure 55 and Figure 56) and concurrently removed from solution by binding to protein.

	F2 in water		F2 in protein solution	
	Mean	St. Error	Mean	St. Error
$M2(\infty)$ (mg)	4.93E-01***	2.00E-02	1.25E+00***	2.91E-01
k_{21} (s^{-1})	4.25E-06***	4.30E-07	6.98E-06***	8.71E-07
k_b (s^{-1})	-		4.09E-04***	7.90E-05

Table 20: Release parameters for release of cisplatin from PLGA 65:35 fibres (F2).

Parameters calculated by non-linear least squares regression using empirical two compartment model with and without protein binding term fitted to protein concentration in the absence or presence of BSA respectively. Parameters are marked *** as they are significant at $p < 0.001$.

	F3 in water		F3 in protein solution	
	Mean	St. Error	Mean	St. Error
$M2(\infty)$ (mg)	1.08E+00***	5.57E-02	1.82E+00***	4.66E-01
k_{21} (s^{-1})	7.45E-06***	1.16E-06	8.90E-06***	1.22E-06
k_b (s^{-1})	-		4.06E-04***	8.64E-05

Table 21: Release parameters for release of cisplatin from PLGA 65:35 fibres (F3). Parameters calculated by non-linear least squares regression using empirical two compartment model with and without protein binding term fitted to protein concentration in the absence or presence of BSA respectively. Parameters are marked *** as they are significant at $p < 0.001$.

This method appears to produce robust results for release of cisplatin from PLGA fibres. For F2 and F3 fibres binding constants were similar using the two compartment model. In addition the release constants were calculated to be similar whether protein was present or not. The total cisplatin present in each formulation was overestimated in the presence of protein although this is not surprising as the release constants, k_{21}, were somewhat overestimated. The rate constant for protein binding, k_b, is calculated $4.1\pm0.9\times10^{-4}$ s^{-1} by this method, higher than, $6.1\pm0.9\times10^{-5}$ s^{-1}, the value measured from protein binding of unbound cisplatin (section 3.6.1). This difference may be caused by the additional removal of cisplatin at each time point. It is also possible that the some component of the fibre increased the rate of protein binding. Alternatively, depot formation may increase the rate of aquation of cisplatin on its release.

The two compartment model successfully offers a reasonable approximation of the unbound cisplatin concentration when cisplatin is released from solid fibres in the presence of protein.

3.6.4 Cisplatin Release from Hollow Fibres and Binding to Albumin

The release profile of PLGA 65:35 F10 hollow fibres was determined in water (Figure 60) and in BSA solution as above (section 2.3.8.3). The two compartment model incorporating irreversible protein binding was used to analyse the concentration-time profile (section 1.6.3).

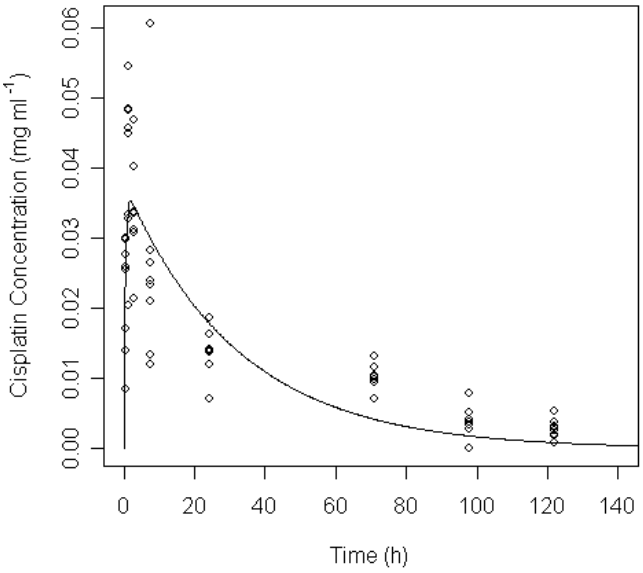

Figure 68: Unbound cisplatin concentration in BSA solution during cisplatin release from PLGA 65:35 hollow fibres.

Cisplatin concentration resulting from release from 5 mg F10 fibres and removal from solution by binding to BSA (n=9). Solid line is predicted value using two compartment model with parameters shown in Table 21.

Figure 68 shows the concentration of cisplatin as it is released from F10 fibres and concurrently removed from solution by binding to protein. As for solid fibres, the protein binding model was a better fit to this dataset than the data from microspheres. Drug concentration initially rises high, before dropping off as the rate of drug release from fibres falls.

	F10 in water		F10 in protein solution	
	Mean	St. Error	Mean	St. Error
$M2(\infty)$ (mg)	1.35E+00***	2.66E-02	2.99E+00**	9.88E-01
k_{21} (s^{-1})	6.99E-06***	5.44E-07	8.60E-06***	1.70E-06
k_b (s^{-1})	-		6.91E-04***	1.78E-04

Table 22: Release parameters for release of cisplatin from PLGA 65:35 fibres.
Parameters calculated by non-linear least squares regression using empirical two compartment model with and without protein binding term fitted to protein concentration in the absence or presence of BSA respectively. Parameters are marked *** as they are significant at $p < 0.001$.

Table 22 shows the parameters of the two compartment model in the presence and absence of BSA. Ethanol precipitation appears to produce robust results for release of cisplatin from PLGA fibres. The binding constant calculated is similar to that calculated based on release from solid fibres (see section 3.6.3). In addition the release constant, k_{21}, was calculated to be similar whether protein was present or not. As for solid fibres the total cisplatin present was overestimated in the presence of protein. The two compartment model successfully predicted the release profile of cisplatin released from fibres in the presence of protein and the results are consistent with *in vivo* values for cisplatin binding to protein.

3.6.5 Summary of Protein Binding Studies

Rate constant of protein binding of unbound cisplatin in solution, k_b, was 6×10^{-5} s^{-1}. The two compartment protein binding model for cisplatin release described the data for irreversible binding to protein following release from PLGA 65:35 solid (k_b = 4×10^{-4} s^{-1}) and hollow fibres (k_b = 7×10^{-4} s^{-1}). The model slightly overestimated the binding constant. This is because of additional removal of cisplatin during sampling that was not accounted for in the model. The method is useful as it does give relevant approximations. This method was not suitable for analysing microspheres due to transfer of microspheres in suspension which effected the measured drug concentrations. To the author's knowledge, this work has demonstrated for the first time that cold ethanol precipitation is a suitable method for determining rate parameters for irreversible protein binding of a drug.

3.7 Bacterial Attachment

3.7.1 Bacterial Attachment to Microspheres

Bacteria bind to all surfaces (section 1.7.2) but the affinity of binding is difficult to quantify. Attachment of *Staphylococcus epidermidis* to PLGA microspheres was observed under SEM (section 2.2.3). Microspheres were sieved before mixing with the bacterial culture so that only microspheres between 53 and 90 μm were present.

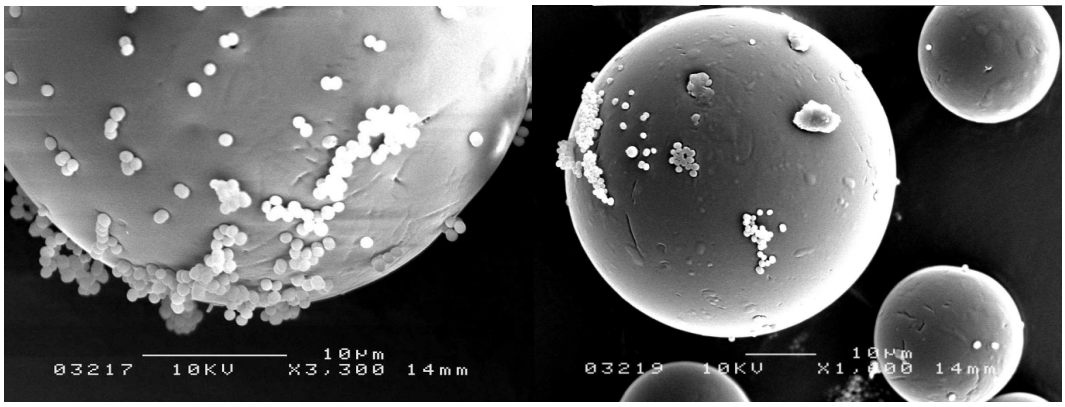

Figure 69: SEM images showing attachment of *S. epidermidis* to PLGA 75:25 microsphere.
Bar is 10 μm.

S. epidermidis were shown to bind to PLGA microspheres (Figure 69). Because the sample had been sieved using a 53 μm sieve, no bacterial sized microspheres were present. This was confirmed using a bacteria free control (not shown). Therefore, the numerous particles of 0.8 μm diameter can be identified as bacterial cells. In the first stages of bacterial attachment, the cells form weak interactions with the microspheres. These images show that the interactions are strong enough to allow attachment to microspheres within a few minutes. It would be interesting to be able to quantify rate of bacterial attachment. Since binding studies would be difficult, slow and expensive using SEM, viable cell count culture techniques were developed to attempt to assess rates of attachment of *S. epidermidis* to microspheres.

To quantify initial bacterial attachment *S. epidermidis* were briefly incubated in PBS with microspheres (section 2.5.2). The microspheres were separated from the culture by centrifuging the mixture at 100 *g*. Relatively slow centrifugation preferentially

sedimented the microspheres but not bacteria which had not become attached. The contaminated microspheres were then incubated with sterile PBS for one minute. As the initial attachment to microspheres is weak, the faster cells become attached in the first incubation, the more cells are available to become unattached during the second incubation. The microspheres were then removed by centrifuging the mixture at 100 *g*. The supernatant was diluted and spread plated on TSA.

Differences between the initial culture concentration and high variance of cell counts hindered analysis. The data were combined and analysed for trends using generalised linear models fitted using the R statistics package. A quasi-Poisson distribution was chosen for the error structure for this count data because negative counts were not possible (as would be allowed assuming a normal distribution). When a Poisson distribution was used for the error structure some outliers had too much influence on the model (leverage). A quasi-Poisson distribution has the same shape as the Poisson distribution but does not require that the mean equals the variance.

AIC cannot be used to compare quasi-Poisson models. Quasi-Poisson models allow the error structure to vary. This means that the likelihood function is not comparable between models (see section 1.6.6). Instead, significant parameters of the combined dataset for the four experiments were determined by model simplification using χ^2 ANOVA. Interactions between parameters could not be calculated due to insufficient sample sizes. For example, for some samples the microspheres were transferred to a fresh Eppendorf before plating. To determine whether this factor is significant a χ^2 test is performed comparing the model with and without transfer. Removing the parameter increases the overall deviance of the data from the model but adds one degree of freedom. The probability that this change is not significant is quite high ($p = 0.10$) and so the parameter is not retained. Attempting to remove the parameter for mass of microspheres produces a large increase in deviance while gaining one degree of freedom. The probability that this change is not significant is low ($p = 4.5\times10^{-5}$) and so the parameter for mass was retained.

$$count = c + d \cdot init + e \cdot mass + f \cdot wash \quad \textbf{(45)}$$

Remaining significant coefficients (equation 45) used to describe *count*, the cell count (cfu ml^{-1}) were *d* affecting *init*, the initial culture concentration (cfu ml^{-1}), *e* (mg^{-1}) affecting *mass*, the mass of microspheres added (mg) and *f* affecting *wash*, a categorical parameter for whether one or two wash steps were used. The intercept, *c*, is equivalent to the mean count at the origin.

Coefficient	Parameter	Estimate	St. Error	Pr(>|t|)
c	(Intercept)	7.85E+00	2.23E-01	< 2E-16***
d	*init*	1.13E-03	1.81E-04	8.14E-09***
e	*mass*	2.56E-02	6.49E-03	1.41E-04***
f	*wash*	-2.14E+00	2.14E-01	< 2E-16***

Table 23: Parameters of minimal generalised linear model of attachment of *S. epidermidis* to PLGA 50:50 microspheres.
Model assumed a quasi-Poisson distribution with coefficient of dispersion = 236.

The parameters of the model (Table 23) correlate with the designs of the experiment. As the link function is the logarithm, these parameters are interpreted by plotting the exponential of the predicted *count*. There was a range of initial culture concentrations from 6×10^2 to 2×10^3 cfu ml^{-1}. It is therefore expected that increasing the concentration of bacteria increased the cell counts. One experiment was performed with only one wash step. The additional wash decreased the cell counts as expected. The combined data showed that increasing the amount of microspheres present with the culture increased the number of bacteria transferred.

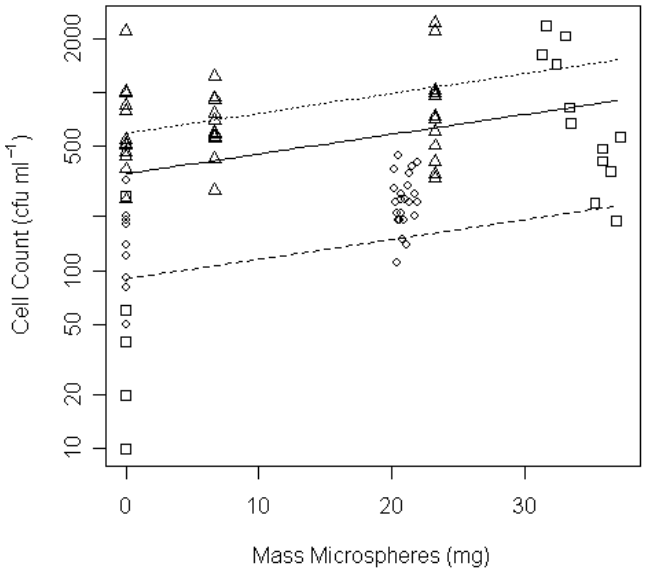

Figure 70: Increasing the mass of microspheres elevates the cell count remaining in tubes after washing.

Plotted values show data and model for *init* = 2025, *wash* = two (□, solid line), *init* = 820, *wash* = two (o, dashed line) and *init* = 592, *wash* = one (Δ, dotted line).

Figure 70 shows the most simplified model describing this dataset. For one of the experiments cell counts were very low and so have not been included in this semi-logarithmic plot but were not excluded from the statistical analysis. It should be noted that although these trends are significant, the variability in the system is very high. For example, doubling the mass of microspheres used from 10 mg to 20 mg with an initial culture of 1000 cfu ml^{-1} and two wash steps will on average cause a 30 % increase in cell count from 141 cfu ml^{-1} to 183 cfu ml^{-1}. Unfortunately, the 95 % confidence interval of these predicted values are 23.5-801 cfu ml^{-1} and 26.8-1180 cfu ml^{-1} respectively.

The highly variable nature of biological systems creates challenges for analysing interactions with interfaces of interest. To successfully make predictions about interactions of bacteria with microspheres, which themselves show variance in their properties a method must be robust, be able to be performed many times rapidly to generate sufficient data for significant analyses and have as few uncontrolled independent variables as possible.

3.7.2 Bacterial Removal from Microspheres

Freeze drying may produce broad spectrum killing of contaminants of microspheres. Freeze drying will not sterilise microspheres since ice crystals will not form to kill the cells. To determine to what level freeze drying reduced bacterial burden samples of blank (M22) and cisplatin containing (M20) microspheres were incubated with *S. epidermidis*. The microspheres were then centrifuged at 100 *g* and the supernatant was aspirated and discarded. The pellet of microspheres was either incubated at room temperature or freeze dried. The pellets were then resuspended in PBS and incubated at room temperature to allow weakly attached microspheres to become detached. The microspheres were pelleted at 100 *g* and the supernatant plated to assess level of cell killing (section 2.5.3).

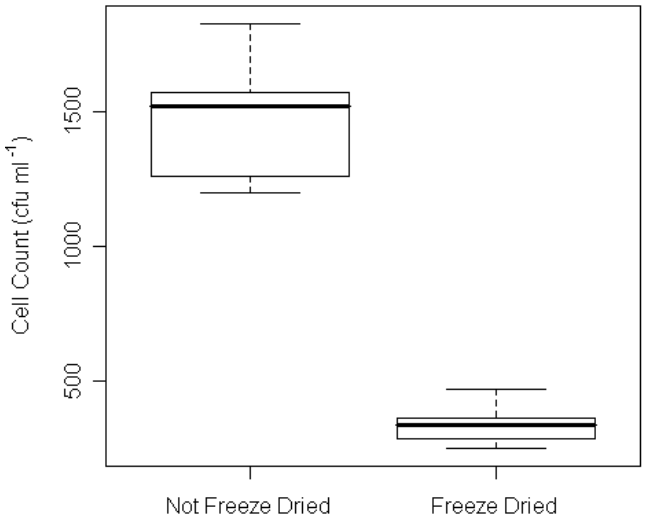

Figure 71: Freeze drying reduced cell count for blank PLGA 65:35 microspheres following coating with *S. epidermidis*.

Bold line shows median count (*n* = 9). Box shows interquartile range. Whiskers show the range of the data.

Three quarters of the bacteria were killed by freeze drying blank PLGA 65:35 microspheres. Freeze drying significantly reduced burden of bacteria on PLGA microspheres (Figure 71). No *S. epidermidis* grew on plates after being incubated with cisplatin microspheres.

3.7.3 Bacterial Attachment to PLGA Fibre

Bacterial attachment to PLGA 65:35 blank fibres (F5) was investigated. Samples of fibre (50 cm and 100 cm) were incubated with a dilute culture of *S. epidermidis*. It was expected that cells would form weak interactions with the fibre and become removed from the culture. Sample with more fibre in was expected to remove more cells due to having twice the area for attachment. The culture was then spot plated as a two-fold dilution series (section 2.5.4). The experiment was repeated with F1 fibres.

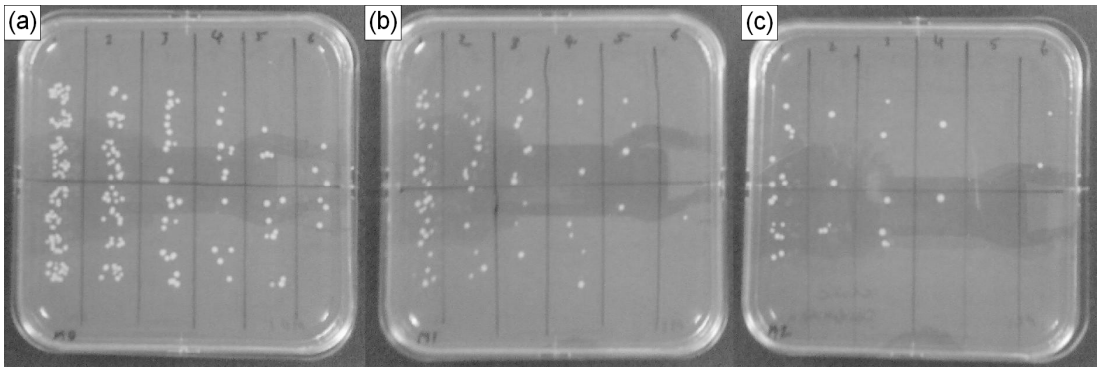

Figure 72: Increasing the amount of PLGA 65:35 solid fibre added to a *S. epidermidis* culture reduced the number of cells remaining in the culture.
Plates of eight spots of 10 µl *S. epidermidis* culture which had been incubated with (a) 0, (b) 50 or (c) 100 cm PLGA 65:35 F5 fibre for 15 minutes plated as six two-fold dilutions.

Figure 12 shows typical spot plates for 10 µl *S. epidermidis* culture which had been incubated with (a) 0, (b) 50 or (c) 100 cm PLGA 65:35 fibre for 15 minutes plated as six two-fold dilutions. A Poisson distribution can be assumed for count data because the normal linear model is not appropriate. A generalised linear model estimates count data values using a logarithmic link function. This avoids negative count predictions and more accurately represents the variance at low counts.

$$count = dd \cdot dil + e \cdot mass \qquad \textbf{(46)}$$

A saturated generalised linear model was fitted to the data for all dilutions and simplified as justified by χ^2 ANOVA. Just two parameters (equation 45) were required to describe *count*, the cell count (cfu ml^{-1}) adequately. Parameters were *dd*

affecting *dil*, the dilution factor (no units), and *e* (mg^{-1}) affecting mass. The experiment number and the type of fibre were not required for the model. Finally the intercept was also removed as it was not significant ($p = 0.12$).

Coefficient	Parameter	Estimate	St. Error	t value	Pr(>|t|)
dd	*dil*	7.7E-02	1.1E-03	73	< 2E-16***
e	*mass*	-1.2E-02	7.2E-04	-17	< 2E-16***

Table 24: Parameters of minimal generalised linear model of attachment of *S. epidermidis* to PLGA 65:35 solid fibres.
Model assumed a Poisson distribution.

The parameters of the model (Table 23) correlate with the designs of the experiment. As the link function is the logarithm, these parameters are interpreted by plotting the exponential of the predicted *count*.

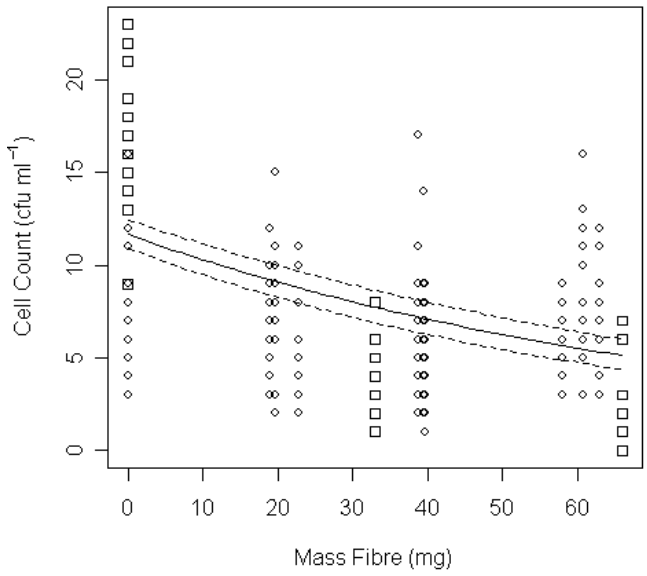

Figure 73: Increasing the amount of PLGA 65:35 fibre present in culture with *S. epidermidis* decreased the cell count in the bathing solution.
Samples of PLGA 65:35 solid fibre, F5 (□) and F1 (o), were added to dilute bacterial cultures. Data shown for most concentrated plating only. Solid line shows generalised linear model fitted to binding data for two batches of PLGA 65:35 solid fibre. Mass and dilution were significant parameters. Dashed lines show 95 % confidence intervals.

Figure 73 shows the cell counts from the most concentrated spots as the amount of fibre added to each sample of culture varied. The effect of mass of fibre was significant. However, the high degree of variation in the data means that quantitative predictions about the binding rate cannot be made.

3.7.4 Ethanol to kill Bacteria attached to PLGA Fibre

Samples of fibre were sanitised with ethanol and rinsed with PBS. A dilute culture of *S. epidermidis* was incubated with the fibres to allow some cells to become attached and then decanted. Half of the samples were incubated at room temperature and half were sanitized with ethanol. The ethanol was decanted and the fibres were rinsed with PBS to remove residual ethanol. The fibres were then incubated with PBS to allow release of weakly attached cells. This incubation medium was then spot plated (section 2.5.5).

Cells survived on the fibres which had not been treated with ethanol. Assuming that this count data had a Poisson distribution the cell count after incubation with F5 fibre was $1.24\pm0.16\times10^{4}$ cfu ml^{-1}. There was no cell growth on plates which had been plated with cultures derived from fibres been treated with ethanol. This implies that cell killing was effective or that no cells which had attached to the fibre were released into the plated buffer after 5 minutes. When these samples of fibre were incubated overnight with 25 ml TSB no colonies grew in the 60 second ethanol treated sample but turbid cultures $>10^{7}$ cfu ml^{-1} grew in the samples without treatment or a short 30 second treatment. A 60 second ethanol treatment had killed all cells associated with the sample as the culture remained clear. It is unlikely that cells had survived the ethanol treatment and not grown under nutrient conditions. Although cells had not been detected by plating following the 30 second treatment, some had survived attached to the fibre. Cells from untreated fibre grew to form a dense, opaque culture.

A single sample does not confirm that every *S. epidermidis* cell will be killed by 60 seconds ethanol or that other species will be as sensitive. However, it does imply that 60 seconds of treatment will dramatically reduce the microbial burden of the fibres and should be implemented as standard. The effect on the release profile of the fibre must be taken into account (see section 3.4.6).

4 Conclusion

4.1 Study Findings

Ovarian cancer is one of the five most common causes of cancer death in women in the USA and UK. The tumour is generally well established in the peritoneum when diagnosed. Current opinion in the medical and scientific literature is that prolonged delivery of cisplatin may offer reduced toxicity compared to IV delivery of a single bolus. Prolonged release can also be achieved by sustained release from a drug depot Sustained release of cisplatin from implantable microspheres or fibres offers the reduced toxicity of prolonged delivery. In addition, the risks associated with resident catheters and costs of extended hospitalization are avoided. Intraperitoneal therapy has been shown to improve survival for patients. Poly(lactide-co-glycolide) (PLGA) is a biodegradable polyester which has been proven safe for medical implantation.

Aim (1) of this work was to develop microsphere depot formulations with improved drug release profiles compared to previous work. PLGA 65:35 microspheres have been manufactured using the ethyl acetate that is a safer solvent than other solvents used by others, such as DCM. The microspheres produced by this improved method have higher cisplatin loadings than previously reported. Formulations with higher drug loading require less excipient.

Aim (2) of this work was to develop and investigate novel cisplatin containing solid and hollow fibres as alternative structures for depot devices. PLGA 65:35 solid fibres have been manufactured with a typical drug loading of 15 % and an equivalent release constant to microspheres. PLGA 65:35 hollow fibres have been manufactured with a typical drug loading of 21 % and an equivalent release constant to microspheres. In addition, between batch and within batch variation of hollow fibres was relatively low compared to microspheres and solid fibres. Manufacturing fibres can be readily adapted to act as a continuous process, making scale up easier to achieve than for microspheres. Fibres could be sliced into pellets for intraperitoneal delivery of cisplatin.

Aim (3) of this work was to examine the drug release profiles of the formulations produced using mathematical models to allow rational comparison of the devices. Determination of release kinetics was achieved using non-linear least squares to fit the semi-empirical and Fickian models to the datasets. First order models such as the two compartment model is a robust model that allows rapid comparison between formulations. An additional exponential improved the description of the data for some formulations. The Higuchi model is only appropriate to describe early release from drug depots but is robust and can converge on a solution even for poor datasets.

PLGA Depot Structure	Rate Constant (s^{-1})	Diffusivity (Higuchi) ($cm^2\ s^{-1}$)	Diffusivity (Fickian) ($cm^2\ s^{-1}$)
Microspheres	5×10^{-6}	1×10^{-10}	4×10^{-11}
Solid Fibres	3×10^{-6}	2×10^{-9}	-
Hollow Fibres	5×10^{-6}	5×10^{-9}	3×10^{-10}

Table 25: Typical kinetic parameters of PLGA 65:35 microspheres, solid fibres, and hollow fibres.

Rates and diffusivities of combined microsphere data (M14, M17, M18-M21), F4 solid fibres and F9 hollow fibres.

The Higuchi model systematically overestimates the diffusivity compared to the Fickian model (Table 25). The Fickian models offer a good mechanistic description of drug release and can generate a physical parameter, the diffusion coefficient, directly. The disadvantage of this model is that it may not achieve convergence for poor or incomplete datasets. All models are approximations to reality, so considering several at once is the best way to inform interpretation of diffusion data.

Cisplatin undergoes a ligand exchange in the presence of water, forming to a potent electrophile. This charged cisplatin species readily forms DNA-platinum adducts. These adducts are thought to be the major mechanism of toxicity to cancer cells. Charged cisplatin also binds other nucleophiles in cells. Cisplatin binding other cellular components reduces the amount of cisplatin available for DNA attack. Irreversible protein binding influences cisplatin pharmacokinetics compared to other drugs.

Aim (4) of this project was to investigate irreversible binding of cisplatin to non-DNA targets, cisplatin binding to protein. The two compartment protein binding model for cisplatin release described the data for irreversible binding to protein following release from PLGA 65:35 solid (k_b = 4×10^{-4} s^{-1}) and hollow fibres (k_b = 7×10^{-4} s^{-1}). Rate constant of protein binding was slightly overestimated compared to decrease of concentration of unbound cisplatin in solution (k_b = 6×10^{-5} s^{-1}). The method is useful as it does give relevant approximations. To the author's knowledge, this work has demonstrated for the first time that cold ethanol precipitation is a suitable method for determining rate parameters for irreversible protein binding of a drug.

All implanted surfaces are susceptible to bacterial attachment. Bacteria are able to survive on implants in a hostile environment-resistant slow growth mode.

Aim (5) of this thesis was to investigate attachment of bacteria to PLGA depots.

S. epidermidis is an important pathogen associated with long term implanted polymeric devices such as intravenous catheters. *S. epidermidis* was found to rapidly bind to PLGA fibres *in vitro*. Attached cell numbers can be reduced by freeze drying or by exposure to 70 % ethanol for 60 seconds.

In conclusion, the novel high cisplatin loading PLGA 65:35 hollow fibres reported in this thesis represent a formulation of continuous release that may offer a therapeutic benefit to ovarian cancer patients as an additional component to current optimum therapy.

4.2 Future Work

High cisplatin loading PLGA 65:35 hollow fibres may offer an improvement to intraperitoneal cisplatin therapy. Cisplatin becomes bound to polyesters when stored at 5°C. Optimization of storage conditions by examining freezing and a desiccated environment may improve the shelf life of cisplatin containing PLGA depots.

High cisplatin loading PLGA 65:35 hollow fibres have a reduced soaking following spinning. To confirm that the NMP levels remaining in the fibre are low the fibres could be analysed using chromatographic methods.

This work has shown that depot morphology plays a role in determining rate of drug release. Preliminary work to extend these studies showed that although carboplatin was released quickly from solid PLGA 65:35 fibres, release was slower from PLGA 75:25 coated double layer hollow fibres. The method of manufacture followed was similar to that used in section 2.1.4, except that the spinneret had an inner and outer polymer channel as well as an aqueous phase central bore (Figure 74).

Figure 74: Double layer hollow fibre spinneret.

PLGA 65:35 dissolved in NMP with carboplatin (50 % of the weight of PLGA 65:35) and PLGA 75:25 dissolved in NMP were spun (by Mr Thomas Richards) through the inner and outer bores of a double layer hollow fibre spinneret respectively with distilled water in the central bore. The release profile of this fibre was determined in water as for other depots analysed in this work with acid digestion to allow detection of the carboplatin (section 2.3.5).

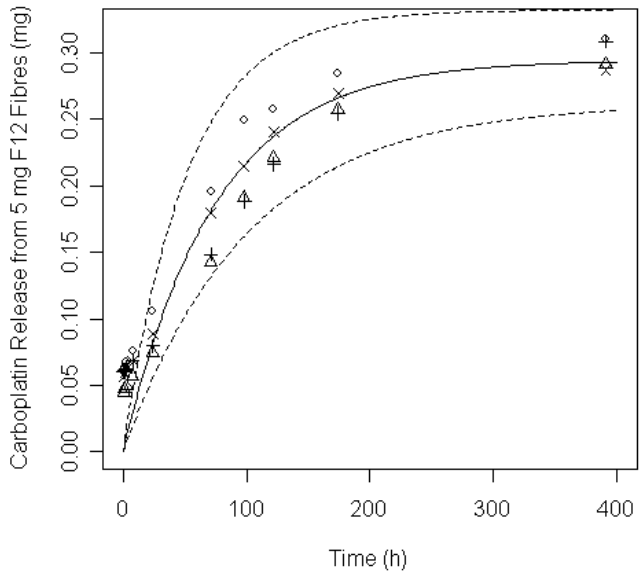

Figure 75: Release of carboplatin from PLGA 75:25 coated PLGA 65:35 double layer hollow fibres.

Solid line shows two compartment release. Dashed lines are 95 % confidence intervals (n = 4).

Figure 75 shows the release of carboplatin from 5 mg of PLGA 75:25 coated PLGA 65:35 double layer hollow fibres. There was insufficient data to fit the three compartment model. The model estimated a drug loading of 0.30 mg carboplatin in 5 mg fibre with a release constant of $3.7 \pm 0.58 \times 10^{-6}$ s^{-1} (parameter ± standard error). This is an order of magnitude reduction in rate of release compared to carboplatin solid fibres which released drug at $2.8 \pm 0.82 \times 10^{-5}$ s^{-1} (section 3.4.7). This additional degree of control is due to the PLGA 75:25 membrane coating the drug containing depot and restricting the rate of diffusion. Although the number of samples examined was low (n = 4), this preliminary experiment suggests that double layer hollow fibres have less variability in profiles of drug release than solid fibres.

As carboplatin is even more soluble than cisplatin the soak following spinning had to be minimised. The fibre was transferred to cylindrical supports after 40 minutes and freeze dried. This caused some sections of the hollow fibre to distend and swell as the pressure fell. This was due to air and water trapped in the lumen of the fibre

evaporating due to the low pressure and not being able to escape through the open ends of the fibre fast enough. Immersing the fibres in liquid nitrogen prior to freeze drying may prevent this. In addition, the fibres remained soft which suggests that NMP remained in the fibre. These difficulties should be possible to overcome offering the potential for improved drug release of more compounds with higher water solubility than cisplatin.

References

ABRAMOFF, M. D., MAGELHAES, P. J. & RAM, S. J. (2004) Image Processing with ImageJ. *Biophotonics International,* 11**,** 36-42.

AKAIKE, H. (1974) A new look at the statistical model identification. *IEEE Transactions on Automatic Control,* 19**,** 716-23.

ALBERTS, D. S., GREEN, S., HANNIGAN, E. V., O'TOOLE, R., STOCK-NOVACK, D., ANDERSON, P., SURWIT, E. A., MALVLYA, V. K., NAHHAS, W. A. & JOLLES, C. J. (1992) Improved therapeutic index of carboplatin plus cyclophosphamide versus cisplatin plus cyclophosphamide: final report by the Southwest Oncology Group of a phase III randomized trial in stages III and IV ovarian cancer. *J Clin Oncol,* 10**,** 706-717.

ALBERTS, D. S., LIU, P. Y., HANNIGAN, E. V., O'TOOLE, R., WILLIAMS, S. D., YOUNG, J. A., FRANKLIN, E. W., CLARKE-PEARSON, D. L., MALVIYA, V. K., DUBESHTER, B., ADELSON, M. D. & HOSKINS, W. J. (1996) Intraperitoneal Cisplatin plus Intravenous Cyclophosphamide versus Intravenous Cisplatin plus Intravenous Cyclophosphamide for Stage III Ovarian Cancer. *N Engl J Med,* 335**,** 1950-1955.

ALTSHULLER, A. P. & EVERSON, H. E. (1953) The Solubility of Ethyl Acetate in Water. *J Am Chem Soc,* 75**,** 1727.

ANDERSON, J. M. & SHIVE, M. S. (1997) Biodegradation and biocompatibility of PLA and PLGA microspheres. *Adv Drug Deliv Rev,* 28**,** 5-24.

ARAKI, H., TANI, T. & KODAMA, M. (1999) Antitumor Effect of Cisplatin Incorporated into Polylactic Acid Microcapsules. *Artif Organs,* 23**,** 161-168.

ARMSTRONG, D. K., BUNDY, B., WENZEL, L., HUANG, H. Q., BAERGEN, R., LELE, S., COPELAND, L. J., WALKER, J. L., BURGER, R. A. & THE GYNECOLOGIC ONCOLOGY GROUP (2006) Intraperitoneal Cisplatin and Paclitaxel in Ovarian Cancer. *N Engl J Med,* 354**,** 34-43.

ARTURSSON, P., BROWN, D., DIX, J., GODDARD, P. & PETRAK, K. (1990) Preparation of Sterically Stabilized Nanoparticles by Desolvation from Graft Copolymers. *J Polym Sci A,* 28**,** 2651-2663.

AVGOUSTAKIS, K., BELETSI, A., PANAGI, Z., KLEPETSANIS, P., KARYDAS, A. G. & ITHAKISSIOS, D. S. (2002) PLGA-mPEG nanoparticles of cisplatin: in vitro nanoparticle degradation, in vitro drug release and in vivo drug residence in blood properties. *J Control Release,* 79**,** 123-135.

BACH, F. D., CARLIER, R. Y., ELIS, J. B., MOMPOINT, D. M., FEYDY, A., JUDET, O., BEAUFILS, P. & VALLÉE, C. (2002) Anterior Cruciate Ligament Reconstruction with Bioabsorbable Polyglycolic Acid Interference Screws: MR Imaging Follow-up. *Radiology,* 225**,** 541-550.

BATES, D. M. & WATTS, D. G. (1981) A Relative Offset Orthogonality Convergence Criterion for Nonlinear Least Squares. *Technometrics,* 23**,** 179-183.

BENET, L. Z. (1985) Mean residence time in the body versus mean residence time in the central compartment. *J Pharmacokinet Pharmacodyn,* 13**,** 555-558.

BENET, L. Z. & TURI, J. S. (1971) Use of the General Partial Fraction Theorems for Obtaining Inverse Laplace Transforms in Pharmacokinetic Analysis. *J Pharm Sci,* 60**,** 1593-94.

BOURNE, D. W. A. & STRAUSS, S. (1995) *Mathematical Modeling of Pharmacokinetic Data*, CRC.

BRAUNECKER, J., BABA, M., MILROY, G. E. & CAMERON, R. E. (2004) The effects of molecular weight and porosity on the degradation and drug release from polyglycolide. *Int J Pharm,* 282**,** 19-34.

BROWN, M. R. W. & SMITH, A. W. (2003) Antimicrobial Agents and Biofilms. IN WILSON, M. & DEVINE, D. (Eds.) *Medical Implications of Biofilms.* Cambridge University Press.

BRUNTON, L. L., LAZO, S. L. & PARKER, K. (2005) *Goodman & Gilman's The Pharmacological Basis Of Therapeutics*, McGraw-Hill.

BURGER, K. N., STAFFHORST, R. W., VIJLDER, H. C. D., VELINOVA, M. J., BOMANS, P. H., FREDERIK, P. M. & KRUIJFF, B. D. (2002) Nanocapsules: lipid-coated aggregates of cisplatin with high cytotoxicity. *Nat Med,* 1**,** 81-84.

BURGHARDT, E., GIRARDI, F., LAHOUSEN, M., TAMUSSINO, K. & STETTNER, H. (1991) Patterns of pelvic and paraaortic lymph node involvement in ovarian cancer. *Gynecol Oncol,* 40**,** 103-106.

CARSLAW, H. S. & JAEGER, J. C. (1959) *Conduction of Heat in Solids,* Oxford, Oxford University Press.

CHEN, J. T., HIRAI, Y., SHIMIZU, Y., HASUMI, K. & MASUBUCHI, K. (1990) New Cisplatin Schedule in Combination with Aclarubicin (ACR) with High Response Rate in Recurrent Gynecological Adenocarcinomas. *Gynecol Oncol,* 38**,** 1-5.

CHEUNG, Y., CRADOCK, J., VISHNUVAJJALA, B. & FLORA, K. (1987) Stability of cisplatin, iproplatin, carboplatin, and tetraplatin in commonly used intravenous solutions. *Am J Hosp Pharm,* 44**,** 124-130.

CLERICI, W. J., HENSLEY, K., DIMARTINO, D. L. & BUTTERFIELD, D. A. (1996) Direct detection of ototoxicant-induced reactive oxygen species generation in cochlear explants. *Hear Res,* 98**,** 116-124.

CORI, C. F. & CORI, G. T. (1929) Glycogen Formation in the Liver from *d*- and *l*-Lactic Acid. *J Biol Chem,* 81**,** 389-403.

CRAMTON, S. E., ULRICH, M., GÖTZ, F. & DÖRING, G. (2001) Anaerobic Conditions Induce Expression of Polysaccharide Intercellular Adhesin in *Staphylococcus aureus* and *Staphylococcus epidermidis*. *Infect Immun,* 69**,** 4079-4085.

CRANK, J. (1975) *The Mathematics of Diffusion,* Bristol, Oxford University Press.

CUTRIGHT, D. E., BEASLEY, J. D. & PEREZ, B. (1971) Histologic comparison of polylactic and polyglycolic acid sutures. *Oral Surg Oral Med Oral Pathol,* 32**,** 165-173.

DE JONG, S. J., ARIAS, E. R., RIJKERS, D. T. S., VAN NOSTRUM, C. F., KETTENES-VAN DEN BOSCH, J. J. & HENNINK, W. E. (2001) New insights into the hydrolytic degradation of poly(lactic acid): participation of the alcohol terminus. *Polymer,* 42**,** 2795-2802.

DE KROON, A. I. P. M., STAFFHORST, R. W. H. M., DE KRUIJFF, B. & BURGER, K. N. J. (2005) Cisplatin Nanocapsules. *Methods Enzymol,* 391**,** 118-125.

DONLAN, R. M. (2001) Biofilms and Device-Associated Infections. *Emerging Infectious Diseases,* 7**,** 227-281.

EASTMAN, A. (1986) Reevaluation of interaction of cis-dichloro(ethylenediamine)platinum(II) with DNA. *Biochemistry,* 25**,** 3912-3915.

EASTMAN, A. & SCHULTE, N. (1988) Enhanced DNA Repair as a Mechanism of Resistance to *cis*-Diamminedichloroplatinum(II). *Biochemistry,* 27**,** 4730-4734.

EINHORN, L. H. (2002) Curing metastatic testicular cancer *PNAS,* 99**,** 4592-95.

EISENKOP, S. M., FRIEDMAN, R. L. & WANG, H.-J. (1997) Complete Cytoreductive Surgery Is Feasible and Maximizes Survival in Patients with Advanced Epithelial Ovarian Cancer: A Prospective Study. *Gynecol Oncol,* 69**,** 103-108.

ELLIS, M. J. & CHAUDHURI, J. B. (2006) Poly(lactic-co-glycolic acid) Hollow Fibre Membranes for use as a Tissue Engineering Scaffold. *Biotechnol Bioeng,* 96**,** 177-187.

ERLICHMAN, C., SOLDIN, S. J., THIESSEN, J. J., STURGEON, J. F. G. & FINE, S. (1987) Disposition of total and free cisplatin on two consecutive treatment cycles in patients with ovarian cancer. *Cancer Chemother Pharmacol,* 19**,** 75-79.

ESPÓSITO, B. P. & NAJJAR, R. (2002) Interactions of antitumoral platinum-group metallodrugs with albumin. *Coord Chem Rev,* 232**,** 137-149.

FABBRI, F., CARLONI, S., BRIGLIADORI, G., ZOLI, W., LAPALOMBELLA, R. & MARINI, M. (2006) Sequential events of apoptosis involving docetaxel, a microtubule-interfering agent: A cytometric study. *BMC Cell Biol,* 7.

FOLEY, I., MARSH, P., WELLINGTON, E. M. H., SMITH, A. W. & BROWN, M. R. W. (1999) General stress response master regulator rpoS is expressed in human infection: a possible role in chronicity. *J Antimicrob Chemother,* 43**,** 164-5.

FRY, W. A., PHILLIPS, J. L. & MENCK, H. R. (2000) Ten-year survey of lung cancer treatment and survival in hospitals in the United States: A National Cancer Data Base Report. *Cancer,* 86**,** 1867-76.

FU, J. C., HAGEMEIR, C. & MOYER, D. L. (1976) A Unified Mathematical Model for Diffusion from Drug-Polymer Composite Tablets. *J Biomed Mater Res,* 10**,** 743-758.

FU, S., KAVANAGH, J. J., HU, W. & JR., R. C. B. (2006) Clinical application of oxaliplatin in epithelial ovarian cancer. *Int J Gynecol Cancer,* 16**,** 1717-1732.

FUJIYAMA, J., NAKASEA, Y., OSAKIB, K., SAKAKURAA, C., YAMAGISHI , H. & HAGIWARA, A. (2003) Cisplatin incorporated in microspheres: development and fundamental studies for its clinical application. *J Control Release,* 89**,** 397-408.

GADDUCCI, A., CARNINO, F., CHIARA, S., BRUNETTI, I., TANGANELLI, L., ROMANINI, A., BRUZZONE, M., CONTE, P. F. & GONO COLLABORATIVE CENTERS (2000) Intraperitoneal versus Intravenous Cisplatin in Combination with Intravenous Cyclophosphamide and Epidoxorubicin in Optimally Cytoreduced Advanced Epithelial Ovarian Cancer: A Randomized Trial of the Gruppo Oncologico Nord-Ovest *Gynecol Oncol,* 76**,** 157-162.

GAO, W. G., PU, S. P., LIU, W. P., LIU, Z. D. & YANG, Y. K. (2003) [The aquation of oxaliplatin and the effect of acid] [Article in Chinese]. *Yao Xue Xue Bao,* 38**,** 223-226.

GEDCKE, D. A. (1972) The Si(Li) X-ray Energy Analysis System: Operating Principles and Performance. *X-Ray Spectrometry,* 1**,** 129-141.

GEORGOULIAS, V., PAPADAKIS, E., ALEXOPOULOS, A., TSIAFAKI, X., RAPTI, A., VESLEMES, M., PALAMIDAS, P. & VLACHONIKOLIS, I. (2001) Platinum-based and non-platinum-based chemotherapy in advanced non-small-cell lung cancer: a randomised multicentre trial. *Lancet,* 357**,** 1478-84.

GILDING, D. K. & REED, A. M. (1979) Biodegradable polymers for use in surgery—polyglycolic/poly(actic acid) homo- and copolymers: 1 *Polymer,* 20**,** 1459-64.

GLUECKAUF, E. & COATES, J. I. (1947) Theory of Chromatography. Part IV. The Influence of Incomplete Equilibrium on the Front Boundary of Chromatograms and on the Effectiveness of Separation. *J. Chem. Soc.***,** 1315–1321.

GOLUB, T. R., SLONIM, D. K., TAMAYO, P., HUARD, C., GAASENBEEK, M., MESIROV, J. P., COLLER, H., LOH, M. L., DOWNING, J. R., CALIGIURI, M. A., BLOOMFIELD, C. D. & LANDER, E. S. (1999) Molecular Classification of Cancer: Class Discovery and Class Prediction by Gene Expression Monitoring *Science,* 15**,** 531-537.

GRAHAM, J. & FALK, S. (2005) ASWCS Chemotherapy Handbook Jan 2005 Update: B2.8 Cisplatin. Avon, Somerset and Wiltshire NHS Cancer Services.

GROSS, M., CRAMTON, S. E., GÖTZ, F. & PESCHEL, A. (2001) Key Role of Teichoic Acid Net Charge in Staphylococcus aureus Colonization of Artificial Surfaces *Infection and Immunity,* 69**,** 3423-26.

HAGIWARA, A., TAKAHASHI, T., KOJINIA, O., YAMAGUCHI, T., SASABE, T., LEE, M., SAKAKURA, C., SHOUBAYASHI, S., LKADA, Y. & HYON, S.-H. (1993a) Pharmacologic Effects of Cisplatin Microspheres on Peritoneal Carcinomatosis in Rodents. *Cancer,* 71**,** 844-850.

HAGIWARA, A., TAKAHASHI, T., SAWAI, K., SAKAKURA, C., TSUJIMOTO, H., OSAKI, K., SAKAKIBARA, T., OHYAMA, T., OHGAKI, M., MURANISHI, S., IKADA, Y. & HYON, S.-H. (1993b) Clinical trials with intraperitoneal cisplatin microspheres for malignant ascites--a pilot study. *Anticancer Drug Des,* 8**,** 463-470.

HALL, M. D., AMJADI, S., ZHANG, M., BEALE, P. J. & HAMBLEY, T. W. (2004) The mechanism of action of platinum(IV) complexes in ovarian cancer cell lines. *J Inorg Biochem,* 98**,** 1614-24.

HAYES, D., CVITKOVIC, E., GOLBEY, R., SCHEINER, E., HELSON, L. & KRAKOFF, I. (1977) High dose cis-platinum diammine dichloride. . *Cancer,* 39**,** 1372.

HEILMANN, C. (2003) Molecular Basis of Biofilm Formation by *Staphylococcus epidermidis*. IN WILSON, M. & DEVINE, D. (Eds.) *Medical Implications of Biofilms*. Cambridge University Press.

HENGSTLER, J. G., HENGST, A., FUCHS, J., TANNER, B., POHL, J. & OESCH, F. (1997) Induction of DNA crosslinks and DNA strand lesions by cyclophosphamide after activation by cytochrome P450 2B1. *Mutat Res,* 373**,** 215-223.

HIGUCHI, T. (1961) Rate of Release of Medicaments from Ointment Bases Containing Drugs in Suspension. *Journal of Pharmaceutical Sciences,* 50**,** 874-5.

HOLSCHNEIDER, C. H. & BEREK, J. S. (2000) Ovarian Cancer: Epidemiology, Biology, and Prognostic Factors. *Semin Surg Oncol,* 19**,** 3-10.

HOLY, C. E., CHENG, C., DAVIES, J. E. & SHOICHET, M. S. (2001) Optimizing the sterilization of PLGA scaffolds for use in tissue engineering *Biomaterials,* 22**,** 25-31.

HORTOBAGYI, G. N., FRYE, D., BUZDAR, A. U., EWER, M. S., FRASCHINI, G., HUG, V., AMES, F., MONTAGUE, E., CARRASCO, C. H., MACKAY, B. & BENJAMIN, R. S. (1988) Decreased cardiac toxicity of doxorubicin administered by continuous intravenous infusion in combination chemotherapy for metastatic breast carcinoma. *Cancer,* 63**,** 37-45.

HRECZUK-HIRST, D., CHICCO, D., GERMAN, L. & DUNCAN, R. (2001) Dextrins as potential carriers for drug targeting: tailored rates of dextrin degradation by introduction of pendant groups. *Int J Pharm,* 230**,** 57-66.

HUO, D., DENG, S., LI, L. & JI, J. (2005) Studies on the poly(lactic-co-glycolic) acid microspheres of cisplatin for lung-targeting. *Int J Pharm,* 289**,** 63-67.

ICH Q3C (R3) (2005) Impurities: Guideline For Residual Solvents. *International Conference On Harmonisation Of Technical Requirements For Registration Of Pharmaceuticals For Human Use.*

IGA, K., HAMAGUCHI, N., IGARI, Y., OGAWA, Y., GOTOH, K., OOTSU, K., TOGUCHI, H. & SHIMAMOTO, T. (1991) Enhanced Antitumor Activity in Mice after Administration of Thermosensitive Liposome Encapsulating Cisplatin with Hyperthermia. *J Pharmacol Exp Ther,* 257**,** 1203-1207.

IKE, O., SHIMIZU, Y., WADA, R., HYON, S.-H. & IKADA, Y. (1992) Controlled cisplatin delivery system using poly(d,l-lactic acid). *Biomaterials,* 13**,** 230-234.

ISHIDA, S., LEE, J., THIELE, D. J. & HERSKOWITZ, I. (2002) Uptake of the anticancer drug cisplatin mediated by the copper transporter Ctr1 in yeast and mammals. *PNAS,* 99**,** 14298-14302.

ISHIHARA, T., IZUMO, N., HIGAKI, M., SHIMADA, E., HAGI, T., MINE, L., OGAWA, Y. & MIZUSHIM, Y. (2005) Role of zinc in formulation of PLGA/PLA nanoparticles encapsulating betamethasone phosphate and its release profile. *J Control Release,* 105**,** 68-76.

JAABACK, K. & JOHNSON, N. (2006) Intraperitoneal chemotherapy for the initial management of primary epithelial ovarian cancer. *Cochrane Database of Systematic Reviews*.

JAMZAD, S., TUTUNJI, L. & FASSIHI, R. (2005) Analysis of macromolecular changes and drug release from hydrophilic matrix systems. *Int J Pharm,* 292**,** 75-85.

JANSSEN PHARMACEUTICAL PRODUCTS INC. (2006) Risperdal Consta® Package Insert.

JEMAL, A., SIEGEL, R., WARD, E., MURRAY, T., XU, J. & THUN, M. J. (2007) Cancer Statistics, 2007. *CA Cancer J Clin,* 57**,** 43-66.

JEONG, B., BAE, Y. H., LEE, D. S. & KIM, S. W. (1997) Biodegradable block copolymers as injectable drug-delivery systems. *Nature,* 388**,** 860-862.

JONES, R. H. & VASEY, P. A. (2003) Part II: Testicular cancer—management of advanced disease. *Lancet Oncol,* 4**,** 738-747.

KARTALOU, M. & ESSIGMANN, J. M. (2001) Mechanisms of resistance to cisplatin. *Mutat Res,* 478**,** 23-43.

KAWASHIMA, Y., YAMAMOTO, H., TAKEUCHI, H., HINO, T. & NIWA, T. (1998) Properties of a peptide containing dl-lactide/glycolide copolymer

nanospheres prepared by novel emulsion solvent diffusion methods *Eur J Pharm Biopharm,* 45**,** 41-48.
KELLAND, L. (2007) The resurgence of platinum-based cancer chemotherapy. *Nature Reviews Cancer,* 7**,** 573-84.
KEREN, I., KALDALU, N., SPOERING, A., WANG, Y. & LEWIS, K. (2004) Persister cells and tolerance to antimicrobials. *FEMS Microbiol Lett,* 230**,** 13-18.
KIM, B.-S., NIKOLOVSKI, J., BONADIO, J., SMILEY, E. & MOONEY, D. J. (1999) Engineered Smooth Muscle Tissues: Regulating Cell Phenotype with the Scaffold. *Exp Cell Res,* 251**,** 318-328.
KIM, H., SUH, H., AHN JO, S., WOO KIM, H., LEE, J. M., KIM, E. H., REINWALD, Y., PARK, S.-H., MIN, B.-H. & JO, I. (2005) In vivo bone formation by human marrow stromal cells in biodegradable scaffolds that release dexamethasone and ascorbate-2-phosphate. *Biochem Biophys Res Commun,* 332**,** 1053-60.
KIRMANI, S., BRALY, P. S., MCCLAY, E. F., SALTZSTEIN, S. L., PLAXE, S. C., KIM, S., CATES, C. & HOWELL, S. B. (1995) A Comparison of Intravenous Versus Intraperitoneal Chemotherapy for the Initial Treatment of Ovarian Cancer. *Obstet Gynecol Surv,* 50**,** 115-117.
KNOX, R. J., FRIEDLOS, F., LYDALL, D. A. & ROBERTS, J. J. (1986) Mechanism of cytotoxicity of anticancer platinum drugs: evidence that cis-diamminedichloroplatinum(II) and cis-diammine-(1,1-cyclobutanedicarboxylato)platinum(II) differ only in the kinetics of their interaction with DNA. *Cancer Res,* 46**,** 1972-1979.
KORST, A. E. C., VAN DER STERRE, M. L. T., GALL, H. E., FICHTINGER-SCHEPMAN, A. M. J., VERMORKEN, J. B. & VAN DER VIJGH, W. J. F. (1998) Influence of Amifostine on the Pharmacokinetics of Cisplatin in Cancer Patients. *Clin Cancer Res,* 4**,** 331-336.
KUMAGAI, S., SUGIYAMA, T., NISHIDA, T., USHIJIMA, K. & YAKUSHIJI, M. (1996) Improvement of intraperitoneal chemotherapy for rat ovarian cancer using cisplatin-containing microspheres. *Jpn J Cancer Res,* 87**,** 412-417.
LA FONTAINE, S. & MERCER, J. F. B. (2007) Trafficking of the copper-ATPases, ATP7A and ATP7B: Role in copper homeostasis *Arch Biochem Biophys,* 463**,** 149-167.
LA MARCA, A. & VOLPE, A. (2007) The Anti-Mullerian hormone and ovarian cancer. *Human Reproduction Update,* 13**,** 265-73.
LAKESHORE BIOMATERIALS DATASHEET Solubility Chart. Lakeshore Biomaterials.
LEE, J., PEÑA, M. M. O., NOSE, Y. & THIELE, D. J. (2001) Biochemical Characterization of the Human Copper Transporter Ctr1. *J Biol Chem,* 277**,** 4380-87.
LEWIN, B. (2000) *Genes VII,* New York, Oxford University Press.
LIDE, D. R. (2005) *CRC Handbook of Chemistry and Physics*, CRC Press, Taylor & Francis Group.
LOS, G., MUTSAERS, P. H., LENGLET, W. J., BALDEW, G. S. & MCVIE, J. G. (1990) Platinum distribution in intraperitoneal tumors after intraperitoneal cisplatin treatment. *Cancer Chemother Pharmacol,* 25**,** 389-394.
LOS, G., VERDEGAAL, E. M., MUTSAERS, P. H. & MCVIE, J. G. (1991) Penetration of carboplatin and cisplatin into rat peritoneal tumor nodules after intraperitoneal chemotherapy. *Cancer Chemother Pharmacol,* 28**,** 159-165.

MA, J., STOTER, G., VERWEIJ, J. & SCHELLENS, J. H. M. (1996) Comparison of ethanol plasma-protein precipitation with plasma ultrafiltration and trichloroacetic acid protein precipitation for the measurment of unbound platinum concentrations. *Cancer Chemother Pharmacol,* 38**,** 391-94.

MACHIDA, Y., ONISHI, H., KURITA, A., HATA, H., MORIKAWA, A. & MACHIDA, Y. (2000) Pharmacokinetics of prolonged-release CPT-11-loaded microspheres in rats. *J Control Release,* 66**,** 159-175.

MARKMAN, M., BUNDY, B. N., ALBERTS, D. S., FOWLER, J. M., CLARK-PEARSON, D. L., CARSON, L. F., WADLER, S. & SICKEL, J. (2001) Phase III Trial of Standard-Dose Intravenous Cisplatin Plus Paclitaxel Versus Moderately High-Dose Carboplatin Followed by Intravenous Paclitaxel and Intraperitoneal Cisplatin in Small-Volume Stage III Ovarian Carcinoma: An Intergroup Study of the Gynecologic Oncology Group, Southwestern Oncology Group, and Eastern Cooperative Oncology Group. *J Clin Oncol,* 19**,** 1001-1007.

MARKMAN, M., KENNEDY, A., WEBSTER, K., ELSON, P., PETERSON, G., KULP, B. & BELINSON, J. (1999) Clinical Features of Hypersensitivity Reactions to Carboplatin. *J Clin Oncol,* 17**,** 1141-1145.

MATSUMOTO, A., MATSUKAWA, Y., SUZUKI, T. & YOSHINO, H. (2005) Drug release characteristics of multi-reservoir type microspheres with poly(dl-lactide-co-glycolide) and poly(dl-lactide). *J Control Release,* 106**,** 172-180.

MAYERSOHN, M. & GIBALDI, M. (1970) Mathematical methods in pharmacokinetics. I. Use of the Laplace transform for solving differential rate equations. *Amer J Pharm Ed,* 34**,** 608-614.

MCGUIRE, W. P., HOSKINS, W. J., BRADY, M. F., KUCERA, P. R., PARTRIDGE, E. E., LOOK, K. Y., CLARKE-PEARSON, D. L. & DAVIDSON, M. (1996) Cyclophosphamide and Cisplatin Compared with Paclitaxel and Cisplatin in Patients with Stage III and Stage IV Ovarian Cancer. *N Engl J Med,* 334**,** 1-6.

MESSARITAKIA, A., BLACKB, S. J., VAN DER WALLEC, C. F. & RIGBY, S. P. (2005) NMR and confocal microscopy studies of the mechanisms of burst drug release from PLGA microspheres *J Control Release,* 108**,** 271-281.

MIYAGI, Y., FUJIWARA, K., KIGAWA, J., ITAMOCHI, H., NAGAO, S., AOTANI, E., TERAKAWA, N. & KOHNO, I. (2005) Intraperitoneal carboplatin infusion may be a pharmacologically more reasonable route than intravenous administration as a systemic chemotherapy. A comparative pharmacokinetic analysis of platinum using a new mathematical model after intraperitoneal vs. intravenous infusion of carboplatin-A Sankai Gynecology Study Group (SGSG) study. *Gynecol Oncol,* 99**,** 591-596.

MOMPARLER, R. L., KARON, M., SIEGEL, S. E. & AVILA, F. (1976) Effect of Adriamycin on DNA, RNA, and Protein Synthesis in Cell-free Systems and lntact Cells. *Cancer Res,* 36**,** 2891-95.

MORTON, G. & THOMAS, G. (1996) Is there a place for whole abdominal radiotherapy in the management of ovarian cancer? *Ann Acad Med Singapore,* 25**,** 429-436.

MUGGLI, D. S., BURKOTH, A. K. & ANSETH, K. S. (1999) Crosslinked polyanhydrides for use in orthopedic applications: Degradation behavior and mechanics. *J Biomed Mater Res A,* 46**,** 271-278.

NAGAI, N. & OGATA, H. (1997) Quantitative relationship between pharmacokinetics of unchanged cisplatin and nephrotoxicity in rats: importance of area under the concentration-time curve (AUC) as the major toxicodynamic determinant in vivo. *Cancer Chemother Pharmacol,* 40**,** 11-18.

NEWMAN, M. S., COLBERN, G. T., WORKING, P. K., ENGBERS, C. & AMANTEA, M. A. (1999) Comparative pharmacokinetics, tissue distribution, and therapeutic effectiveness of cisplatin encapsulated in long-circulating, pegylated liposomes (SPI-077) in tumor-bearing mice. *Cancer Chemother Pharmacol,* 43**,** 1-7.

NISHIYAMA, N., OKAZAKI, S., CABRAL, H., MIYAMOTO, M., KATO, Y., SUGIYAMA, Y., NISHIO, K., MATSUMURA, Y. & KATAOKA, K. (2003) Novel cisplatin-incorporated polymeric micelles can eradicate solid tumors in mice. *Cancer Res,* 63**,** 8977-8983.

NIWA, T., TAKEUCHI, H., HINO, T., KUNOU, N. & KAWASHIMA, Y. (1993) Preparations of biodegradable nanospheres of water-soluble and insoluble drugs with -lactide/glycolide copolymer by a novel spontaneous emulsification solvent diffusion method, and the drug release behavior *J Control Release,* 25**,** 89-98.

NOH, S.-M. (2003) Measurement of Peritoneal Fluid pH in Patients with Non-Serosal Invasive Gastric Cancer. *Yonsei Med J,* 44**,** 45-48.

O'BRIEN, C. N. & GUIDRY, A. J. (1996) Formulation of Poly(DL-Lactide-Co-Glycolide) Microspheres and Their Ingestion by Bovine Leukocytes. *J Dairy Sci,* 79**,** 1954-1959.

OFFICE FOR NATIONAL STATISTICS (1995) Cancer survival trends in England and Wales, 1971-1995: deprivation and NHS Region (CDROM).

OKADA, H. (1997) One- and three-month release injectable microspheres of the LH-RH superagonist leuprorelin acetate. *Adv Drug Deliv Rev,* 28**,** 43-70.

OMURA, G., BLESSING, J. A., EHRLICH, T. C. E., MILLER, A., YORDAN, E., CREASMAN, W. T. & HOMESLEY, H. D. (1986) A Randomized Trial of Cyclophosphamide and Doxorubicin With or Without Cisplatin in Advanced Ovarian Carcinoma: A Gynecologic Oncology Group Study. *Cancer,* 57**,** 1725-30.

PARKIN, D. M., BRAY, F., FERLAY, J. & PISANI, P. (2005) Global Cancer Statistics, 2002. *CA Cancer J Clin,* 55**,** 74-108.

PELEG-SHULMAN, T., GIBSON, D., COHEN, R., ABRA, R. & BARENHOLZ, Y. (2001) Characterization of sterically stabilized cisplatin liposomes by nuclear magnetic resonance. *Biochem Biophys Acta,* 1510**,** 278-291.

PERERA, S. P. & TAI, C. C. (2006) Hollow Fibres. UK.

PETIT, T., VELTEN, M., D'HOMBRES, A., MARCHAL, C., MONTBARBON, X., MORNEX, F., QUETIN, P., GÉRARD, J.-P., ROMESTAING, P. & CARRIE, C. (2006) Long-term survival of 106 stage III ovarian cancer patients with minimal residual disease after second-look laparotomy and consolidation radiotherapy *Gynecol Oncol,* 104**,** 104-108.

PLUNKETT, W., HUANG, P., XU, Y., HEINEMANN, V., GRUNEWALD, R. & GANDHI, V. (1995) Gemcitabine: metabolism, mechanisms of action, and self-potentiation. *Semin Oncol,* 22**,** 3-10.

POLYZOS, A., TSAVARIS, N., KOSMAS, C., GIANNIKOS, L., KATSIKAS, M., KALAHANIS, N., KARATZAS, G., CHRISTODOULOU, K., GIANNAKOPOULOS, K., STAMATIADIS, D. & KATSILAMBROS, N.

(1999) A Comparative Study of Intraperitoneal Carboplatin versus Intravenous Carboplatin with Intravenous Cyclophosphamide in Both Arms as Initial Chemotherapy for Stage III Ovarian Cancer. *Oncology,* 56**,** 291-296.

POPOVA, E. (2006) WebComputing Service Framework. *Int. Journal Information Theories & Applications,* 13**,** 246-254.

PRIOR, S., GANDER, B., BLARER, N., MERKLE, H. P., SUBIRÁ, M. L., IRACHE, J. M. & GAMAZO, C. (2002) In vitro phagocytosis and monocyte-macrophage activation with poly(lactide) and poly(lactide-co-glycolide) microspheres. *Eur J Pharm Sci,* 15**,** 197-207.

QIN, J. & CHUNG, T.-S. (1999) Effect of dope flow rate on the morphology, separation performance, thermal and mechanical properties of ultrafiltration hollow fibre membranes. *J Membr Sci,* 157**,** 35-51.

R DEVELOPMENT CORE TEAM (2007) R: A language and environment for statistical computing., R Foundation for Statistical Computing, Vienna, Austria.

REEDIJK, J. (2003) New Clues for Platinum Antitumor Chemistry: Kinetically Controlled Metal Binding to DNA. *PNAS,* 100**,** 3611-3616.

RICHARDS, M. J., EDWARDS, J. R., CULVER, D. H. & GAYNES, R. P. (2000) Nosocomial infections in combined medical-surgical intensive care units in the United States. *Infect Control Hosp Epidemiol,* 21**,** 510-515.

RITGER, P. L. & PEPPAS, N. A. (1987) A simple equation for description of solute release I. Fickian and non-Fickian release from non-swellable devices in the form of slabs, spheres, cylinders or discs. *J Control Release,* 5**,** 23-36.

ROSENBERG, B., VAN CAMP, L. & KRIGAS, T. (1965) Inhibition of Cell Division in *Escherichia coli* by Electrolysis Products from a Platinum Electrode. *Nature,* 205.

SALTZMAN, W. M. & RADOMSKY, M. L. (1991) Drugs released from polymers: diffusion and elimination in brain tissue. . *Chem. Eng. Sci. ,* 10**,** 2429-44.

SAMIMI, G., VARKI, N. M., WILCZYNSKI, S., SAFAEI, R., ALBERTS, D. S. & HOWELL, S. B. (2003) Increase in Expression of the Copper Transporter ATP7A during Platinum Drug-Based Treatment Is Associated with Poor Survival in Ovarian Cancer Patients. *Clin Cancer Res,* 9**,** 5853-5859.

SHANKARAN, V., IKEDA, H., BRUCE, A. T., WHITE, J. M., SWANSON, P. E., OLD, L. J. & SCHREIBER, R. D. (2001) IFN and lymphocytes prevent primary tumour development and shape tumour immunogenicity. *Nature,* 410**,** 1107-11.

SHEARER, H., ELLIS, M. J., PERERA, S. P. & CHAUDHURI, J. B. (2006) Effects of Common Sterilization Methods on the Structure and Properties of Poly(D,L Lactic-Co-Glycolic Acid) Scaffolds. *Tissue Engineering,* 12**,** 2717-27.

SIRCAR, S. & HUFTON, J. R. (2000) Why does the Linear Driving Force Model for Adsorption Kinetics Work? *Adsorption,* 6**,** 137-147.

SMITH, A. W. (2005) Biofilms and antibiotic therapy: Is there a role for combating bacterial resistance by the use of novel drug delivery systems? *Advanced Drug Delivery Reviews,* 57**,** 1539-50.

SORBE, B. (2003) Consolidation treatment of advanced (FIGO stage III) ovarian carcinoma in complete surgical remission after induction chemotherapy: A randomized, controlled, clinical trial comparing whole abdominal

radiotherapy, chemotherapy, and no further treatment *International Journal of Gynecological Cancer,* 13**,** 278-286.

SORENSON, C. M., BARRY, M.A.,EASTMAN, A. (1990) Analysis of events associated with cell cycle arrest at G2 phase and cell death induced by cisplatin. *J Natl Cancer Inst,* 82**,** 749-755.

STEN-KNUDSEN, O. (2002) *Biological Membranes: Theory of Transport, Potentials and Electric Impulses* Cambridge University Press.

SULLIVAN, J. B. J. & KRIEGER, G. R. (1992) *Hazardous Materials Toxicology-Clinical Principles of Environmental Health.,* Baltimore, MD, Williams and Wilkins.

SWEETMAN, S. C. (2004) *Martindale:The Complete Drug Reference*, Pharmaceutical Press, London.

SWENERTON, K., JEFFREY, J., STUART, G., ROY, M., KREPART, G., CARMICHAEL, J., DROUIN, P., STANIMIR, R., O'CONNELL, G., MACLEAN, G. & AL., E. (1992) Cisplatin-cyclophosphamide versus carboplatin-cyclophosphamide in advanced ovarian cancer: a randomized phase III study of the National Cancer Institute of Canada Clinical Trials Group. *J Clin Oncol,* 10**,** 718-726.

TABATA, Y. & IKADA, Y. (1988) Effect of the size and surface charge of polymer microspheres on their phagocytosis by macrophage. *Biomaterials,* 9**,** 356-362.

TAKAHARA, P. M., FREDERICK, C. A. & LIPPARD, S. J. (1996) Crystal Structure of the Anticancer Drug Cisplatin Bound to Duplex DNA. *J Am Chem Soc,* 118**,** 12309-12321.

TAMAI, H., IGAKI, K., KYO, E., KOSUGA, K., KAWASHIMA, A., MATSUI, S., KOMORI, H., TSUJI, T., MOTOHARA, S. & UEHATA, H. (2000) Initial and 6-Month Results of Biodegradable Poly-l-Lactic Acid Coronary Stents in Humans. *Circulation,* 102**,** 399-404.

TAMURA, T., IMAI, J., MATSUMOTO, A., TANIMOTO, M., SUZUKI, A., HORIKIRI, Y., SUZUKI, T., YOSHINO, H. & IKE, O. (2002) Organ distribution of cisplatin after intraperitoneal administration of cisplatin-loaded microspheres. *Eur J Pharm Biopharm,* 54**,** 1-7.

TAP PHARMACEUTICAL PRODUCTS INC. (2003) Lupron Depot® Package Insert.

TOWNSEND, D. M., DENG, M., ZHANG, L., LAPUS, M. G. & HANIGAN, M. H. (2003) Metabolism of Cisplatin to a Nephrotoxin in Proximal Tubule Cells. *J Am Soc Nephrol,* 14**,** 1-10.

TRACY, M. A., WARD, K. L., FIROUZABADIAN, L., WANG, Y., DONG, N., QIAN, R. & ZHANG, Y. (1999) Factors a!ecting the degradation rate of poly(lactide-co-glycolide) microspheres in vivo and in vitro. *Biomaterials,* 20**,** 1057-1062.

TROPE, C., KAERN, J., HOGBERG, T., ABELER, V., HAGEN, B., KRISTENSEN, G., ONSRUD, M., PETTERSEN, E., ROSENBERG, P., SANDVEI, R., SUNDFOR, K. & VERGOTE, I. (2000) Randomized study on adjuvant chemotherapy in stage I high-risk ovarian

cancer with evaluation of DNA-ploidy as prognostic instrument. *Ann Oncol,* 11**,** 281-288.

URIEN, S. & LOKIEC, F. (2004) Population pharmacokinetics of total and unbound plasma cisplatin in adult patients. *Br J Clin Pharmacol,* 57**,** 756-763.

VON EIFF, C., JANSEN, B., KOHNEN, W. & BECKER, K. (2005) Infections Associated with Medical Devices: Pathogenesis, Management and Prophylaxis. *Drugs,* 65**,** 179-214.

VON HOFF, D. D., SCHILSKY, R., REICHERT, C. M., REDDICK, R. L., ROZENCWEIG, M., YOUNG, R. C. & MUGGIA, F. M. (1979) Toxic effects of cis-dichlorodiammineplatinum(II) in man. *Cancer Treat Rep,* 63**,** 1527-1531.

WALLACE, D. W., STAUDT-BICKEL, C. & KOROS, W. J. (2006) Efficient development of effective hollow fiber membranes for gas separations from novel polymers *J Membr Sci,* 278**,** 92-104.

WANG, D., LI, K. & TEO, W. K. (1996) Polyethersulfone hollow fiber gas separation membranes prepared from NMP/alcohol solvent systems. *J Membr Sci,* 115**,** 85-108.

WARME, W. J., ARCIERO, R. A., SAVOIE III, F. H., UHORCHAK, J. M. & WALTON, M. (1999) Nonabsorbable Versus Absorbable Suture Anchors for Open Bankart Repair *Am J Sports Med,* 27**,** 742-746.

WARNER, D. F. & MIZRAHI, V. (2003) Mechanisms of Stationary-Phase Mutagenesis in Bacteria and their Relevance to Antibiotic Resistance. IN COATES, A. R. M. (Ed.) *Dormancy and Low-Growth States in Microbial Disease.* Cambridge University Press.

WATTS, P. J., DAVIES, M. C. & MELIA, C. D. (1990) Microencapsulation using emulsification/solvent evaporation: an overview of techniques and applications. *Crit Rev Ther Drug Carrier Syst,* 7**,** 235-259.

WEN, X. & TRESCO, P. A. (2006) Fabrication and characterization of permeable degradable poly(dl-lactide-co-glycolide) (PLGA) hollow fiber phase inversion membranes for use as nerve tract guidance channels *Biomaterials,* 27**,** 3800-09.

WENCLAWIAK, B. W. & WOLLMANN, M. (1996) Separation of platinum(II) anti-tumour drugs by micellar electrokinetic capillary chromatography *J Chromatogr A,* 724**,** 317-326.

WILSON, R. H., LEHKY, T., THOMAS, R. R., QUINN, M. G., FLOETER, M. K. & GREM, J. L. (2002) Acute Oxaliplatin-Induced Peripheral Nerve Hyperexcitability. *J Clin Oncol,* 20**,** 1767-1774.

WIRTH, T., ZENDER, L., SCHULTE, B., MUNDT, B., PLENTZ, R., RUDOLPH, K. L., MANNS, M., KUBICKA, S. & KÜHNEL, F. (2003) A Telomerase-dependent Conditionally Replicating Adenovirus for Selective Treatment of Cancer. *Cancer Res,* 63**,** 3181-88.

WITZIG, T. E., GORDON, L. I., CABANILLAS, F., CZUCZMAN, M. S., EMMANOUILIDES, C., JOYCE, R., POHLMAN, B. L., BARTLETT, N. L., WISEMAN, G. A., PADRE, N., GRILLO-LÓPEZ, A. J., MULTANI, P. & WHITE, C. A. (2002) Randomized Controlled Trial of Yttrium-90–Labeled Ibritumomab Tiuxetan Radioimmunotherapy Versus Rituximab Immunotherapy for Patients With Relapsed or Refractory Low-Grade, Follicular, or Transformed B-Cell Non-Hodgkin's Lymphoma *J Clin Oncol,* 20**,** 2453-63.

YEN, M.-S., JUANG, C.-M., LAI, C.-R., CHAO, G.-C., NG, H.-T. & YUAN, C.-C. (2001) Intraperitoneal cisplatin-based chemotherapy vs. intravenous cisplatin-based chemotherapy for stage III optimally cytoreduced epithelial ovarian cancer *Int J Gynecol Obstet,* 72**,** 55-60.

ZWEIZIG, S., ROMAN, L. D. & MUDERSPACH, L. I. (1994) Death from Anaphylaxis to Cisplatin: A Case Report. *Gynecol Oncol,* 53**,** 121-122.

ZYLBERBERG, B., RAVINA, J., SALAT-BAROUX, J., DORMONT, D., LIPP, B. & GUILLET, J. (1986) [Polychemotherapy of ovarian cancer via combined intravenous and intraperitoneal routes. Technic and preliminary results]. *J Gynecol Obstet Biol Reprod,* 15**,** 671-6.

Appendices

Appendix A – Solvents of PLGA

Name	Ethyl acetate	Dichloro-methane	Trichloro-methane	Propanone	N,N-Dimethyl formamide	Tetra-hydrofuran	Hexafluoro-Isopropanol	N-Methyl-2-Pyrrolidone
CAS	(141-78-6)	(75-09-2)	(67-66-3)	(67-64-1)	(68-12-2)	(109-99-9)	(920-66-1)	(872-50-4)
Density (g cm^{-3})	0.90^{20}	1.33^{20}	1.48^{25}	0.78^{25}	0.9445^{25}	0.88^{25}	1.46^{21}	1.02^{25}
Solubility of PLGA 50:50	SS	S	S	SS	S	SS	S	S
Solubility in water	S	SS	SS	M	M	M	M	VS
Boiling point (°C)	77	40	61	56	153	65	59	202
Rat oral LD_{50} (mg kg^{-1})	5600	1600	940	5800	2800	2200	1300	4000

Table A1: Solvents of PLGA 50:50.

Density of liquid at superscript temperature (°C) compared to the density of water at 4°C. Boiling points measured at 101.3kPa. S = soluble, SS = slightly soluble, VS = very soluble, M = miscible. Density (at temperature), solvent solubility in water and boiling point from Lide, 2005 (Lide, 2005). Solubility of PLGA 50:50 in solvent from Lakeshore Biomaterials datasheet (Lakeshore Biomaterials datasheet). LD_{50} values from material safety data sheets (see Table A2 for MSDS online locations).

Chemical	LD50 (mg kg^{-1})	Source	MSDS Online Location
Ethyl acetate	5620	Fisher	https://fscimage.fishersci.com/msds/08750.htm
	5620	Oxford	http://physchem.ox.ac.uk/MSDS/ET/ethyl_acetate.html
Dichloromethane	1600	Fisher	http://www.soest.hawaii.edu/krubin/MSDS/dichloromethane.html
	1600	Oxford	http://physchem.ox.ac.uk/MSDS/DI/dichloromethane.html
Trichloromethane	695	Fisher	https://fscimage.fishersci.com/msds/93015.htm
	1194	Oxford	http://ptcl.chem.ox.ac.uk/MSDS/CH/chloroform.html
Acetone	5800	Fisher	https://fscimage.fishersci.com/msds/00140.htm
	5800	Oxford	http://ptcl.chem.ox.ac.uk/MSDS/PR/propanone.html
N,N-Dimethylformamide	2800	Fisher	https://fscimage.fishersci.com/msds/07860.htm
	2800	Dupont	http://msds.dupont.com/msds/pdfs/EN/PEN_09004a2f8061e698.pdf
Tetrahyrdofuran	1650	Fisher	https://fscimage.fishersci.com/msds/23011.htm
	2816	Oxford	http://physchem.ox.ac.uk/MSDS/TE/tetrahydrofuran.html
Hexafluoroisopropanol	1500	Fisher	https://fscimage.fishersci.com/msds/94544.htm
	1040	Dupont	http://msds.dupont.com/msds/pdfs/EN/PEN_09004a2f8062a65e.pdf
N-Methyl-2-Pyrrolidinone	3914	Fisher	https://fscimage.fishersci.com/msds/08690.htm
	4150	Whitaker	http://www.whitakeroil.com/MSDS/COM%20td%20ehswww%20servlet%20FileStreamServlet.pdf

Table A2: Oral LD_{50} of organic solvents for rats.

LD_{50} from material safety data sheets from two online sources each. Where values differ, mean is used in thesis text.

Appendix B – Derivation of Two Compartment Pharmacokinetic Model

Rate equations can be determined by assuming a two compartment model (Figure 4). The pharmacokinetics of cisplatin can be derived from the rate equations using Laplace transformations (Mayersohn and Gibaldi, 1970). Converting a function into Laplace space allows operations to be performed on the expressions more easily than in regular space. The Laplace transform (equation 47) is widely used in science and engineering for solving integrals.

$$L\{f(t)\} = \int_0^\infty \exp(-s \cdot t) f(t) dt \qquad \textbf{(47)}$$

Complex expressions can be solved using tables of transformations. Some common transforms are shown in Table B1.

Function: f(t)	Laplace: f(s)
1	$\frac{1}{s}$
A	$\frac{A}{s}$
$A \cdot e^{-at}$	$\frac{A}{s+a}$
$A \cdot (1 - e^{-at})$	$\frac{A}{s(s+a)}$
$\frac{A}{(b-a)}(e^{-at} - e^{-bt})$	$\frac{A}{(s+a)(s+b)}$

Table B1: Useful Laplace transforms (Mayersohn and Gibaldi, 1970).

For solving pharmacokinetic problems the rate equations are generally straightforward. However, solving for the concentration of a compartment with several mass transfer

directions can be challenging. Fortunately there is a method for solving problems that are not tabulated.

The general partial fraction theorem states that the function $P(u)/Q(u)$ can be expressed as a sum of partial fractions, where $P(u)$ is a polynomial with a lower degree in u than another polynomial, $Q(u)$. General partial fraction theorem can be used to solve first order rate equations (Benet and Turi, 1971).

$$L^{-1}\left\{\frac{P(s)}{Q(s)}\right\} = \sum_{i=1}^{n} \frac{P(\lambda_i)}{Q_i(\lambda_i)} \exp(\lambda_i t) \quad \textbf{(48)}$$

This method (equation 48), described as the fingerprint method (Bourne and Strauss, 1995), states that the inverse Laplace transformation of a quotient of two polynomials of the form $P(s)/Q(s)$ can be expressed as the sum of the expression with each root substituted in turn. This is true provided that $Q(s)$ has a higher degree in s and contains the factor $(s - \lambda_i)$ which is not repeated. $P(\lambda_i)$ is the value of the numerator for each s term. $Q_i(\lambda_i)$ is the value of the denominator when λ_i is substituted for s terms apart from the term containing λ_i which is excluded.

Using these Laplace transform methods the pharmacokinetics can be determined for this drug. Figure 4 shows a two compartment pharmacokinetic model where an initial dose, D_W, is injected into the blood of a patient, becoming rapidly mixed throughout the whole central compartment with volume, V. The concentration of cisplatin in the central compartment, $W1$, is determined by the rate of transfer into, c_{12}, and out of, c_{21}, the peripheral compartment, the concentration of cisplatin in the peripheral compartment, $W2$, and the rate of elimination, c_{el}.

$$\frac{dW1}{dt} = c_{21}W2 - c_{12}W1 - c_{el}W1 \quad \textbf{(1)}$$

$$\frac{dW2}{dt} = c_{12}W1 - c_{21}W2 \quad \textbf{(2)}$$

In Laplace space:

$$s \cdot \overline{W1} - W1(0) = c_{21}\overline{W2} - c_{12}\overline{W1} - c_{el}\overline{W1} \quad \textbf{(49)}$$

$$s \cdot \overline{W2} - W2(0) = c_{12}\overline{W1} - c_{21}\overline{W2} \quad \textbf{(50)}$$

Where $\overline{W1}$ and $\overline{W2}$ are the concentrations in the central and peripheral compartments transformed into Laplace space. The boundary conditions are that when $t = 0$, $W2 = 0$ and $W1 = D_W/V$.

$$\left(s + \overline{W1}\right) \cdot \overline{W2} = c_{12}\overline{W1} \quad \textbf{(51)}$$

Substitute 51 into 49 to give:

$$s \cdot \overline{W1} - D_W/V = \frac{c_{21}c_{12}}{\left(s + c_{21}\right)}\overline{W1} - c_{12}\overline{W1} - c_{el}\overline{W1}, \text{ or;}$$

$$\overline{W1} \cdot \left\{s\left(s + c_{21}\right) + c_{12}\left(s + c_{21}\right) + c_{el}\left(s + c_{21}\right) - c_{21}c_{12}\right\} = \left(D_W/V\right)\left(s + c_{21}\right), \text{ so;}$$

$$\overline{W1} = \frac{\left(D_W/V\right)\left(s + c_{21}\right)}{s^2 + s\left(c_{21} + c_{12} + c_{el}\right) + c_{el}c_{21}} \quad \textbf{(52)}$$

The denominator can be factorised using two roots, α_W and β_W to give;

$$\overline{W1} = \frac{\left(D_W/V\right)\left(s + c_{21}\right)}{\left(s + \alpha_W\right)\left(s + \beta_W\right)} \quad \textbf{(53)}$$

where;

$$\alpha_W \beta_W = c_{el} c_{21} \tag{54}$$

and;

$$\alpha_W + \beta_W = c_{21} + c_{12} + c_{el} \tag{55}$$

This can be transformed into real space using the fingerprint method for the inverse Laplace transform giving equation 56.

$$W1 = \frac{(D_W/V)}{\beta_W - \alpha_W}\left\{(-\alpha_W + c_{21})\exp(-\alpha_W \cdot t) - (-\beta_W + c_{21})\exp(-\beta_W \cdot t)\right\} \tag{56}$$

This is commonly simplified to the empirical form in equation 3 where A_W and B_W are the aggregated constants.

$$W1 = A_W \exp(-\alpha_W \cdot t) + B_W \exp(-\beta_W \cdot t) \tag{3}$$

From this model (equation 56) the pharmacokinetics of cisplatin can be calculated.

	Estimate	Std. Error	t value	Pr(>|t|)
D_W/V	3.54E+00	8.48E-02	41.7	1.30E-11
α_W	1.00E-03	9.62E-05	10.4	2.53E-06
β_W	3.96E-06	6.60E-07	6.00	2.04E-04
c_{21}	3.44E-04	3.91E-05	8.80	1.02E-05

Table B2: Fit parameters for pharmacokinetic model of cisplatin distribution to mean plasma cisplatin concentration data from Erlichman, et al., 1987 using R.

Table B2 shows the fit parameters for mean data from Erlichman, et al., 1987. Using the known relationships of the roots (equations 54 and 55), $c_{el} = 1.2\times10^{-5}$ s^{-1} and $c_{12} = 6.5\times10^{-4}$ s^{-1}. Based on a dose of 50 mg m^{-2} with an estimated mean surface area of 1.69 m^2, volume of distribution in the aqueous compartment was 24 l, similar to the volume of distribution of 21 l reported elsewhere (Urien and Lokiec, 2004).

From the two compartment model incorporating protein binding (Figure 5) the rate equations can be derived.

$$\frac{dU1}{dt} = j_{21}U2 - j_{12}U1 - j_{el}U1 - k_bU1 \quad \textbf{(57)}$$

Equation 57 for unbound cisplatin is similar to equation 1 for total cisplatin but incorporates the protein binding effect. The concentration of unbound cisplatin in the central compartment can be determined as above but with different parameters since;

$$\alpha_W\beta_W = k_b\left(k_b + j_{el} + j_{12}\right) - j_{21}j_{12} \quad \textbf{(58)}$$

and;

$$\alpha_W + \beta_W = 2k_b + j_{12} + j_{el} \quad \textbf{(59)}$$

Appendix C – Derivation of Semi-Empirical Release Models

The equation which predicts empirical release of drug from a depot device (such as a PLGA microsphere or fibre) can be derived from the rate equations using Laplace transformations (Mayersohn and Gibaldi, 1970). Figure 15 shows the scheme of cisplatin release, where *X1* is the amount released into solution, $M2(\infty)$ is amount of cisplatin in the depot which will be released after a long time and k_{21} is the release constant. From this model it can be seen that the concentration of cisplatin, *X1*, changes at a rate;

$$\frac{dX1}{dt} = k_{21} \cdot X2 \qquad \textbf{(4)}$$

The concentration of cisplatin remaining in the fibre, *X2*, falls at a rate;

$$\frac{dX2}{dt} = -k_{21} \cdot X2 \qquad \textbf{(60)}$$

These differential equations can be solved using the Laplace transformation. In Laplace space these equations have the form;

$$s \cdot \overline{X1} - X1(0) = k_{21}\overline{X2} \qquad \textbf{(61)}$$

$$s \cdot \overline{X2} - X2(0) = -k_{21} \cdot \overline{X2} \qquad \textbf{(62)}$$

Here $\overline{X1}$ and $\overline{X2}$ are $X1$ and $X2$ in Laplace space. The initial conditions are $X1(0) = 0$ and $X2(0) = M2(\infty)$ so therefore;

$$\overline{X2} = \frac{M2(\infty)}{(s + k_{21})} \qquad \textbf{(63)}$$

Substituting this back into equation 61 gives;

$$\overline{X1} = \frac{k_{21} M2(\infty)}{s(s + k_{21})} \quad \textbf{(64)}$$

Using an anti-Laplace transform (Table B1) to convert equation 64, which is in Laplace space, back into real space gives;

$$X1 = M2(\infty) \cdot \left(1 - e^{-k_{21}t}\right) \quad \textbf{(5)}$$

The two compartment model in Figure 15 is described by equation 5 (as long as k_{21} is kept constant by sink conditions). A single exponential is a poor fit for some formulations if there is a significant initial burst release. To improve the fit if a one compartment model is insufficient a second release pool within the device can be added. Physically this might represent a rapid dissolution of drug crystals in accessible pores near the surface of the device followed by slower release of well dispersed drug from the matrix.

Figure 16 shows the release scheme which in physical terms these represent a surface pool, $M3(\infty)$, of readily released cisplatin at rate k_{31} and a well dispersed pool, $M4(\infty)$, of slowly released cisplatin at a rate, k_{41}. The sum of drug in both pools $M3(\infty)$ and $M4(\infty)$ is the total drug loading. For the two compartments in the fibre the rate equation will be of the form;

$$\frac{dX3}{dt} = -k_{31} \cdot X3 \quad \textbf{(65)}$$

So in Laplace space;

$$\overline{X3} = \frac{M3(\infty)}{s + k_{31}} \tag{66}$$

While for the solution compartment;

$$\frac{dX1}{dt} = k_{31} \cdot X3 + k_{41} \cdot X4 \tag{67}$$

In Laplace space is;

$$\overline{X1} \cdot s = k_{31} \cdot \frac{M3(\infty)}{s + k_{31}} + k_{41} \cdot \frac{M4(\infty)}{s + k_{41}}, \text{ or;}$$

$$\overline{X1} = \frac{k_{31} \cdot M3(\infty)(s + k_{41}) + k_{41} \cdot M4(\infty)(s + k_{31})}{s(s + k_{31})(s + k_{41})} \tag{68}$$

Equation 68 can be solved using the fingerprint method (Appendix B) The degree in *s* of the polynomial in the denominator of equation 68 is higher than the polynomial in the numerator and there are no repeating terms so the fingerprint method may be applied. The roots are found by letting each factor of the denominator be zero so $s = 0$, $-k_{31}$ and $-k_{41}$. To transform this into an expression in real space each root is substituted for *s* in turn (excluding the polynomial term) and then multiplied by the exponential of the product of time and the root, $\exp(\lambda_i t)$. The sum of these three values is the integrated function *X1*.

$$L^{-1}\left\{\overline{X1}\right\} = X1 = \begin{pmatrix} \frac{k_{31} \cdot k_{41}(M3(\infty) + M4(\infty))}{k_{31} \cdot k_{41}} \\ + \frac{k_{31} \cdot M3(\infty)(-k_{31} + k_{41})}{-k_{31}(-k_{31} + k_{41})} \cdot e^{-k_{31} \cdot t} \\ + \frac{k_{41} \cdot M4(\infty)(-k_{41} + k_{31})}{-k_{41}(-k_{41} + k_{31})} \cdot e^{-k_{41} \cdot t} \end{pmatrix}, \text{ or;}$$

$$X1 = \{M3(\infty) + M4(\infty)\} - M3(\infty) \cdot e^{-k_{31} \cdot t} - M4(\infty) \cdot e^{-k_{41} \cdot t} \quad \textbf{(7)}$$

The amount of drug released can be derived from the rate equations as to give the model shown in equation 7.

Appendix D – Derivation of Protein Binding Equations

The empirical release models can also be applied to the case where protein removes cisplatin from solution. The two compartment case can be solved as for no clearance of the drug but with rate equation 69 replacing equation 4.

$$\frac{dX1}{dt} = k_{21} \cdot X2 - k_b \cdot X1 \quad \textbf{(69)}$$

This means that in Laplace space the substituted equation becomes;

$$\overline{X1} = \frac{k_{21} M2(\infty)}{(s + k_{21})(s + k_b)} \quad \textbf{(70)}$$

When this is transformed back into real space using the fingerprint method (see Appendix B) the concentration is predicted by equation 8. Transforms can also be carried out using tables of Laplace transforms where available.

$$X1 = \frac{k_{21} M2(\infty)}{(-k_{21} + k_b)} \cdot e^{-k_{21}t} + \frac{k_{21} M2(\infty)}{(-k_b + k_{21})} \cdot e^{-k_b t}, \text{ or;}$$

$$X1 = \frac{k_{21} M2(\infty)}{(k_b - k_{21})} \cdot \left(e^{-k_{21}t} - e^{-k_b t}\right) \quad \textbf{(8)}$$

```
TWOCMPRF2<-nls(cispF2~
        k_21*M*(exp(-k_21*timpF2s)-exp(-k_b*timpF2s))/(k_b-k_21)
,start=list(k_21=1e-5,k_b=1e-4,M=0.6))
```

Table D: Code for non-linear least squares fitting of two compartment protein binding model to cisplatin release data using R.

The parameters to be estimated are $M2(\infty)$, the total drug, k_{21}, the release constant and k_b, the binding constant of cisplatin to BSA.

This model is suitable in many situations for determining the cisplatin concentration in the presence of protein. In cases where the three compartment model gives an improved fit the model can also be derived.

From the rate equations of the three compartment model (Figure 20) the amount of cisplatin in solution can be derived. The rate equation for the solution compartment is given by equation 71.

$$\frac{dX1}{dt} = k_{31} \cdot X3 + k_{41} \cdot X4 - k_b \cdot X1 \qquad \textbf{(71)}$$

This can be transformed into Laplace space and can be combined with expressions for the fibre compartments (equation 66) to give;

$$\overline{X1}(s + k_b) = k_{31} \cdot \frac{M3(\infty)}{s + k_{31}} + k_{41} \cdot \frac{M4(\infty)}{s + k_{41}}, \text{ or;}$$

$$\overline{X1} = \frac{k_{31} \cdot M3(\infty)(s + k_{41}) + k_{41} \cdot M4(\infty)(s + k_{31})}{(s + k_b)(s + k_{31})(s + k_{41})} \qquad \textbf{(72)}$$

In this case the roots, $s = -k_b$, $-k_{31}$ and $-k_{41}$.

$$X1 = \left(\begin{array}{l} \dfrac{k_{31} \cdot M3(\infty)(-k_b + k_{41}) + k_{41} \cdot M4(\infty)(-k_b + k_{31})}{(-k_b + k_{31})(-k_b + k_{41})} \cdot e^{-k_b t} \\ + \dfrac{k_{31} \cdot M3(\infty)}{(-k_{31} + k_b)} \cdot e^{-k_{31} t} \\ + \dfrac{k_{41} \cdot M4(\infty)}{(-k_{41} + k_b)} \cdot e^{-k_{41} t} \end{array} \right) \quad \textbf{(9)}$$

It should be noted that the three compartment model for protein binding (equation 9) introduces two additional parameters which may make the model less significant than the more simple equation 8.

Appendix E – Derivation of Higuchi Kinetics

Fick's Law can be written for an infinite slab as equation 73 where $M(t)/A$ is the amount of drug released after an amount of time per unit area, D is the diffusivity, C_s is the limit of solubility of the drug in the bathing solution and h is the theoretical distance into the slab from which drug has begun eluting.

$$\frac{d\,M(t)/A}{dt} = \frac{DC_s}{h} \qquad \textbf{(73)}$$

Higuchi kinetics (Higuchi, 1961) assumes that there is a perfect sink at the edge of the slab. The solubility of drug in the matrix ($C(0)$) must be much higher than its solubility in water (C_s). Also the drug particles must be much smaller than the layer.

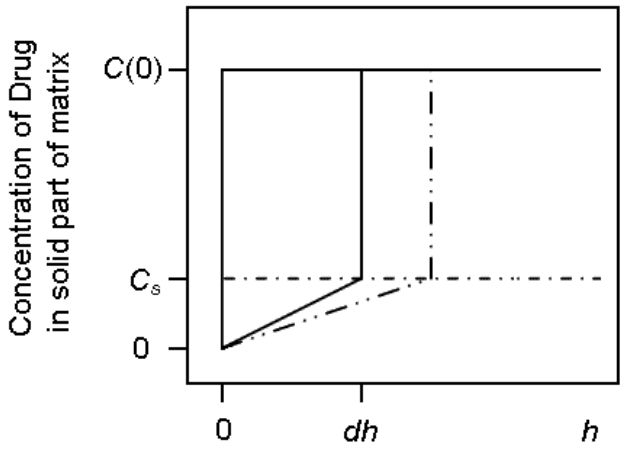

Figure E: The amount of drug released from the solid matrix of a slab into solution after an amount of time is determined by the loading of drug in the matrix ($C(0)$) and its solubility in water (C_s).
This is calculated using h, the theoretical distance into the slab from which the drug has started to elute. Adapted from Higuchi, 1961.

Figure E shows that the amount of drug released from the solid matrix of a slab into solution after an amount of time is determined geometrically by the solubility of drug in the matrix ($C(0)$) and in water (C_s) by the relationship given in equation 74.

$$d\,M(t)/A = C(0)dh - \frac{1}{2}C_s dh \tag{74}$$

This can be combined with equation 73 to give equation 75.

$$2C(0)\frac{dh}{dt} - C_s\frac{dh}{dt} = \frac{2DC_s}{h} \tag{75}$$

This rearranges to:

$$\frac{h(2C(0) - C_s)dh}{2DC_s} = dt \tag{76}$$

Integrating equation 76 gives:

$$\frac{(2C(0) - C_s)h^2}{4DC_s} + k = t \tag{77}$$

When $t = 0$, $h = 0$, so $k = 0$. These boundary conditions give:

$$h = 2 \cdot \sqrt{\frac{DC_s t}{2C(0) - C_s}} \tag{78}$$

So integrating equation 74 with respect to h and substituting equation 78 for h gives equation 11.

$$\frac{M(t)}{A} = (C(0) - \frac{1}{2}C_s) \cdot 2 \cdot \sqrt{\frac{DC_s t}{2C(0) - C_s}}$$, or;

$$\frac{M(t)}{A} = \sqrt{DC_s(2C(0) - C_s)t} \quad \textbf{(11)}$$

Appendix F – Derivation of Release from Fick's Second Law in Spherical Coordinates

Fick's first law in spherical coordinates is defined by equation 15, where $C(r, t)$ is the concentration, D is the diffusivity and r is the radius.

$$j(r,t) = -D\frac{\partial C(r,t)}{\partial r} \quad \textbf{(15)}$$

Fick's second law for spherical coordinates can be derived by finite element analysis. By examining the flow of material through an element of the structure, the overall mass transfer can be determined. The volume element, ΔV, of a spherical matrix is a spherical shell of inner radius r, outer radius $r + \Delta r$. The material entering ΔV during Δt is an amount, ${}^{\text{in}}Q_r{}^{\Delta t}$, which crosses the inner surface of the shell with area $4\pi r^2$ (equation 74).

$${}^{\text{in}}Q_r{}^{\Delta t} = j(r,t)4\pi \cdot r^2 \Delta t \quad \textbf{(79)}$$

Here, $j(r, t)$ is the radial flux at a distance r from the centre of the sphere at time t. Concurrently an amount, ${}^{\text{out}}Q_r{}^{\Delta t}$, is leaving the volume ΔV across the outer surface of the shell with area $4\pi(r + \Delta r)^2$ (equation 75).

$${}^{\text{out}}Q_{r+\Delta r}{}^{\Delta t} = j(r+\Delta r,t)4\pi \cdot (r+\Delta r)^2 \Delta t \quad \textbf{(80)}$$

Therefore, the amount accumulated in the volume ΔV after Δt, $Q_{\Delta V}{}^{\Delta t}$, is the difference between the two quantities (equation 81). Terms in Δr^2 can be excluded as they rapidly tend to zero.

$$Q_{\Delta V}{}^{\Delta t} = {}^{\text{in}}Q_r{}^{\Delta t} - {}^{\text{out}}Q_{r+\Delta r}{}^{\Delta t} \quad \textbf{(81)}$$

$$Q_{\Delta V}{}^{\Delta t} = 4\pi\left(j(r,t)r^2 - j(r+\Delta r,t)(r+\Delta r)^2\right)\Delta t \text{, or}$$

$$Q_{\Delta V}{}^{\Delta t} = 4\pi \cdot r\big(j(r,t)r - j(r+\Delta r,t)r - j(r+\Delta r,t)2\Delta r\big)\Delta t \qquad \textbf{(82)}$$

Assuming that the concentration profile changes slowly then $j(r,\ t)$ approximates $j(r,\ t+\Delta t)$ and $j(r+\Delta r,\ t)$ approximates $j(r+\Delta r,\ t+\Delta t)$. The accumulated amount of drug, $Q_{\Delta V}{}^{\Delta t}$, equals the change in concentration, $\Delta C^{\Delta t}$ multiplied by the volume, ΔV during Δt. Since $\Delta V = 4\pi r^2 \Delta r$ the accumulated amount of drug can be calculated from the concentrations in ΔV at t and $t + \Delta t$ which are $C(r',\ t)$ and $C(r',\ t+\Delta t)$ respectively (equation 89) where $r \le r' \le r + \Delta r$ so that $r' \rightarrow r$, as $\Delta r \rightarrow 0$.

$$Q_{\Delta V}{}^{\Delta t} = \Delta C^{\Delta t} \Delta V$$

$$Q_{\Delta V}{}^{\Delta t} = \big(C(r',t+\Delta t) - C(r',t)\big)4\pi \cdot r^2 \Delta r \qquad \textbf{(83)}$$

Combining equations 82 and 77 and dividing by $4\pi \cdot r^2 \Delta r \Delta t$ produces equation 84, an expression relating flux to concentration.

$$\frac{C(r',t+\Delta t) - C(r',t)}{\Delta t} = -\frac{1}{r}\left(\frac{r\big(j(r+\Delta r,t) - j(r,t)\big)}{\Delta r} + 2\,j(r+\Delta r,t)\right) \qquad \textbf{(84)}$$

At the limits where $\Delta t \rightarrow 0$ and $\Delta r \rightarrow 0$ then $r' \rightarrow r$ and $j(r + \Delta r,\ t) \rightarrow j(r,\ t)$, which reduces to partial derivatives (equation 16).

Appendix G – Derivation of Release from Fick's Second Law in Cylindrical Coordinates

Finite element analysis can be performed for cylinders. The cylinder is assumed to be radially homogenous for all angles of θ and along its length for all values of z. Therefore, concentration is treated as not being a function of z or θ so these terms are excluded from the concentration profile (equation 20).

$$\frac{\partial C(r,\theta,z)}{\partial z} = \frac{\partial C(r,\theta,z)}{\partial \theta} = 0 \qquad \textbf{(85)}$$

The volume element, ΔV, is a cylindrical ring of height Δz, inner radius r, and outer radius $r + \Delta r$. The change in concentration in ΔV during Δt is an amount, ${}^{\text{in}}Q_r{}^{\Delta t}$, which crosses the inner surface of the ring of radius r and area, $2\pi \cdot r\Delta z$. This is summarized by equation 86.

$${}^{\text{in}}Q_r{}^{\Delta t} = j(r,t)2\pi \cdot r\Delta z\Delta t \qquad \textbf{(86)}$$

Here, $j(r, t)$ is the radial flux at a distance r from the cylinder axis at time t. Concurrently an amount, ${}^{\text{out}}Q_r{}^{\Delta t}$, is leaving the volume ΔV (equation 87).

$${}^{\text{out}}Q_{r+\Delta r}{}^{\Delta t} = j(r+\Delta r,t)2\pi \cdot (r+\Delta r)\Delta z\Delta t \qquad \textbf{(87)}$$

Therefore, the amount accumulated in the volume ΔV after Δt, $Q_{\Delta V}{}^{\Delta t}$, is the difference between the two quantities (equation 88).

$$Q_{\Delta V}{}^{\Delta t} = {}^{\text{in}}Q_r{}^{\Delta t} - {}^{\text{out}}Q_{r+\Delta r}{}^{\Delta t}$$

$$Q_{\Delta V}{}^{\Delta t} = 2\pi \cdot \Delta z\left(j(r,t)r - j(r+\Delta r,t)(r+\Delta r)\right)\Delta t \qquad \textbf{(88)}$$

Assuming that the concentration profile changes slowly then $j(r,\ t)$ approximates $j(r,\ t+\Delta t)$ and $j(r+\Delta r,\ t)$ approximates $j(r+\Delta r,\ t+\Delta t)$. The accumulated amount of drug, $Q_{\Delta V}{}^{\Delta t}$, equals the change in concentration, $\Delta C^{\Delta t}$ multiplied by the volume, ΔV during Δt. Since $\Delta V = 2\pi \cdot r\Delta r\Delta z$, the accumulated amount of drug can be calculated from the concentrations in ΔV at t and $t+\Delta t$ which are $C(r',\ t)$ and $C(r',\ t+\Delta t)$ respectively (equation 89) where $r \le r' \le r+\Delta r$ so that $r' \rightarrow r$, as $\Delta r \rightarrow 0$.

$$Q_{\Delta V}{}^{\Delta t} = \Delta C^{\Delta t} \Delta V$$

$$Q_{\Delta V}{}^{\Delta t} = \left(C\left(r', t+\Delta t\right) - C\left(r', t\right)\right) 2\pi \cdot r\Delta r\Delta z \qquad \textbf{(89)}$$

Combining equations 88 and 89 and dividing by $2\pi \cdot r\Delta r\Delta z\Delta t$ produces equation 90, an expression relating flux to concentration.

$$\frac{C\left(r', t+\Delta t\right) - C\left(r', t\right)}{\Delta t} = -\left(\frac{j\left(r+\Delta r, t\right) - j\left(r, t\right)}{\Delta r} + \frac{j\left(r+\Delta r, t\right)}{r} \right) \qquad \textbf{(90)}$$

At the limits where $\Delta t \rightarrow 0$ and $\Delta r \rightarrow 0$ then $r' \rightarrow r$ and $j(r+\Delta r,\ t) \rightarrow j(r,\ t)$ reducing to partial derivatives (equation 21).

For a cylinder with a uniform initial concentration of drug the solution to equation 30 simplifies to equation 32 (Crank, 1975) where $a\alpha_n$ has the values shown in Table G1 for $n = 1,\ldots,20$.

n	$a\alpha_n$	n	$a\alpha_n$
1	2.40482	11	33.77582
2	5.52007	12	36.91709
3	8.65372	13	40.05842
4	11.79153	14	43.19979
5	14.93091	15	46.34118
6	18.07106	16	49.48261
7	21.21163	17	52.62405
8	24.35247	18	55.76551
9	27.49347	19	58.90698
10	30.63460	20	62.04847

Table G1: The first twenty positive roots of the Bessel function of the first kind of zero order.

Roots calculated using webMathematica (Popova, 2006).

$$M(t) = M(\infty)\cdot\left(1-\sum_{n=1}^{\infty}\frac{4}{(a\alpha_n)^2}\exp\left(-D\alpha_n^2 t\right)\right) \quad \textbf{(32)}$$

For a solid fibre the range of the fibre, r, extends from the origin so B in equation 28 must be zero so that the result falls within the boundary conditions.

```
Cylinder<-nls(cisplatin~
        M*(1-((4*exp(-D*(2.404825558/0.024)^2*time)/2.404825558^2
        +4*exp(-D*(5.52007811/0.024)^2*time)/5.52007811^2
        +4*exp(-D*(8.653727913/0.024)^2*time)/8.653727913^2)))
,start=list(M=0.4,D=1e-12))
```

Table G2: Code for non-linear least squares fitting of a third order Taylor series approximation of cylindrical diffusion equation to cisplatin release data using R.

The parameters to be estimated are *M*, the total cisplatin, and *D*, the diffusivity. The radius of the cylinder is 0.024 cm and the Bessel zeros are from Table G1.

Appendix H – Modification of Fick's Second Law for Hollow Cylinders

Equations for heat flow in an infinite hollow cylinder (Carslaw and Jaeger, 1959) can be used to describe diffusion of a solute from a hollow fibre (Crank, 1975). The solid cylinder could be simplified because the Bessel function of the second kind in equation 28 could not be part of the solution at $r = 0$. For a hollow fibre however r does not include the origin and so the Bessel function of the second kind is set to zero at $r = 0$ by the boundary conditions.

n	α_n	n	α_n
1	3.91017	11	43.19529
2	7.84526	12	47.12242
3	11.77511	13	51.04952
4	15.70356	14	54.97661
5	19.63143	15	58.90368
6	23.55900	16	62.83075
7	27.48641	17	66.75780
8	31.41372	18	70.68485
9	35.34095	19	74.61189
10	39.26814	20	78.53893

Table H1: The first twenty positive roots of the Bessel function used for solving release from hollow fibres.

Roots of the Bessel function $J_0(a\alpha_n)Y_0(1.8\alpha_n)-J_0(1.8\ \alpha_n)Y_0(a\alpha_n)$ were calculated using webMathematica (Popova, 2006) where 1.8 is the ratio of outer against inner radii for F9 hollow fibres.

```
Hollow_Fibre<-nls(cisplatin~
        M*(1-4*((((bessel_J0(97.75422897*0.040)-bessel_J0(97.75422897*0.072))
        /(97.75422897^2*(bessel_J0(97.75422897*0.040)+bessel_J0(97.75422897*0.072))))
        *exp(-D*97.75422897^2*time)
        +((bessel_J0(196.1315516*0.040)-bessel_J0(196.1315516*0.072))
        /(196.1315516^2*(bessel_J0(196.1315516*0.040)+bessel_J0(196.1315516*0.072))))
        *exp(-D*196.1315516^2*time)
        +((bessel_J0(294.3778788*0.040)-bessel_J0(294.3778788*0.072))
        /(294.3778788^2*(bessel_J0(294.3778788*0.040)+bessel_J0(294.3778788*0.072))))
        *exp(-D*294.3778788^2*time)))/(0.072^2-0.040^2))
,start=list(M=1,D=5e-11))
```

Table H2: Code for non-linear least squares fitting of a third order Taylor series approximation of hollow fibre diffusion equation to F9 cisplatin release data using R.
The parameters to be estimated are *M*, the total cisplatin, and *D*, the diffusivity. The first three Bessel zeros from Table H1 have been divided by the inner radius, 0.040 cm.

Appendix I – Calculation of Diffusivity of Cisplatin in Microspheres using Higuchi Kinetics

To estimate the surface area of a 100 mg sample of microspheres the density is needed. This was estimated by displacement of water.

Volume (sample)	= Mass / Density
	= 100 mg / 780 mg cm^{-3}
	= 0.128 cm^3
Volume (one microsphere)	$= \frac{4}{3}\pi R^3$
	= 1.13×10^{-7} cm^3
Number of microspheres (sample)	= Volume (sample) / Volume (one microsphere)
	= 0.128 cm^3 / 1.13×10^{-7} cm^3
	= 1.13×10^{6}
Surface area (one microsphere)	$= 4\pi R^2$
	= 1.13×10^{-4} cm^2
Surface area (sample)	= 1.13×10^{-4} cm^2 * 1.13×10^{6}
	= 128 cm^2

The surface area can be used in conjunction with the Higuchi model to estimate the diffusivity of cisplatin in the polymer matrix.

$$D = \frac{(k/A)^2}{C_s\left(2M(\infty)/V - C_s\right)} \quad \textbf{(13)}$$

The Higuchi constant, k, was $1.1\pm0.04\times10^{-3}$ mg $s^{-0.5}$ for large PLGA 50:50 microspheres. The surface area of the sample is 128 cm^2 based on an approximate mean radius of 30 μm and a density of 780 mg cm^{-3}. The solubility of cisplatin, C_s, is

2 mg cm^{-3}. The concentration of cisplatin in the sample is 1.2 % of the 100 mg sample or 0.012 mg mg^{-1}.

$$D = \frac{(0.0011\,\text{mg}\,\text{s}^{-0.5} / 128\,\text{cm}^2)^{\,2}}{2\,\text{mg}\,\text{cm}^{-3} \cdot (2 \cdot (0.012\,\text{mg}\,\text{mg}^{-1} \cdot 780\,\text{mg}\,\text{cm}^{-3}) - 2\,\text{mg}\,\text{cm}^{-3})}$$

Using this calculation the diffusivity of cisplatin in small PLGA 50:50 microspheres is estimated as 2×10^{-12} cm^2 s^{-1}.

Appendix J – Calculation of Diffusivity of Cisplatin in Fibres using Higuchi Kinetics

The surface area of a sample of fibres was estimated for each type of fibre. For example, for F2 fibres the surface area of the fibre was estimated from its bulk properties.

Density (sample) = Mass (sample) / Volume (sample)

= 41.2 mg / 0.14 cm^3

= 290 mg cm^{-3}

Volume (sample) = π * Radius (sample)^2 * Length (sample)

Radius (sample) $= \sqrt{\frac{0.14\,\mathrm{cm}^3}{\pi \cdot 75.3\,\mathrm{cm}}}$

= 0.024 cm

The volume is in agreement with the mean value measured using digital callipers. For 5 mg fibre the typical length was 9.1 cm.

Surface area (fibre) = 2 π * Radius (fibre) * Length (fibre)

+ 2 π * Radius (fibre)^2

= 1.4 cm^2

Appendix K – Batch Data for PLGA Microspheres and Fibres

Label	L:G Ratio	Mass PLGA (g)	Mass EA (g)	Mass Cisplatin (g)	Volume PVA (ml)	Cisplatin Loading (%)	Homogeniser Speed (rpm)	Homogenisation Time (min)
M1	50:50	2.58	23.24	1.34	150	9	9500	13
M3	"	3.37	30.41	1.51	"	2-6	"	"
M4	"	"	"	"	125*	6-8	"	"
M7	"	3.60	32.45	1.18	150	1-2	"	"
M8	65:35	3.61	32.57	"	"	1-4	"	"
M14	"	2.64	23.76	1.06	160	7	6500	11
M16	"	"	"	1.06‡	"	0	"	"
M17	"	2.84	25.58	1.00	"	11	"	"
M18	"	"	17.46	"	"	13	"	"
M19	"	"	12.99	"	"	11	"	"
M20	"	"	25.58	1.01	"	12	"	"
M21	"	"	"	1.00	"	7-9	"	"
M22	"	"	"	1.00‡	"	0	"	"
M25	"	"	"	1.00	"	6	"	"
M26	"	"	"	"	"	4	"	"
M27	"	"	25.59	"	"	5	"	"

Table K1: Conditions of manufacture of batches of PLGA microspheres.

* Twice volume of dope added to PVA. † Dichloromethane replaced ethyl acetate. ‡ Phenolphthalein replaced cisplatin. ◊ Carboplatin replaced cisplatin.

Label	L:G Ratio	Mass PLGA (g)	Mass NMP (g)	Mass Cisplatin (g)	Flow Rate (ml h^{-1})	Hollow	Diameter (cm)	Density (g cm^{-3})	Cisplatin Loading (%)	Water Flow (ml h^{-1})
F1	75:25	5.54	27.7	0.6	60	N	0.044	212	0	NA
F2	65:35	2.14	9.91	1.07	"	"	0.048	294	10-11	"
F3	"	2.15	9.98	1.11	"	"	"	267	9-24	"
F4	"	2.14	9.92	1.06	"	"	0.052	287	15	"
F5	"	"	"	0	"	"	0.059	240	0	"
F6	"	"	"	1.31◊	"	"	0.097	271	5	"
F7	"	3.21	14.87	1.61	"	"	0.065	223	ND	"
F8	"	3.03	14.05	1.52‡	50	Y	0.110	506	0	70
F9	"	"	14.04	1.52	200	"	0.127	276	21-22	200
F10	"	5.8	26.87	2.91	"	"	0.149	357	27-28	"

Table K2: Conditions of manufacture of batches of PLGA fibres.

‡ Phenolphthalein replaced cisplatin. ◊ Carboplatin replaced cisplatin.

Appendix L – Modelling Cisplatin Release from PLGA Microspheres

Parameter	Mean M3, M7 1-38 μm		Mean M3, M7 38-90 μm	
	Estimate	St. Error	Estimate	St. Error
Higuchi k (mg $s^{-0.5}$)	3.41E-03***	1.31E-04	1.11E-03***	3.68E-05
AIC Higuchi	45.0		-36.8	
Empirical 2 $M2(\infty)$ (mg)	4.89E+00***	9.53E-01	1.18E+00***	1.04E-01
Empirical 2 k_{21} (s^{-1})	1.40E-06**	4.27E-07	2.51E-06***	4.37E-07
AIC Empirical 2	54.1		-33.8	

Table L1: Parameters for release of cisplatin from PLGA 50:50 microspheres.
Higuch and empirical two compartment models calculated by non-linear least squares regression. There was insufficient data for three compartment model and spherical Fickian models to converge. AIC is comparable between models not between microsphere datasets. Parameters are marked *** if they are significant at $p < 0.001$ and ** at $p < 0.01$.

Parameter	Mean M14, M17-M21	
	Estimate	St. Error
Higuchi k (mg $s^{-0.5}$)	1.37E-02***	4.22E-04
AIC Higuchi	NA	
Spherical $M(\infty)$ (mg)	1.22E+01***	3.67E-01
Spherical D/R^2 (s^{-1})	2.10E-07***	2.68E-08
AIC Spherical	484	
Empirical 2 $M2(\infty)$ (mg)	1.14E+01***	2.64E-01
Empirical 2 k_{21} (s^{-1})	4.639E-06***	4.19E-07
AIC Empirical 2	532	
Empirical 3 $M3(\infty)$ (mg)	3.51E+00***	4.68E-01
Empirical 3 $M4(\infty)$ (mg)	8.73E+00***	4.64E-01
Empirical 3 k_{31} (s^{-1})	8.34E-05**	2.96E-05
Empirical 3 k_{41} (s^{-1})	2.22E-06***	3.54E-07
AIC Empirical 3	480	

Table L2: Parameters for release of cisplatin from six batches of PLGA 65:35 Microspheres.

Higuchi, spherical Fickian, two and three compartment models were fitted by non-linear least squares regression using R. AIC is comparable between models not between microsphere datasets. Parameters are marked *** if they are significant at $p < 0.001$ and ** at $p < 0.01$.

Parameter	M21 (aged)		M25	
	Estimate	St. Error	Estimate	St. Error
Spherical $M(\infty)$ (mg)	5.40E-01***	7.91E-03	4.74E-01***	4.84E-03
Spherical D/R^2 (s^{-1})	1.37E-06***	1.28E-07	1.41E-06***	8.81E-08
AIC Spherical	-195.9		-228.6	
Empirical 2 $M2(\infty)$ (mg)	5.15E-01***	9.37E-03	4.53E-01***	7.32E-03
Empirical 2 k_{21} (s^{-1})	4.51E-05***	4.37E-06	4.62E-05***	3.64E-06
AIC Empirical 2	-156.1		-170.7	
Empirical 3 $M3(\infty)$ (mg)	2.26E-01***	2.78E-02	2.20E-01***	1.61E-02
Empirical 3 $M4(\infty)$ (mg)	3.24E-01***	2.73E-02	2.64E-01***	1.58E-02
Empirical 3 k_{31} (s^{-1})	1.87E-04***	4.82E-05	1.47E-04***	2.00E-05
Empirical 3 k_{41} (s^{-1})	9.71E-06***	1.46E-06	8.88E-06***	8.71E-07
AIC Empirical 3	-199.4		-249.6	

Table L3: Parameters for release of cisplatin from aged (M21) and sieved (M25) PLGA 65:35 microspheres.

Parameters calculated by non-linear least squares regression using spherical Fickian and empirical two and three compartment models. Higuchi model was not appropriate for this dataset. AIC is comparable between models not between microsphere datasets. Parameters are marked *** as they are significant at $p < 0.001$.

Parameter	M26		M27	
	Estimate	St. Error	Estimate	St. Error
Spherical $M(\infty)$ (mg)	3.50E-01***	3.43E-03	4.35E-01***	5.92E-03
Spherical D/R^2 (s^{-1})	7.86E-07***	4.16E-08	1.40E-06***	1.17E-07
AIC Spherical	-301.0		-203.0	
Empirical 2 $M2(\infty)$ (mg)	3.26E-01***	5.66E-03	4.13E-01***	7.89E-03
Empirical 2 k_{21} (s^{-1})	2.60E-05***	2.53E-06	4.85E-05***	4.61E-06
AIC Empirical 2	-218.1		-157.7	
Empirical 3 $M3(\infty)$ (mg)	1.99E-01***	1.11E-02	1.88E-01***	1.74E-02
Empirical 3 $M4(\infty)$ (mg)	1.60E-01***	1.06E-02	2.56E-01***	1.72E-02
Empirical 3 k_{31} (s^{-1})	6.36E-05***	5.33E-06	1.84E-04***	3.47E-05
Empirical 3 k_{41} (s^{-1})	4.32E-06***	5.01E-07	9.08E-06***	1.10E-06
AIC Empirical 3	-327.3		-217.6	

Table L4: Parameters for release of cisplatin from sieved (M27, M27) PLGA 65:35 microspheres.

Parameters calculated by non-linear least squares regression using spherical Fickian and empirical two and three compartment models. Higuchi model was not appropriate for this dataset. AIC is comparable between models not between microsphere datasets. Parameters are marked *** as they are significant at $p < 0.001$.

Appendix M – Modelling Cisplatin Release from PLGA Fibres

Parameter	F2		F3		F4	
	Estimate	St. Error	Estimate	St. Error	Estimate	St. Error
Cylindrical $M(\infty)$ (mg)	1.95E+00	1.86E+00	1.18E+00***	1.06E-01	8.27E+00	1.83E+01
Cylindrical D (cm^2 s^{-1})	8.60E-09	1.75E-08	3.42E-10**	1.04E-10	9.82E-13	4.40E-12
AIC Cylindrical	-275.4		0.2158		-69.14	
Higuchi k (mg $s^{-0.5}$)	5.76E-04***	1.15E-05	1.45E-03***	5.74E-05	7.61E-04***	3.36E-05
AIC Higuchi	-276.7		12.82		-71.30	
Empirical 2 $M2(\infty)$ (mg)	4.93E-01***	2.00E-02	1.08E+00***	5.57E-02	7.43E-01***	8.41E-02
Empirical 2 k_{21} (s^{-1})	4.25E-06***	4.30E-07	7.45E-06***	1.16E-06	2.96E-06***	7.65E-07
AIC Empirical 2	-253.6		4.466		-66.25	
Empirical 3 $M3(\infty)$ (mg)	1.18E-01***	2.96E-02	1.69E-01	1.10E-01	8.46E-02	5.33E-02
Empirical 3 $M4(\infty)$ (mg)	5.54E-01***	1.10E-01	9.54E-01***	1.05E-01	8.32E-01**	2.40E-01
Empirical 3 k_{31} (s^{-1})	3.95E-05*	1.79E-05	1.64E-04	2.51E-04	1.65E-04	2.97E-04
Empirical 3 k_{41} (s^{-1})	1.49E-06*	6.66E-07	5.18E-06**	1.60E-06	1.64E-06	1.01E-06
AIC Empirical 3	-274.4		3.006		-66.28	

Table M: Parameters for release of cisplatin from PLGA 65:35 solid fibres.

Parameters were calculated by non-linear least squares regression using cylindrical Fickian, Higuchi and empirical two and three compartment models. AIC is comparable between models not between fibre datasets. Parameters are marked *** if they are significant at $p < 0.001$, ** at $p < 0.01$, * at $p < 0.05$ and are not marked if they are not significant.

Appendix N – Effect of Ethanol on Fibre Release Parameters

Parameter	F9		F9 (ethanol)	
	Estimate	St. Error	Estimate	St. Error
Hollow $M(\infty)$ (mg)	1.10E+00***	3.51E-02	1.19E+00***	2.27E-02
Hollow D (cm^2 s^{-1})	3.27E-10***	3.18E-11	3.78E-10***	2.60E-11
AIC Hollow	-185.8		-151.7	
Higuchi k (mg $s^{-0.5}$)	1.13E-03***	2.64E-05	1.29E-03***	3.12E-05
AIC Higuchi	-93.45		-57.41	
Empirical 2 $M2(\infty)$ (mg)	1.04E+00***	2.59E-02	1.15E+00***	1.54E-02
Empirical 2 k_{21} (s^{-1})	5.02E-06***	3.28E-07	5.30E-06***	2.32E-07
AIC Empirical 2	-177.7		-163.6	
Empirical 3 $M3(\infty)$ (mg)	1.12E-01*	5.15E-02	6.72E-02*	2.91E-02
Empirical 3 $M4(\infty)$ (mg)	9.59E-01***	4.76E-02	1.10E+00***	2.83E-02
Empirical 3 k_{31} (s^{-1})	1.55E-04	1.59E-04	2.85E-04	4.06E-04
Empirical 3 k_{41} (s^{-1})	3.94E-06***	5.30E-07	4.75E-06***	3.05E-07
AIC Empirical 3	-184.2		-171.0	

Table N1: Release parameters for release of cisplatin from PLGA 65:35 F9 hollow fibres before and after ethanol treatment.

Parameters were calculated by non-linear least squares regression using cylindrical Fickian, Higuchi and empirical two and three compartment models. AIC is comparable between models not between fibre datasets. Parameters are marked *** if they are significant at $p < 0.001$, * at $p < 0.05$ and are unmarked if they are not significant.

Parameter	F10		F10 (ethanol)	
	Estimate	St. Error	Estimate	St. Error
Hollow $M(\infty)$ (mg)	1.40E+00***	3.64E-02	1.48E+00***	2.12E-02
Hollow D (cm^2 s^{-1})	2.95E-10***	2.71E-11	5.12E-10***	3.12E-11
AIC Hollow	-137.8		-169.0	
Higuchi k (mg $s^{-0.5}$)	1.48E-03***	2.86E-05	1.72E-03***	4.08E-05
AIC Higuchi	-55.76		29.39	
Empirical 2 $M2(\infty)$ (mg)	1.35E+00***	2.19E-02	1.45E+00***	1.59E-02
Empirical 2 k_{21} (s^{-1})	4.78E-06***	2.45E-07	7.86E-06***	3.20E-07
AIC Empirical 2	-177.0		-202.5	
Empirical 3 $M3(\infty)$ (mg)	2.53E-02	2.70E-02	6.25E-02	5.78E-02
Empirical 3 $M4(\infty)$ (mg)	1.33E+00***	3.11E-02	1.40E+00***	5.56E-02
Empirical 3 k_{31} (s^{-1})	7.76E-04	3.47E-03	2.17E-04	4.88E-04
Empirical 3 k_{41} (s^{-1})	4.62E-06***	3.03E-07	7.34E-06***	5.26E-07
AIC Empirical 3	-174.1		-202.7	

Table N2: Release parameters for release of cisplatin from PLGA 65:35 F10 hollow fibres before and after ethanol treatment.

Parameters were calculated by non-linear least squares regression using cylindrical Fickian, Higuchi and empirical two and three compartment models in R. AIC is comparable between models not between fibre datasets. Parameters are marked *** if they are significant at $p < 0.001$ and are not marked if they are not significant.

Appendix O – Modelling Carboplatin Release from Solid Fibres

Parameter	F6	
	Estimate	St. Error
Cylindrical $M(\infty)$ (mg)	2.46E-01***	1.49E-02
Cylindrical D (cm^2 s^{-1})	6.96E-09**	2.27E-09
AIC Cylindrical	-140	
Empirical 2 $M2(\infty)$ (mg)	2.42E-01***	1.41E-02
Empirical 2 k_{21} (s^{-1})	2.75E-05**	8.16E-06
AIC Empirical 2	-141	

Table O: Release parameters for release of carboplatin from PLGA 65:35 F6 fibres. Parameters were calculated by non-linear least squares regression using cylindrical Fickian, and empirical two compartment models. Higuchi and three compartment models were not significant. Parameters are marked *** if they are significant at $p < 0.001$ and ** at $p < 0.01$.